Characterizing of Robo downstream signalling to promote direct neurogenesis

Doctoral Thesis presented by

Salma Moustafa Mahmoud Amin

Thesis Director: Dr. Victor Borrell Franco

PhD Program in Neuroscience

Neurosciences Institute

Universidad Miguel Hernández de Elche

- 2023 -

Characterizing of Robo downstream signalling to promote direct neurogenesis

Doctoral Thesis presented by

Salma Moustafa Mahmoud Amin

Thesis Director: Dr. Victor Borrell Franco

PhD Program in Neuroscience

Neurosciences Institute

Universidad Miguel Hernández de Elche

- 2023 -

Sant Joan d'Alacant, 14 Marzo 2023

This Doctoral Thesis, entitled "Characterizing of Robo downstream signalling to promote direct neurogenesis", is submitted under the format of thesis by compendium of the following publication:

Amin, S., & Borrell, V. (2020). The Extracellular Matrix in the Evolution of Cortical Development and Folding. Frontiers in cell and developmental biology, 8, 604448. https://doi.org/10.3389/fcell.2020.604448.

Yours sincerely

Salma Moustafa Mahmoud Amin

INSTITUTO DE NEUROCIENCIAS

DIRECTOR'S REPORT

Sant Joan d'Alacant, 14 Marzo 2023

Dr. D. Victor Borrell Franco, Director of the doctoral thesis entitled "Characterizing of Robo downstream signalling to promote direct neurogenesis"

CERTIFIES:

That Ms. Salma Moustafa Mahmoud Amin has carried out under my supervision the work entitled "Characterizing of Robo downstream signalling to promote direct neurogenesis " in accordance with the terms and conditions defined in her Research Plan and in accordance with the Code of Good Practice of the University Miguel Hernández of Elche, satisfactorily fulfilling the objectives foreseen for its public defence as a doctoral thesis.

I sign for appropriate purposes, at Sant Joan D'alicante, 14 of March of 2023

Thesis director

Dr.D. / Victor Borrell Franco

E-mail : vborrell@umh.es
https://in.umh-csic.es/en/

Tel: +34 965 919245

Av Ramón y Cajal s/n
CAMPUS DE SANT JOAN
03550 SANT JOAN D'ALACANT– ESPAÑA

REPORT OF THE DOCTORAL PROGRAMME COORDINATOR

Sant Joan d'Alacant, 14 Marzo 2023

Dra. Elvira de la Peña García, Coordinator of the Neurosciences PhD programme at the Institute of Neurosciences in Alicante, a joint centre of the Miguel Hernández University (UMH) and the Spanish National Research Council (CSIC),

INFORMS:

That Ms. Salma Moustafa Mahmoud Amin has carried out under the supervision of our PhD Programme the work entitled "Characterizing of Robo downstream signalling to promote direct neurogenesis*"* in accordance with the terms and conditions defined in its Research Plan and in accordance with the Code of Good Practice of the University Miguel Hernández de Elche, fulfilling the objectives satisfactorily for its public defence as a doctoral thesis.

Which I sign for appropriate purposes, at Sant Joan D'alicante, 14 of March of 2023

Dra. Dña. / Elvira de la Peña García

Coordinator of the PhD Programme in Neurosciences

E-mail : elvirap@umh.es
https://in.umh-csic.es/en/

Tel: +34 965 919533
Fax: +34 965 919549

Av Ramón y Cajal s/n
CAMPUS DE SANT JOAN
03550 SANT JOAN D'ALACANT– ESPAÑA

FUNDING

During my studies, I received funding "La Caixa " – Severo Ochoa doctoral Scholarship from Obra Social ”la Caixa”, to carry out my PhD thesis entitled “Characterizing of Robo downstream signalling to promote direct neurogenesis.”

Acknowledgments

I'd like to express my heartfelt gratitude to everyone who helped me get to the end of this journey. I couldn't have done it without the unwavering support of my family and friends. Throughout my studies, they have been my rock and cheerleaders.

I'd like to thank Dr. Victor Borrell for giving me the opportunity to do my thesis in his lab and for guiding me through these years. I am grateful for all of the skills and knowledge he has passed on to me. I'd like to thank the "La Caixa' Foundation for funding my PhD; Thank you for your trust in me, providing me with the necessary independence as well as your constant scientific guidance and availability. I'm confident that my time in your lab shaped my mind as a researcher and enabled me to be at the forefront of innovative science.

I would like to thank previous and current members of the Borrell lab, Adrian, Virginia, Esther Llorens, Trini, Ana, Alex, Enrico, Lucia, Anna, Yuki, Eduardo, and Rafael, for providing me with all kinds of support and scientific discussions, including physical support (nitrogen and water trips), during my PhD. I don't want to forget Elosia Herrera Lab, which has been like a sister lab to us; I'd like to thank them especially for their generosity and helpfulness.

I'd also like to thank the La Caixa, UMH, and CAPD cordinators, Dr. Elvira Maria De La Peña, Dr. Maria Cruz, Maria Virtudes Garcia Fernandez, Bibian Garcia, and Marina Carratala Gutierrez, for guiding me through visa renewal every year, Phd paperwork, and thesis submission processes from afar.

I'd like to thank the following INA members for their assistance: Khalil Kass Youssef, Juan Galceran, Mari Trini, Angel Marquez, Jose Lopez Atalaya, and Antonio Caler. They were a vital part of my PhD research.

I would like to thank my friends and click that were responsible for the good times. Lucia, Anna, Alvaro, Ana, Aida, Michael, Kat, Khalid, Pablo, Irene, Khalil, and Amr, it was a pleasure to spend time with you and share food and good times. Thank you for accepting me and caring about me.

Finally, I couldn't have done it without my family and friends' unwavering support. They have been my rock and cheerleaders throughout my studies. I'm dedicating my work to my father and mother, who have been there for me every step of the way. Because of them, I am who I am today. I'd like to express my gratitude to my brother Mahmoud and his wife Shereen for always being available to advise and listen to me for hours. I'd like to thank Lucia, who was my constant companion during this period, and I know I couldn't have done it without her. You stood by me, and you and your family were my second home. I am really happy I met you.

Thank you to everyone who helped me grow as a person and researcher. I'd like to continue paying it forward.

To whom it may concern:

I captured all of the images used as section cover pages in this thesis using imaging facilities at the Institute of Neuroscience, Alicante.

Table of Contents

Abbreviations

Abbreviations

aRGCs	apical Radial Glia Cells
AJs	Adherent Junctions
BBB	Blood Brain Barrier
bIPs	Basal Intermediate Progenitors
Bp	Basal process
BrdU	Bromodeoxyuridine
bRGCs	basal Radial Glia Cells
Cas9	CRISPR associated protein 9
CGE	Caudal Ganglionic Eminence
CK	Chicken
CMV	Citomegalovirus promotor
CNS	Central Nervous System
CP	Cortical Plate
CR	Cajal Retzius
CRISPR	Clustered Regularly Interspaced Short Palindromic Repeats
CSF	Cerebrospinal Fluid
DAPI	4′,6-diamidino-2-phenylindole
Dll1	Delta like canonical Notch ligand 1
E(X)	Embryonic day (x)
ECM	Extracellular Matrix
F	Foward
GABA	γ-aminobutyric-acid
GEF	Guanine nucleotide exchange factor
GFAP	Glial Fibrillary Acidic Protein
GFP	Green Fluorescent Protein
GLAST	Glial High Affinity Glutamate Transporter
gRNA	Guide RNA
ICD	Intracellular domain
INM	Interkinetic Nuclear Migration
ISVZ	Inner Subventricular Zone
IPCs	Intermediate Progenitor Cells
IZ	Intermediate Zone

LC-MS	Liquid chromatography–Mass Spectrometry
LGE	Lateral Ganglionic Eminences
MGE	Medial Ganglionic Eminences
Ms	Mouse
MS	Mass Spectrometry
MUNCs	Mammalian Uncoordinated proteins
MZ	Marginal Zone
NBT	Nitroblue Tetrazolium
NCx	Neocortex
NE	Neuroepithelium
NECs	Neuroepithelial Cells
NeuN	Neuronal Nuclei protein
NeuroD2	Neuronal Differentiation 2 protein
NNE	Non neural ectoderm
NPC	Nuclear Pore Complex
Nup	Nucleoporin
OB	Olfactory bulb
OSVZ	Outer Subventricular Zone
ONM	Outer Nuclear Membrane
INM	Inner Nuclear Membrane
Par3	Partitioning defective 3
Pax6	Paired box 6
PFC	Prefrontal cortex
PH3	Phospho-Histone 3
POA	Preoptic Area
qPCR	quantitative Polymerase Chain Reaction
R	Reverse
Robo1	Roundabout guidance receptor 1
Robo2	Roundabout guidance receptor 2
SAPs	Subapical Progenitors
scRNA seq	single cell RNA sequencing
Shh	Sonic hedgehog
Sn	Snake
s/rGAPs	Slit/Robo GTPase activating proteins

SVZ	Subventricular Zone
Tbr2	T-box transcription factor 2
Tuj1	Neuron-specific class III beta-tubulin
VZ	Ventricular Zone
Wnt	Wingless/ Integrated
WT	Wild Type

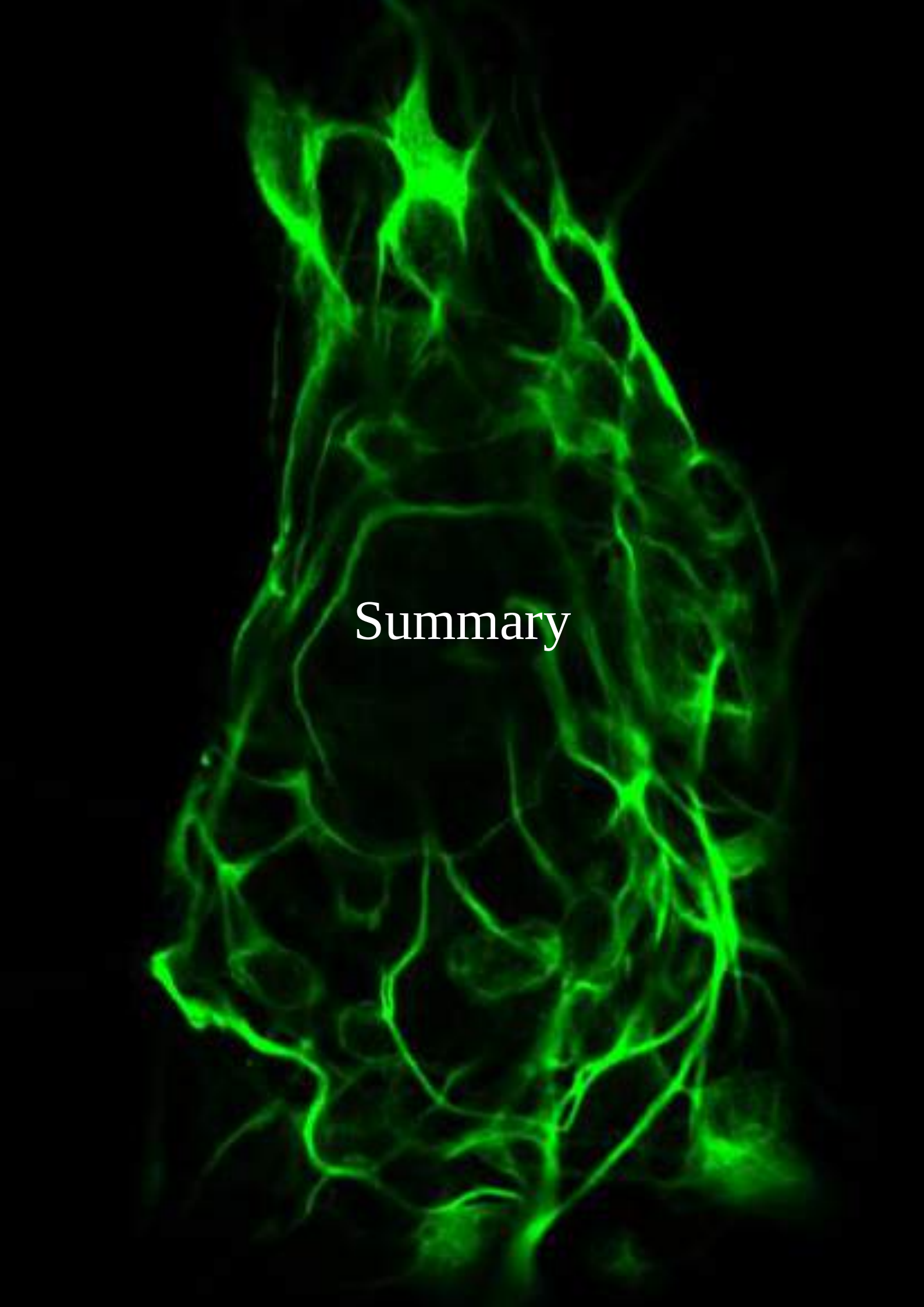
Summary

Summary

The size and degree of folding of the mammalian cortex are pivotal factors that affect species' cognitive abilities and sensorimotor skills. The cerebral cortex is the main region in the mammalian brain that governs complex cognitive behaviors. The development of the cortex depends on the amplification of neural stem cells (NSCs), neural progenitors (NPs) and the generation and differentiation of postmitotic neurons. There are two main types of NPs in the mouse neocortex (NCx): apical radial glia (aRGCs) and intermediate progenitor cells (IPCs). Robo receptors play an important role in regulating the amplification of cortical progenitors. The absence of Robo receptor signalling plus the alteration of the Notch signalling pathway in the mouse NCx leads to an overproduction of poorly functional IPCs. Ancient amniotic cortices exhibit a predominance of direct neurogenesis during development, where aRGCs produce neurons directly. Intriguingly, Robo receptors as well as Notch signalling play a major role in attenuating the mode of neurogenesis. This hypothesis was validated in several brain structures with phyletic antiquity, confirming that Robo receptors are essential in the shift towards indirect neurogenesis during the evolution and expansion of the cerebral cortex. However, little is known about the precise signalling cascade or interactors employed by Robo to initiate direct neurogenesis. In this thesis, we demonstrated the transcriptomic differences between the developing mouse NCx and OB (where direct neurogenesis is predominant in the OB vs NCx) using single cell RNA sequencing (scRNA). We showed aRGCs populations that are differently enriched between these regions. We traced lineage trajectories of indirect and direct neurogenesis, as well as validating the expression of several differentially expressed genes between the two regions.

We used Robo intracellular domain (ICD)—this region is considered a constitutively active form of Robo receptor—and demonstrated the protein interactors that bind it. Following that, we demonstrated Robo ICD localization to the nucleus. We discovered that Robo conserved cytoplasmic domains play an important role in Robo ICD nucleocytoplasmic localization and direct neurogenesis induction in the mouse NCx. Next, we showed that Robo ICD localizes to chromatin, and causes transcriptional changes that occur upon the experimental gain of function of Robo ICD in the NCx and *in vitro*. Additionally, we showed that loss of function of Nup107, a nuclear pore complex (NPC) protein and one of Robo ICD protein interactors, induces direct neurogenesis in mouse NCx and chick lateral pallium. Taken together, our

findings suggest the transcriptional role Robo ICD exerts by binding DNA and, consequently, its conserved role in moderating direct neurogenesis.

Resumen

El tamaño y el grado de plegamiento de la corteza cerebral son factores fundamentales que afectan a las capacidades cognitivas y habilidades sensoriomotoras de los mamíferos. La corteza cerebral es la principal región del cerebro que gobierna conductas cognitivas complejas. El desarrollo de la corteza depende de la amplificación de células madre neurales (CMN), progenitores neurales (PN) y de la generación y diferenciación de neuronas postmitóticas. Hay dos tipos principales de PN en la neocorteza o neocórtex (NCx) del ratón: las células de glía radial apical (CGRa) y las células progenitoras intermedias (CPI). Los receptores Robo juegan un papel importante en la regulación de la amplificación de los progenitores corticales. La ausencia de señalización del receptor Robo sumada a la alteración de la vía de señalización de Notch en el NCx de ratón conduce a una sobreproducción de CPI poco funcionales. La corteza de especies amniotas anteriores en la evolución a los mamíferos (como los reptiles y las aves) exhiben un predominio de neurogénesis directa durante el desarrollo, por el cual las CGRa producen neuronas directamente. Curiosamente, los receptores Robo, así como la señalización de Notch, desempeñan un papel importante en la atenuación de esta modalidad de neurogénesis a lo largo de la evolución. Esta hipótesis ha sido validada en varias estructuras cerebrales con antigüedad filética, confirmando que los receptores Robo son esenciales en el cambio hacia la neurogénesis indirecta durante la evolución y la consecuente expansión de la corteza cerebral. Sin embargo, se sabe poco sobre la cascada de señalización de Robo, así como de los mensajeros secundarios empleados por este receptor para iniciar el proceso de neurogénesis directa. En esta tesis, demostramos las diferencias transcriptómicas que existen entre el NCx y el bulbo olfatorio (BO) de ratón en desarrollo (sabiendo que la neurogénesis directa es predominante en BO frente al NCx). Para ello usamos la técnica de secuenciación de ARN de células individuales (single-cell RNA sequencing (scRNAseq) en inglés). Mostramos que hay poblaciones de RGCa que están diferentemente enriquecidas entre estas regiones. Trazamos trayectorias de linaje de neurogénesis indirecta y directa y validamos la expresión de varios genes expresados diferencialmente entre las dos regiones.

Utilizamos el dominio intracelular (DIC) de Robo (esta región se considera una forma constitutivamente activa del receptor) y demostramos los mensajeros secundarios que se unen. Después, demostramos la localización del DIC de Robo en el núcleo. Descubrimos que sus dominios citoplasmáticos, muy conservados a lo largo de la evolución, tienen un papel importante en la localización núcleo-citoplasmática del DIC y la inducción directa de

neurogénesis en el NCx de ratón. A continuación, mostramos que una vez en el núcleo, el DIC se une a la cromatina y provoca cambios transcripcionales que tienen como resultado una la ganancia de función de Robo tanto en el NCx como *in vitro*. Además, demostramos que la pérdida de función de Nup107, una proteína que forma parte del complejo del poro nuclear (CPN) además de ser una proteína de interacción del DIC de Robo, induce neurogénesis directa en el NCx de ratón y en el palio lateral de pollo. En conjunto, nuestros resultados sugieren el papel de modulación transcripcional que ejerce el DIC de Robo al unirse al ADN y, en consecuencia, su rol conservado a lo largo de la evolución en la disminución de la neurogénesis directa.

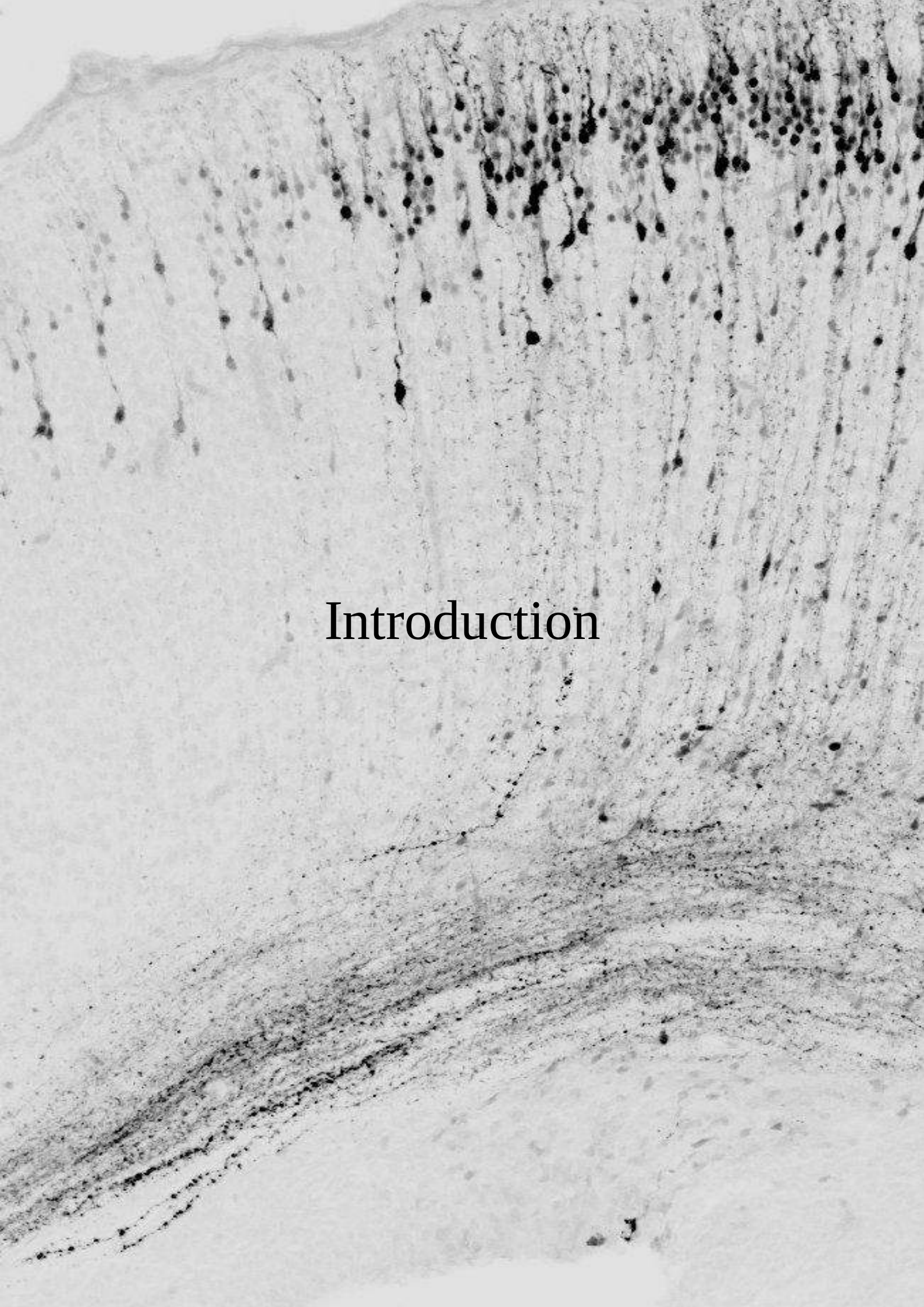

Introduction

1. Introduction

The human brain is an immensely complex organ composed of billions of precisely interconnected neurons. The increase in both size and complexity of the brain, and in particular of the prefrontal cortex (PFC), defines humans more than any other evolutionary event (Bystron et al., 2008; Cadwell et al., 2019; Hill & Walsh, 2005; Kostovic & Rakic, 1990; Stepniewska et al., 2007). The human cerebral cortex is generally considered the most complex organ. It is the structure that we hold responsible for the repertoires of behaviour distinguishing us from our closest living and extinct relatives (Molnár & Pollen, 2014).

The awareness of physical and social circumstances, the ability to have thoughts and feelings (emotions), to be sexually attracted to others, to express our thoughts to our fellow humans through language, and to store such information in memories, certainly rank among the most intriguing functions of the human brain. Given their importance in daily life—and for human culture generally— it is not surprising that much of the human brain is devoted to these and other complex mental functions (Purves et al., 2019). The cerebral cortex constitutes half the volume of the human brain and is presumed to be responsible for the neuronal computations underlying complex phenomena such as perception, thought, language, attention, episodic memory, and voluntary movement (Purves et al., 2019).

The cerebral cortex is derived from the dorsal telencephalon, also known as the pallium, which has classically been divided into medial, dorsal, and lateroventral areas. The neocortex has undertaken a disproportionate number of changes and grown in size relative to other brain regions during evolution, implying that anatomical, cellular, and molecular changes in the cerebral cortex may have occurred in tandem with human cognition (Silver et al., 2020).

Importantly, the human cerebral cortex's extraordinary size and organizational-functional complexity emerge from an extraordinary and complex developmental process. This process involves the massive proliferation of a significant number of neural stem cells, which produce a multitude of neurons and glial cells in the mature cerebral cortex. Furthermore, as new cortical neurons are born, they must migrate away from their birth site to their final location near the brain's surface, a critical process governed by very strict genetic regulation (Llinares-Benadero & Borrell, 2019; Ross & Walsh, 2001; Sidman & Rakic, 1973). Perturbation of any one of these steps commonly results in significant changes in size, shape and organizational anomalies, leading to severe learning deficits, cognitive disability and intractable

epilepsy(Barkovich et al., 2012; De Juan Romero & Borrell, 2015). These major changes in size and composition of the human cerebral cortex arise from early changes in progenitor behaviour during development. This leaves us with many fundamental questions, whether unique developmental processes are the cause for the changes in size and function. What are the molecular cascades and cellular processes that affect this cerebral cortex development?

2. Ontogeny of the cerebral cortex

The embryonic process of neurulation establishes the base for the development of the central nervous system (Betts et al., 2013). The ectoderm is in charge of the vast majority of CNS development. It subspecializes to form the neural plate. The neural plate folds and closes into itself, becoming the neural tube, which extends rostro-caudally. The closure of the neural tube is accompanied by its disproportionate expansion in the anterior part, generating a series of constriction marks that set boundaries between the major primordia of different brain regions: the forebrain, midbrain, and hindbrain. Further on in development, additional constrictions arise transversally subdividing brain regions (**Fig. 1**) (Rubenstein et al., 1998; Vaage, 1969).

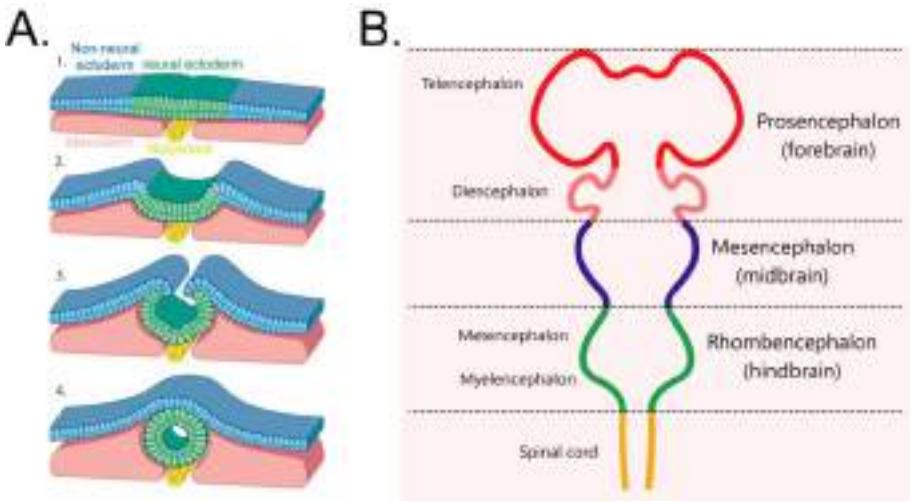

Figure 1. Early embryonic development of the nervous system. (A) (1–4) Schematic transverse sections that illustrate the neural ectoderm folding inwards to form a neural tube. (1) flat neural plate stage, (2) hinge-point formation and neural-fold elevation, (3) apposition of the neural folds with the neural ectoderm covered by the non-neural ectoderm (NNE), and the (4) meeting and remodelling of the neural ectoderm and NNE to form a closed neural tube covered by a single layer of NNE. (B) Regionalization of the neural tube, the top portion is subdivided and forms the three primary brain

vesicles: the prosencephalon (forebrain), the mesencephalon (midbrain), and the rhombencephalon (hindbrain). These primary vesicles then give rise to the five secondary brain vesicles: Telencephalon, Diencephalon, Mesencephalon, Metencephalon, and Myelencephalon (Adapted from Purves et al., 2019).

2.1. Prosomeric model

The prosomeric model states that the prosencephalon (forebrain) is subdivided into two distinct regions: the telencephalonand diencephalon. The telencephalon and the diencephalon are separated by histological and gene expression landmarks. The more caudal portion of the prosencephalon contains a rostrocaudal sequence of the presumptive preoptic, optic, hypothalamic, and posterior tuberculum areas, each of which crosses the midline. On the other hand, areas fated to become part of the eminentia thalami, ventral thalamus, dorsal thalamus, pretectum, and alar plate of the midbrain, hindbrain, and spinal cord form a similar rostrocaudal sequence at the lateral part of the neural plate. Thereon, the rostral prosencephalon becomes the telencephalon, formed of two bilaterally symmetric telencephalic vesicles that include pallial and subpallial regions. The pallium will give rise to the rudiments of the cerebral cortex and hippocampus, while the subpallial territory gives rise to the basal ganglia (derived from embryonic structures called the ganglionic eminences), basal forebrain nuclei, and the olfactory bulb (Purves et al., 2019; Rubenstein et al., 1998).

2.2. Phylogenetic origin of the cortex

The embryonic telencephalon develops from the forebrain's most anterior part. The cerebral cortex develops from further subdivisions of the dorsal part or pallium, which is subdivided according to its structure and function into three distinct territories: the medial archicortex, the lateral paleocortex, and in between them the neocortex, the largest region (**Fig. 2**). The neocortex is an evolutionary novel acquisition that stemmed from the phylogenetically ancient archicortex and paleocortex, and accounts for the overall increase in brain size and contributes to the increase in complexity in recently evolved species (Krubitzer & Kaas, 2005; Manuel et al., 2015; O'Leary et al., 2007).

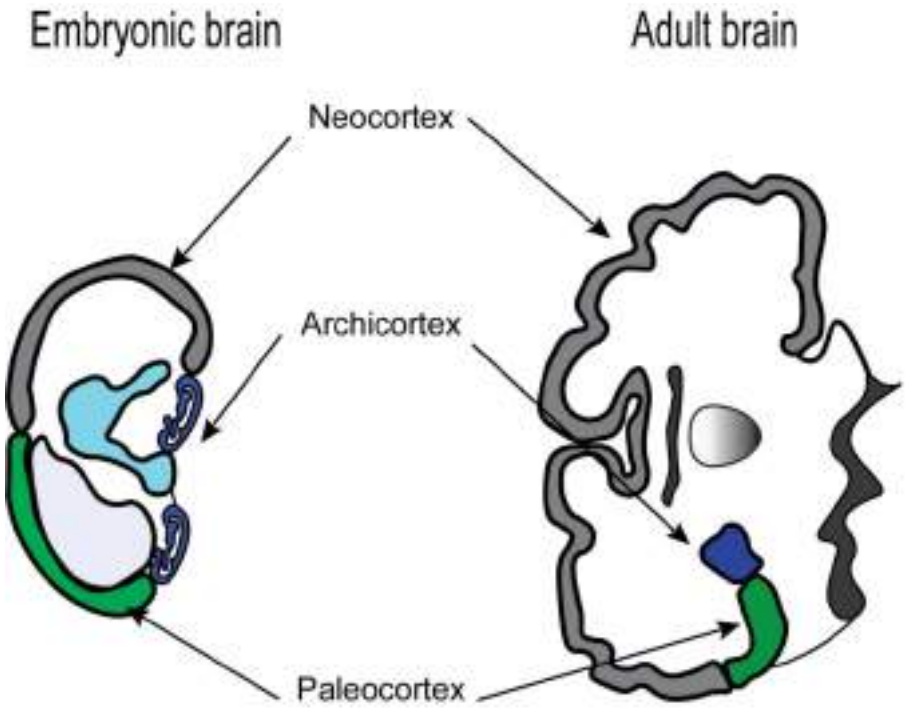

Figure 2. Embryological development of the cerebral cortex. On the left the embryo schema and on the right the developed brain. The paleocortex is the oldest portion of the hemisphere. It forms the floor of the cerebral hemisphere and corresponds with the olfactory cortex and the olfactory bulb. The archicortex curls up to form the hippocampus. The neocortex is the largest area and forms the outer aspect of the cerebral cortex (Adapted from Salatino, 2014).

2.2.1. Archicortex

The archicortex is a phylogentically ancient cortex comprised of the entorhinal cortex, retrosplenial cortex, the subiculum and hippocampus (Manuel et al., 2015). In mammals, the hippocampal formation is composed of 4 subregions (the dentate gyrus, the hippocampus, subiculum and entorhinal cortex). The hippocampus processes sensory and other neural information, interacts with storage areas to consolidate long-term memories, and plays an indirect role in cognition (Insausti, 1993; Insausti & Amaral, 2003).

2.2.2. Paleocortex

The paleocortex (olfactory piriform cortex) is also an ancient cortical area where olfactory fibers project. Generally, it is formed by three layers and is found on the ventral surface of the cerebral hemispheres. Given its physical contact with the ventral telencephalon, adjacent to the lateral ganglionic eminence (LGE), during development and its striatal derivatives in maturity, the paleocortex is considered to be a linking structure between the ventral and dorsal telencephalon (Manuel et al., 2015; O'Leary et al., 2007; Purves et al., 2019).

2.2.3. Neocortex

The neocortex covers the bulk of the cerebral hemispheres.It represents 80% of the brain mass in humans and is the largest region of the cerebral cortex.The neocortex is organized in the radial dimension into neuronal layers that are further divided into sublayers (Garey, 1999). Cortical folding is one of the anatomical features that correlate with complex behaviour, such as language and the ability to create and use tools and technology, and that distinguishes humans from other species (Geschwind & Rakic, 2013; Molnár, 2011). Relative to non-human primates, Humans have a higher brain-to-body ratio, which means they have more neurons and a greater degree of brain lateralization (Lewitus et al., 2013; Sousa et al., 2017), and a complex pattern of gyri and sulci (Borrell & Götz, 2014). Furthermore, these cortical features develop in humans over a longer gestational period and an extended adolescent period that lasts until the third decade of life (Petanjek et al., 2011).

3. Organization of the cerebral cortex

3.1. Cytoarchitecture

The neocortex in all species, including humans has two distinct characteristics: it is a cellular sheet composed of projection (or pyramidal) and local circuit neurons (or interneurons) deployed in layers horizontally, and in columns vertically (radially). The cortical column is the basic functional unit of the cortex, which is formed by an array of neurons that extends vertically, perpendicular to the pial surface, with all 6 cellular layers are present in each column (Mountcastle, 1997; Rakic, 2007). Neurons occupying the same column are interconnected in the vertical dimension and share extrinsic connectivity and dynamic cortical operations (Eccles, 1981). Cortical expansion in evolution occurred mainly due to an expansion of the cortical surface area. This expansion results from an increase in the number of cortical columns, and is accompanied by degrees of variability in the laminar appearance of the cortex, the cellular composition and packing of each layer, myelination, and interconnections between adjacent areas. This variability is particularly pronounced in more evolved cortices and depends on the function of that region (Fatterpekar et al., 2002; Kandel et al., 2000; Kornack & Rakic, 1995).

During corticogenesis, neurons are born in an orderly fashion from stem cells and migrate radially to their final position in the same order. The earliest generated neurons end up occupying the deepest layers, and the latest to be born end up located in the most superficial layers. This inside-out sequence is achieved because neurons migrate radially past those previously generated, before they stop (Fatterpekar et al., 2002; Kandel et al., 2000;

Mountcastle, 1997; Purves et al., 2019; Sidman & Rakic, 1973; Torii et al., 2009). Once radial migration is complete, the neocortex is composed of six layers of cells (**Fig. 3**):

Layer I: is the Molecular Layer (Plexiform Layer), a sparsely cellular lamina due to the scarcity of cell bodies, instead full of dendrites and axons from neurons in deeper layers.

Layer II: is also called the External Granular Cell Layer. It consists primarily of closely packed granule cells with a small pyramidal morphology.

Layer III: is also called the External Pyramidal Cell Layer. It is mainly composed of large pyramidal cells with scattered non pyramidal cells. Neurons located deep in layer III are typically larger than those located more superficially. Frequently, neurons of layers II and III are considered together (II/III), as they both project their axons to other cortical regions and receive intracortical afferents.

Layer IV: the Internal Granular Cell layer is usually the narrowest of the cortical layers and contains densely packed stellate cells and a variety of granule cells. It is subdivided into a supragranular portion (IVA) and a deep infragranular portion (IVB) that is permeated by a very dense horizontal plexus of myelinated fibers, forming the external band of Baillarger. This layer is the main target of thalamic afferents but also receives intracortical connections.

Layer V: The Internal Pyramidal Cell layer, contains large pyramidal cells and scattered non-pyramidal cells. The superficial portion (Va) contains scattered pyramidal cells, whereas the deep portion (Vb) contains both pyramidal cells and a horizontal plexus of myelinated fibers designated the internal band of Baillarger. The internal band of Baillarger (layer Vb) is much thinner than layer IVB, forms a less densely interconnected plexus of myelinated fibers.

Layer VI: The Multiform Layer (Fusiform or Pleomorphic Layer) is relatively thin and compact, composed of spindle-shaped cells infused with fiber bundles. It forms the deeper limit of the cortex and contains axons to and from the cortex. Neurons in layer V project their axons to layers II/III and V, whereas neurons in layer VI project to layer IV.

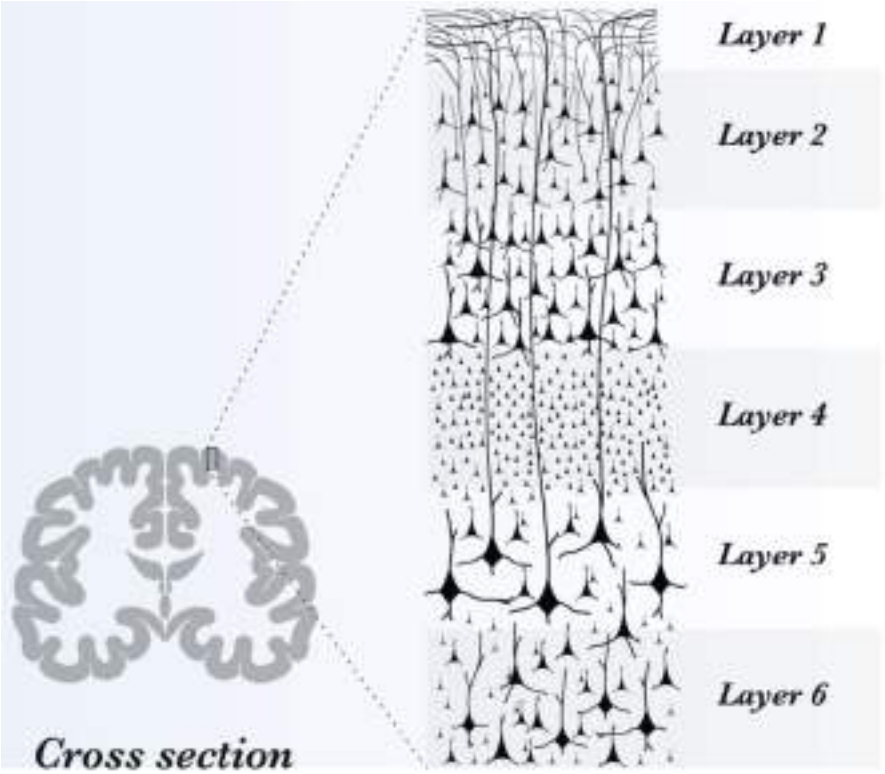

Figure 3. A general scheme of cortical layering. Cross section showing the six layered cortex (adapted from Mai & Paxinos, 2011).

3.2. Cellular composition of the neocortex

The neocortex comprises hundreds of neuronal cell types and a diverse number of glia cell types. In mammals, each functional cortical column contains two main classes of neurons: inhibitory (GABAergic) interneurons, which make local connections and receive extrinsic input, and excitatory projection (glutamatergic) neurons, which extend axons to farther intracortical, subcortical, and subcerebral regions (Molyneaux et al., 2007; Rakic, 2007).

3.2.1. Excitatory neurons

Excitatory neurons are spiny pyramidal neurons that use glutamate as their main neurotransmitter (glutamatergic). Pyramidal cells are long-axon cells that are located in all layers except layers I. These cells are very abundant in all cortical areas, approximately accounting for 70-85% of the total population of neurons (DeFelipe & Fariñas, 1992). Pyramidal neurons relay information between different areas of the neocortex or to other areas of the brain. During development, they arise from progenitors in the neocortical germinal zones, located in the apical region of the dorsolateral wall of the telencephalon.

Pyramidal neurons are quite heterogeneous, distinguished into multiple subpopulations depending on their location in different cortical layers and areas, morphological features, expression of transcription factors, and function. The complexity and diversity of projection neuron subtypes make their classification complex, but the most accurate classification system is based on a combination of morphology, electrophysiological properties, and patterns of gene expression, in addition to their axonal projections (DeFelipe & Fariñas, 1992; Molyneaux et al., 2007).

3.2.2. Inhibitory neurons

Cortical inhibitory interneurons represent a small percentage (20-30%) of the total population of neurons (Sultan & Shi, 2018). They use γ-aminobutyric acid as neurotransmitter, which is thought to be the cerebral cortex's primary inhibitory neurotransmitter (Flames et al., 2007; Gelman & Marín, 2010; Llorca & Marín, 2021). They also mediate the precise gating of information through specific signalling pathways, representing fundamental modulatory and integrative elements for cortical function (Llorca & Marín, 2021). The majority of interneurons arise from progenitors in the ventral telencephalon (subpallium), mainly in the medial ganglionic eminence (MGE), the caudal ganglionic eminence (CGE), and the preoptic area (POA), from where they migrate long distances to their final destination in the neocortex. A small population is produced in the lateral ganglionic eminence and septal area, contributing to the formation of the olfactory bulb (Gelman & Marín, 2010; Molyneaux et al., 2007).

GABAergic interneurons exhibit a variety of morphological, physiological, molecular, and synaptic characteristics. Despite these differences, interneurons share similar characteristics that allow their classification into specific subtypes. Interestingly, the expression of calcium binding proteins such as parvalbumin (PV), calbindin (CB), or calretinin (CR), as well as neuropeptides such as somatostatin (SST), vasoactive intestinal peptide (VIP), neuropeptide Y (NPY), or cholecystokinin (CCK), is used to classify different subtypes of interneurons in the neocortex (Flames et al., 2007).

3.2.3. Cajal Retzius cells

The third and categorically smallest portion of cortical neurons are Cajal-Retzius cells (CR). Since very early in development, CR cells have populated Layer I, covering the entire cortex. CR cells express Reelin, a large molecule known for its role in regulating radial migration and the establishment of appropriate cortical layering, as well as influencing progenitor cell behaviour. CR cells are glutamatergic and are mainly generated from the cortical hem, in addition to other regions outside the neocortex, mainly the subpallium-pallium boundary and the septum (Bar et al., 2000; Molyneaux et al., 2007; Soriano & Del Río, 2005; Taverna et al., 2014).

3.2.4. Glial cells

The term "glia" comes from the Greek word "glue." In the mature brain, there are three types of glia: astrocytes, oligodendrocytes, and microglia. Glia cells maintain the ionic medium of nerve cells, modulate the rate of nerve firing, and regulate synaptic propagation by controlling neurotransmitter uptake, in addition to acting as a scaffold for some neurodevelopmental events (Jäkel & Dimou, 2017).

Astrocytes: represent the most highly abundant type of glial cells in the brain. They are generated at late stages of cortical development. Astrocytes have a star like appearance. Astrocytes maintain water and ion homeostasis, participate in the formation of tripartite synapse and maintain the integrity of the blood brain barrier (BBB) (Jäkel & Dimou, 2017; Purves et al., 2019).

Oligodendrocytes: they are restricted to the central nervous system (CNS). During development, oligodendrocytes are generated in the ventral telencephalon, and then migrate tangentially to cortex. Oligodendrocytes form myelin sheaths along the length of axons. Myelin is necessary for saltatory nerve impulse conduction, which is very apparent in multiple sclerosis where chronic demyelination and oligodendrocyte loss contributes to axonal dystrophy and neurodegeneration (Bradl & Lassmann, 2010).

Microglia: these are the immune and phagocytic cells of the brain. They originate from yolk-sac progenitors that are in the brain only during development. Similar to astrocytes, microglia cells respond rapidly to any injury and extend cellular processes or migrate to the lesion site, participating in scar formation (Jäkel & Dimou, 2017; Silver, 2016).

4. Development of the neocortex

4.1. Neocortex germinal layers

4.1.1. The ventricular zone

The cortex is primarily made up of a primary germinal or ventricular zone (VZ), which contains the primary type of cortical progenitor cells and is bounded by the lateral telencephalic ventricle. Neuroepithelial cells (NECs) form the ventricular zone (VZ) during early neurogenesis and are responsible for the lateral expansion of the neocortex. Early on, Neuroepithelial stem cells (NECs) occupy the VZ, followed by apical Radial Glia Cells (aRGCs) and subapical Radial Glia. These are the primary type of cortical progenitor cells, generating neurons and Intermediate Progenitor Cells (IPCs), which go on to constitute the Subventricular Zone (SVZ) (**Fig. 4**)(Arai & Taverna, 2017).

4.1.2. Subventricular Zone (SVZ)

The subventricular zone (SVZ), a mitotically active transient compartment, is considered a significant source of cortical projection neurons as well as glial cells and possibly some interneuron subpopulations.The SVZ is populated by newborn neurons, IPCs and basal RGCs (bRGCs). The SVZ also contains radial and tangential fibers, including crossing axons. As neurogenesis progresses, IPCs residing in the SVZ undergo terminal symmetric division, producing neurons that are destined to populate the upper cortical layers. The significant enlargement of SVZ and upper neuronal layers across mammalian phylogeny strongly suggests the evolutionary role of IPCs in cortical expansion (Arnold et al., 2008; Kelava et al., 2012; Rash & Grove, 2006; Smart, 2002). The enlargement of the SVZ in gyrencephalic species like humans and monkeys due to the abundance of bRGCs and IPCs results in the subdivision of the SVZ into an inner SVZ (ISVZ) and an outer SVZ (OSVZ) (**Fig. 4**).

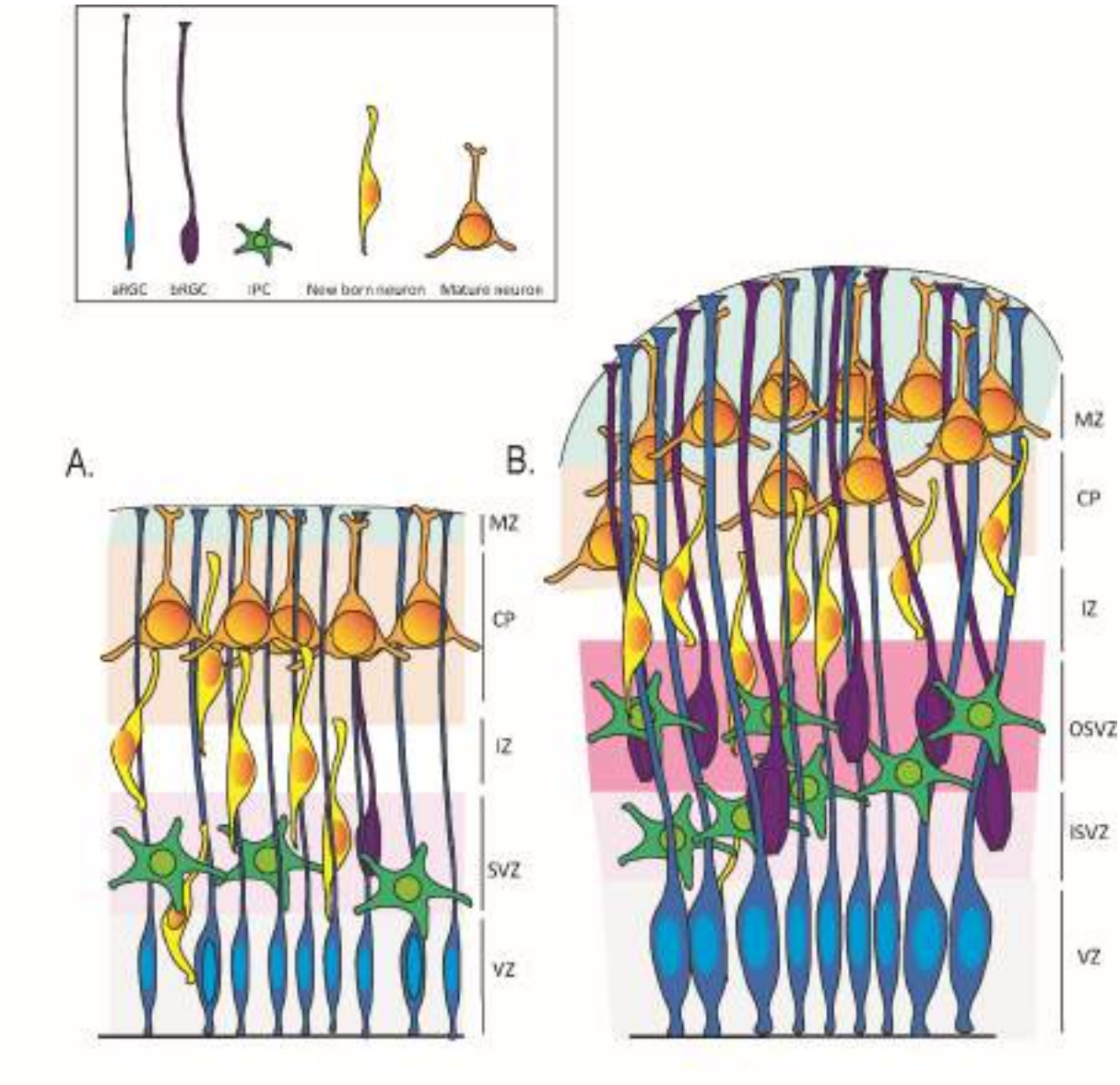

Figure 4. Neocortex germinal layers. (A) Lisencephalic species have few bRGCs (purple) and neurons (blue) that migrate parallel to aRGCs (green) radial fibers to their targeted layers. (B) Gryencephalic species have more bRGCs, which increases the number of radial fibers thereby diverging the entire scaffold and expanding the cortical surface (adapted from Borrell & Götz, 2014).

4.2. Neural progenitor cell types

Progenitor cells in the developing neocortex are classified according to their different location of mitosis (apical, basal), apico-basal polarity, and capacity for proliferation. The three principal types of neural progenitors in the developing neocortex are apical, subapical, basal progenitors.

4.2.1. Apical progenitors

4.2.1.1. Neuroepithelial stem cells (NECs)

All neurons in the neocortex originally derive from NECs. NECs constitute the pseudo-stratified neuroepithelium monolayer that constitutes the early neural tube mentioned previously. NECs exhibit strong apico-basal polarity, extending along the entire thickness of the neural tube by contacting the apical surface and the basal membrane. Adherens junctions (AJs) and tight junctions are located in the apical end of NECs lateral to the plasma membrane. AJs are necessary to maintain the apico-basal polarity of NECs. Knocking out AJs disturbs the organisation of these cells (De Juan Romero & Borrell, 2015; Götz & Huttner, 2005). Initially, NECs undergo symmetric division, expanding their population and ultimately aiding the lateral and radial growth of the neocortical primordium. Later on, NECs transform into aRGCs (Florio & Huttner, 2014; Götz & Huttner, 2005).

4.2.1.2. Apical Radial Glia Cells (aRGCs)

Prior to the initiation of neurogenesis, NECs start acquiring astroglial markers and become aRGCs (**Fig. 5**). aRGCs continue to express NECs markers such as Pax6 and Nestin, aRGCS also express apical hallmarks such as Prominin-1, Par3/Par6/aPKC, β-catenin, and N-cadherin. Although aRGCs suppress the expression of tight junction proteins, this has no effect on AJ proteins like ZO1. aRGCs characteristically exhibit a primary cilium, an organelle that protrudes from the apical plasma membrane into the ventricular lumen. It serves as a sensor for molecular signals in the cerebrospinal spinal fluid (CSF), activating different signalling pathways, including Shh, Wnt, and IGF (Taverna et al., 2014). Interestingly, the polarity of aRGCs is reflected on the distribution of its cellular components. aRGCs' centromere and Golgi apparatus are located apically, away from the basal process. It's worth mentioning that apical-basal polarity plays a role in prompting symmetric versus asymmetric division, which is defined by equal versus unequal distribution of cellular components to daughter cells. However, it's not the only determining factor controlling fate determination (Taverna et al., 2014). These newly generated cells accumulate across the apical surface of the cortex, forming the VZ, while the basal process of the aRGCs, usually referred to as radial glial fiber, crosses all layers until reaching the vicinity of the basement membrane (Fernández et al., 2016; Florio & Huttner, 2014; Namba & Huttner, 2017). The basal end of the apical process of aRGCS is anchored to the basement membrane, which is rich in extracellular matrix molecules and G-protein coupled receptors. These molecules act as signalling molecules between the basement membrane and RGCs (Amin & Borrell, 2020; K. R. Long & Huttner, 2019). Originally, the basal process was thought to only act as a scaffold for newly born migrating neurons, but recent studies demonstrated that it has a

critical role in fate specification and signalling (De Juan Romero & Borrell, 2015; K. R. Long & Huttner, 2019; Taverna et al., 2014)

Similar to NECs, aRGCs undergo symmetric self-proliferating divisions or asymmetric differentiating divisions. Interestingly, in contrast to NECs, as neurogenesis proceeds, aRGCs switch from symmetric self-amplifying divisions, to asymmetric divisions generating one aRGC plus a different type of cell, a basal progenitor (most frequently) or a neuron (Fernández et al., 2016).

4.2.1.3. Apical Intermediate Progenitors

Apical intermediate progenitors (aIPs) ─previously known as short neuron precursors─ are a small population of progenitors that occupy the VZ (**Fig. 5**). These cells exhibit apico-basal polarity, but unlike aRGCs their basal process resides in the VZ. aIPs downregulate astroglial markers like BLBP and GLAST and lack the expression of t-box brain protein 2 (TBR2), but they are integrated in AJs, express PAX6 and undergo apical division, similar to aRGCs. aIPs are highly neurogenic, and they divide symmetrically producing two neurons, augmenting the neuronal output achieved by apical mitoses (Gao et al., 2014).

4.2.2. Subapical Progenitors

Subapical progenitors (SAPs) are located in abventricular position within the VZ (**Fig. 5**). They possess an apical process that extends to VZ even during mitosis. SAPs divide in the basal portion of the VZ, and express the astroglial markers Pax6 and/or Tbr2. These cells may undergo several rounds of division, and they have relatively low abundance in the embryonic mouse cortex (Pilz et al., 2013).

4.2.3. Basal progenitors

Basal progenitors are classified into two types: intermediate progenitors cells (IPCs) and basal Radial Glia Cells (bRGCs). They are generated from NECs, aRGCs, or basal progenitors themselves.

4.2.3.1. Intermediate Progenitors cells

Intermediate Progenitors Cells (IPCs) are non-epithelial cells generated from aRGCs. After birth, they downregulate Pax6 and start expressing Tbr2, detach from AJs in the VZ, retract their apical process, lose their apico-basal polarity, and migrate basally to the SVZ, where

they undergo mitosis. This prompt retraction of the apical process is critical for cell cycle progression (Borrell & Reillo, 2012; Noctor et al., 2004, 2008). Once IPCs are located in the SVZ, they may undergo one or more rounds of proliferative symmetric divisions, which serve to amplify their numbers. In lissencephalic species, IPCs mostly undergo self-consuming neurogenic divisions, producing two daughter neurons. But in gyrencephalic species, IPCs in ISVZ and OSVZ frequently undergo self-amplification in parallel with, or before, producing neurons (Fietz et al., 2010; Haubensak et al., 2004; Miyata et al., 2004).

4.2.3.2. Basal Radial Glia Cells (bRGCs)

bRGCs were originally described in the developing cortex of humans and ferrets, and later in rodents (Florio & Huttner, 2014; Kelava et al., 2012). bRGCs are also known as outer, or translocating, RGCs, and were also previously referred to as intermediate radial glia (**Fig. 5**). bRGCs share some morphological features with aRGCs, particularly a basal process that extends to the basement membrane, thus maintaining a high apico-basal polarity. Unlike aRGCs, bRGCs lack an apical process because they don't contact the VZ. Hence, bRGCs lack contact with apical AJs and signals from the CSF (Florio & Huttner, 2014; Namba & Huttner, 2017).

bRGCs express molecular markers typical of RGCs like Pax6, Tbr2, GFAP (in primates), and phosphorylated vimentin, a very useful marker to characterise bRGCs by identifying the basal radial fiber during mitosis. Long ex-vivo videomicroscopy analyses of the developing cerebral cortex have demonstrated that the morphology of bRGCs is extremely diverse and dynamic in the OSVZ of primates (Dehay et al., 2015). Beyond the classical features of bRGC (basal process during mitosis), there are other morphotypes of bRGCs: those with an apical and a basal process (bipolar bRGC), and bRGC that have only an apical process during mitosis. In the mouse cortex, bRGCs have an extremely low abundance, and mostly generate neurons through symmetric self-consuming divisions. The relevance of bRGCs in mouse cortical development remains unclear, but in species with large and folded cortices, bRGCs undergo symmetric proliferative divisions generating two daughter bRGCs, thus amplifying the basal progenitor pool, or neurogenic asymmetric divisions generating one bIP or a neuron (Hansen et al., 2010; Reillo et al., 2011).

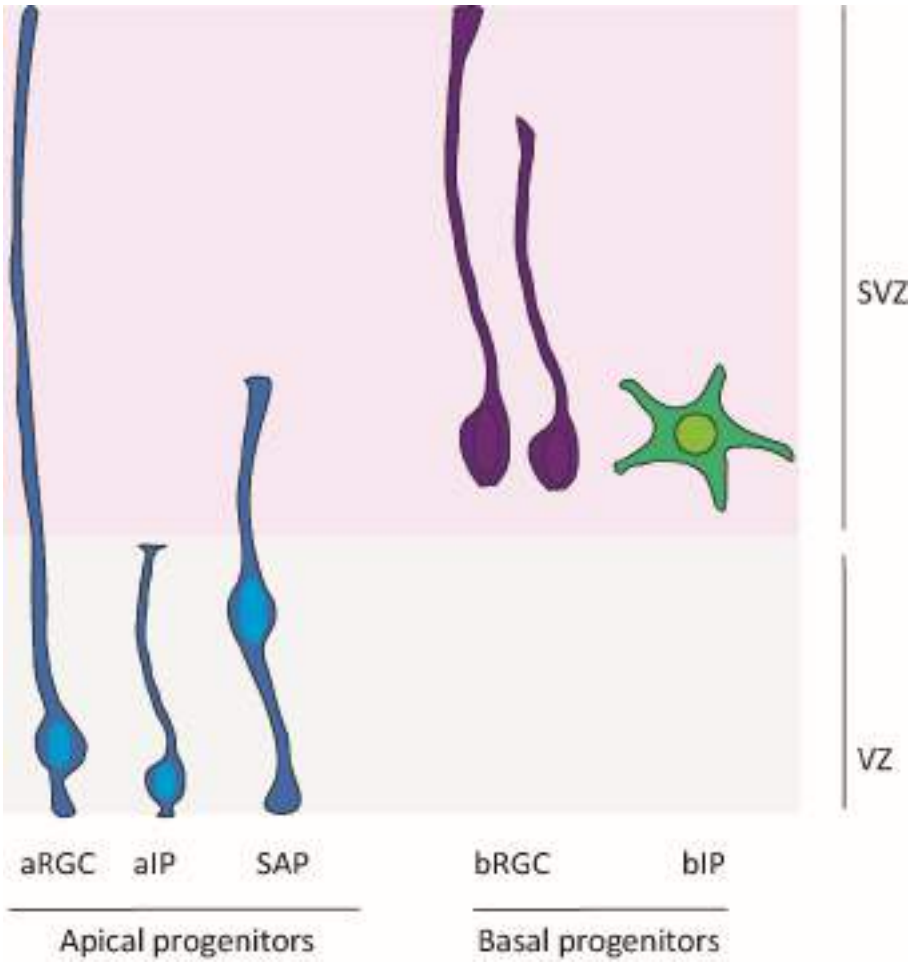

Figure 5. Neural progenitor cell types in the developing cortex. Apical progenitors entail apical radial glia cells (aRGCs), apical intermediate progenitors (aIPs), and subapical progenitors (SAPs); all of these progenitors undergo mitosis in the ventricular plane, with the exception of SAPs, which undergo mitosis in an abventricular location while remaining in contact with the ventricular zone. Basal progenitors, that include basal radial glia cells (bRGCs) and basal intermediate progenitors (bIPs), divide in the abventricular region and have no contact with other cells (adapted from Florio & Huttner, 2014).

4.4. Overview of dynamics of cortical neurogenesis and development

The mouse cerebral cortex arises from the telencephalic pseudostratified neuroepithelium. It's lined by a uniform monolayer of neuroepithelial cells (NECs) that emerges at mid-embryogenesis forming the telencephalic vesicles (Borrell & Reillo, 2012). NECs divide symmetrically self-amplifying and generating two identical daughter cells, therefore increasing the surface area of the telencephalic neuroepithelium and providing an adequate pool of progenitor cells (A. Kriegstein et al., 2006). At mid-gestation between embryonic days 8 and 9, the first wave of neurons is born, marking the beginning of neurogenesis. With

the initiation of neurogenesis, NECs begin expressing glial markers such as GLAST and BLBP, and acquire their Radial Glial Cell (RGC) identity. Apical RGCs (aRGCs) constitute the main proliferative region of the cerebral cortex: the VZ (De Juan Romero & Borrell, 2015). All cerebral glutamatergic neurons are produced by aRGCs, either directly or indirectly via Intermediate Progenitor Cells (IPCs) (De Juan Romero & Borrell, 2015; Noctor et al., 2002). They also contribute to producing the two main macroglial cell types: astrocytes and oligodendrocytes (Kriegstein & Alvarez-Buylla, 2009).

During the early period of corticogenesis, aRGCs mainly self-amplify through symmetric division, expanding their own pool. Progressively, they go on to divide asymmetrically, producing one daughter aRGC and one neuron, or IPC. Ultimately, at late stages of neurogenesis, aRGCs undergo a final self-consuming symmetric division producing two non-RGC cells. aRGCs produce neurons either directly (direct neurogenesis) or indirectly via IPCs (indirect neurogenesis). This underlines the probability that undergoing each type of division is dependent on the developmental stage. Direct neurogenesis occurs less frequently in mice even at early stages, compared to birds and reptiles (Attardo et al., 2008; Cárdenas & Borrell, 2019; De Juan Romero & Borrell, 2015; Haubensak et al., 2004; Kowalczyk et al., 2009). Indirect neurogenesis is a two-step process where IPCs amplify the neuronal yield of RGCs, and is characteristic of the mammalian neocortex.

As corticogenesis procedes, IPCs ―the second prevalent type of progenitors in the cortex― start appearing. IPCs are non-epithelial progenitor cells that are produced by aRGCS on the apical surface of the VZ and migrate basally to form the SVZ. Mouse IPCs in the SVZ undergo symmetric neurogenic divisions to generate two neurons (Kriegstein et al., 2006; Kriegstein & Noctor, 2004), hence multiplying the neuronal yield produced by aRGCs. After E12.5, the majority of neurons forming all cortical layers are produced from IPCs (Kowalczyk et al., 2009; Kriegstein et al., 2006; Noctor et al., 2004). This continues until later stages of corticogenesis, when aRGCs begin to produce large number of neurons directly (Fernández et al., 2016).

In the majority of gyrencephalic species, whether primates or non-primates, the SVZ is enlarged and contains an abundant number of progenitors, unlike in lissencephalic species. This enlargement leads to the creation of two distinct sublayers: ISVZ and OSVZ (Borrell & Reillo, 2012; Fietz et al., 2010). These subdivisions of the SVZ are absent in the mouse cortex (Stahl et al., 2013). The emergence of the OSVZ in the cortex of gyrencephalic species and its

abundant numbers of self-amplifying progenitors are considered to play major roles during the evolution and expansion of gyrencephalic brains (Fernández et al., 2016; Nonaka-Kinoshita et al., 2013). The OSVZ plays a major role during cortical neurogenesis by producing the majority of supragranular neurons (Arai & Pierani, 2014). Moreover, they add a large number of radial glia fibers to the pre-existing scaffold, thus driving the tangential dispersion of radially migrating cortical neurons in gyrencephalic brains (Reillo et al., 2011).

At the onset of neurogenesis, the first cohorts of neurons form the preplate (PP). Later-generated cortical neurons migrate into the PP, splitting it into two parts: the marginal zone (outside) and the subplate (inside) (**Fig. 6**). These later-generated neurons thus begin forming the cortical plate, which eventually will give rise to most of the grey matter. Newly generated cortical neurons migrate radially using radial glia fibers as a scaffold (Dehay & Kennedy, 2007; Fernández et al., 2016). The laminar fate of postmitotic neurons is a birthdate dependant-mechanism, where the earliest born neurons form deep layers and later born neurons form superficial cortical layers. Therefore each newly generated was of neurons bypasses previously generated neurons. Therefore, cortical layers are from deep to superficial with exception of layer I (**Fig. 6**) (Manuel et al., 2015). While glutamatergic projection neurons are generated in the cortex, GABAergic interneurons arise from multiple germinal regions of the subpallial telencephalon, mainly from the MGE. GABAergic interneurons are produced over a long period of embryogenesis. In mice, they are generated from E12.5 (**Fig. 6**) until birth. Olfactory interneurons are generated from birth throughout adult life (Batista-Brito et al., 2008).

At the end of neurogenesis around E16.5-E17.5 (**Fig. 6**) (Caviness et al., 2003; Jiang & Nardelli, 2016a; Nomura & Hanashima, 2014), the majority of aRGCs in the VZ transform into astrocytes, but they also begin producing macroglial cells: astrocytes and oligodendrocytes, which lose their attachment to the VZ and migrate toward the cortical plate. The switch of aRGCs from generating neurons to glia is controlled by complex neuron-glial interactions in addition to spatiotemporal, intrinsic, and extrinsic factors (Jiang & Nardelli, 2016b; Kriegstein & Götz, 2003; Kriegstein & Alvarez-Buylla, 2009).

The generation of astrocytes and oligodendrocytes is maximal during the first postnatal month in mice, and they will maintain mitotic activity throughout life (Jiang and Nardelli, 2015). During early postnatal and adult mammalian brains, neurogenesis continues primarily in the

SVZ of the lateral ventricle, providing neurons to the olfactory bulb and the hippocampal dentate gyrus (Alvarez-Buylla & Garcıa-Verdugo, 2002).

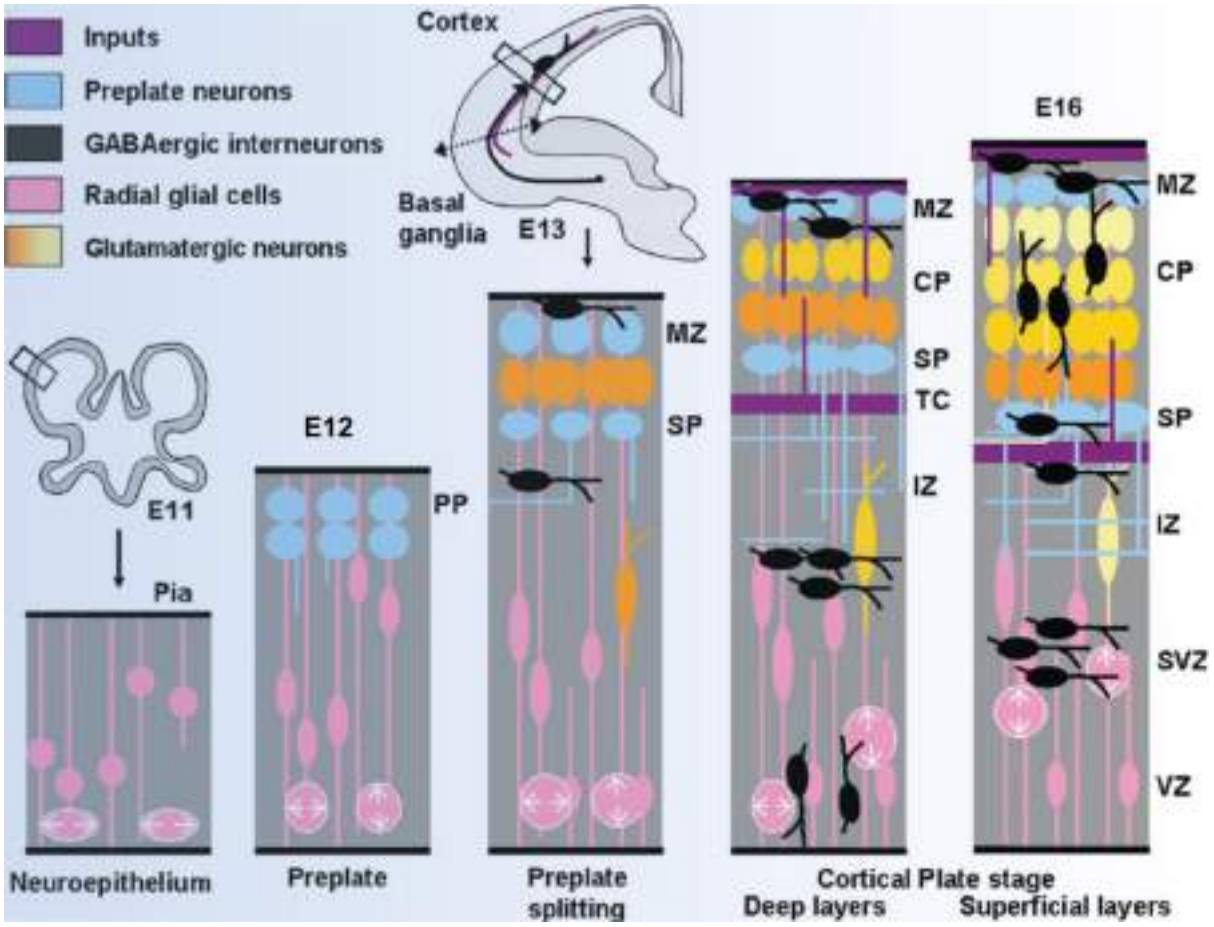

Figure 6. A schematic representation showing cortical development. Migrating interneurons from subcortical areas are shown in purple and black. Cortical development begins with the formation of the VZ at E11. Once neurogenesis starts and neurons migrate to the pial surface and complete their differentiation in the cortical plate. Deep layer neurons are generated and migrate earlier, while neurons that are going to occupy superficial layers are formed later. At E12-E13, the cortex is bilaminar where it's formed of VZ and a primitive preplate. At E17-E18 the thickness of the cortex increases due to the exiting of neurons from their cell cycles and migrating to their destined cortical layer. CP, cortical plate; IZ, intermediate zone; MZ, marginal zone; PP, preplate; SP, subplate; TC, thalamocortical axons; SVZ, subventricular zone (adapted from Vitalis & Rossier, 2011).

4.5. Modes of division in cortical progenitors

Cortical progenitors have two modes of division: symmetric and asymmetric. Either mode of division can result in a proliferative or a consumptive division. There are four types of divisions: symmetric proliferative, symmetric consumptive, asymmetric proliferative and asymmetric consumptive.

Symmetric proliferative division produces two identical daughter cells. This mode of division is a key factor in progenitor pool size determination. This is evolutionary significant,

especially in the BPs, where they have gained a greater proliferative capacity in gyrencephalic species compared to lissencephalic species. bIPs and bRGCs in gryencephalic species possess a high self-proliferative capacity that increases the progenitor pool remarkably in gyrencephalic species compared to lissencephac species (Betizeau et al., 2013; Betizeau & Dehay, 2016; Hansen et al., 2010; Reillo et al., 2011). On the other hand, an asymmetric consumptive division occurs when a progenitor divides, producing two neurons, this division occurs in bIPs in primates and occurs rarely in mice and ferrets (Gertz & Kriegstein, 2015; Haubensak et al., 2004; Miyata et al., 2004).

Asymmetric proliferative division occurs when one progenitor cell divides to give rise to one identical daughter progenitor cell and another different cell type. A standard example of asymmetric proliferative division is aRGC dividing to generate a daughter aRGC and a neuron or a BP (bIP, bRGC). In asymmetric consumptive division, progenitors divide, producing two different cell types, like in aRGCs that divide, producing a neuron and a BP (bIP or bRGC).

The asymmetric inheritance of specific cellular components causes adaptation to an asymmetric mode of division. This is possibly explained by the polarised distribution of cellular components prior to mitosis in the mother progenitor (Knoblich, 2001; Lancaster & Knoblich, 2012). Some neurodevelopmental disorders are caused by premature switching between different modes of division. In microcephaly (a human disease characterised by a smaller brain size at birth), APs switch from symmetric proliferative division to asymmetric division and from asymmetric proliferative division to asymmetric consumptive division prematurely (Fish et al., 2006, 2008).

5. Transcription factors in corticogenesis

During cortical neurogenesis, the differentiation and proliferation of progenitor cells is regulated by a number of transcription factors (TFs). These TFs are important in determining the composition of neuronal subtypes, cortical thickness, and cortical surface area. Expression of TFs is regulated via extrinsic and intrinsic signals (Sindhu et al., 2012). Some TFs are used as markers of specific progenitor and neuronal subtypes. TFs regulate the expression of downstream genes by binding to DNA, and thus they can modulate a repertoire of processes ranging from mitotic activity to cell fate determination and differentiation (Eguchi et al., 2014).

TFs involved in modulating corticogenesis belong to superfamilies that regulate tissue and organ development throughout the embryo: homeodomain, paireddomain, Basic helix–loop–helix (bHLH), winged helix, nuclear orphan receptor, Ets, zinc finger, and T-domain families. TFs featured in corticogenesis are expressed in specific patterns depending on the region, area, gradient zone, and layer. These patterns are usually correlated with their specific functions. For example, Tbr1 (a T-box TF) is expressed in the IZ and CP, where postmitotic neurons reside, and is involved in regulating neuronal and cortical layer specification (Sindhu et al., 2012). TF expression gradients during cortical development are correlated with progenitor proliferation and differentiation via direct and indirect neurogenesis.

Prior to the onset of neurogenesis, TF function is primarily to regulate forebrain regionalization and area patterning, suppress neuronal differentiation, and promote progenitor proliferation. Forebrain regionalization refers to the establishment of boundaries in the embryonic cortex separating the dorsal telencephalon from the ventral telencephalon (Subcortical regions). Among the TFs involved in forebrain regionalization are: Pax6 (paired homeodomain TF), Ngn1, Ngn2 (bHLH TFs), Emx1, Emx2 (homeodomain TFs) (Muzio et al., 2002; Scardigli et al., 2003; Schuurmans & Guillemot, 2002) (**Fig. 7**). Each of the previous TFs plays a role in neurogenesis and regional patterning, which is the subdivision of the cortex into specialized motor, visual, sensory and auditory regions. This regionalization depends on the rosto-caudal and mediolateral expression gradients of these TFs.

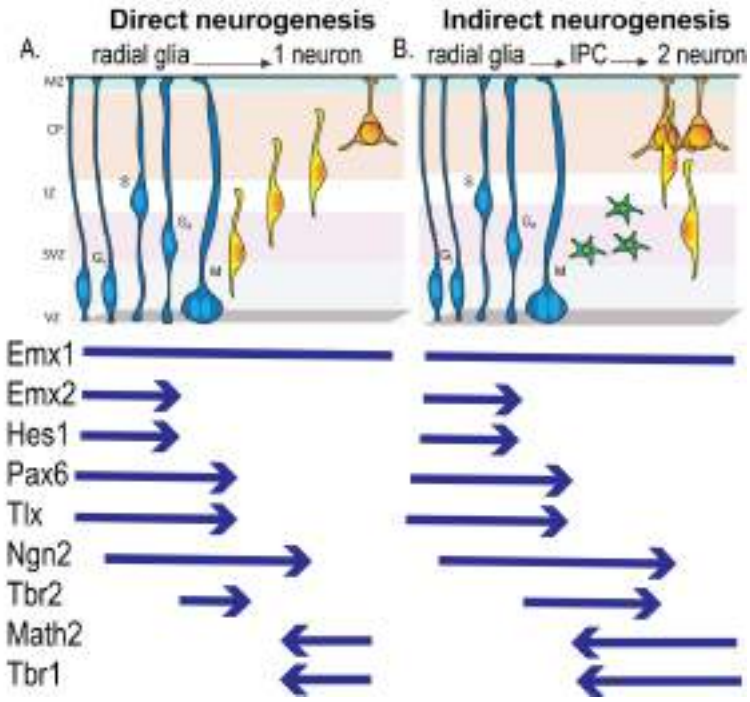

Figure 7. Cortical neurogenesis via direct and indirect pathways is correlated to transcription factor expression. (A) Direct neurogenesis Self-replicating aRGC divide in the VZ, producing one neuron that migrates radially to the CP. (B) indirect neurogenesis aRGC divide in the VZ to self-replicate and produce an IPC. The IPC migrates into the SVZ or remains in the basal VZ, where it divides to produce two or more neurons that migrate radially to the CP. Transcription factors indicated below are expressed through the differentiation sequence of progenitors. Emx1 and Emx2 are expressed throughout cortical neurogenesis, while the latter promotes symmetric proliferation. Hes1 is expressed in the VZ only, suppressing neuronal differentiation. Pax6 is expressed in progenitors and is downregulated in IPC and new born neurons. Tlx is expressed in the VZ, it prevents precocious differentiation. Ngn2 is expressed in subtypes of progenitors that are supposed to be neurogenic, in addition to some immature neurons. Tbr2 is expressed in IPCs and in preplate neurons. Math2 and Tbr1 are expressed in postmitotic neurons mainly in the IZ and cortical plate (adapted from Vaid & Huttner, 2020).

6. Transcription factor expression sequence during corticogenesis

Once neurogenesis commences, Pax6 is expressed by aRGCs in the VZ. When IPCs are born from aRGCs, they downregulate Pax6 and begin expressing Tbr2, which is important in regulating IPC production and, later, neuronal maturation. NeuroD is also expressed in some IPCs that are mainly located in the SVZ (J. K. Lee et al., 2000). As IPCs mature and approach the transition to neurons, they start expressing low levels of NeuN (Neuron Nuclei). Newborn neurons begin downregulating Tbr2 and start expressing Tbr1 as they migrate through the IZ and subplate, until reaching the CP and MZ (Englund et al., 2005; Hevner, 2006). Tbr1 is expressed at its highest level in newborn glutamatergic cortical neurons. Hence, these patterns of TFs outline a sequence of TF expression during cortical neurogenesis, where RGCs express Pax6, IPCs express Tbr2 and newly born glutamatergic neurons express Tbr1 (Englund et al.,

2005; Hevner, 2006). This sequence of TFs expression is conserved in areas where glutamatergic neurons are produced, including the cerebral cortex, hippocampus, cerebellum, and olfactory bulb (Imamura et al., 2011).

7. Signalling pathways and cortical neurogenesis

Cortical progenitors are influenced by numerous extrinsic and intrinsic factors during development. Among these factors are signalling pathways triggered by receptor proteins at the plasma membrane. The Notch, Wnt, Shh, and Fgf pathways are among the most important signalling pathways influencing neurogenesis and proliferation in the developing cerebral cortex.

7.1. Fibroblast growth factor (Fgf) signalling

The mammalian fibroblast growth factor (Fgf) family consists of 22 polypeptides that range in length from 150 to 300 amino acids in humans and are divided into seven subfamilies based on sequence phylogeny (T. Iwata & Hevner, 2009). They play a major role in forebrain patterning, in addition to regional specification, proliferation, differentiation, and survival (Borello et al., 2008; Hébert, 2011). Fgf binds to their cognate tyrosine kinase receptors (Fgfr 1 to 4) activating downstream signalling pathways such as: mitogen-activated protein kinase (MapK), Protein kinase B (Pkb)/Akt, Phospholipase Cγ (PLCγ), and Rac-Cdc42-Rho pathways. Several FGFs have major roles in cortical development, mainly in NECs' transition to RGCs. For example, Fgf receptor 2 (Fgfr2) promotes premature acquisition of the NECs-RGCs transition (Sahara & O'Leary, 2009). Fgf10 overexpression increases radial glial markers in developing mouse cortex, whereas Fgf10 mutant mice have an extended period of NE proliferation and a delayed onset of neurogenesis (Kang et al., 2009). Fgf plays a role in regulating the transition of RGCs to BPs. Fgf ligand regulate maturation of cortical progenitors by regulating the duration of cell cycle. The duration of the cycle and especially G1 phase duration are increased, when progenitors enter neurogenic divisions (Calegari et al., 2005). Fgf2 maintains progenitors in a self-replicating mode by controlling their cell cycle length. Fgf2 upregulates the expression of Cyclin D1 and inhibits the cyclin dependent kinase inhibitor P27, shortening the G1 phase and decreasing the percentage of neurogenic divisions (Lukaszewicz et al., 2002; Raballo et al., 2000).

7.2. Wnt signalling

Wnt proteins are secreted glycoproteins that interact with two distinct receptor families: the Frizzled (Fz or Fzd) receptors and the LDL receptor-related proteins 5 and 6 (LRP5 and LRP6). The formation of Wnt-Fz-LRP6 complex and the recruitment of dishevelled (Dvl) result in the recruitment of Axin to the complex. Activation of this complex inhibits Axin-mediated β- catenin phosphorylation, which leads to the accumulation of stabilized β-catenin and transportation to the nucleus, where it forms a complex with TCF/LEF, activating Wnt pathway target genes. Loss- and gain-of-function studies of Wnt pathway components implicate them in promoting proliferation and self-amplification of RGCs (Chenn & Walsh, 2002; Machon et al., 2003; Woodhead et al., 2006). Moreover, studies at later stages show the role of the Wnt pathway in promoting the transition of RGCs to BPs, and promoting their proliferation via N-myc and the proneural gene Neurogenin 1 (Ngn1). On the other hand, there are studies suggesting the role of Wnt signalling in the neural differentiation of BPs (Munji et al., 2011). Given these data, it should be taken in to account that all these studies were performed manipulating β-catenin, which also plays a role in cell adhesion, implying that all these phenotypes might not only dependant on Wnt signalling (MacDonald et al., 2009).

7.3. Sonic hedgehog (Shh) pathway

The Shh signalling pathway has important roles in CNS development in vertebrates, including pattern formation, cell fate specification, axon guidance, proliferation, survival, and differentiation of neurons. Malfunction of Shh signalling is the cause of many nervous system diseases. This pathway is activated via Shh ligand binding to the Patched receptor. This is followed by the accumulation of Smoothened and activation of the TF Gli, which regulates downstream gene transcription by either activation or repression (Paridaen & Huttner, 2014). Shh is expressed early during telencephalic development around E7.5, before the closure of the neural tube, at the ventral midline of the forebrain. Studies manipulating the levels of Shh or Patched revealed that Shh signalling has a role in regulating the proliferation of cortical progenitors, in RGCs transitioning into IPCs, and affecting IPC proliferation via cell cycle regulation (Shikata et al., 2011).

7.4. Notch pathway

Notch signalling pathway is an evolutionary conserved pathway that controls an extraordinary number of cell fate and developmental processes (Ables et al., 2011; Gaiano & Fishell, 2002; Hori et al., 2013; Mizutani et al., 2007). Notch is a transmembrane receptor, with four

variants in mammals: Notch1 through 4, and several transmembrane ligands: Jagged 1 (Jag1) and Jag2 (homologs of *Drosophila* Serrate), and Delta-like proteins (Dll). These transmembrane ligands bind the transmembrane Notch receptors on neighbouring cells, which initiates a series of cleavage events that end with the γ-secretase-mediated cleavage of the transmembrane domain of Notch, releasing a Notch intercellular domain (NICD) into the cytoplasm. NICD is then trafficked into the cell nucleus, where it binds to the protein complex Recombining Binding Protein Suppressor of hairless, also called CSL or CBF-1 (RBPJ), in addition to other transcriptional activators. This is finally followed by DNA binding and transcriptional activation of target downstream genes.

The Hes family of TFs, particularly Hes1 and Hes5, are the most well-known Notch target genes. These genes encode bHLH proteins that repress proneural bHLH such as Mash1 and Nrg1, resulting in neuronal differentiation suppression in these cells with an activated Notch pathway (Imayoshi et al., 2013; Pierfelice et al., 2011). Importantly, Nrg1 promotes expression of the Notch ligand Dll1, so activation of Notch signalling in a cell will drive its repression of *Dll1* transcription. Daughter cells generated from asymmetric division of RGCs show asymmetric Delta-Notch signalling levels, mirroring the fate that they acquire. According to the downstream effects of Notch activation, daughter cells with high Notch signalling will remain as RGCs, while cells with low Notch signalling will have high expression of Dll1 and proneural genes, initiating neural differentiation (Paridaen & Huttner, 2014). This mechanism where cells inhibit the differentiation of their neighbouring cells is known as lateral inhibition. Widespread absence of Notch signaling results in the premature differentiation of early-born cells, generating a low number and diversity of cell types (Kageyama, Ohtsuka, Shimojo, et al., 2008).

The basics of the Notch lateral inhibition mechanism lead to the expression of Hes1 and Hes5 in some cells and the expression of Dll1 in their neighbours in a stochastic manner. This creates a typical salt and pepper pattern of gene expression that sustains asymmetric division, producing one progenitor cell and one differentiating neuron (Kageyama et al., 2008). In-depth analyses of this signalling system have demonstrated that proneural genes and Notch effector TFs are expressed in an oscillatory manner (i.e, Hes1), proposing that the salt and pepper pattern changes dynamically rather than a subtle initial difference that is nullified by lateral inhibition (Kageyama et al., 2008).

The salt-and-pepper pattern of Notch pathway ligand expression is regulated by negative feedback. Hes1 follows an activation/inhibition cycle of transcription by binding directly to its own promoter, whereas Ngn2 and Dll1 display a negative correlation with Hes1 expression

in neural progenitors. This oscillation of notch pathway between progenitor cells is essential to maintaining a pool of undifferentiated progenitors. When Hes1 expression is low in one cell, Ngn2 and Dll1 expression is high, these expression levels are countered in the lateral cell by activating Notch signalling and upregulating Hes1 expression, which inhibits Ngn2 and Dll1 expression. These oscillations are reversed in approximately in hourly intervals serving the purpose of maintaining progenitors undifferentiated. These oscillations of Hes1 expression highlight that not only the expression but also the dynamics of these genes is important for fate determination. This makes the Notch pathway a context-dependant pathway, highly dependent on the niche and cellular physiology, which ultimately will determine the fate of progenitor cells (Hori et al., 2013; Kageyama, Ohtsuka, Shimojo, et al., 2008; Shimojo et al., 2011).

The onset of Notch signalling in the cerebral cortex coincides with the onset of neurogenesis and the transition of NECs to RGCs, as evidenced by the high expression of Dll1, Hes1, and Hes5. This hypothesis was supported by experiments promoting notch signalling, which prematurely led to a strong induction of RGC markers in progenitors (Gaiano & Fishell, 2002). The Notch signalling pathway has also been implicated in the generation of BPs from RGCs (Mizutani et al., 2007; Ohata et al., 2011). Although Hes genes are canonical regulators of Notch signalling (by regulating the expression of its ligands), other genes such as Cyclin D1, P21 (Cdkn1a), Erbb2, Abcg2, Nfia, the astroglial markers (BLBP, GFAP), and Nepro appear to have an effect on Notch downstream signalling to inhibit neurogenesis, early during cortical development (Pierfelice et al., 2011).

7.5. The effects of mitochondrial genes and energy processes on neurogenesis

Mitochondria are cellular organelles that are the powerhouse of the cell, have emerged as key players in progenitor fate determination. Generally, mitochondria are known for their role in ATP generation, which is used as cell fuel; however, mitochondria regulate a range of functions, from metabolic and redox signalling to nuclear gene expression and epigenetic functions (Chandel, 2014). Interestingly, mitochondrial regulatory functions are context-dependant, varying between different cell types such as cancer cells, progenitor cells, and postmitotic (differentiated) cells. Recent studies have revealed that mitochondria play a dynamic role in neural development. The differentiation of NSCs to enter the neurogenic lineage is accompanied by a shift in metabolism shift from glycolytic metabolism to mitochondrial oxidative phosphorylation (OXPHOS) (**Fig. 8**) (Khacho & Slack, 2018). This metabolic shift that occurs during neuronal differentiation isn't limited to ATP levels but encompasses cell cycle regulation and appropriate neuronal differentiation. Mitochondria

change morphology depending on the cell type. Recent studies show that in progenitors shortly after dividing, daughter cells committed to progenitor self-renewal undergo mitochondrial fusion, while daughter cells that undergo extensive mitochondrial fission are committed to neuronal fate (Iwata et al., 2020).

These changes in mitochondrial morphology in particular regulate metabolic and reactive oxygen species (ROS) generation. ROS have a direct effect on NSCs commitment to a progenitor fate rather than differentiating. The upregualtion of mitochondrial ROS led to stabilization of NRF2- redox master regulator- that is trafficked to the nucleus and ultimately upregulate differentiation genes and repress genes that regulate self-replication (**Fig. 8**) (Khacho et al., 2019).

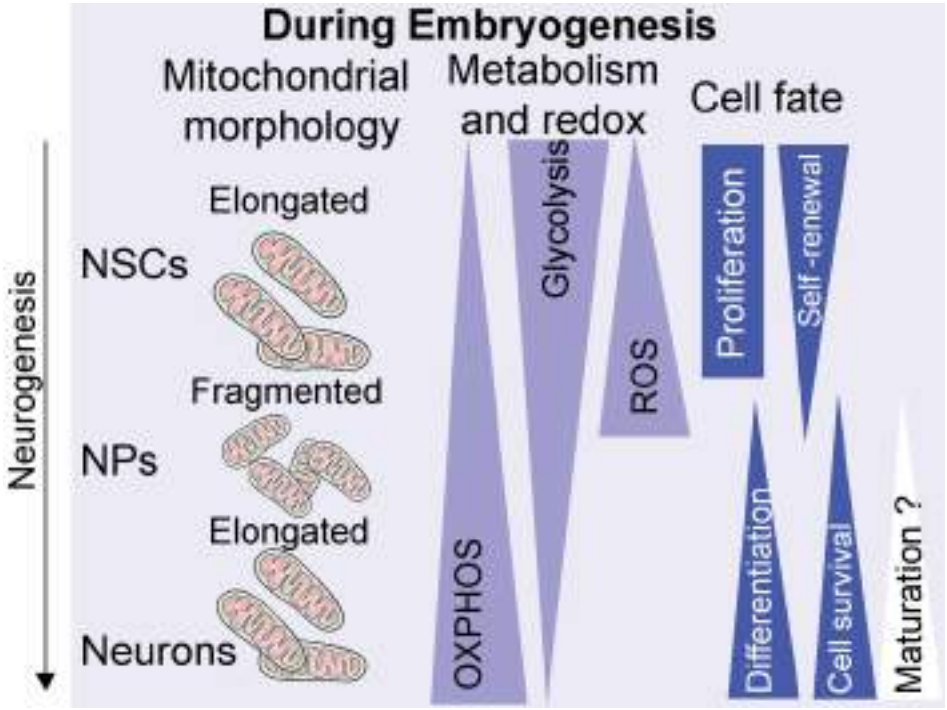

Figure 8. Mitochondria structure and neurogenesis. Schematic representation showing the changes that occur in mitochondria shape and metabolism during embryonic neurogenesis. During embryonic neurogenesis, cells progress from neural stem cells (NSCs) passing neural progenitors (NPs) and to neurons. During the NPs phase mitochondria become fragmented then elongated upon differentiation to neurons. During differentiation, NSCs and NPs start to depend less on glycolysis and more on oxidative phosphorylation (OXPHOS). Reactive oxygen species (ROS) production occurs during the transition from NSCs to NPCs (adapted from Khacho et al., 2019).

8. Cell Cycle

Cell cycle length has a major role in neurogenesis. During cortex development, progenitors exiting the cell cycle take either a neurogenic or a gliogenic identity. Mitotic studies of cortical progenitors during corticogenesis show a lengthening in cell cycle length, especially during the G1 phase. This lengthening of the cell cycle coincides with an increase in the proportion of cells exiting the cell cycle during differentiative division. The increased rate of neurogenesis, which peaks in the middle of corticogenesis, is a direct result of the increased production of progenitors at the start of corticogenesis. The slowing of neurogenesis at the end of corticogenesis is caused not only by the cell cycle stopping, but also by the progenitor pool perching. The length of the cell cycle in primates differs from that of rodents in both time and structure. In contrast to rodents, primate VZ progenitors have a different duration of the S and G1 phases; their cell cycle is shorter at mid-corticogenesis due to variations in the length of the S and G1 phases. This variation in S phase duration during corticogenesis appears to be a primate-specific cell cycle feature. Moreover, the length of the cell cycle in primate cortical precursors is significantly longer than in rodents. This lengthening of the cell cycle in primate cortical progenitors is thought to be an evolutionary adaptive feature (Calegari et al., 2005; Calegari & Huttner, 2003; Dehay et al., 2015; Taverna et al., 2014).

8.1. Interkinetic nuclear migration

Interkinetic nuclear migration (INM) is a benchmark phenomenon where the nucleus of NECs and apical progenitors (AP) migrates up and down through the thickness of the VZ during cell cycle, in coordination with the cell cycle phases. Mitosis takes place on the apical surface of the VZ. The nucleus moves to the basal side during G1, where it remains during the S phase, when DNA is synthesised. During G2, the nucleus returns to the apical surface, where mitosis occurs once more. INM is responsible for the appearance of the pseudostratified neuroepithelium of the VZ and is dependent on the mechanical action of Myosin II (**Fig. 9**) (De Juan Romero & Borrell, 2015; Götz & Huttner, 2005; Miyata et al., 2010; A. Reiner et al., 2005; O. Reiner et al., 2012). Why do only apical progenitors undergo INM and mitosis at the apical surface is an unanswered question. One possible explanation is that the primary cilium is located at the apical surface of apical progenitors and contains the centromeres of the apical progenitor, which are required for mitosis. SAPs and BPs, on the other hand, do not undergo INM during cell cycle progression, indicating that INM is restricted to cells with apico-basal polarity. However, nucleokinesis is not limited to APs (Tsai & Gleeson, 2005),

and Myosin II contractility is also important for BPs that undergo nuclear migration after delaminating from the VZ and migrating towards the SVZ. another possible explanation for INM being restricted to APs and followed by mitosis on the apical surface could be that APs contain many polarity cues and are in contact with signalling cues present in the CSF, which could influence the decision of symmetric or asymmetric divisions in daughter cells (Huttner & Kosodo, 2005).

The primary function proposed for INM is to provide the VZ with a pseudostratified appearance (nuclear resistance). INM is a critical step in the proliferation of apical progenitors and the evolution of the cerebral cortex. The nuclear residence hypothesis holds that the fate of apical progenitors is influenced by a variety of factors throughout the apico-basal niche. Notch signalling is one of those well-known factors that prevent progenitors from differentiating. As a result, INM influences proliferating APs' exposure to neurogenic versus proliferating signal (Taverna et al., 2014).

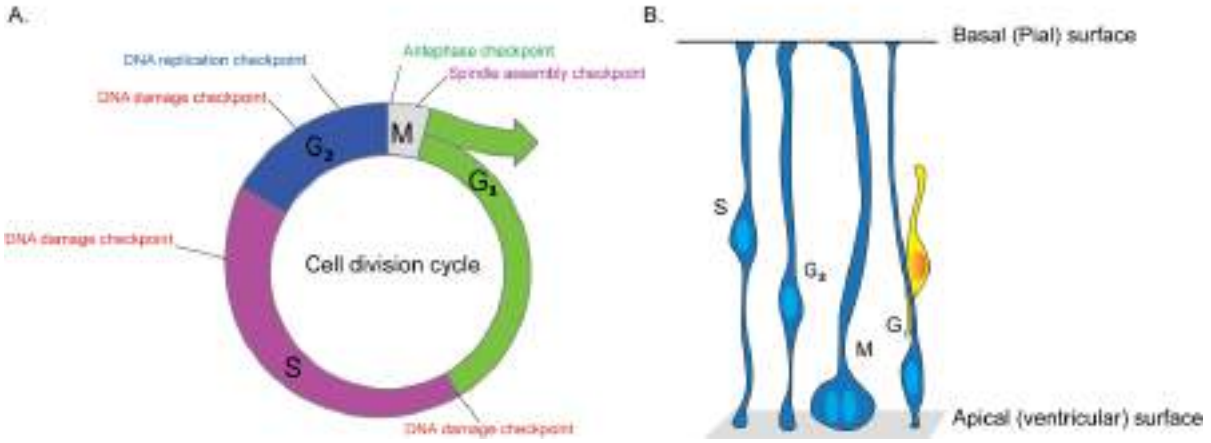

Figure 9. Cell cycle and interkinetic nuclear migration (INM). (A) Cell cycle and checkpoints applied during progenitor replication, where there are checkpoints for DNA damage, proper anaphase, and checkpoints for spindle assembly. (B) A schema representing INM, showing soma dynamics during cell cycle. Progenitors are in blue, and newly born neurons are in yellow (adapted from Arai & Taverna, 2017).

8.2. Mitotic spindle orientation

The mitotic spindle plays a key role in regulating the symmetric and asymmetric modes of division (Taverna et al., 2014). Studies show that manipulating mitotic spindle components (microtubules and centrosomes) has an impact on neurogenesis. Mitotic spindle orientation affects neurogenesis, especially in polarised cells like NECs and aRGCs. In the developing

mouse cortex, aRGCs and NECs have a mitotic spindle largely oriented perpendicularly to the apico-basal axis of the cell, making it in synchrony with apico-basal polarity signals from the apical membrane, basal process, and AJs (Fish et al., 2006; Lancaster & Knoblich, 2012). Horizontal or oblique orientation of the mitotic spindle is accompanied with bRGCs generation in rodents and primates (Gertz & Kriegstein, 2015; Pilz et al., 2013; Shitamukai et al., 2011). Mutation of mitotic spindle proteins is one of the hallmarks of microcephaly. These mutations lead to premature neurogenesis and depletion of the progenitor pool. Studies report that mutations in proteins that are constituents of or interact with, the centrosome like Lis1, mInsc, LGN, Aspm, Cdk5rap2, and MCPH, impair neurogenesis and result in microcephaly or lissencephaly (Taverna et al., 2014).

8.3. Proneural genes and cell cycle

Cell cycle exit is a critical step that precedes neuronal differentiation and neuronal identity determination. Basic helix loop helix (bHLH) genes are transcription factors that play a major role during neurogenesis in the CNS. Proneural genes code typical bHLH transcriptional activators, which bind DNA as active heterodimers with ubiquitously expressed E proteins. bHLH proneural genes promote cell cycle exit via CKIs activation, specifically p27/Kip1 (Farah et al., 2000). Expression of proneural proteins in stem cells is enough to promote cell cycle exit and neuronal fate commitment. Proneural genes expressed in the mouse cerebral cortex include Neurogenin1 (Ngn1), Neurogenin2 (Ngn2), and Mash1 (Fode et al., 2000; Nieto et al., 2001). Ngn2 is the most important proneural gene in cortical development and neurogenesis. Ngn2 promotes Ngn1 expression while suppressing Mash1 expression. Ngn1 and Ngn2 are the proneural genes required in the dorsal telencephalon to determine the glutamatergic identity of cortical neurons as well as the identity of other cortical neurons. Mash1 is required for the identification of GABAergic neurons in the ventral telencephalon. This demonstrates that these two proneural genes are thought to be determinants of two distinct neuronal lineages. (Wilkinson et al., 2013). Proneural genes are critical in activating the expression of the Notch ligand Dll1, as well as other factors important to maintaining the progenitor identity in the neighbouring cell via lateral inhibition (**Fig. 10**).

Progenitor-associated genes have more open chromatin compared to neuronal differentiation-associated genes that require a specific epigenetic remodel before activation. One example is that during the cell cycle, when Cyclin-dependent kinases are active, the hyperphosphorylated form of Ngn2 has less DNA binding affinity, which is sufficient to target progenitor-

associated specific promoters. On the other hand, upon cell cycle lengthening and the reduction of cyclin-dependant kinase activity, Ngn2 phosphorylation decreases, this event is associated with an increase in DNA binding affinity and providing the necessary epigenetic remodelling for activating neuronal differentiation associated genes. As cyclin-dependant kinase expression decreases during the cell cycle, the expression of progenitor genes remains basal, while the expression of differentiation genes increases, promoting differentiation (Hardwick & Philpott, 2014).

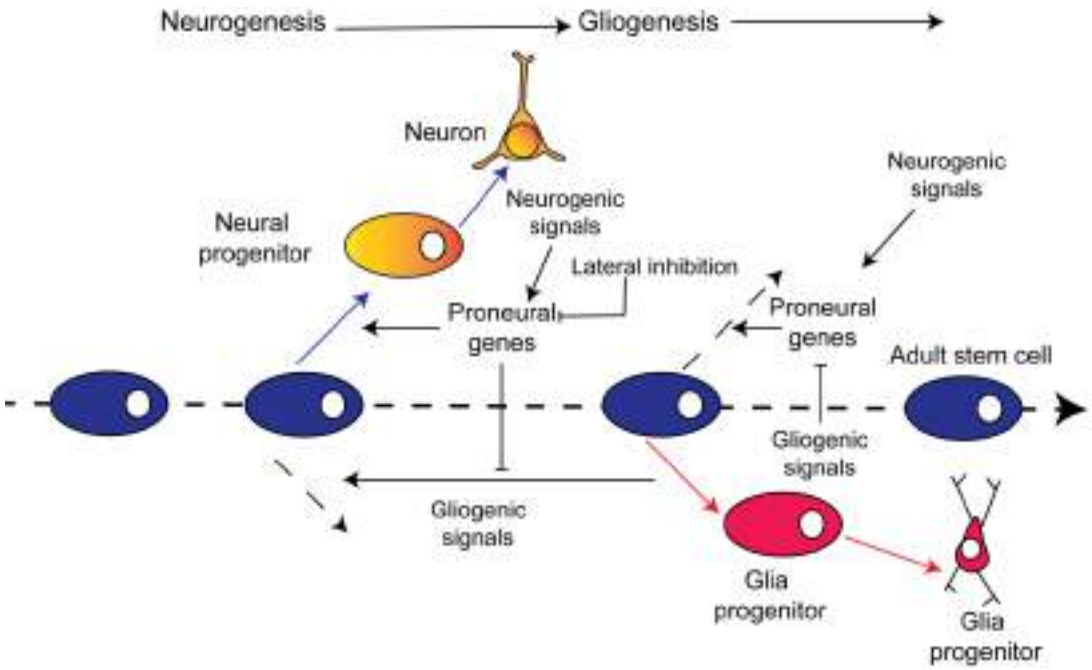

Figure 10. A schematic representation showing the role of proneural genes during neurogenic and gliogenic stages of neural development. Multipotent neural stem cells are able to generate all types of neural cells. First neural stem cells generate neurons, then glia. However, the switch between neurogenesis and gliogenesis is controlled by extrinsic and intrinsic factors. Proneural genes are intrinsic determinants controlling the balance between neurogenesis and gliogenesis in addition to lateral inhibition, where notch signalling inhibits neighbouring cells from neuronal differentiation, thereby maintaining the balance between self-replicating progenitors and progenitors entering neural differentiation (adapted from Bertrand et al., 2002).

8.4. Cell Cycle determinants that directly affect neurogenesis

D-type cyclins are known for their role in regulating the G1 phase. Cyclin Ds activate Cdk4 and Cdk6 promoting the passage of cell cycle checkpoints and commitment to a proliferative fate. Although Cyclin D1 and Cyclin D2 are functionally redundant, Cyclin D2 has an important role in BPs pool expansion during neocortical expansion in gyrencephalic brains, this role can't be compensated by Cyclin D1 (Hardwick et al., 2015) (**Fig. 11**). On the other hand, Cyclin D1 promotes neuronal differentiation. This was shown in spinal cord studies, where overexpressing Cyclin D1 led glia cells to adapt a neurogenic fate. This conflicting

effect of Cyclin D2 and Cyclin D1 is due to the different regulation of Hes genes. Cyclin D1 upregulates Hes 6, and Cyclin D2 upregulates Hes5, a neurogenesis promotor (Panaliappan et al., 2018).

Beside the roles of Cyclins and CDKs, Cell cycle Inhibitors (CKIs) have an important role in regulating the proliferation of neural progenitor cells. CKIs are divided into two classes: the Ink4 family (p15, p16, p18, p19) and the Cip/Kip family (p27, p21, p57). P57-deficient mice display increased proliferation of progenitors during development, which causes a hyperplastic anterior pituitary gland (Bilodeau et al., 2009). Overexpression of P27 and P57 induces premature cell cycle exit in cortical as well as retinal progenitor cells (Tarui et al., 2005; Tury et al., 2011).

P21 (Cdkn1a) protein is considered to be the founding member of CKIs family. It is encoded by the *Cdkn1a* gene and it is controlled transcriptionally by P53 dependent and independent pathways. Its transcription is increased upon various intracellular and extracellular stimuli to arrest the cell cycle and ensure DNA stability. P21 is involved in differentiation, transcription, cell migration, cytoskeleton organization, and apoptosis. Activation of P53—the critical driver of P21 transcription—is followed by cell cycle arrest. It suppresses cell cycle genes by forming a dimerization complex that consists of the RB-like, E2F, and MuvB (DREAM) complexes (Engeland, 2018). Depending on the cell type and niche context, several studies show that P21 can either exert a positive or a negative role on differentiation. P21 promotes differentiation of mouse oligodendrocytes. Moreover, P21 cytoplasmic localization has a positive role in normal cell differentiation, as observed in mature human monocytes and rat neurons by suppressing apoptosis, and stimulating neurite outgrowth (Tanaka et al., 2002).

Overexpression of P21 has been shown to induce differentiation of mouse embryonic stem cells by suppressing Sox2. Nevertheless, maintaining a basal expression of p21 is critical to protect stem cells from exhaustion, while P21 overexpression initiates differentiation and restricts the self-replication capacity of adult stem cells (Kreis et al., 2019).

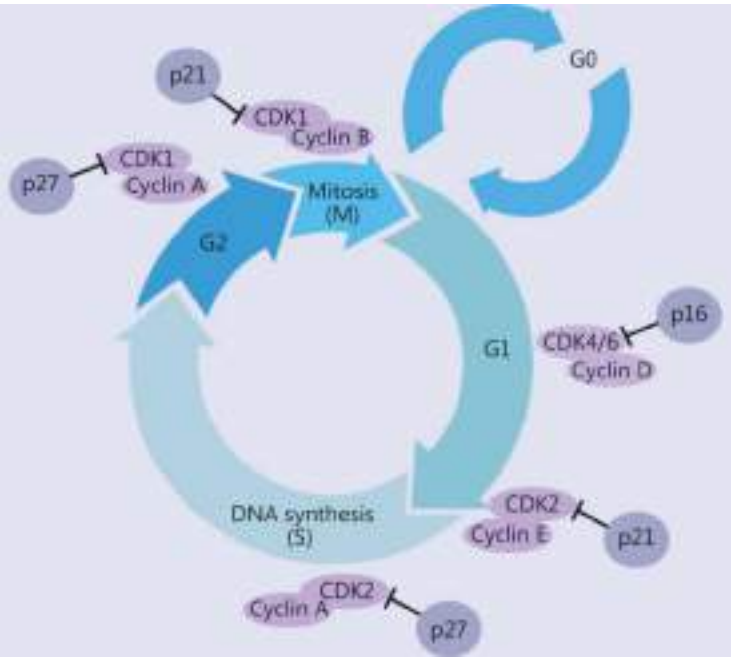

Figure 11. A schematic representation of cell cycle determinants. Each phase of the cell cycle is regulated by cyclin-dependent kinases (CDKs) and other regulatory partner proteins, the cyclins, and CDK inhibitors.

9. Nuclear envelope

The nuclear envelope (NE) is the membrane that separates the nucleus from the cytoplasm in eukaryotic cells. The NE acts as a barrier between the cytoplasm and DNA. It consists of two membranes: the outer nuclear membrane (ONM) and the inner nuclear membrane (INM) (**Fig. 12**). Both INM and ONM are perforated with nuclear pore complexes (NPCs). NPCs act as gateways that allow efficient and selective translocation of many macromolecules. The protein components of NPCs have been identified, but the mechanism for exactly how NPCs come together still remains unknown. NPCs are formed by a highly stable scaffold, where more dynamic and exchangeable parts can be targeted to change nuclear transport properties and eventually cell state (Rabut et al., 2004).

ONM is characterised by having continuous endoplasmic reticulum (ER). INM connects to filamentous proteins called Lamins (such as LaminA, LaminB1, LaminB2, LaminC) forming a web with DNA and NPCs, that provides structural stability. ONM and INM are formed by a diverse group of proteins that are abundant in the ER. Many of these proteins that form INM, ONM, and NPCs are evolutionarily conserved, both structurally and functionally. This highlights that the mechanisms controlling the organisation of nuclear content could be partially conserved (Akhtar & Gasser, 2007; Hetzer, 2010; Mekhail & Moazed, 2010). It has

been suggested that the interconnection of ONM-INM-NPCs is important for nuclear movement and positioning (**Fig. 12**) (Burke, 2019).

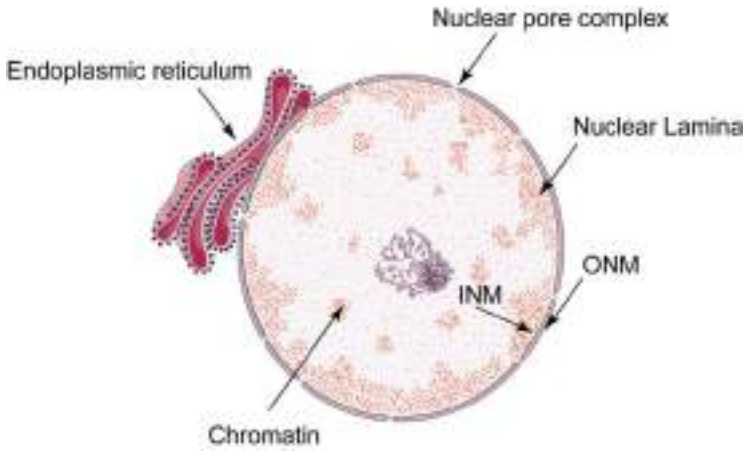

Figure 12. A schema of the nuclear envelope (NE) composition. The NE is composed of INM and ONM and separates the nucleus from the cytoplasm. The nuclear lamina is connected to the INM, linking the chromatin to the NE. Nuclear pore complexes (NPC) are dispersed across the NE where the INM and ONM are fused together (adapted from Schrimer & Gerace, 2002).

9.1. Nuclear envelope reorganization during division

The NE in higher eukaryotic cells disintegrates completely during cell division, giving the mitotic spindle access to chromosomes. This means that every mitotic cell has to reform its own NE and reconstruct the identity of its nuclear compartment (Güttinger et al., 2009).

NE reorganisation in mitotic cells is a highly dynamic process that requires many players. By late G2, the genome and the number of NPCs had duplicated, and the surface area of the NE had increased. When the cell enters Prophase, the NE undergoes breakdown (NEBD), losing the compartmentalization between nucleus and cytoplasm (Burke & Ellenberg, 2002). During early anaphase, when chromosomes are segregated and chromatin is not surrounded by any membranes, NE are found in the cytoplasm and the transmembrane NE is located in the ER (Dultz et al., 2008; Wandke & Kutay, 2013). During late Anaphase, ER membrane reassociates and quickly encloses the chromatin. In Prometaphase, a few nuclear pore complex proteins such as Nup107-160 localize to the kinetochore and play a role in correct mitotic spindle assembly during mitosis (Rasala et al., 2006; Walther et al., 2003) (**Fig. 13**). At the end of the cell cycle, the NE is reconstituted and the barrier between the nucleus and the cytoplasm is re-established, along with selective transport between the nucleus and the cytoplasm (Kutay & Hetzer, 2008).

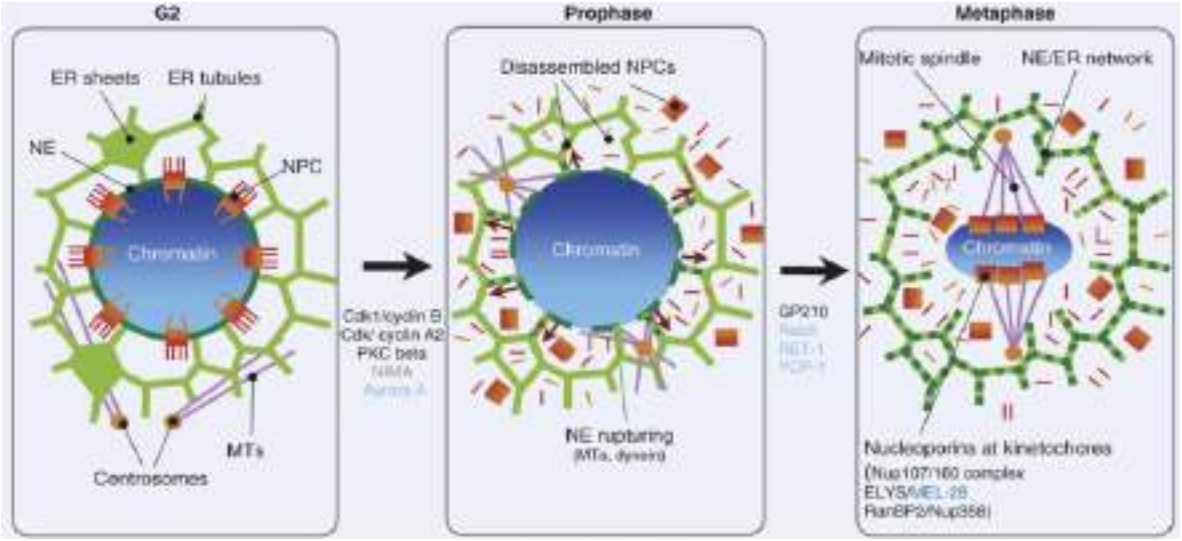

Figure 13. A schematic representation of nuclear envelope breakdown (NEBD) during division. In G_2, the cell nucleus has finished replicating its DNA. When the cell enters mitosis, the NE (dark green) is reabsorbed and the NPCs (red) are disassembled into the ER (green). In prophase, centrosomes (orange dots) and microtubules (purple) move to the NE, participating in its disassembly. At metaphase, the NE has completely disappeared, but some NPC complexes are associated with the kinetochore and spindle formation (adapted from Kutay & Hetzer, 2008).

9.2. Nuclear Pore Complex composition

NPC is made up of several copies of about 30 different proteins known as nucleoporins (Nups). The first category of Nups are rich in phenylalanine-glycine (FG domain repeats, which serve as a permeability barrier.(Frey & Görlich, 2009; Mohr et al., 2009) (**Fig. 14**). The second category of nucleoporins lack FG repeats and are known as structural nucleoporins. Finally, the third category of nucleoporins acts as anchors of NPC to the NE. These proteins are pore membrane proteins (Poms); however, only three Poms are identified in vertebrates until now: Pom121, Ndc1, and Gp210 (Antonin et al., 2005; Cohen et al., 2003; Mansfeld et al., 2006) (**Fig. 14**). Nucleoporins tend to interact with each other, forming subcomplexes. These subcomplexes are considered the building blocks of the NPC. Three nuclear pore subcomplexes have been identified: Nup107-160, Nup62, and Nup93 (Rabut et al., 2004).

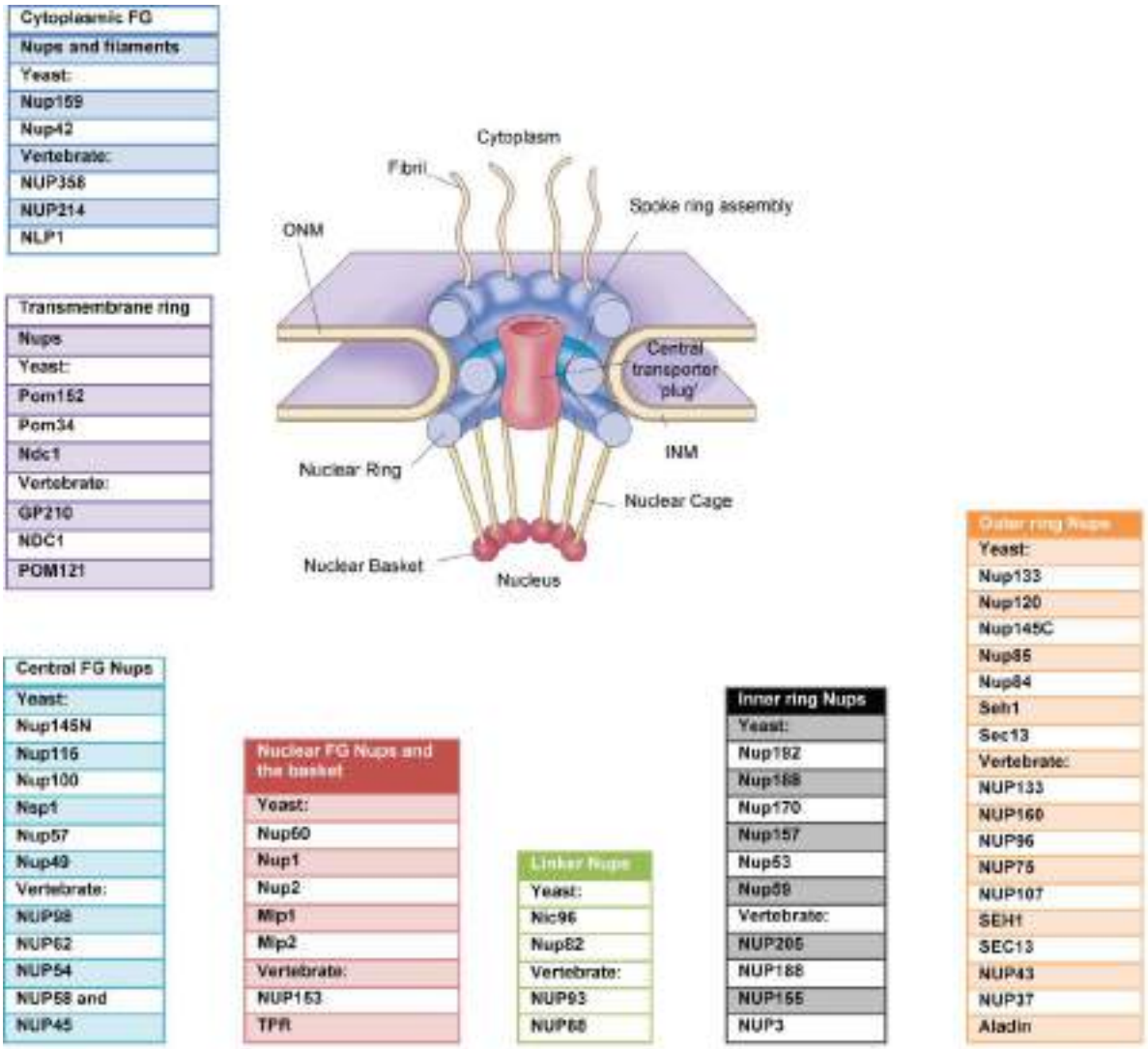

Figure 14. Nuclear pore complex (NPC) structure and composition. NPC is a cylinder made up of eight spokes that surround a central tube that connects the nucleoplasm to the cytoplasm. The outer and inner nuclear membranes (ONM, INM) fuse to form a space for NPC to reside. The NPC is anchored to the NE by a transmembrane structure that connects to the core structure. Inner and outer Nups are known to be biochemically stable and are thought to have a role in NE assembly and NPC formation. GP210, glycoprotein 210; Mlp, myosin-like protein; Ndc1, nuclear division cycle protein 1; Nic96, Nup-interacting component of 76 kDa; NLP1, Nup-like protein 1; Pom, pore membrane protein; Seh1, SEC13 homologue 1; TPR, translocated promoter region (adapted from Strambio-De-Castillia et al., 2010).

9.3. NPC function

The primary function of NPC is transporting macromolecules between the cytoplasm and the nucleus. However, it was recently highlighted that NPCs also play a role in the dynamic organization of the genome, affecting DNA stability and repair (Mekhail & Moazed, 2010).

9.3.1. NPC and molecular trafficking

The majority of macromolecules that shuttle in and out of the nucleus share the same active transport mechanism, consisting of nuclear transport factors (NTFs) that bind to transport signals on the cargoes. NTFs belong to the karyopherin (Kap) protein family, and are referred to as importins and exportins. Importins import cargo from the cytoplasm to the nucleus, while exportins export cargo from the nucleus to the cytoplasm. The transport signal present on the cargo is a short amino acid sequence called the nuclear localization sequence (NLS) for cargo import and the nuclear export sequence (NES) for cargo export (**Fig. 15**).

Cargo transport occurs in three steps. First, NTFs recognise and bind to any NLS or NES present on the cargo. Second, NTFs mediate interaction between central FG rich nucleoporins present in the central channel of the NPC. Third, when the cargo-NTFs complex arrives to its destination whether nucleus or cytoplasm, the NTFs dissociate from the cargos releasing it. In case of importing cargo to the nucleus, this dissociation is mediated by RanGTP. In case of exporting cargo to the cytoplasm, in the nucleus the association of NES of the cargo and NTFs is mediated by RanGTP. Once in the cytoplasm, the dissociation of NTF-cargo is performed by GTP hydrolysis. This process releases RanGDP and NTFs that can be recycled and used in future transports (Kuersten et al., 2001; Lange et al., 2007; Lu et al., 2021).

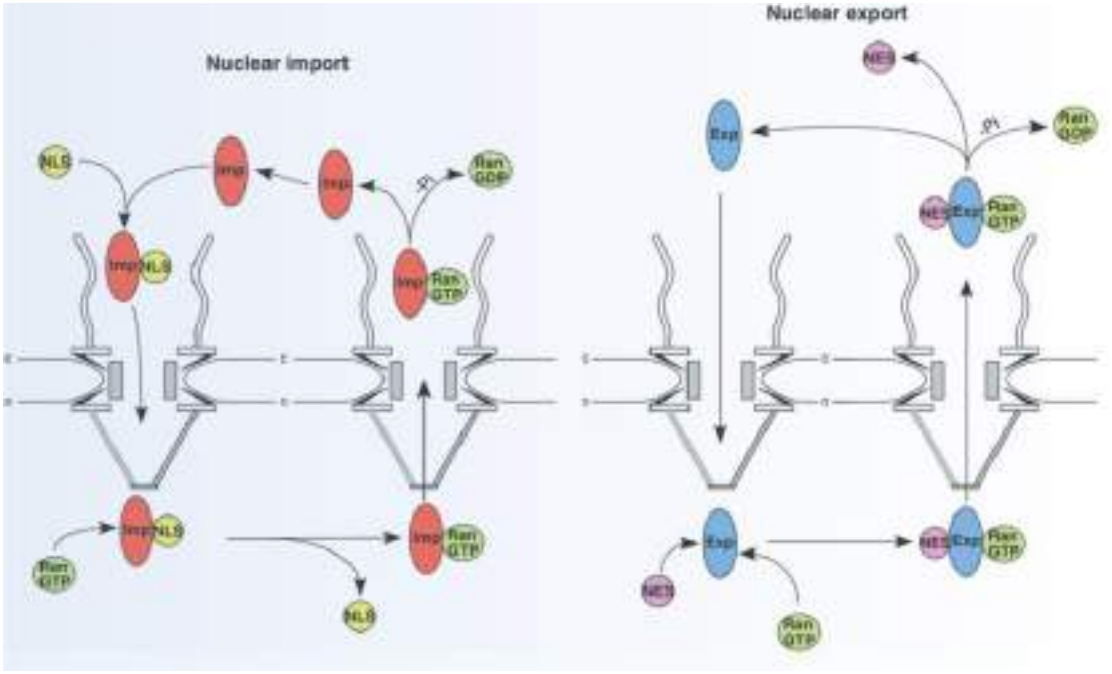

Figure 15. Nuclear import and export of cargo. Importins bind to molecules that have a NLS in the cytoplasm, then they mediate interaction with NPC for cargo translocation. In the nucleus, RanGTP binds to importin, inducing conformational changes that are followed by cargo releases from the NPC complex. The importin-Ran-GTP complex is recycled back in to the cytoplasm and hydrolysed to Ran-GDP. Exportins bind to cargo that have a NES, this process requires Ran-GTP, which is hydrolyzed into Ran-GDP at the cytoplasm after cargo release. (Imp) importin; (Exp) exportin (adapted from Fahrenkrog, 2006).

9.3.2. NPC and gene expression

Chromatin is highly organized within the nucleus, distinguished by its diverse packaging and compactness. Chromatin compactness is one of the factors that regulates repression or activation of gene expression. Chromatin is classified into heterochromatin and euchromatin. Heterochromatin is condensed chromatin packaged tightly with nucleosomes. In contrast, euchromatin is loosely packaged, and the extent of packaging with nucleosomes is dynamically regulated. The exact protein composition of the nuclear periphery is still unidentified. The nuclear periphery may be enriched with activator and repressor domains and cofactors that affect transcriptional activation or repression. Nuclear periphery domains has been associated with gene silencing; where studies in yeast showed that transcriptionally inactive regions like telomeres and centromeres are associated to the NE (Hediger et al., 2002). Additionally, transcriptional silencing associated with the nuclear periphery is dependent on histone deacetylase, which suggests that only some genes can be sensitive to histone deacetylation at the nuclear periphery. Altogether, these observations unveil a

complex heterogeneity at the nuclear periphery that entails cross-talk between genes and genetic elements and perinuclear domains in the NE (Mekhail & Moazed, 2010).

The nuclear lamina is a meshwork structure formed of Lamin proteins that lies just below the NE and is thought to play important roles in gene expression at the nuclear periphery (Andrés & González, 2009). Studies using microscopy analyses in mammalian cells show a close link between nuclear Lamins interacting with heterochromatin, where LaminA and Lamin associated peptide 2 (Lap2-a) anchor heterochromatin to the NE, which causes transcriptional repression (Dechat et al., 2010; Lee et al., 2009). But does the NPC only repress gene transcription? The answer to this question is no. Chromatin immunoprecipitation assay (ChIP) in *S. cerevisiae* showed that NPC such as Nup116, Nup60 and Nup2 are associated with highly transcribed genes (Casolari et al., 2004). This association between NPC and highly transcribed genes is also found in *Drosophila* and other eukaryotic cells, where Nup98 is associated with gene regulation via chromatin dissociation from the NPC (Hou & Corces, 2010). Another example is the transmembrane nucleoporin Nup210, which plays a role in myogenesis of embryonic stem cells and differentiation into neural progenitors. Knocking out Nup210 in embryonic stem cells blocked myogenesis, and the differentiation of embryonic stem cells into neural progenitors. Nup210 expression during myogenesis and differentiation of embryonic stem cells into neural progenitors was accompanied by a change in gene transcription, which wasn't due to changes in nuclear transport (**Fig. 16**) (D'Angelo et al., 2012).

The link between NPC and gene transcription regulation arises partly from being dependent on DNA zip codes called gene recruitment sequences (GrSs) (Ahmed et al., 2010). GrSs allow targeting of nuceloplasmic loci to the NPC. GrSs are functional in fission yeast, supporting evolutionary conservation. These genes might hold an explanation for the preference of some genes to be transcribed close to, or away from, the nuclear periphery. The role of NPC in gene regulation is more complex than it seems, NPC mainly mediates transport between the nucleus and the cytoplasm, and this allows it to have a dynamic architectural organization. This dynamic organization allows various components of the NPC to be trafficked between the nuclear pores and the nucleoplasm. It has been proposed that nucleoporin localization to the nucleoplasm may play a role in the transcriptional activation of internally localized genes. A chromosome wide mapping of Nup93 in mammalian cells in the presence and absence of histone deacetylase showed the recruitment of silent chromatin by active domains at the NPC, causing significant changes in chromatin organization and

transcriptional regulation (Pepenella & Hayes, 2007). Overall, these findings show that the association of DNA-NPC may have a differential effect depending on the context: cell type, organism, signalling cues and trafficking of NPC components.

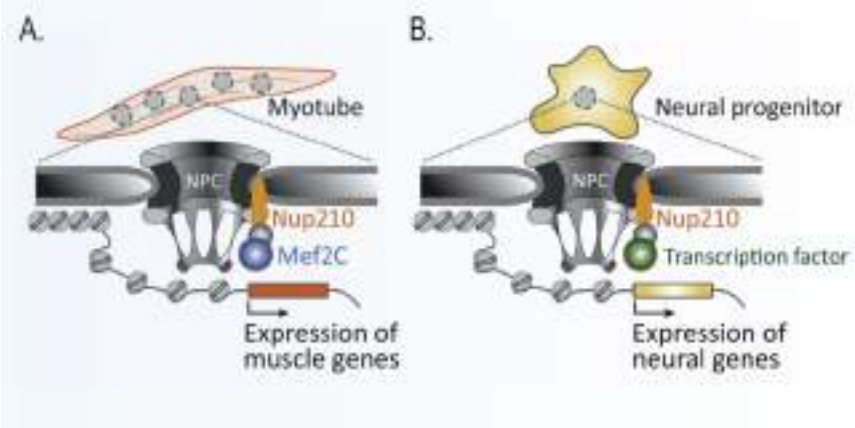

Figure 16. NPC and gene expression regulation. (A) During early differentiation in myoblasts, Nup210 induction by Mef2c leads to inducing gene expression and myogenesis. (B) Nup210 recruitment in embryonic stem cells and induction of its differentiation into neural progenitors are thought to be due to recruitment of transcription factors to the NPC that ultimately affect the expression of neural genes (Satomura & Brickner, 2017).

9.3.3. NPC and cell cycle

NPC disassembly is considered a critical step for nuclear envelope breakdown (NEBD), as it allows the influx of molecules that may be critical for cell cycle progression. One of these molecules is Cdk1, which requires access to lamins and INM to properly regulate mitosis. The hyperphosphorylation of NE proteins, which is thought to play a role in disrupting protein complexes or activating certain factors involved in the process, is another critical event during NEBD. Cdk1/CycB1, protein kinase C (PKC), Nima, and Aurora A have all been implicated in NEBD (Portier et al., 2007). Cdk1 is an important kinase in this process because it phosphorylates lamins and Nups, including the Nup107-160 subcomplex, the Nup93 subcomplex, Nup53, Nup98, Ndc1, and gp210 (Güttinger et al., 2009). The dissociation of INM like Lap2-a and Lamin b receptor (LBR) appears to depend on Cdk1 (Courvalin et al., 1992). Furthermore, some nucleoporins are critical for cell cycle progression; among them is Nup107-160 complex, which is implicated in many mitotic assembly processes such as: mitotic spindle assembly, spindle assembly checkpoint (SAC) activity, kinetochores functions, chromosome passenger complex (CPC) localization, nucleation of microtubules at kinetochores at mitosis, and progression of cytokinesis (Katsani et al., 2008; Mishra et al., 2010; Orjalo et al., 2006; Platani et al., 2009; Rasala et al., 2006; Zuccolo et al., 2007).

Next, I will describe the composition and function of Nup107-160 subcomplex and its spatio-temporal role in regulating mitosis.

10. Nup107-160 subcomplex composition

Nup107-160 complex forms a fundamental part of the outer rings of the NPC. In most eukaryotes, it is composed of equal parts of: Nup107, Nup96, Nup160, Nup133, Sec13, and Seh1. Nup107-160 counterpart in yeast is Nup84 complex, which is identical to Nup107-160 complex but lacks Nup43 and Nup37 subunits. Depending on the species, Nup37, Nup43 and ElYS might be included or absent in Nup107-160 sub complex formation. Nup85, Nup43, and Seh1 form one of the two short arms, while Nup160, Nup37, and ELYS form the other. These two arms are connected to Nup96 and Sec13, while Nup96 is connected to Nup107 and Nup133 to form the long stem (Nup96-Nup107-Nup133) of the Y-shaped molecule. Several copies of the Nup107-160 subcomplex form the outer rings facing the nuclear and cytoplasmic sides of the NPC assembly (Asakawa et al., 2019; Kampmann & Blobel, 2009; Newton et al., 2018).

10.1 Nup107-160 subcomplex role in mitotic spindle assembly

Nup107-160 subcomplex is thought to play a critical role in mitotic spindle assembly; it localizes to the kinetochore in mammalian cells during mitosis. Nup37, Nup43, Seh1 and Sec13 are all components of Nup107-160 subcomplex that are targeted by kinetochores during prophase until anaphase of mitosis. Also, Nup96 was observed at the mitotic spindles and spindle pole during mitosis (Enninga et al., 2003; Walther et al., 2003). Studies examining the exact role of Nup107-160 subcomplex using mitotic Xenopus extract revealed that depletion of Nup107-160 subcomplex rendered the mitotic spindle assembly deformed. This function is suggested to be independent of the initial Ran-GTP mediated mitotic assembly. Orjala et al. (2006) demonstrated in the study defective mitotic spindle due to depletion Nup107-160 complex could be corrected by the addition of Ran-GTP (Orjalo et al., 2006). However, several studies have emerged refuting the critical role of Nup107-160 in mitotic spindle, this is based on studies in human HeLa cells, where depleting Nup107-160 complex had no effect on mitotic spindle assembly. However, in Hela cells Nup107 was found to be located near the kinetochore and the spindle pole. This suggests that the role of Nup107-160 subcomplex might differ between Xenopus and humans (Platani et al., 2009; Zuccolo et al., 2007).

10.2. Nup107-160 subcomplex role in spindle assembly checkpoint (SAC)

The spindle assembly checkpoint (SAC) is considered the trigger safety of cells in eukaryotic cells, assuring the fidelity of chromosome segregation during mitosis. The SAC inhibits chromosome missegregation and cases of aneuploidy. Defects in SAC lead to tumorigenesis. Until now, the uncovered components of the SAC mechanism are: MAD (mitotic-arrest deficient) genes MAD1, MAD2, and MAD3 (BUBR1 in humans), and the BUB (budding uninhibited by benzimidazole) gene, BUB1. These components were found to be conserved in all eukaryotic cells; they are involved in active SAC during the prometaphase.

During mitosis in mammalian cells, the SAC is recruited and anaphase is blocked upon the discovery of a single unattached kinetochore (known as mono-orientation or monotelic attachment). Unattached kinetochore activates the mitotic spindle checkpoint (MCC). MCC blocks Cdc20 from activating anaphase-promoting complex-cyclosome (APC/C). SAC cascade is negatively regulated by the correct attachment of all sister kinetochore pairs to kinetochore microtubules and the maintenance of their bidirectional orientation. The release of Cdc20 activates APC/C, this results in the degradation of Cyclin B1 and Securin (SEC). The activation of SEC leads to the activation of Separase, which degrades the cohesion ring linking sister chromatids. The degradation of Cyclin B prohibits initiation of cytokinesis and mitotic exit program, which depend on Cdk1-Cyclin B1 binding.

Studies in *Xenopus* extract show that Nup107 is upregulated near unattached Kinetochore to the microtubule (Orjalo et al., 2006), However in this same study they show that SAC recruitment to the Kinetochore upon disrupting microtubule assembly is independent of Nup107 complex.

Interestingly, in metazoan species, specifically *Caenorhabditis elegans* (*C. elegans*) Nup107 mutants displayed compromised SAC, strongly suggesting that Nup107 is important for chromosome segregation during mitosis (Ródenas et al., 2012).

10.3. Nup107 and the kinetochore

The Nup107 subcomplex is thought to c ontribute to the kinetochore. The kinetochore is a disc-shaped protein complex associated with duplicated chromatids during mitosis (**Fig. 17**). The kinetochore has a trilaminar composition, dividing it into an inner, outer, and central kinetochore. The inner part of the kinetochore interacts with centromeric chromatin, while the outer part of the kinetochore is the area that interacts with spindle microtubules. The two main components of the outer part of the chromosome are Ndc80 complex and CENPF. Ndc80 complexes is formed by: Ndc80, Nuf2, Spc24, Spc25. Ndc80 complex bind to Mis12, forming Kinetochore microtubule network (KMN) which is indispensible for microtubule-kinetochore

interaction. Studies in Hela cells showed that Nup107 complex localization to the Kinetochore is mediated by Ndc80. Functional experiments depleting Nuf2 and Nudc80 led to a reduction in Nup107 complex recruitment to the kinetochore. Immunofluorescence assays and yeast two hybrid assay revealed an interaction between Nup133 and CENPF, however functional studies depleting CENPF in Hela cells only affected Nup133 localization to the kinetochore. These results point to a potential function of Nup107 complex in the correct attachment of microtubules to the kinetochore (Zuccolo et al., 2007).

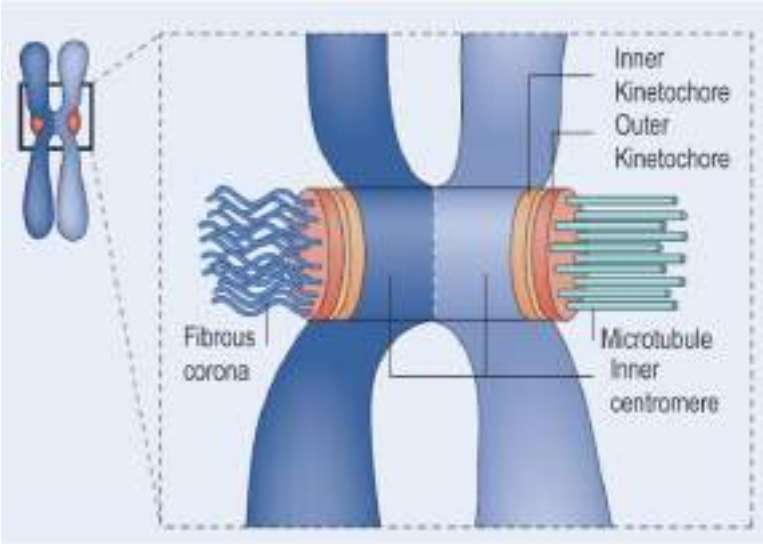

Figure 17. Kinetochore structure. Schematic representation of a mitotic chromosome that has two paired sister chromatids. The chromatid on the right is attached to microtubules, and the chromatid on the left is unattached. In addition to the inner, and outer kinetochore, inner centromere and fibrous corona (adapted from Cheeseman & Desai, 2008).

11. Robo receptor

11.1 The history of Robo receptor

Most organisms develop their CNS along a bidirectional axis of symmetry located at the midline. The ventral midline, also known as the floor plate, organises the secretion of diffusible proteins, which regulate neuron migration, axon and dendrite growth across the midline. Surprisingly, glia and neuronal cells delineate the midline and control axon guidance in the developing cerebral cortex (Chédotal, 2007).

Robo and its ligand Slit are evolutionary conserved molecules (Brose et al., 1999). Roundabout receptors (Robo) and their ligands, known as Slits, were discovered in the early 1990s and are important players in axon guidance. Slit was originally thought to function as an extracellular matrix protein in Drosophila, but subsequent research revealed that it is a diffusible chemorepellent for axons crossing the midline. Robo was discovered during a gene

screen in Drosophila to look for genes involved in midline crossing. Slit and Robo have been linked to a variety of neuronal and non-neuronal processes such as cell migration, neurogenesis, angiogenesis, and tumorigenesis (Kidd et al., 1998; Wang et al., 2003).

11.2. The structure of Robo receptors and their Slit ligands

The Robo receptor family is a highly conserved family of receptors. The members of the Robo family vary between vertebrates and invertebrates. Vertebrates have four Robo receptors (Robo1, Robo2, Robo3, and Robo4). Robo1–3 show a high degree of structure and function similarity and are expressed in many tissues, including the CNS. However Robo3 has a very low affinity for Slits and it is selectively phosphorylated by Netrin-1. Robo3 plays a role in midline crossing by antagonizing the repellent signal from Robo1 and Robo2. Robo4 is distinct from the other members, it is specifically found in endothelial cells, acting in angiogenesis, not being expressed in the CNS. Robo receptors are members of the immunoglobulin (Ig) superfamily and cell adhesion molecules (CAMs). They are able to undergo heterophilic and homophilic interactions. In the majority of vertebrates, Robo receptors are expressed in the brain. The standard structure of Robo receptor is composed of five Ig motifs, three fibronectin type III domains, and four conserved cytoplasmic domains. These cytoplasmic domains are expressed in different combinations in the Robo family. Robo3 lack CC1 domain, while in Robo1/2, cytoplasmic domains (CC0-CC3) have no inherent catalytic activity, but confer a downstream signal by recruiting various factors to conserved proline-rich domains (W. D. Andrews et al., 2007; Ballard & Hinck, 2012; Hohenester, 2008; Ypsilanti et al., 2010) (**Fig. 18**).

Robo receptors undergo alternative splicing that generates various isoforms. 5'-coding sequence alternative splicing produces two distinct isoforms, A and B. These differ at their N terminal, where A isoform is longer (16-40 residues) than B (Chédotal, 2007).

Robo receptors' primary ligands are Slits (Kidd et al., 1998). Three Slit genes are expressed in mammals, all of which are found in the nervous system and other organs. Slits are glycoproteins with an N-terminal signal peptide, four domains (D1-D4) containing leucine-rich repeats (LRR), several EGF-like sequences, a laminin-G domain, and a cysteine-rich knot at the C-terminus. Slits are cleaved to produce a C-terminal fragment with unknown function and an N-terminal fragment that is active and mediates Robo receptor binding (Brose et al., 1999; Ypsilanti et al., 2010).

Studies performed in *Drosophila* showed that Robo receptors bind to the Slit D2 domain via their Ig1 and Ig2 domains. Slit-Robo binding complexes are evolutionary conserved across species (Morlot et al., 2007). Heparan sulphate proteoglycans (HSPG) stabilise the Slit-Robo homodimer by interacting with the Slit D4 domain, an interaction that seems to potentiate Slit activity (Seiradake et al., 2009) (**Fig. 18**).

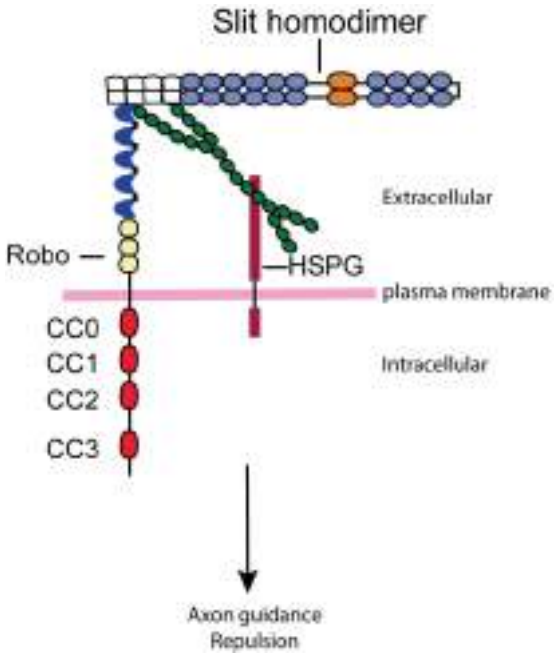

Figure 18. A schematic representation demonstrating Robo-slit signalling. Slits bind to Robo receptor's immunoglobulin (Ig1) domain via its (D2) domain, which contains leucine rich repeats (LRR). Syndecan (Sdc) and other heparin sulphate proteoglycans (HSPGs) are Robo and Slit co-receptors. HSPG is made up of core heparin sulphate chains that form a ternary complex with the Ig1 domain of Robo and the D2 domain of Slit to stabilise Robo and Slit binding (adapted from Ypsilanti et al., 2010).

11.3. Downstream Robo/slit signalling molecules

Robo/Slit downstream signalling molecules are mainly cytoplasmic kinases, regulatory molecules related to actin polymerization and cytoskeleton reorganization. These molecules affect cell mobility, including kinases such as Hakai, Myo9b and GTPases like Rac, Cdc42, and RhoA, that are part of the Rho family, and other molecules like Abl and Ena that regulate cytoskeleton (Tong et al., 2019) (**Fig. 19**).

Abl is a tyrosine kinase that inhibits Robo signalling by phosphorylation of Robo at CC1 domain, and alters cell adhesion by activating Robo signalling on binding to cables, and affecting βcatenin and N-cadherin activity (Rhee et al., 2007; Wills et al., 2002). *In vitro* studies showed an anti-tumorigenic effect of P-cadherin that is modulated by Robo3 in oral squamous cell carcinoma cell line (Bauer et al., 2011). Furthermore, GTPases, which are

small GTP-binding proteins that regulate cell polarity and mobility. GTPase activity is modulated by many molecules, such as: s/rGAPs (Slit/Robo GTPase activating proteins), Dock/Nck (Nck in mammals) and GEFs (guanine nucleotide exchange factors), all these molecules can be sequestered by Robo (Ypsilanti et al., 2010). Recently, de novo targets of Slit/Robo have been identified, like ubiquitin kinase Hakai that inhibits growth and migration of lung cancer. All together, these molecules further highlight Slit/Robo as a potential target for cancer therapeutics (Tong et al., 2019) (**Fig. 19**).

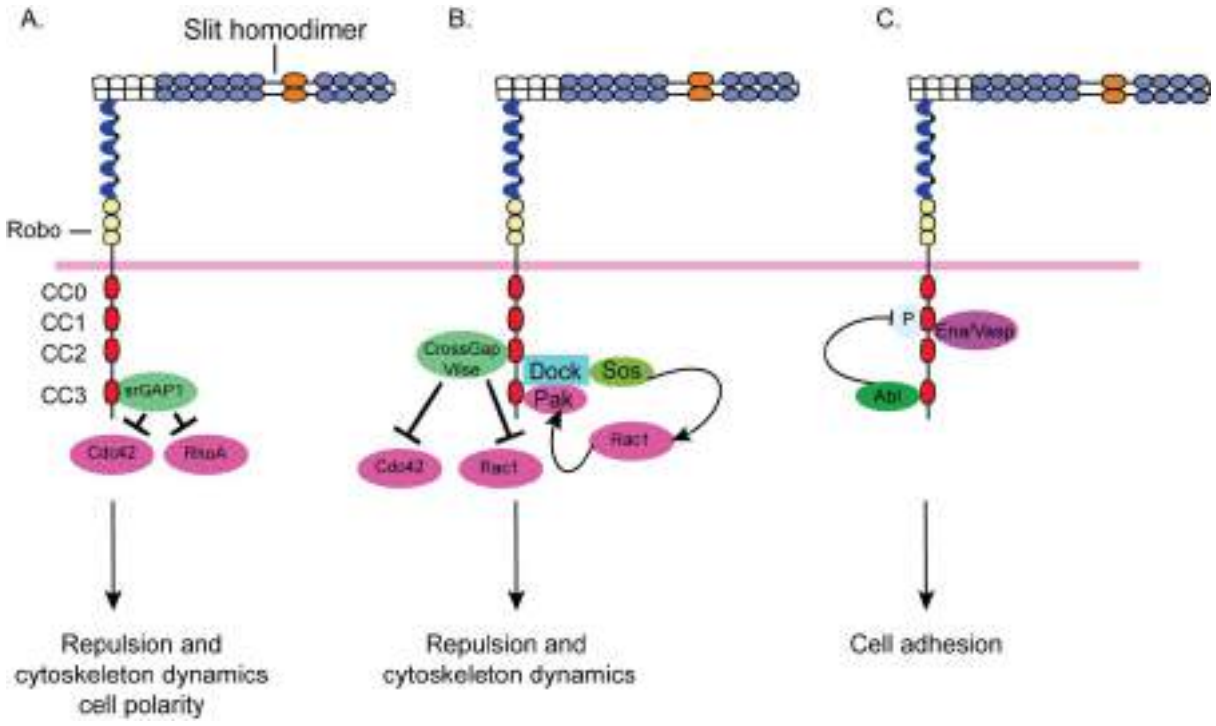

Figure 19. A schematic representation showing key regulators of Robo downstream signalling. (A) In the presence of Slit, RoboGAP1 (srGAP1) binds to Robo CC3 domain and inhibits RhoA and Cdc42 activation. This cascade is involved in the mediation of repulsion, cell polarity, and the control of cytoskeleton dynamics. (B) In the presence of Slit, Visle/cross GAP binds to Robo CC2 domain. Rac1 and Cdc42 are inhibited by this interaction. Rac1 can also be activated by the son of sevenless, a GEF, via the adaptor protein Dock, which binds to Robo CC2-3 domain. This cascade activates Rac1 and (Pak) P21 activated kinase, both of which bind Robo CC2-3 domain. These Robo downstream targets are involved in cytoskeleton dynamics and repulsion. (C) Tyrosine Kinase Abelson (Abl) binds Robo CC3 domain, blocking Robo signalling by phosphorylating Robo CC1 domain and moderates cell adhesion. Enabled (Ena), a substrate of Abl, also binds Robo CC1 and CC2 domains (adapted from Ypsilanti et al., 2010).

11.4. Robo cleavage and new regulatory complexes

Previous studies focusing on post-translational modifications of Robo have shown that the downstream signalling pathways and receptor regulation could be more complicated than previously proposed. The cleavage of Robo intracellular domain was reported in hepatoma cells, where the intracellular domain is cleaved via γ secretase, yielding two distinct intracellular Robo1 fragments: Robo1-CTF1, Robo1-CTF2. In this study, several NLSs were identified in Robo1 intracellular domain. This suggests the possible transcriptional role of Robo1. Further biochemical fractionation assays using a proteasome inhibitor showed that Robo-CTF2 is exclusively localized to the nucleus, while Robo-CTF1 is located in the membrane, cytoplasm, and nucleus. This suggests that proper localization of intracellular domain to different cellular compartments might be important in its regulatory role. Moreover, removal of the several NLS sequences didn't abolish Robo1 nuclear localization, suggesting the presence of a non-canonical mechanism (Seki et al., 2010) (**Fig. 20**). In addition to intercellular cleavage, Robo and other axon guidance receptors undergo extracellular cleavage, producing proteins that are important to regulate migration. A study performed in *Drosophila* showed the role of metalloprotease–disintegrin Kuzbanian (ADAM10 in mammals) in the cleavage of the Robo extracellular domain. This process is important in neuronal cells that require Robo/Slit repulsion when crossing the midline. Furthermore, cleavage of Robo extracellular domain appears to be important in receptor activation following Slit stimulation. It was also shown that Robo cleavage by Kuz/ADAM10 is important for sequestering son of sevenless (Sos) and other molecules important for Robo/Slit midline repulsion (Coleman et al., 2010) (**Fig. 20**).

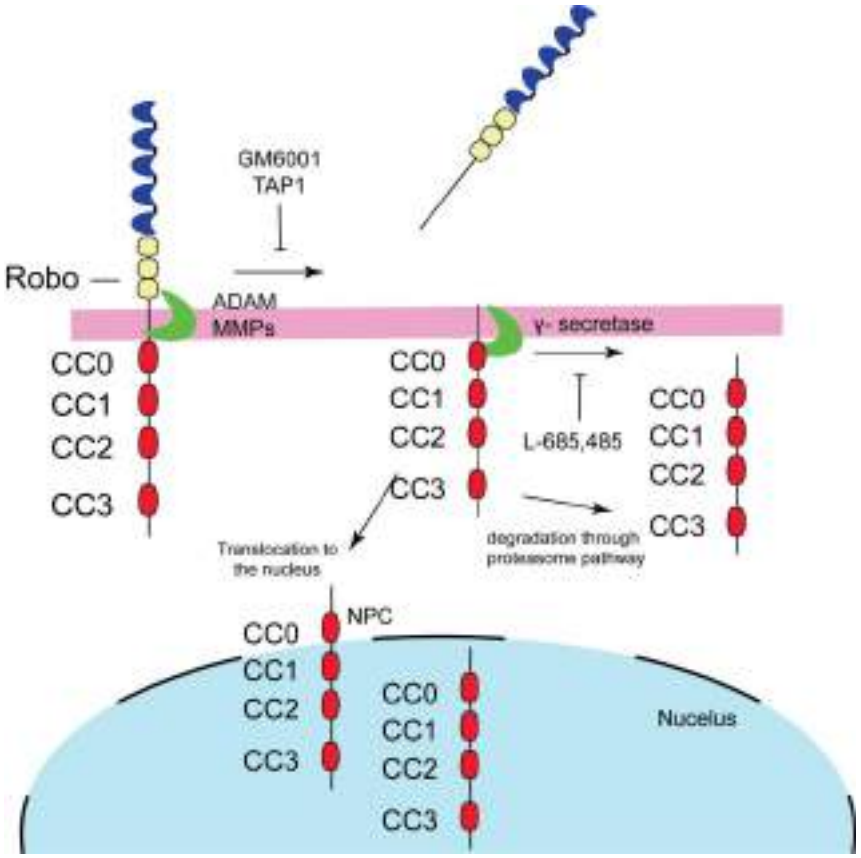

Figure 20. Schema showing Robo proteolysis and translocation to the nucleus. Robo extracellular terminal is shed by metalloproteases (MMPs, ADAM). This process can be blocked by GM6001 and TAP1. Membrane-bound Robo cytoplasmic terminal is then cleaved by γ-secretase, which can be inhibited by γ secretase inhibitors L-685,485. Robo cytoplasmic terminal undergoes further proteolytic degradation or translocates to the nucleus (adapted from Seki et al., 2010).

11.5. Robo receptor and neuronal migration

Robo-Slit signaling plays a major role in axon guidance systems in rodents, especially in the formation of major forebrain axonal tracts and commissures, in the visual system, and in the spinal cord (Andrews et al., 2008; Long et al., 2004). But Robo1 expression is also associated with regions used by newborn interneurons to migrate, correlating with Calbindin (a marker of GABA containing interneuron) (Andrews et al., 2007). Robo1 receptor is expressed in the SVZ, ganglionic eminence (GE), the MZ and lower part of the IZ. Robo1 knockout mice exhibit a disruption in interneuron migration, suggesting the involvement of Robo in regulating interneuron migration. Interneurons in Robo1 KO accumulate in the striatum, a phenotype not observed in Slit1 KO mice. This suggests that Robo regulates interneuron migration in a Slit1-independent manner (Andrews et al., 2007; Marín & Rubenstein, 2003). One possible explanation for this mechanism is the interaction between Robo and Sema-Neurophilin (Nrp)/Plexin signalling. Previous work showed an Interaction between Robo1

first to Ig domain to Nrp (Liu et al., 2004). This interaction was further emphasized with Nrp1 knockout mice that exhibit a similar phenotype to that of Robo Knockout mice (Marín & Rubenstein, 2001).

Moreover, Robo receptors play a major role in neurons' radial migration during cortical development (Gonda et al., 2013; Marillat et al., 2002; Whitford et al., 2002). Knocking out Robo1 in layer II/III leads to a delay in neuronal migration from the IZ to the CP (Gonda et al., 2013), this phenotype was reminiscent of N-cadherin overexpression phenotype (Kawauchi et al., 2010). Robo1 inhibits the interaction between N-cadherin and β catenin (Rhee et al., 2002, 2007), which might cause N-cadherin endocytosis. Robo4 knockdown neurons lead to neuronal retention in the white matter, these neurons don't show a big change in polarization but have a leading process with a specific direction, suggesting the role Robo4 might play in directing migrating neurons by interacting with RGCs basal process (W. Zheng et al., 2012).

11.6. Role of Robo receptors in cortical progenitor proliferation

During early corticogenesis, many signalling pathways and molecules have been implicated in affecting progenitor proliferation and division modes. Robo1/2 is expressed in VZ cortical progenitors. Loss of this expression in Robo1/2 KO mice led to a decrease in the number of proliferating aRGCs. Robo1/2 KO mice have an increase in IPCs that are $Tbr2^{+}$ but are poorly functional. These IPCs that are found in the Robo mutant VZ have an apical process that tethers them to the apical surface. These data strongly suggest that Robo receptors play a role in regulating IPCs generation from aRGCs and their delamination from the apical surface (Borrell et al., 2012).

This study showed that Robo regulation of aRGCs proliferation was communicated via Hes1, a notch downstream transcription factor. Notch is a transmembrane protein that is known for its function in promoting RGCs proliferation and inhibiting IPCs generation. Robo1/2 KO mice exhibited low Hes1 expression in the cortex, suggesting that Robo signalling activates Hes1 expression. Moreover, luciferase assays performed in Neuro2A cells that lack notch signalling, showed that Hes1 is activated by Robo and that this activation is independent of Robo CC3 domain. This implied that Robo activation of Hes1 is independent from Notch (Borrell et al., 2012) (**Fig. 21**).

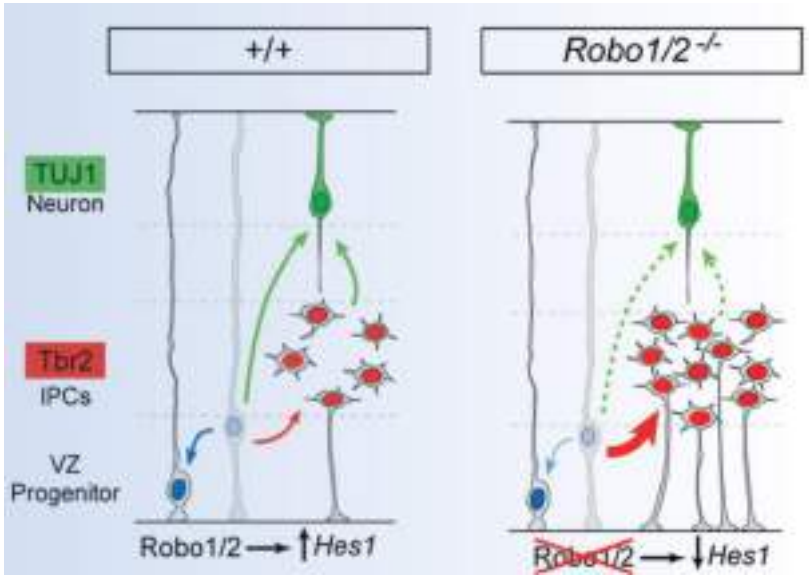

Figure 21. A schema of the model proposed in (Borrell et al., 2012) for the role of Robo signalling in the progenitors of the developing telencephalon. In the case of normal cortical development (+/+), Robo signalling activates Hes1 transcription in neocortical progenitors where it plays a role in keeping the balance between VZ progenitors self-renewal and generation of $TBr2^+$ intermediate progenitors and $Tuj1^+$ neurons. In the case of the absence of Robo signalling (-/-) in the developing telencephalon , Hes1 transcription is downregulated and the VZ progenitors dynamics become unbalanced, favouring the generation of more $Tbr2^+$ intermediate progenitors over self-renewal. In the developing cortex of Robo1/2 mutants $Tbr2^+$ cells have an apical process that prevents them from entering mitosis (adapted from Borrell et al., 2012).

11.7. Robo receptors regulate the balance between Direct and Indirect neurogenesis

Recently Robo receptors were demonstrated to play a role in ammonite cortical evolution. Direct neurogenesis is an evolutionarily old mode of neurogenesis that was followed by the emergence of Indirect neurogenesis, a newer mode of neurogenesis (Cárdenas et al., 2018). The mammalian brain is made up of various regions, each with its own evolutionary timeline; for example, the neocortex is thought to be the newest region developed in the mammalian brain, whereas the hippocampus, olfactory bulb (OB), and spinal cord are thought to be ancient brain structures. Direct neurogenesis is more common in these structures as a mode of progenitor division (Cárdenas & Borrell, 2019; Díaz-Guerra et al., 2013; Luzzati, 2015). A recent study demonstrated that the prevalent mode of neurogenesis, whether indirect in the neocortex or direct in the OB, is controlled by the levels of Slit-Robo signalling (Cárdenas et al., 2018). High expression levels of Robo1/Robo2 induced Direct neurogenesis, while low expression levels of Robo1/Robo2 in the neocortex are required to maintain Indirect neurogenesis (Cárdenas et al., 2018). Robo regulates direct vs. indirect neurogenesis via the modulation of Notch ligand expression (Cárdenas et al., 2018). This study compared the role of Robo1/2 in reptiles, birds, and the mammalian telencephalon, showing a negative correlation between Robo expression levels and Indirect neurogenesis. Where the highest

levels of Robo expression and the highest level of Direct neurogenesis was observed in reptiles, moderate Robo1/2 expression in birds was associated with more Indirect neurogenesis in birds. All this data confirmed the role of Robo receptors in regulating the mode of neurogenesis and how low expression of Robo in the neocortex directly affects progenitor proliferation (**Fig. 22**).

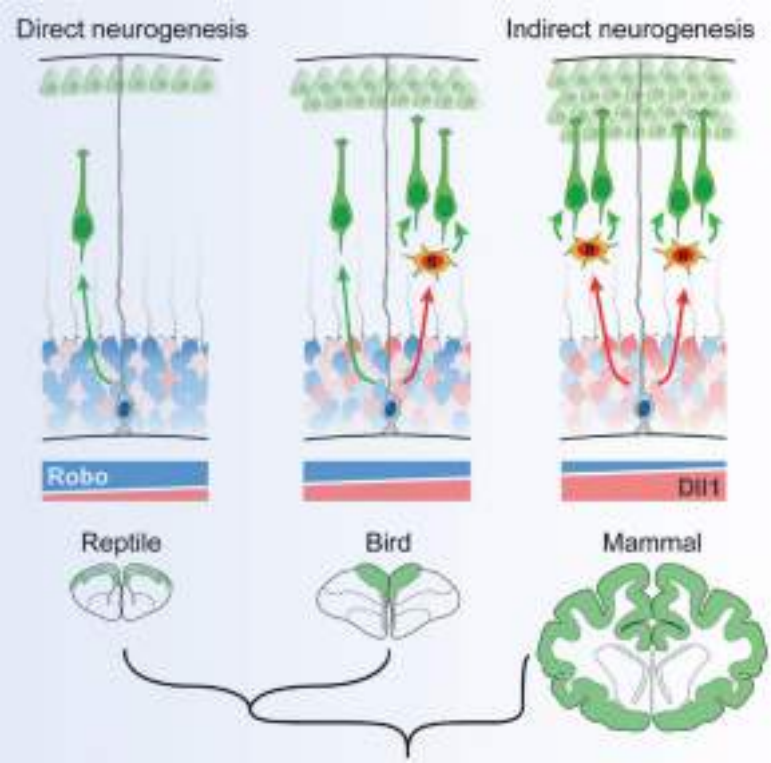

Figure 22. A schema showing that the levels of Robo and Notch signalling across amniotes. Robo and Notch signalling influence the mode of neurogenesis and, as a result, the size and complexity of the cerebral cortex. The mammalian neocortex is dominated by indirect neurogenesis, while reptiles and birds are dominated by direct neurogenesis. In mammalian cortex, low Robo and high Dll1 expression are important for indirect neurogenesis, whereas high Robo and low Dll1 expression are important for direct neurogenesis in reptiles and birds (adapted from Cárdenas et al., 2018).

12. Cortical evolution across ammonites

Brain development, morphological aspects, and the formation of neural networks is highly divergent in vertebrate species. These characteristics adapt to the species' environment. Specialized traits appear under the force of natural selection to adapt to different ecological niches. Amniotes have a special brain organization that serves their behavioural repertoire. Mammals and birds are endowed with a well-developed telencephalon, which correlates with their higher cognitive abilities (Butler & Hodos, 2005; Jarvis et al., 2005; Medina, 2007; Nomura & Hanashima, 2014). The anatomical cytoarchitecture of the telencephalon is highly divergent: mammals have six layers as a feature of their telencephalon, while the avian

telencephalon is composed of several neuronal nuclei. On the other hand, reptiles have a single-layered structure. Interestingly, the evolutionary mechanism that led to this divergence of the telencephalon remains unclear.

The Amniote lineage diverged into two main clades: sauropsids and synapsids. Mammals belong to synapsids, while reptiles and birds belong to sauropsids. Sauropsids are further subdivided into lepidosaurs, encompassing tutara, snakes, and lizards, and archosaurs that encompassed crocodiles, birds and turtles (Goffinet, 2017; Nomura & Hanashima, 2014; Tzika et al., 2011).

Gene expression levels, neural connectivity maps, and cell migration patterns show that the amniote embryonic cortex is composed of three main divisions: medial, dorsal and ventral. The tetrapartite pallium model postulates that the dorsal pallium of sauropsids (non-mammals) is homologous as a whole to mammalian cortical regions, medial pallium is homologous to the hippocampus and the ventrolateral pallium is homologous to the olfactory cortex, olfactory bulb and the claustrum laterally (L. Puelles et al., 2016; Luis Puelles, 2017; Luis Puelles et al., 2013). Birds and reptiles (sauropsids) develop a prominent nucleus located in the ventral pallium known as the dorsal ventral ridge (DVR), which rostrally is thought to receive thalamic sensory information and caudally includes the amygdala (Desfilis et al., 2018; Luzzati, 2015; Manger et al., 2002). The reptile dorsal cortex is formed of three layers: two sparsely dense layers (outer and inner) and a densely packed neuronal layer in between (Nomura et al., 2013). This three-layered organization is conserved in ancestral structures such as: the Hippocampus, and the piriform cortex, and the olfactory bulb. The six-layered cortex emerged with rise of mammals, making it a special distinguishing evolutionary trait. Cortical layers in the mammalian cortex develop distinct connectivity between another brain regions and the spinal cord. Neurons in layers 5 and 6 project to the thalamus; layer 5 projects to the spinal cord, and neurons in layer 4 receive thalamic input. Layer 2 and 3 connect superficially to other brain regions. This laminar organization, while present in mammals and reptiles, is absent in birds, that exhibit projections connecting different nuclei. In birds, excitatory neurons' input and output projections occur in a similar way, resembling the organization present in the mammalian cortex (Dugas-Ford & Ragsdale, 2015; Jarvis et al., 2005; Katz & Callaway, 1992).

Recently, single cell RNA sequencing (ScRNA-seq) studies in mice showed the neuronal diversity that exists not only between cortical layers, but also between cortical regions (Yao et

al., 2021); this technique also provided a key insight to the conservation of cortical molecular signatures in birds and reptiles. A key finding emerging from these ScRNA-seq studies is that birds, reptiles and mammals dorsal cortex express the same transcription factors but in different combination. Given, transcription factors that are considered markers of superficial and deep cortical layers in mammals have already existed in the dorsal pallium of our ancestors, this implies that a genetic signature distinguishing different cortical layers in the mammalian cortex has emerged due to modifications in the neuron genetic programme (Tosches et al., 2018).

13. Proposed hypothesis for the evolution of the neocortex

During evolution, cortical expansion is disproportionate to other regions of the brain. Cortical expansion and folding resulted from the combination of different variables that included an increase in neuronal yield, neuron packaging and migration, connectivity patterns, extended neurogenic period, changes in the extracellular matrix composition, an increase in cortical progenitors, and the generation of new neuronal subtypes, the suppression of direct neurogenesis, and the prevalence of indirect neurogenesis (Amin & Borrell, 2020; Florio & Huttner, 2014; Geschwind & Rakic, 2013). In this section, I am going to discuss some of these factors.

13.1. Molecular factors affecting progenitor cell dynamics

Changes in the timing, duration, and expression amplitude of different signalling pathways, attributed to cortical neurogenesis and pallial structure formation during amniotes' cortical evolution (Nomura & Hanashima, 2014). Interestingly, the Notch pathway has been implicated as an evolutionarily conserved pathway for progenitor fate determination and differentiation. Observations in different species of amniotes, showed the importance of Notch signalling variation. The Notch pathway has higher levels of activation in gecko, mosaic expression in turtles and birds and a lower expression in mouse cortex. This expression pattern correlated to the rate of neuronal differentiation of different species. Loss of function of Notch pathway in gecko increased neuronal differentiation, highlighting the importance of notch pathway in neurogenesis induction at least in gecko pallium (Nomura et al., 2013). These noticeable spatio-temporal differences of notch signalling across species may provide the molecular set up necessary for the differences in cortex neurogenic rates.

Studies showed that Wnt and Notch pathways are direct targets of Cyclin and CDks, which are known for their essential role in cell cycle progression. These findings indicate the important role these molecules play in cortical expansion (Braunreiter & Cole, 2019; Nomura & Hanashima, 2014).

13.2. SVZ emergence and BP abundance

One of the most important functions of aRGCs is the production of BPs -including IPCs and bRGCs-, which leads to an increase in the rate of neurogenesis. A key event following the emergence of BPs is their detachment from the VZ and their coalescence into the SVZ (Cárdenas & Borrell, 2019). The SVZ is a structure that is absent from the cortex of most reptiles; however, a very simplified SVZ like structure can be observed in turtles and the dorsal pallium of birds. The establishment of the SVZ is correlated with the evolutionary expansion of the neocortex. The SVZ is considered as a proliferative zone, where $Tbr2^{+}$ cells reside. In birds and reptiles, $Tbr2^{+}$ cells are present but in a more scattered pattern and have no proliferative capacity in some of these species (De Juan Romero & Borrell, 2015; Veronica Martínez-Cerdeño et al., 2006; Suzuki & Hirata, 2013). This evidence suggests that the expression of $Tbr2^{+}$ in reptiles and birds may be important for maintaining the glutamatergeric lineage rather than increasing the neuronal output (Sessa et al., 2010).

Studies performed on Macaque cortices demonstrated the massive size of the SVZ in these species. The macaque cortex possesses a much larger number of progenitors in comparison to mouse cortex. At the peak of neurogenesis in the mouse cortex, 15-20% of basal mitosis occurs in the SVZ, while in human, around 85% of basal mitosis occurs in the SVZ. This massive accumulation of basal progenitors in the SVZ, eventually led to its subdivision into ISVZ and OSVZ. Interestingly, the abundance of progenitors in the SVZ varies between different species (Reillo et al., 2011), there are many studies supporting the correlation between the abundance of progenitors in these germinal layers and cortical folding and expansion that emerged in gyrencephalic species (De Juan Romero & Borrell, 2015; Fernández et al., 2016; Llinares-Benadero & Borrell, 2019).

13.3. Extracellular matrix role in cortical expansion and folding

Many intrinsic factors are considered candidates for cortical expansion and folding, but one important candidate that has emerged recently is the extracellular matrix (ECM). ECM represents the scaffold of protein network that surrounds cells during development. It is

present in the developing neural tissue of many species. Recently, ECM has been revealed to play a more complex role in cortical development than previously assumed (**Fig. 23**).

ECM plays a major role in cell proliferation, migration, and cortical folding (Amin & Borrell, 2020; Long & Huttner, 2019). Transcriptomic studies performed on germinal cortical layers in lissencephalic (mice) and gyrencephalic (human, ferret, macaque) species showed an increase of ECM components in the latter compared to the former. This suggests that ECM could have been attributed to the evolutionary expansion and folding of the cerebral cortex (Fietz et al., 2012; Florio et al., 2016; Pollen et al., 2015).

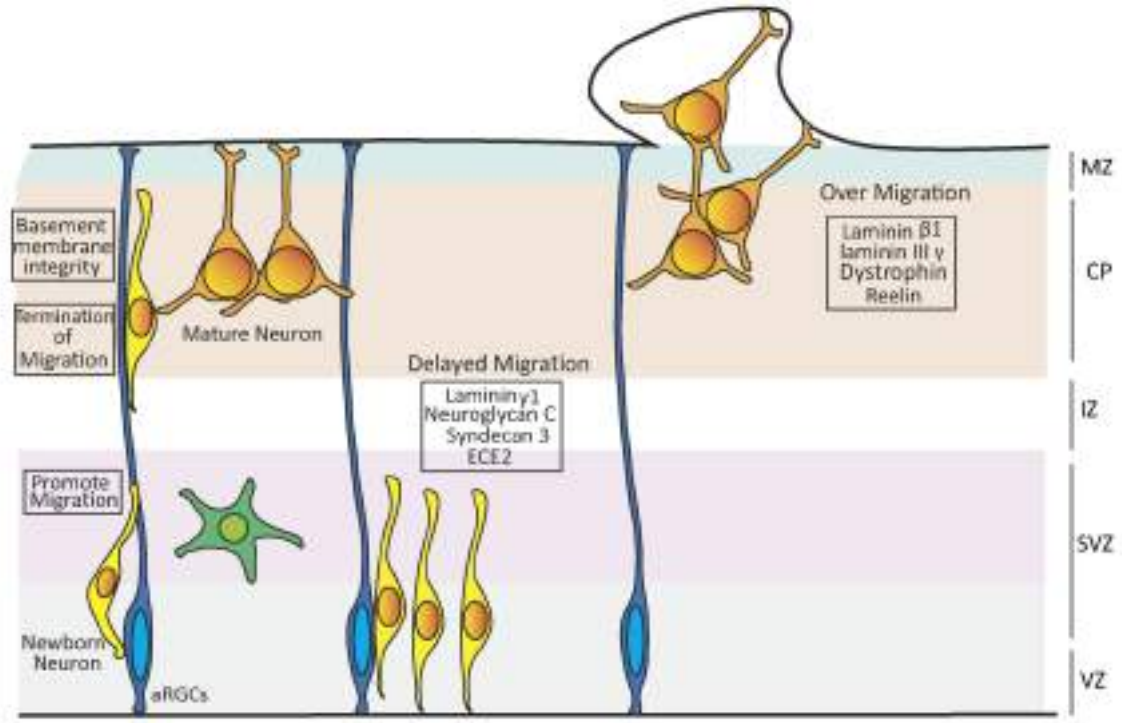

Figure 23. A schematic representation demonstrating the role ECM plays in neuronal migration. ECM components influence migration promotion and termination, as well as the integrity of the basement membrane in the developing cortex of mice. Depletion of Laminin, Neuroglycan, and Syndecan 3 results in migration delay, whereas depletion of Laminin 1, Laminin III, Dystrophin, and Reelin results in over migration and basement membrane rupture (Amin & Borrell, 2020).

Studies manipulating ECM components (such as: Perlecan, syndecan, chondroitin sulphate proteoglycan (CSPG) that are expressed in the germinal layers of the mouse developing cortex, affected progenitor proliferation and differentiation (Maeda, 2015; Park et al., 2003; Sirko et al., 2010). Moreover, ECM components influence INM of aRGCS. This role is evolutionary conserved, as manipulating laminin γ1 analogue in zebrafish and β1 integrin receptor in mouse VZ affected INM and aRGCs attachment to the apical surface (**Fig. 24**).

On the other hand, loss of function experiment of integrin αvβ3- another laminin receptor- led to an exclusive significant decrease in bRGCs in the developing ferret cortex. This showed that ECM is essential for bRGCs abundance in the OSVZ in gyrencephalic species (**Fig. 24**) (de Juan Romero et al., 2015; Dehay et al., 2015; Fietz et al., 2010).

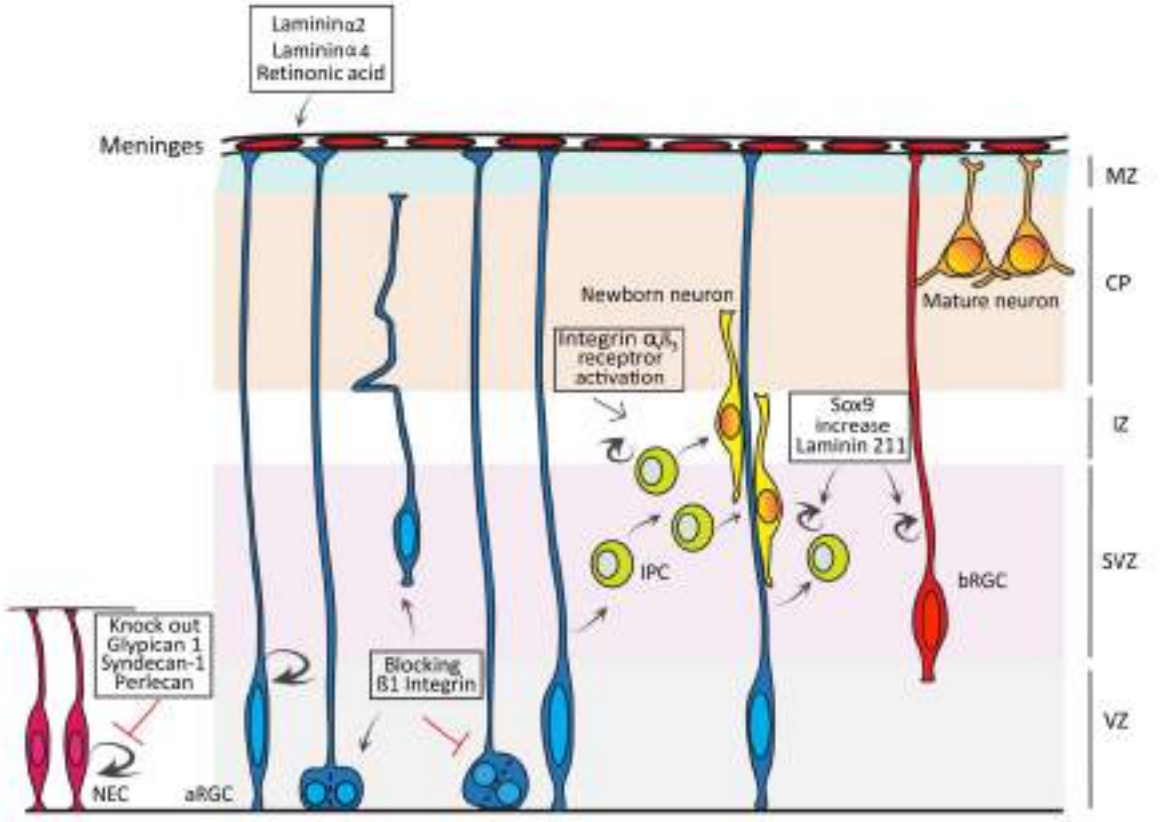

Figure 24. A schematic representation showing the role ECM components play on progenitors in the developing cortex. Neuroepithelial cells (NECs), apical radial glia cells (aRGCs), basal radial glia cells (bRGCs), and intermediate progenitor cells are all affected by ECM components (IPCs). NEC proliferation is reduced when Glypican 1, Syndecan-1, and Perlecan are depleted. Blocking β1 Integrin causes aRGCs to detach from the apical surface and impairs asymmetric division in the VZ. The loss of Laminin α2, Laminin α4, and Retinoic acid from the external meninges reduces aRGC attachment to the basement membrane. Integrin $\alpha v\beta^3$ upregulation increases the production of IPCs as well as their rate of cell cycle entry. Sox9 activation leads to an increase in bRGC proliferation via Laminin 211.(Amin & Borrell, 2020).

To add to this, ECM components HAPLN1, Lumican, and Collgen I have been shown to induce cortical plate folding in human fetal explant cultures (Long et al., 2018). These findings suggest the crucial role ECM plays in the morphology of the cerebral cortex.

Taken together, all these data show the role ECM plays in regulating progenitor proliferation, basal progenitors' abundance, increasing the rate of neurogenesis, and the emergence of cortical folding.

14. Direct vs Indirect neurogenesis in ammonite cortical development

The emergence of indirect neurogenesis plays an important role in the evolutionary expansion of the cerebral cortex (De Juan Romero & Borrell, 2015; Kriegstein et al., 2006). The generation of IPCs and their migration to the SVZ provided the developing cortex with the necessary neuronal output essential for the cortex's six-layer layout (Miyata et al., 2010). The development and expansion of the cerebral cortex in amniotes necessitated a shift from direct to indirect neurogenesis. This interchange from direct to indirect neurogenesis was accompanied with an abundant increase in IPCs and an aberrant suppression of direct neurogenesis as a mode of differentiation utilized by aRGCs. Observing repitle pallium development, we find that it is completely devoid of IPCs (Verónica Martínez-Cerdeño et al., 2012; Nomura & Hanashima, 2014), suggesting that all the neurons are produced via direct neurogenesis. The neuronal output produced by direct neurogenesis is further reduced due to the longer cell cycle, hence leading to the formation of a rudimentary three-layered cortex. Recently, experiments manipulating the levels of Robo1 and Dll1 expression, by repression Robo1 expression and overexpressing Dll1, in snake pallium led to an increase in IPCs and a formation of a de novo SVZ. This suggests that reptiles use direct neurogenesis as a default mode of division (Cárdenas et al., 2018). Moving onto birds, specifically in chicken cortical development, their SVZ exhibit a small number of basal mitoses and have $Tbr2^{+}$ IPCs (Charvet et al., 2009; Cheung et al., 2007; Martínez-cerdeño et al., 2017). This observation suggests that the emergence of basal mitosis and its tendency to favour indirect neurogenesis in birds lead to the aberrant expansion of their pallium compared to reptiles. Interestingly, overexpressing Robo1/2 and knocking out Dll1 expression in chick pallium, induced direct neurogenesis and decreased basal mitosis. The limited period of neurogenesis is limited in birds and reptiles, where it ranges from (2-4) days, while mammals have a more extended period (7 days in mice to 21 weeks in humans), Taking all these factors into consideration suggests that the concurrence of direct neurogenesis and a short neurogenic period.

In mammals, IPCs are the major source for neuronal production. Direct neurogenesis was repressed in mammalian cortex to only generate around 10-20% of neurons. The evolutionary expansion of the cortex involved the suppression of Direct neurogenesis, the emergence of

IPCs, BPs, and their various subtypes (Kalebic et al., 2019) and their higher self-proliferative capacity. These factors greatly increase the final neurogenic yield. The molecular mechanisms generating basal progenitors still remain poorly understood. Transcriptomic analysis and new technologies were able to uncover some molecules implicated in basal progenitor proliferation. Among these molecules are: Cux2, Tbr2, Dll-Notch, Shh-Smo, Robo receptors, Fgfr3, Arx, Magoh, Trnp1 and others (Borrell et al., 2012; Colasante et al., 2009; Cubelos et al., 2008; Martínez-cerdeño et al., 2017). Basal progenitor generation includes detachment from AJs and delamination from the VZ; it also has been proposed that oblique and horizontal divisions of aRGCs produce basal progenitors. During evolutionary expansion of the neocortex, direct neurogenesis is repressed, and there is a change in genetic and epigenetic signatures that allows the generation of basal progenitors. In addition to a significant change in cell cycle, especially during cell cycle re-entry, where basal progenitors are able to self-proliferate many times before entering self-consuming neurogenic division. IPCs divisions observed in mouse cortex showed that they undergo only one round of divisions to produce two neurons, while in primates, basal progenitors undergo numerous self-proliferative divisions (Betizeau et al., 2013). Hence, this developmental mechanism has a significant impact on producing a much larger number of neurons per aRGC, resulting in greater cortex expansion (De Juan Romero & Borrell, 2015; Llinares-Benadero & Borrell, 2019).

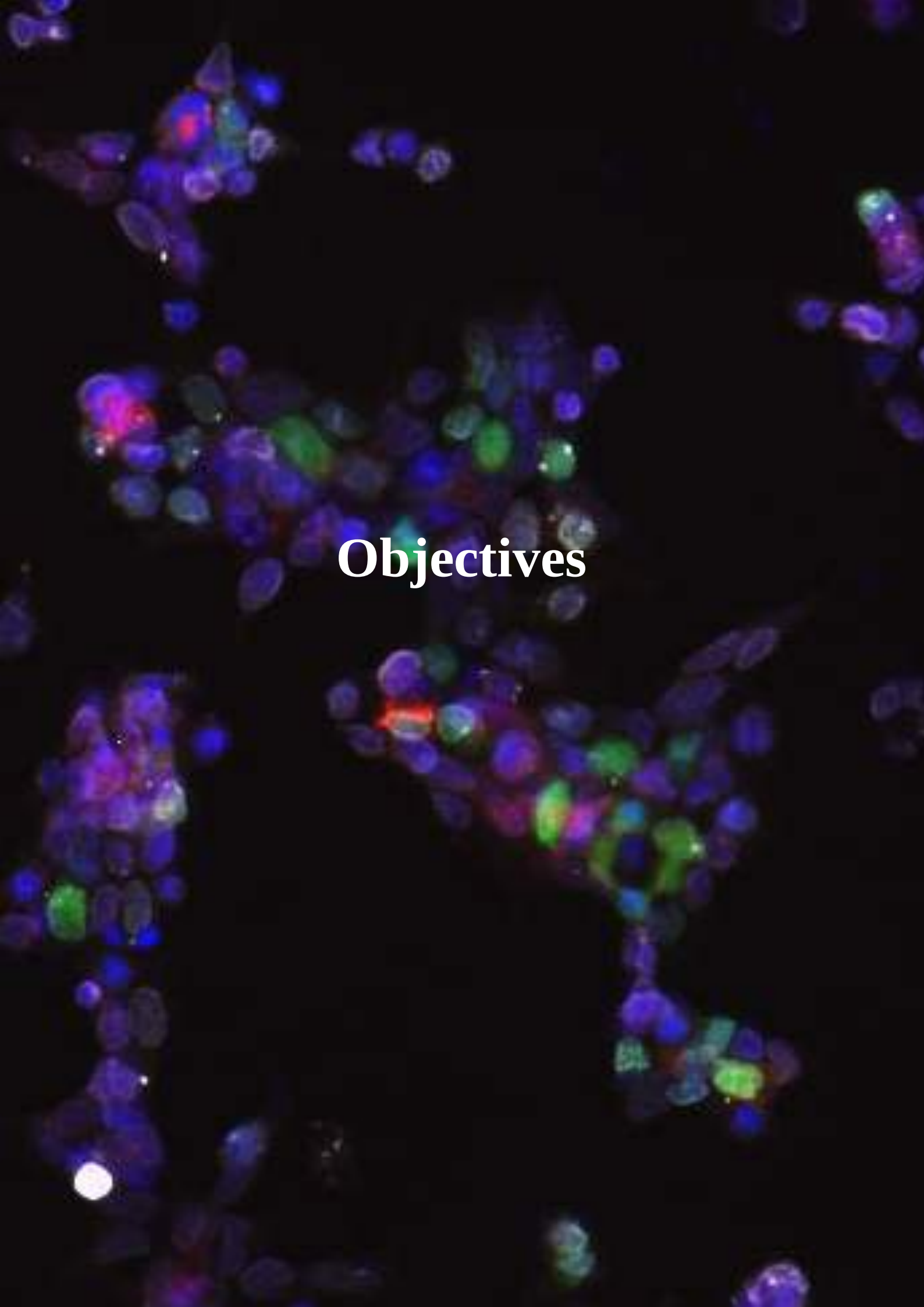

Objectives

Objectives

The primary goal of this project is to identify and characterise the signalling cascade initiated by Robo1/2 ICD to induce Direct neurogenesis, with a particular focus on proteins interacting with Robo and their evolutionary relevance. In order to address this question, we set the following specific objectives:

1. To characterize and compare the transcriptomic profiles and trajectories of progenitor cell types in the mouse developing NCx and OB, as paradigmatic examples of indirect and direct neurogenesis respectively.

2. To identify proteins interacting with the intracellular domain (ICD) of activated Robo1/2 receptors.

3. To study the subcellular localization of Robo1/2-ICD, and its link to Direct neurogenesis.

4. To characterize transcriptional changes in mouse cortical progenitors undergoing Direct neurogenesis as a result of Robo-ICD signaling, and the functional link between Robo and gene transcription.

5. To understand how the interaction of Robo-ICD with nuclear proteins drives Direct neurogenesis in mouse and during amniote evolution.

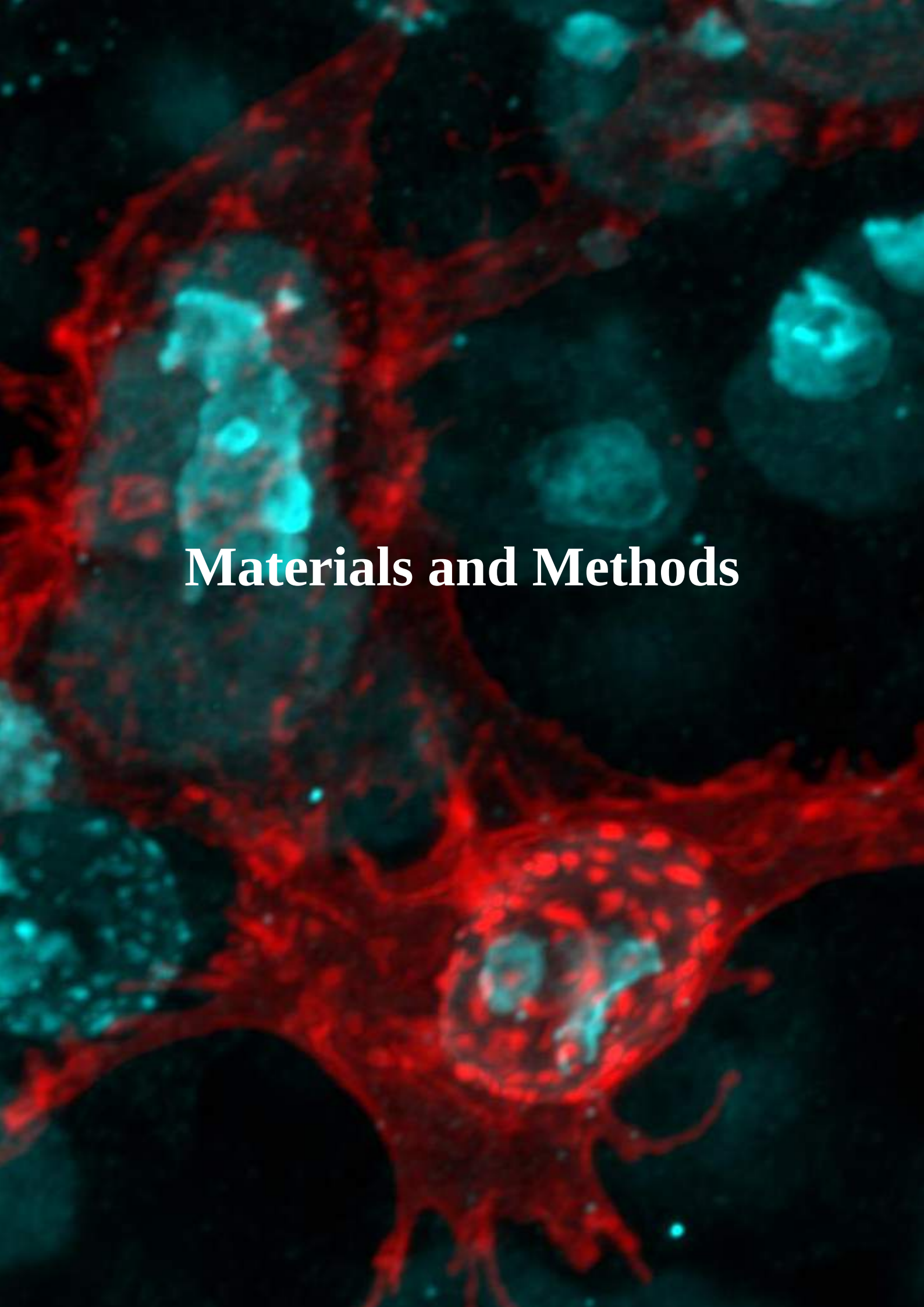

Materials and Methods

Materials and Methods

1. Cell culture

P19 cells were a gift from the lab of Dr.Vijay Twari's (Queen's university, Belfast, UK). The cells were cultured in Growth medium which consists of (MEM α, nucleosides (Thermo fisher, ref: 12571063) with FBS 10% (Thermo fisher, ref: 16140071), 1% Glutamax (Gibco, ref: 35050038), 1% penicillin-streptomycin (Gibco, ref: 15140122)). Cells were incubated in an incubator with a tightly regulated temperature at 37℃ and 5% CO2 with saturating humidity. The cells were regularly checked and routinely tested for mycoplasma. Confluent cells were split (1:3) using Trypsin-EDTA (0.25%) (Gibco, ref: 25200072).

P19 cells were transfected using Lipofectamine 2000 (Thermo fisher ref: 11668019). First, we plated 5×10^6 cells in a T75 flask (Corning, ref: 353136). On the next day transfections were carried out using plasmids pCAG-Robo1-flag (Vector builder), pCAG-Robo2-flag (Vector builder) and Crispr Dll1 and the negative control PCAG-EGFP (a generous gift from the Gage lab (Salk institute for biological science, USA) with Lipofectamine 2000 (Thermo fisher, ref: 11668027). We left the transfection complexes at room temperature (RT) for 20 minutes. After applying the transfection complexes to the cells, the transfected flasks were left in the incubator for 5 hours, and then medium was changed. Cells were left post transfection for 48 hours, and then we proceeded with cell lysis followed by protein quantification, immunoprecipitation, and western blot.

2. Mouse Primary culture and transfection

The neocortex was isolated from the brains of E12.5 wild type (WT) ICR embryos. The neocortical tissue was dissociated by incubating it in trypsin, 0.25% -EDTA, and DNAse at 37 ^{o}C for 8 minutes, followed by gentle trituration with a P200 pipette. Dissociated cells were plated on glass coverslips coated with poly-lysine at a density of 65 X 10^3 cells per coverslip. Next, cells were cultured in Ns5 medium (DMEM glutamax media (Gibco, ref: 21969-035),1% pencillin- streptomycin,0.5% N2 supplement (Thermofisher, ref: 17502048), 1% B27 (Thermofisher, ref:12587010),0.1% bFGF (Peprotech, ref:100-18B), 0.1% EGF (Peprotech, ref: AF-100-15) and incubated at 37 ^{o}C and 5% CO2. Lipofectamine 2000 (Invitrogen) was used to transfect primary dissociated cell cultures with Robo1-Flag + Robo2-Flag. Two days after transfection, cells were fixed for 10 minutes in 4% PFA and 4% sucrose solution for immunofluorescence assays.

3. Experimental model animals

Wild type mice (*Mus musculus*) were kept in an Institute of Cancer Research (ICR) genetic background. Cell culture and expression analysis experiments were carried out on ICR mice. Mice were kept at the animal facility of the Instituto De neurociencias de Alicante, at a standard 16h:8h dark/light cycle, in accordance with Spanish regulations (RD 53/2013) and European Union regulations. The Universidad Miguel Hernández Institutional Animal Care and Use Committee (IACUC) approved the experimental protocols. The embryonic day (E0.5) was the day of the vaginal plug. All of the animals used in this study were tested naive, with no previous procedures performed on them.

Fertilized chicken (*Gallus gallus*) eggs were obtained from a poultry farm in Córdoba (Granja Santa Isabel) and incubated at 38oC. Day 0 post-ovoposition was defined as the day of lay (dpo).

Fertilized snake eggs (*Lamprophis fuliginosus*) were obtained from a breeding colony affiliated with Dr. Michel C. Milinkovitch's lab at the University of Geneva and stored in accordance with Geneva Canton regulations (authorization 1008/3421/1R). The day of lay was considered 0 dpo, and eggs were maintained at 28ºC under humidity.

4. Constructs

For overexpression experiments, we used pCAG mRobo1-Myc, pCAG mRobo2-Myc and crispr Dll1 constructs (Cárdenas et al., 2018). These constructs are expressing a myristoylated (Myr(m)) sequence that facilitate the tagged Robo intracellular domain attachment to the memebrane. We designed mRobo1-Flag and mRobo2-Flag under pCAG promtor, and CMV GFP to identify transfected cells (purchased from vector builder). We used a GFP encoding construct downstream of a CAG promoter into an MMLV retroviral packaging vector in the control samples (a generous gift from F.H. Gage).

Crispr plasmids for knocking out Nup107 expression in mice and chicken were created by annealing the following oligomers into the pSpCas9(BB)-2A-GFP plasmid (PX458, Addgene) after a BbsI digestion as described in Zhang Lab's protocol.

4.1. The following newly designed guides were used:

Ms Nup107 F: CACCGGGGCTTCCGCTCTCTGTGCC
Ms Nup107 R: AAACGGCACAGAGAGCGGAAGCCCC
Ck nup107 F: CACCGAATCATCTGATGCGTTCGTT
CK nup107 R: AAACAACGAACGCATCAGATGATTC

The pSpCas9 (BB)-2A-GFP plasmid (PX458, Addgene) without crispr guide was used in the control knockout experiments.

For mRobo1 and mRobo2 cytoplasmic domain truncated constructs, mRobo2-Myc truncated plasmids (R2D1 ,R2D2, R2D3) were a generous gift from Dr.Le Ma (Thomas Jefferson University, USA). We designed mRobo1 cytoplasmic domain truncated plasmids (R1D1, R1D2,R1D3). mRobo1 myc plasmid was cut in two restriction sites using NotI and BtgZI (NEB, ref: R0189S, R0703S), backbone vector was gel purified to be used for all constructs. We designed primers for the different mRobo1 fragments that contain the myr truncated cytoplasmic domain and myc tag using the Nebuilder® assembly tool.

4.2. Gibson assembly myr Robo 1 truncated cytoplasmic domain primers:

MYR F: GTCTCATCATTTTGGCAAAGGAATTCGCGGCCGCTAGC
CC0 R: CTTGTCGTCATCGTCTTTGTAGTCGTCCACATCACCATAAACAGTTGAC
MYC F: GACTACAAAGACGATGACGACAAGTGGCGGCCGCTCGAGTCT
MYC R: ATTTTTGGCAGAGGGAAAAAGATCTCAGTGGTATTTGTGAGCCAGGG
CC1 R: CTTGTCGTCATCGTCTTTGTAGTCGATGAGCTGCGTGGTGGC
CC2 R: CTTGTCGTCATCGTCTTTGTAGTCTGGGGGAGGATGCGCTGG

Fragments were generated using Xpert high fidelity DNA polymerase kit (Grisp, ref: v7E502), and gel purified. A fragment vector mixture was prepared with a 2:1 fragment to vector-ratio. Gibson buffer 2A was added to this mixture and incubated for 30 minutes at 50^0C. The generated plasmids were then transformed and sequenced to validate them.

5. Immunoprecipitation

Two days post-transfection with the plasmid combination mentioned above we removed the medium from the cells and washed them twice with cold 1X DPBS (Thermofisher, ref: 14190144). Whole cell protein was extracted by scraping cells using 500 µl of HSBN lysis

buffer (10 mM HEPES-KOH pH 7,4 (Sigma, ref: H4034), 150 mM NaCl (VWR, ref: 27810.295), 1% Nonidet P40 (Applichem, ref: A1694.0250), one Tablet complete EDTA-free (Roche, ref: 04693159), one Tablet PhosStop (Roche, ref: 04906837), 100 µg/ml DNaseI (Applichem, ref: A3778.0050 10mg), 100 µg/ml RNaseA (Applichem, ref: A2760.0500 10mg)). Cells were sheared using 0.55 needle gauge. Cell lysate was then centrifuged at 16 × 10^3g at 4 ^{O}C. The cleared lysate was then transferred to precooled tubes. After that, 40 µl of anti m2 flag sigma magnetic beads (Millipore, ref: M8823) were added to the cell lysate to pull down Robo1 ICD flag and Robo2 ICD flag. The tubes were placed in a rotating shaker at 30 rounds per minute (rpm) speed at 4 ^{O}C for 1 hour. After incubation, the magnetic beads were washed once with HSBN lysis buffer using a magnetic rack (Sigma, ref: 20-400) followed by two washes with HBS buffer (10 mM HEPES-KOH pH 7.4, 150 mM NaCl, 1 Tablet PhosStop). In order to elute the protein bound to the beads, we added 40 µl of Glycine PH 2.8 (Sigma, ref: G8898) four times consecutively and left them to incubate for five minutes in between elutions, excluding the first quick elution. Next, we saved 30µl of the eluted protein for immunoprecipitation validation, and the remaining eluted protein was stored at -20 ^{O}C and shipped for mass spectrometry analysis.

6. Western Blot

We used the Pierce^{TM} BCA protein assay kit (Thermo fisher, ref: 23227) for protein quantification. Protein samples were denatured with 1X Laemmli buffer for 5 minutes at 95 ^{O}C. 30 µg of protein samples were resolved on 8% SDS-PAGE gel for 2.5 hours at 100 mV in 1X Running buffer (25mM Tris base (Sigma, ref: T1503-1KG), 190mM glycine (Sigma, ref:G8898-1KG) and 0.1%SDS (Sigma, ref: L3771-100G)) using the Mini Protean® electrophoresis system (Biorad, ref: 1658005EDU). Following that, A 0.45-m nitrocellulose membrane was used to transfer the proteins (GE Healthcare Life Science, ref: 10600002) via overnight wet transfer at 4 ^{O}C and 30 V using a mini Trans-blot ® electrophoretic transfer cell (Biorad, ref: 170-3930) and already cooled transfer buffer (25 mM Tris base, 190 mM glycine, 0.1% SDS, and 20% Methanol (JTBaker, ref: 8405). The membrane was blocked in 5%BSA (Sigma, ref: A9576-50ML) dissolved in TBST 0.25% (20mM Tris-HCl (Sigma, ref: T3253-1KG), 150 mm NaCl, 0.25% Tween 20 (Sigma, ref: P7949-500ML)) for 1 hour. Membranes were incubated with antibodies diluted in 5% BSA TBST overnight at 4 ^{O}C. The following day, membranes were washed 4X with TBST 0.25% for 15 minutes; after that, membranes were incubated with secondary peroxidase antibody for 45 minutes at Room temperature. The membranes were then washed four times for 15 minutes with TBST 0.25%.

In order to develop the membranes, we applied Chemiluminescent HRP substrate (Millipore, ref: WBKLS0100). Images were captured using Amersham Imager 680 Bio imager (GE healthcare, ref: 29270771).

Primary antibodies: anti flag M2 (1:1000, Mouse monoclonal, Sigma, ref: F1804), anti Nup107 (1:5000-1:1000, Sigma, ref: SAB3500333), anti Gadph (1:5000,mouse monoclonal, Santa Cruz biotechnology, ref: sc-32233), ant lamin B1 (1:1000, rabbit polyclonal, Abcam, ref: ab220797), Anti-Robo2 Antibody, clone 4C6.1 (1:500, mouse monoclonal, Sigma, MABN122), anti Robo1 (C-terminal region) Antibody (1:500, rabbit polyclonal, ECM biosciences, RP2791)

Secondary antibodies: peroxidase conjugated anti-mouse IgG, IgM (H+L) (1:10000, Thermo fisher, ref: 31444), peroxidase conjugated anti-rabbit IgG (H+L) (1:0000, Thermo fisher, ref: 31462).

7. Protein nuclear fractionation

For nuclear fractionation assay, P19 cells transfected with the plasmid combination mentioned above were used to detect mRobo 1/2 flag. Native P19 cells were used to detect native Robo1/2 cytoplasmic terminals. Cells were trypsinized with (0.25%) Trypsin-EDTA and resuspended in 10 ml growth medium. Cells were pelleted by centrifuging at 100 X g for 5 minutes. The pellet was washed twice with 1X DPBS. Next 4X pellet volume was added to the pellet of B10 buffer (10 mM HEPES-KOH pH 7.9,10 mM KCl (VWR, ref: 26759.291),5 mM $MgCl_2$ (VWR, ref: 25108.295), 0.5 mM EDTA (Sigma, ref: ED-100G),0.5 mM mercaptoethanol (Thermo fisher, ref: 31350-010), 1 tablet complete EDTA-free, 1 tablet PhosStop). This was followed by 10 minutes of incubation on ice, then by douncing the lysate 40 times using a 100 µl mini homogenizer (GPE, ref: 20404). Next, the lysate was centrifuged at 500 X g for 5 minutes at 4 ^{O}C and the supernatant was saved afterwards as the cytoplasmic and membrane fraction. To extract the cytoplasmic fraction the previous supernatant was centrifuged at 10 min 16000 x g at 4°C and supernatant saved as cytoplasmic fraction. The pellet remaining from the previous step was washed twice with B10/200 buffer (10 mM HEPES-KOH pH 7.9, 10 mM, 10 mM 0.5 Mm KCl (Panreac, ref: 131232.12), 200mM Sucrose, 0.1% NP-40, 5 mM $MgCl_2$, EDTA (Sigma, ref: ED-100G), 0.5 mM β-mercaptoethanol (Thermo fisher, ref: 31350-010), one tablet complete EDTA-free, one tablet PhosStop). The pellet was then resuspended in 500 µl of B10/200N buffer which was overlayed on 2ml of B10/800 (10 mM HEPES-KOH pH 7.9, 10 mM KCl, 800 mM Sucrose, 5

mM MgCl 2, 0.5 mM EDTA, 0.5 mM MeSH, Protease and Phosphatase Inhibitor) buffer cushion. The mixture was centrifuged at 2500 x g during 10 minutes at 4°C. The nuclear pellet was extracted by adding B400 buffer(10 mM HEPES-KOH pH 7.9, 0.5% NP-40, 10 mM KCl, 400 mM NaCl, 5 mM MgCl 2, 0.5 mM EDTA, 0.5 mM MeSH, 20% Glycerol, DNase. RNase, Protease and Phosphatase Inhibitor) 4X times the pellet volume and sheared through 0.5 mm gauge needle. The nuclear extract was centrifuged 10 min 16000 x g at 4°C. The supernatant from this step is the nuclear extract of the protein lysate.

8. Immunofluorescence

Upon reaching the desired embryonic stage, cervical dislocation was used to sacrifice pregnant female mice. We fixed the brains for 30 minutes to 1 hour using 4% Paraformaldehyde (Sigma, ref: 441244-1KG) dissolved in 0.1 phosphate buffer (PH 7.4) at 4 ^{O}C. Next, we cryoprotected the brains using 30% sucrose (Panreac, ref: 131621.0914) solution dissolved in 1X PBS PH 7.4 followed by immersion in Cryo-Medium NEG-50 (Thermo fisher, ref: 6502). Brains were frozen and sectioned at 20 µm thickness using cryostat and collected in super frost slides (Thermo fisher, J1800AMNZ).

Slides were left to dry at 37 ^{O}C for 3 hours, then sections were washed with 1X PBS and permeabilized with 1X PBS-T (0.25% Triton (Sigma, ref: T8787-250ML)). Next, sections were incubated with blocking solution (normal horse serum 10% (Gibco, ref: 16050), Triton 0.25%, and 0.25% BSA) dissolved in PB 0.1M for 2 hours, and slides were incubated with primary antibodies dissolved in blocking solution at the proper concentration overnight at 4 ^{O}C. The following day, sections were washed with 1X PBS-T and incubated with the suitable fluorophore conjugated secondary antibody at the proper concentration for 2 hours at RT. Sections were counterstained with Dapi (4′, 6-Diamidine-2′-phenylindole dihydrochloride) (Sigma, ref: D9542-5mg). Finally, sections were then dehydrated using a series of alcohols and mounted with coverslips using Entellan mounting medium (Sigma, ref: 1.07960).

For immunofluorescence of cells *in vitro*, cells were fixed with 4% PFA and 4% sucrose for 10 minutes at RT. Cells were then washed with 1X PBS and permeabilized for 20 minutes with 1X PBS-T 0.25% before being incubated for 1 hour with blocking solution. This was followed by incubation with the primary antibody overnight at 4 ^{O}C. The following day, cells were washed with 1X PBS-T and incubated with fluorophore-conjugated secondary antibodies for 2 hours at RT. Cells were counterstained with Dapi and mounted using MOWIOL® (Calbiochem, ref: 475904).

Primary antibodies	Host	Concentration	Company	Reference
GFP	Chicken	1:1000	Aves lab	(GFP-1020)
His	Mouse	1:1000	Thermo scientific	(37-2900)
Tuj1	Mouse	1:1000	Covance	(MMS-435P)
Tbr1	Rabbit	1:750	Abcam	ab31940
Ph3	Mouse	1:1000	Sigma	05-806
Pax6	Rabbit	1:500	Sigma	AB2237
Myc	Rabbit	1:500	Santa Cruz	sc-789
Flag	Mouse	1:1000	Sigma	F3165
Robo 1 CT	Rabbit	1:500	ECM biosciences	RP2791
Sox2	Goat	1:400	R&D systems	AF2018

9. *In situ* Subcellular Fractionation

P19 cells were seeded at a density of 65,000 cells per well on polylysine-treated coverslips in a 24 well plate (Falcon, ref: 353047) and incubated at 37 ^{o}C, 95% humidity, and 5% CO_2. Cells were transfected with the plasmids indicated in each experiment after 24 hours in culture using Lipofectamine 2000 (Invitrogen). Two days post transfection; cells were washed twice with ice cold 1X PBS while tilting the plate. For immunofluorescence assays, coverslips representing whole cells were fixed in 4% PFA and 4% sucrose solution for 10 minutes. To remove the cytoplasmic fraction and the loosely held nuclear fraction, 200µl CSK buffer (10mM PIPES (P6757-25G), 300mM Sucrose, 100mM NaCl, 3mM MgCl2, 1mM EGTA (Sigma, ref: E4378-10G)) + 0.1% (V/V) Triton X-100) was applied directly onto each remaining coverslip and incubated on ice for 1 minute. The tightly held nuclear fraction was washed with ice cold 1X PBS, fixed for 10 minutes with 4% PFA and 4% sucrose solution, and saved for immunofluorescence assays. Next, to remove the tightly held nuclear fraction, the remaining coverslips were washed with ice cold 1X PBS for 1 minute, and 200µl CSK buffer + 0.5% (V/V) Triton X-100 was applied directly onto each remaining coverslip and incubated on ice for 20 minutes. The chromatin fraction was washed with 1 ml of ice cold 1X PBS and fixed with 4% PFA and 4% sucrose solution for 10 minutes for immunofluorescence assays (Sawasdichai et al., 2010).

10. Probe cloning for *in situ* hybridization

For ISH probe synthesis, RNA was extracted from E12.5 or E14.5 mouse cortex, chick (Gallus gallus) E6 dorsal pallium, and snake (Lamprophis fuliginosus) E8 pallium using the RNeasy mini kit (Qiagen, ref: 74104). cDNA was generated using maxima first strand kit (Thermofisher, ref: K1641). PCR products of DNA fragments targeting different genes were generated using Gotaq flexi DNA polymerase (Promega, ref: M8305). PCR products were purified from agarose gel using illustra GFX kit (GE healthcare, ref: 28-9034-70). PCR products were ligated into PGEM-T vectors or PGEM-T easy vectors using Promega T4 ligase (Promega, ref: A3600, A1360, M1801). Ms Robo1, Ms Robo2, MsDll1, Ms Hes1, Ms Hes2, Ms Pax6 *in situ* probes were previously designed in the lab (Cárdenas et al., 2018).

10.1. Primers:

CK Nup107 ISH F: TCTGCTCGGCAATCAGTCAA
CK Nup107 ISH R: AACAGGCTGTACCTCGTTTCC
Ms Nup107 ISH F: GAGCCGAAGCCTACTGAGAC
Ms Nup107 ISH R: CTAATGGGAGCGTCTGGGTC
Ms Ptprz1 ISH F: AGGCTTAACAGTTCCTCACTCG
Ms Ptprz1 ISH R: AAAGCGACCCCTATCTATGTCA
Ms Hey2 ISH F: GAGAAAGAGAAGAAGCAGGCAA
Ms Hey2 ISH R: GTTTATCGCTTTCTCCACACAG
Ms Tbr1 ISH F: CACTCGCTCTTTCACTTGACC
Ms Tbr1 ISH R: GGAGTGGGGTCTGAAAAGATAG
Ms Etv4 ISH F: TGACTCCCCCAGACAAATCG
Ms Etv4 ISH R: GAGCGGCTCAGCTTGTCATA
Sn Nup107 ISH F: GGCCCAAAGACTCTGCAAAAG
Sn Nup107 ISH R: GCAGTGTGCTTCTCACATACT

11. *In situ* Hybridization

Overnight, brains were fixed in 4% paraformaldehyde (PFA) in PB pH7.3 at 4 ºC overnight. Brains were cryoprotected with 30% sucrose solution, then frozen and sectioned at 20 µm in Cryo-medium Neg-50 (Thermo Scientific).

According to the manufacturer's instructions, sense and anti-sense cRNA probes were synthesised and labelled with digoxigenin (DIG; Roche Diagnostics). In situ hybridization (ISH) was carried out as previously described (Reillo et al., 2011). Briefly, frozen brain

sections of E12.5 ICR mouse, E6 chick embryos and E8 snake embryos were hybridized with DIG-labeled cRNA probes overnight in hybridization solution [50% formamide (Ambion), 10% dextran sulfate, 0.2% tRNA (Invitrogen), 1x Denhardt's solution [from a 50× stock; SIGMA), 1x salt solution (containing 0.2 M NaCl, 0.01 M Tris, 5 mM NaH2PO4, 5mM Na2HPO4, 5 mM EDTA, pH 7.5)]. Next, sections were washed with washing buffer and blocked for 2 hours at room temperature in MABT buffer solution 1x, 10% sheep serum, 10% blocking reagent. Sections were incubated with alkaline phosphatase-conjugated anti-digoxigenin antibodies (Roche, ref: 11093274910). Signal visualization of the labeled cRNAs dig probes was performed by incubating the sections in a nitroblue tetrazolium (NBT)/5-bromo-4-chloro-3-indolyl phosphate (BCIP) solution [3.4 µl/ml from NBT stock and 3.5 µl/ml from BCIP stock in reaction buffer (100 mg/ml NBT stock in 70% dimethylformamide; 50 mg/ml BCIP stock in 100% dimethylformamide; Roche)].

12. *In utero* electroporation

At embryonic day E12.5, mouse embryos were electroporated *in utero* in the neocortex. Pregnant women were deeply anaesthetized with 2-2.5% isoflurane and their uterine horns were exposed. Using pulled borosilicate glass micropipettes (Ref #WPI 1B150F-4), DNA solution (approximately 1L) was injected into the lateral ventricle, and square electric pulses (30-35V, 50ms on - 950ms off, 5 pulses) were applied with an electric paddle (Cuy21EDIT Bex C., LTD) using round electrodes (CUY650P5, Nepa Gene or CUY650P7, Nepa Gene).

The following plasmid concentrations were used: 0.25 ug/l Nup107 MS crispr, 0.25 ug/ul empty MS crispr, and 0.7 ug/ul GFP.

1ug/µl of mR1 flag, 1ug/µl mR2 flag, 1ug/µl Crispr Dll1, 1ug/µl GFP, 1ug/µl mR1D1, 1ug/µl mR2D1, 1ug/µl mR1D2, 1ug/µl mR2D2, 1ug/µl mR1D3, 1ug/µl mR2D3, 1ug/µl GFP.

13. In-ovo electroporation

Fertilized eggs were incubated as previously described until 4 dpo for chicken *in ovo* electroporations. A small window was opened in the eggshell the day before electroporation, and 2ml of albumen was aspirated to allow for further manipulation. DNA solution was injected into the lateral telencephalic ventricle of embryos at 4 days post-ovoposition (dpo), and square pulses (30 V, 5 ms, 5 pulses each 500 ms) were applied with an electric stimulator (TSS20 OVODYNE ELECTROPORATOR, MCI) using round electrodes (CUY650P3, Nepa Gene).

Electroporated embryos were then left to developing under the same temperature and humidity conditions. Embryos were fixed for 1 hour in cold 4% PFA, and their brains were processed for immunofluroescence.

Plasmid concentration used: 1 ug/ul of Nup107 CK crispr, 1 ug/ul crispr empty, 0.7 ug/ul GFP.

14. Mass spectrometry

Elutes from co-IP experiments in 0.1M glycine were adjusted to pH 7.5-8 with 1 M Tris. Subsequently, proteins were digested in-solution with trypsin and Lys-C and analyzed by nanoflow LC-MS/MS according to procedures described previously (Groessl et al., 2012; Shevchenko et al., 1996; Vasilj et al., 2012) with slight modifications. In brief, digestion was performed with 2x 200ng trypsin (Trypsin Gold, Promega) for 16-24h each followed by digestion with 100ng rLys-C (Promega) for another 16-24h. Digests were desalted by C-18 UltraMicroColumns (Nest Group) and subsequently dried, and stored until analysis at -20°C. For LC-MS/MS analyses the peptides were recovered in 3µl 30% formic acid supplemented with 25fmol/µl standard peptides (Retention Time Calibration Mixture, Thermo Pierce), diluted with 20µl of water and 5µl were injected. NanoLC-MS/MS analyses were performed with a Q-Exactive HF mass spectrometer (ThermoScientific, USA/Germany) hyphenated to a nanoflow LC system (Dionex3000 RSLC, ThermoDionex, Germany). Peptides were separated in a linear gradient of 0.1% aqueous formic acid (eluent A) and 0.1% formic acid in 60% acetonitrile (eluent B) for 120min and the mass spectrometer was operated in data-dependent acquisition mode (DDA, TopN 10). Label-free quantitative analysis based on the most intense peptide ions (MI3/HI3) was carried out with the Progenesis QIP V4.2 software (Nonlinear Dynamics, Newcastle u.T., UK) (Groessl et al., 2012; Silva et al., 2006). Protein identification was performed with Mascot V2.6 (Matrixscience, UK) (Perkins et al., 1999).

15. Luciferase assay

P19 cells were cultured and transfected as mentioned above. One-day post transfection, cells were treated for the detection of luciferase and Renilla activity. Briefly, cells were washed, and whole cell extracts were obtained using PLB lysis buffer (Promega). The signal was detected with a Berthold luminometer using the Dual-Luciferase® Reporter Assay (Promega). Constructs used for transfection were: Dll1 Luc (Castro et al., 2006), RL-CMV (Promega),

empty vector pCI (Promega),mRobo1 flag, mRobo1 myc, Jag1 (Cárdenas et al., 2018), and GFP.

16. FACS sorting for Bulk RNA sequencing analysis

16.1. Bulk RNA sequencing from embryonic cortical tissue: E12.5 electroporated mouse embryos with mRobo1, mRobo2, Crispr Dll1, GFP and GFP for negative control were used for this experiment. The electroporated embryos were sacrificed at E13.5, brains were extracted in ice cold HBSS (Thermo fisher, ref: 14025092). Electroporated cortical areas resembling rosto-caudal and medio-lateral locations reported in (Cárdenas et al., 2018) were dissected. The dissected tissue from several embryos was dissociated using Trypsin-EDTA 0.05% (Thermo fisher, ref: 25300062) diluted in dissociation Medium (HBSS without Ca^{2+} and $Mg2^{+}$ (Thermo fisher, ref: 14170112) supplemented with 10%FBS, 1% P/S) and left for 8 minutes in a 37 ^{O}C water bath. Cells were then centrifuged, and the pellet was suspended in 500 µl of Dissociation medium and filtered with a 40 µm PES filter (Corning, ref: 352340). Cells were FACS sorted using (FACS Aria II, BD). Cells with High GFP^{+} intensity were collected in 100 µl of extraction buffer from Arcturus PicoPure™ RNA isolation kit (Thermofisher, ref: KIT0204).

16.2. Bulk RNA sequencing from P19 cells: Cells were plated in a 6 well plate (Falcon, ref: Falcon 351146) at a density of 500,000 cells per well. As mentioned previously, transfection was carried out using mRobo1flag plasmid and GFP plasmid as control. Medium was removed 2 days post transfection and cells were trypsinized and resuspended in culture medium. GFP^{+} cells for both conditions were FACs sorted and collected in 100 µl of extraction buffer from Arcturus PicoPure™ RNA isolation kit (Thermofisher, ref: KIT0204).

Following sample collection, RNA was extracted using the Arcturus PicoPureTM RNA isolation kit according to the manufacturer's protocol. RNA integrity was determined using a Bioanalyzer (Agilent 2100), and samples with RIN values greater than 8 were chosen for RNA sequencing. Three independent replicas per condition were sequenced for each biological replica. Libraries were prepared using the SMART-seq v4 Library Prep Kit and sequenced using 50 bp single reads on an Illumina HISeq 2500 sequencer.

17. Bulk RNA sequencing analysis

Reads were quality-checked with FASTQC v0.11.9. RNA-Seq output reads were quality-trimmed and filtered for adapters using Trim Galore v0.6.5 and aligned to the genome

assembly (GRCm38.p6) using HISAT2 (D. Kim et al., 2015). Gene-level read counts were computed using HTSeq v0.11.1 (parameters: -m union –no_stranded and Ensembl gene annotations) (Anders et al., 2015). Differentially expressed genes were identified using DESeq2 v1.28.1(Love et al., 2014). Gene Ontology (GO) functional enrichment analysis for DEGs and Kyoto Encyclopedia of Genes and Genomes (KEGG) pathway enrichment analysis were performed using Gene Set Enrichment Analysis (GSEA) method (Subramanian et al., 2005). The meta analysis of the GO terms was performed using Cytoscape v3.8.1, EnrichmentMap v3.3.1 and WordCloud v3.1.3 (Merico et al., 2010; Oesper et al., 2011; Shannon et al., 2003).

18. Tissue microdissection and Single cell RNA sequencing analysis

E12.5 brains of wild type ICR embryos were isolated, and the meninges were cleaned. During dissection, brains were immersed in L15 buffer no phenol red + glutamine (Thermofiher, ref: 21083-027). Brains were embedded in agarose and kept at 42^0(Low melting temperature) (Lonza, ref: 50100). After the agarose solidified, agarose blocks containing the brains were cut by Vibratome (Leica, ref: VT1000S) into sections 250 µm thick with vibratome speed set at 2 mm/sec and frequency 50-60 HZ. Sections were then collected in L15, the primordium of the olfactory bulb (OB) and a section of the adjacent neocortex (NCx) was microdissected using microsclapel under steromicroscopic guidance (Leica, ref: MZ16). Tissue for both regions was pooled from 6-8 littermates. The tissue was incubated in HBSS-phenol red without $Ca^{2+,}$ Mg^{2+} (Thermofisher, ref: 14170112) and 40µl of Trypsin-EDTA 0.05% (Thermo fisher, ref: 25300062) for 4 minutes in a 37 ^{O}C water bath. This was followed by adding 200 µl of FBS to neutralize the effect of the trypsin. The cells were then pipetted for 6-8 times with pipette set at 1000 µl volume. This was followed by passing the dissociated cells through 40µm strainer (Pluriselect, ref: 43-10040-40) pre-wetted with HBSS. Cells were centrifuged for 5 minutes at 1000 RPM speed and resuspended in 50µl of 1X PBS PH7.4 (Gibco, ref: 10010023) + 0.1% BSA.

The number of cells was calculated using Neubauer chamber and trypan blue (Sigma, ref: T8154) to validate cell viability.

19.10 X genomics Workflow

Briefly, we used 10X genomics chromium platform to generate the libraries of Single cell Rna Seq samples from the OB and NCx (Chromium Single Cell 3' GEM, Library & Gel Bead

Kit v3, 4 rxns PN-1000092, Chromium Single Cell B Chip Kit, 16 rxns PN-1000074, Chromium i7 Multiplex Kit, 96 rxns PN-120262). This platform is based on microfluidic principles. Using an 8-channel microfluidic chip, the 10X system isolates a large of single cells in using gel bead into emulsion (GEM). The droplet-based encapsulation of the cells is achieved by gel beads, where each gel bead is functionalized with oligonucleotide that has a unique barcode, a UMI, primers, a sequencing adaptor and a 30 bp Oligo dT. Cell lysis, reverse transcription, cDNA amplification, molecular tagging, and library construction all take place in the same workflow. We aimed in each replicate around 10,000 cells to be processed in the workflow. Libraries were sequenced in an Illumina HiSeq2500 instrument with a modified 75 bp paired-end protocol.

20. Single cell RNA data analysis

Raw 10X single cell RNA seq data was analyzed using a custom pipeline. Reads were aligned to the ensemble GRCm39 (Genome Reference Consortium Mouse Reference 39) with STARsolo (v2.7.3a) (Dobin et al., 2013). To select cells for downstream analysis, cell barcodes associated with the most UMIs were selected using DropletUtils (v1.6.1) (Lun et al., 2019). Parameters used for cell filtering: (1) Cells were removed by filtering if they have < 250 UMIs mapped to the mouse genome, (2) cells were removed if they have < 200 unique genes detected, (3) removed cells with > 3 standard deviations above the mean number of genes detected for each batch separately, (4) Removed genes detected in < 3 cells, (5) cell were removed if they have Percentage of MT (Mitochondrial) genes >15.

Normalization, clustering, and integration of data were performed using Seurat (V3.1.5) (Butler et al., 2018). Using a linear model with Seurat ('ScaleData' function), the effects of sequencing depth, replicate, and library preparation batch were removed. Principal component analysis (PCA) was used to reduce the dataset's dimensionality to the top 40 PCs. Cells are then grouped together in order to optimise the density of links within clusters versus links between clusters. Cell clusters with fewer than 30 cells were excluded from further investigation. Cells were clustered using Clustree (v0.4.2) and Seurat (v3.1.5) and cluster names were assigned based on bibliography. Clusters were integrated with SCTransform normalization based on sample origin. The clusters were regressed out effects of cell cycle and mitochondrial genes. 11 clusters were discarded due to having high expression of mitochondrial genes, low number of UMIs and no differential expressed genes. Monocle 3b was used to construct single-cell pseudo-time trajectories in the integrated data set for OB and

NCx samples (Trapnell et al., 2014). Differential expressed genes (DEGs) and gene cluster enrichment analysis were determined in R. DEGs and gene cluster enrichment analysis was performed for each cluster versus all other cells in the dataset for genes that are present in minimally 10% of the cells in the cluster. Genes were considered enriched if they have a P value < 0.5 and 0.2 $\log^2$fold.

21. Chromatin immunopreciptation (ChIP)

ChIP and ChIP-qPCR experiments were performed on P19 cells with the same transfection parameters as described in the previous experiments. To test the effect of overexpressing mRobo1flag and Crispr Dll on the chromatin landscape and validate the binding of Robo1flag certain DNA regions. The cells were fixed and DNA was cross- linked using 1% formaldehyde for 10 minutes at RT. Then they were neutralized with 0.125 M glycine, scraped off and rinsed with cold 1X PBS. Next, cells were centrifuged for 7 minutes at 4^{o}C at 600g. the pellets were resuspended in 10 ml of L1 buffer (50 mM HEPES KOH pH 7.5, 1 mM EDTA pH 8, 140 mM NaCl, 10% glycerol, 0.25% Triton X-100, 5% NP-40). This was followed by incubation for 10 minutes at 4^{o}C and a centrifugation for 5 minutes at 4^{o}C at 1300 g. The pellet obtained from the previous centrifugation was resuspended in L2 buffer (200 mM NaCl, 0.5 mM EGTA pH 8, 1 mM EDTA pH 8, 10 mM Tris pH 8), and incubated for 10 minutes at RT. This was followed by a 5-minute centrifugation at 4^{o}C at 1300 g. The pellet was then resuspended in L3 buffer, which contains protease inhibitors (1 mM EDTA pH 8, 10 mM Tris pH 8, 0.5 mM EGTA pH 8, 0.1% Na-deoxycholate 100 mM NaCl, and 0.17 mM N-lauroyl sarcosine). The pellet was then sonicated using bioruptor sonicator ad incubated overnight at 4^{o}C. The lysate was cleared of debris by centrifuging at 14,000g for 10 minutes at 4^{o}C. 60µg of chromatin was incubated overnight with mouse anti-flag antibody after 1 hour of preclearing, the mixture of the chromatin and the antibody was incubated with with 40 µl of protein A- or G-Sepharose beads that were pre-blocked with tRNA and BSA for 3 hours at 4°C. The beads were washed twice with 1 ml of buffer L3 and once with 1 ml of DOC buffer (10 mM Tris (pH 8), 0.5% Na-deoxycholate, 1 mM EDTA], 0.25 M LiCl, 0.5% NP-40). Bound chromatin was eluted with 1% SDS/0.1 M NaHCO3. The eluted chromatin was then treated for 30 minutes at 37°C with RNase A (0.2 mg/ml), followed by 2.5 hours at 55°C with proteinase K (50 g/ml). The chromatin crosslinking was then reversed overnight at 65°C with gentle shaking. The chromatin was recovered in 40 µl of TE buffer after purification with phenol-chloroform extraction and ethanol precipitation. ChIP-seq libraries

were prepared using standard Illumina protocols and sequenced on a Next-seq platform with 42 bp paired-end reads (Pataskar et al., 2016).

22. ChIP-seq analysis

ChIP-seq reads quality was assessed using FASTQC program. Robo1-Crispr Dll1 ChIP-seq was generated from P19 cells in one biological replicate, followed by validation of the peaks using ChIP-qPCR. Bowtie2 (Langmead & Salzberg, 2012). The paired end reads were aligned to the mouse genome mm10 using default parameters and UCSC annotations (Waterston et al., 2002). The SAM file was converted to BAM file using SAMTOOLS (Danecek et al., 2021; Raney et al., 2014). The peaks were called using MACS2 using paired end parameters. WIG files were generated using QuasR (Gaidatzis et al., 2015) and the genomewide peaks enrichment was visualized using UCSC genome browser (Raney et al.,2014). The peaks were annotated using Homer. The promoter motifs were analysed by submitting the gene list to the homer findMotifs.pl programme (Heinz et al., 2010).

23. Image quantification and statistical analyses

Image acquisition was done using Olympus FV10 confocal microscope, Zeiss Apotome microscope, and Zeiss airy scan.

23.1. Electroporation analysis

To reduce the significant variability between litters in mouse experiments, counts in the hemisphere of each experimental embryo were normalised with the non-electroporated hemisphere at the same rostro-caudal and latero-medial level. At least three independent embryos were quantified. The images were captured using an Olympus FV10 confocal microscope.

23.2. Cell culture analysis

To quantify the cytoplasmic and the nuclear localization for Robo1 ICD flag, Robo 2 flag and Robo1/2 myc truncated constructs in p19. We captured a minimum of seven images per culture replicate using Olympus FV10 confocal microscope with a 63X oil objective, Individual cells from at least 3 different cover-slips were quantified. Colocalization signal was quantified using Fiji to measure signal, area, and integrated density.

24. Statistical analysis

GraphPad Software version 8.0.0 for Windows, San Diego, California, USA, www.graphpad.com, was used for statistical analysis. When statistical significance was assumed, p values were set below 0.05. All values are the mean standard deviation of the mean (SEM). Independent samples or pairwise t-test To compare statistical differences between two experimental groups, the t-test was used.

One way ANOVA was used to compare the statistical differences between at least three experimental groups. It was assumed that the variance in the experimental distributions would be similar. The samples were obtained independently, and the observations were sampled at random. Embryos from at least two different females were used in each experiment. The experimental n, statistical test used, and statistical significance are all detailed in the legend of each figure.

Tables

Table 1. Results obtained from *in vitro* mass spectrometry analysis of proteins bound to flag tag upon overexpression of mRobo1/2-ICD-flag and Cripsr-Dll1. 104 proteins were found to be more enriched in the mRobo1/2-ICD-flag sample compared to the control sample. The table lists the gene names of enriched proteins and their log2 fold-change.

Gene names	log2 Fold-Change Flag/CTL
Robo2	31.49769
Robo1	31.27825
Cap2	28.86476
Hdx	27.36131
Rpl22	27.00072
Mkl1	26.98522
Qpctl	26.24518
Wipf1	26.15827
Rnf219	26.15025
Mtfr1	25.98076
Setx	25.86432
Aldh1l1	25.79266
Mob2	25.73182
Slain2	25.46557
Dhx57	25.45127
Slc17a6	25.17058
Rbm6	25.10161
Atp5j2	25.07637
Pi4ka	24.90355
Arhgap39	24.83718
Eif2b1	24.83405
Sgk223	24.52453
Arhgap32	24.51533
1700021F05Rik	24.40331
Phactr2	24.38027
BC003331;Odr4	24.2094
Cox6a1	24.17562
Nedd4l	24.06521
Eif2ak3	23.92262
Ell	23.91502
Wipf3	23.83779

Tab3	23.71942
Srsf10;Srsf12	23.59815
Dda1	23.58394
Atp13a1	23.54887
Nedd8	23.51135
Spire2	23.48757
Prpf39	23.44
Akt2	23.43237
Rab18	23.4247
Arhgap27	23.31969
Mrpl45	23.21985
Mpdz	23.19016
Mtss1l	23.15892
Aftph	23.14079
Ube2o	23.12226
Nisch	23.03565
Ccdc132	22.87736
Mta3	22.8674
Nck1;Nck2	22.86571
Gorasp2	22.84412
Hectd1	22.81255
Haus6	22.80823
Vps53	22.79521
Mrps5	22.78187
Rtn1	22.76557
Lrch2	22.72057
Ccdc97	22.6049
Nudt16l1	22.56092
Gpam	22.55075
Phactr1	22.48468
Lrrfip1	22.40925
Fbxo22	22.34408
Gtf3c4	22.27994
Atat1	22.2182
Ncaph2;Gm7535	22.1699
Otx2;Otx1	22.16269
Tbc1d15	22.12428
Vps51	22.12384
Trappc8	22.11288

Mettl16	22.08858
Irf2bpl	22.07024
Slc27a4	21.99196
Opa1	21.95968
Gna11;Gna14	21.92299
Rmdn3	21.89946
Golim4	21.89089
Stim1	21.86561
Tab2	21.83592
Rcn3	21.80882
Vps16	21.80546
Wdr48	21.79648
Pmpca	21.76923
Nde1;Ndel1	21.73364
Sepsecs	21.69434
Tcstv1	21.68648
Nup107	21.68427
Gpc1	21.68069
Morc2a	21.66789
Hmox1	21.51268
Pcca	21.46949
Meis2	21.35391
Mms19	21.35278
Timmdc1	21.35062
Dscc1;DSCC1	21.28362
Syne2	21.26928
Wdr7	21.06825
Bccip	20.68534
Dctn3	20.44804
Chd7;Chd8;Chd6;Chd9	19.62257
Sapcd2	18.48334

Table 2 DEGs identified upon expression of mRobo1/2-ICD-myc together with Crispr-Dll1. Bulk RNA-seq was performed on FACS-sorted cells at E13.5, one day post IUE. A total of 1573 genes were differentially expressed between cortical cells overexpressing mRobo1/2-ICD + Crispr-Dll1 and control samples. The names of the top 100 upregulated and downregulated DEGs is listed. The table indicates gene names, Log_2 Fold Change and adjusted P value (padj).

GeneName	log2FoldChange	padj
Robo1	5.506	3.44E-28
Ano3	5.504	7.79E-23
Eda2r	4.877	1.26E-29
Cdkn1a	3.925	1.65E-87
Zic1	3.547	0.049174071
Gm5869	3.379	2.82E-07
Ddx60	3.132	5.26E-05
Pmaip1	2.944	9.23E-07
Ifitm3	2.937	1.38E-34
Mx2	2.869	2.94E-05
Phlda3	2.857	1.45E-50
Hs3st3a1	2.794	0.000834792
Dglucy	2.677	2.59E-22
Psmb8	2.585	0.003752897
Oas1b	2.456	2.96E-06
Gbp3	2.336	1.13E-05
Cldn9	2.286	0.005023889
Tfap2d	-2.272	0.001151076
Rn7sk	2.209	4.00E-05
Sema3c	-2.047	0.001303116
Adra2c	-2.04	0.006121534
Ehhadh	2.031	0.019164547
Irgm1	2.025	7.79E-23
C1qa	2.023	0.014736617
Usp18	2.018	1.14E-29
Rtp4	2.014	5.26E-10
Rasgef1c	1.992	0.040761074
Calb2	1.988	0.002333547
Bst2	1.954	2.15E-15
Robo2	1.95	9.99E-64
Lyz2	1.914	0.002798033

Cxcl12	-1.893	0.045203856
Erap1	1.887	0.008675048
Gbp7	1.88	0.00312961
Lhx6	-1.878	0.007149083
9530059O14Rik	-1.83	0.004760451
B2m	1.819	1.53E-13
Gm9987	-1.815	0.042896733
Cabp7	-1.815	0.0176182
Bmp7	1.772	0.003276047
Fndc3c1	1.759	0.000440098
Isg15	1.737	2.08E-05
Sulf2	1.734	7.64E-13
Ifi27	1.708	0.002843408
Abca1	-1.67	0.000112439
Cox6b2	1.657	2.43E-05
Trim21	1.632	5.46E-05
Cyp4f13	1.621	0.031978032
Mirg	1.621	0.01043701
D130062J10Rik	-1.612	0.027804279
Ceacam1	-1.588	0.007841624
Ddx58	1.577	3.35E-09
Fggy	1.574	0.033697876
Serpine2	1.568	0.00121034
Dlk1	1.567	8.70E-17
Eml2	-1.566	1.38E-05
Ccdc80	-1.552	0.044029657
Hr	-1.551	0.00967788
H2-Q4	1.541	0.005272875
Rmst	1.539	3.26E-06
Prdm12	-1.539	0.029999938
Nmi	1.528	0.007898525
Sstr3	-1.523	0.000107609
Kcnh3	-1.518	0.000114556
Cux2	-1.517	1.35E-12
Slitrk3	-1.516	0.032201977
Pcdhb6	-1.509	0.035846805
Pappa	1.504	2.91E-05
Gypc	1.496	3.02E-05
Pvt1	1.494	0.002575865

Sh3rf3	-1.486	0.000612909
Adamts5	-1.483	0.002018864
Bbc3	1.478	1.14E-15
Vit	-1.478	0.014528869
Cpxm2	1.475	0.002339452
Parp9	1.466	1.24E-08
Gm42946	-1.459	0.000863471
Veph1	-1.448	3.61E-05
St8sia5	-1.445	0.046790281
Sorl1	-1.436	0.044374858
Slc7a3	1.432	0.003549111
Rcan2	1.43	2.24E-12
Gpr153	1.426	0.006848204
Fgf15	1.421	0.000272902
Mgat5b	-1.419	0.018622211
Smpdl3b	1.413	0.003589445
Tap1	1.41	0.008016242
Tle2	-1.404	0.000282254
Tlcd4	-1.402	0.026574144
Gm16487	-1.396	0.029067943
Hey2	1.389	0.001420166
Unc5a	-1.37	0.000785575
Tbc1d24	-1.369	8.00E-07
Tafa2	-1.367	0.044072424
Osbpl7	-1.362	0.004874498
Irf9	1.357	4.53E-11
Hrk	1.356	0.004779149
Arhgdig	1.348	0.014193504
Fchsd1	-1.34	0.001607411

Table 3. DEGs identified by in vitro mRobo1 ICD flag RNA sequencing in p19 cells. Here are the top 100 DEGs genes. In this table we are listing gene name (Genes), Log2 fold change (Log2C), and adjusted P value (padj).

GeneNames	Log2FoldChange	Padj
Robo1	3.688855452	1.6536E-188
Upp1	-1.444127255	9.30613E-40
Gpr62	-3.793211754	1.99566E-36
Ier3	-1.824350514	2.31735E-35
Ddit4	-1.162104074	4.42543E-34
Adm	-2.420204871	4.72309E-29
Dusp6	-1.824020587	4.13415E-28
Trap1a	-1.563248601	5.44519E-28
Stc1	-1.412251926	4.74795E-25
Optn	-1.508974336	6.65809E-24
Egln1	-1.037018326	6.28299E-23
Gm46060	-2.168150152	2.65474E-22
Ankrd37	-1.396001668	4.27424E-22
Ldha	-1.139787704	6.08498E-22
Fam162a	-0.981464451	1.06647E-20
Tnrc18	0.779461348	1.41731E-18
Eno1	-0.830026547	3.56254E-18
Anxa2	-0.998163455	1.62026E-17
Pfkfb3	-1.247862656	1.62026E-17
Pgk1	-0.872137322	3.8639E-17
Lfng	1.089251733	5.68737E-17
Dmbx1	1.514247938	2.75665E-16
Tpi1	-0.883044736	2.95327E-16
Sec24d	1.057491915	3.50382E-16
Kcng3	-2.255799041	6.66347E-16
Slc7a3	-1.092778222	6.86274E-16
Higd1a	-0.864085202	1.3823E-15
Abcg4	1.531730243	3.11379E-15
Spry2	-1.723931991	4.07058E-15
Rtn4rl1	0.829098257	4.52678E-15
Aldoa	-0.823247611	4.59911E-15

Col5a2	0.740176733	4.90547E-15
Ppp1r3c	-1.865581665	5.55585E-15
Gm31340	-1.286761747	6.94955E-15
Sema6a	-1.112596671	7.34216E-15
Gbe1	-0.894725244	8.51075E-15
Ppp1r3g	-1.213633975	8.62875E-15
Erbb3	0.967028627	1.11343E-14
Nptx1	1.275877352	1.19342E-14
Bnip3	-0.880920191	1.96851E-14
Rem2	1.199936594	2.22404E-14
Eno1b	-0.836423053	2.31197E-14
Pfkl	-0.927971882	3.20865E-14
Rbpms	-0.897021075	4.5435E-14
Plod2	-0.842608967	5.94877E-14
Alg12	1.171898093	6.36949E-14
Ero1a	-0.862476069	8.70232E-14
Zfp428	-0.801380881	9.43933E-14
Nol4l	0.961645442	9.69019E-14
Pdia4	0.606407238	9.77526E-14
Itprip	0.963408423	2.13501E-13
Rasl10b	0.775850214	2.30787E-13
Slc39a14	-1.292473782	2.86151E-13
Egln3	-0.995060418	3.48631E-13
Bmf	1.132014118	3.96054E-13
Hprt	-0.733935519	3.99378E-13
Igdcc4	0.892812049	4.02447E-13
Mkrn1	-0.826916001	4.77019E-13
Pfkp	-0.932239317	4.77019E-13
Tex19.2	-2.579149487	5.3508E-13
Mlec	0.664336529	7.30914E-13
Myc	-0.771967643	7.44629E-13
Ephb3	0.839452555	1.25794E-12
Itga5	0.723573757	1.73769E-12
Snx33	1.206203094	2.00317E-12
Ripor1	0.838125142	2.54689E-12

Pcolce2	-0.836585294	2.54689E-12
Pkdcc	-0.982688379	2.8725E-12
Pyroxd2	1.029429246	3.24252E-12
Derl3	1.043754681	3.46375E-12
Dusp4	-1.547046475	4.78339E-12
Hid1	1.329555674	5.98848E-12
Rhbdl3	0.86102243	6.21629E-12
Stk32a	1.013818928	1.01672E-11
Gpi1	-0.69856642	1.01672E-11
Ciart	-1.011136454	1.5237E-11
Cxcl12	0.827572297	1.62407E-11
Aldoart1	-0.801317684	1.80089E-11
Sncb	-1.198877505	1.80089E-11
Aldoc	-0.874129356	2.14674E-11
G2e3	-0.840517661	3.3964E-11
Gprc5c	0.794465434	3.76423E-11
Hmgb3	-0.755241818	5.16854E-11
Pgam1	-0.71647423	5.3102E-11
Gdap10	-0.933574964	6.22835E-11
Timp2	0.835819776	7.58173E-11
Etv5	-0.982855454	8.02291E-11
Spon1	-1.890283929	8.75656E-11
Mt2	-1.236264525	1.12878E-10
Slc4a5	1.170091917	1.29684E-10
Trim71	-0.756268898	1.36889E-10
Pcyt2	-0.739809411	1.48929E-10
Fndc3b	0.679649387	1.79319E-10
L1td1	-0.73892964	1.8932E-10
Tmem38a	0.629384821	2.02106E-10
Ago4	1.157470564	2.04515E-10
Naglu	1.103572437	2.21448E-10
Bdh1	-0.79269575	2.3872E-10
Stat4	1.001349354	2.40705E-10

Table 4. DEGs from NCx and OB RGCs clusters obtained from E12.5 NCx and OB scRNA-seq. The top 100 DEGs genes with the highest average log fold change (avg logFC) in each region's RGCs clusters are listed.

Ncx RGCs DEGs		OB RGCs DEGs	
Gene	**avg_logFC**	**Gene**	**avg_logFC**
Ybx1	0.904709	**Nnat**	1.261887
Ppp1r14b	0.872075	**Stmn2**	1.254725
Anp32b	0.849103	**Rtn1**	1.120431
Jund	0.825162	**Zic1**	1.081744
Gm47283	0.784001	**Fabp7**	1.07238
Lhx2	0.763463	**Kitl**	1.061225
H1f10	0.748968	**Mest**	1.026979
Srsf2	0.748529	**Zic4**	1.005824
Hnrnpd	0.719171	**Ptprz1**	0.686462
Srsf9	0.702195	**Gap43**	0.617218
CT010467.1	0.702109	**Zic3**	0.570155
Taf10	0.694844	**Tuba1a**	0.567954
Gas1	0.683258	**Etv1**	0.558961
Id4	0.682775	**Dcx**	0.518517
Nsmce4a	0.660334	**Zbtb20**	0.515153
Epha5	0.646537	**Ptn**	0.492257
Set	0.645452	**Atp1a2**	0.468742
Neurog2	0.640563	**A730094K22Rik**	0.455966
C1qbp	0.635405	**Tmsb4x**	0.435521
Cenpv	0.62281	**Klf7**	0.434054
Rcc2	0.60372	**Otx2**	0.432062
Mpp6	0.596852	**Ldhb**	0.414367
Rpl35a	0.587306	**Mageh1**	0.402201
Gm28438	0.582499	**Luzp2**	0.401443
Hist1h2ap	0.575941	**Slc1a2**	0.394637
Cdv3	0.569758	**Fgf15**	0.379972
Glrx5	0.5668	**Col25a1**	0.365983
Psip1	0.559213	**Islr2**	0.364488
Lmnb1	0.558212	**Efna5**	0.338937
Rab5if	0.553798	**Tubb2b**	0.332773

Bri3	0.545398	**Il17rd**	0.288269
Ccnd2	0.539705	**Vim**	0.274016
Alyref	0.530176	**Selenow**	0.262285
Hnrnpab	0.523833	**Sorcs1**	0.251915
Nt5dc2	0.522551	**H3f3b**	0.240148
mt-Rnr1	0.504059	**Gsn**	0.197209
Ppp2ca	0.500095	**Ftl1**	0.195508
Ppp1cc	0.497183	**Gm37812**	0.157993
Nfib	0.489793	**Gm37457**	0.140732
Polr2m	0.48727	**Ptma**	-0.15296
Tcf4	0.479813	**Dmrt3**	-0.18067
Gspt1	0.477221	**Rpl41**	-0.18296
Ybx3	0.476823	**Rpl17**	-0.18866
Bod1	0.475064	**Riox1**	-0.19218
Sap30	0.466347	**Rpl36a**	-0.19993
Hdgf	0.465889	**Hsp90aa1**	-0.20919
Hes1	0.46588	**Car14**	-0.21414
Hnrnpa0	0.464482	**Coq2**	-0.21791
Ube2m	0.457231	**Pdcd2**	-0.2201
Ptms	0.452059	**Snrpg**	-0.22024
Marchf5	0.446555	**Yars2**	-0.22251
Hras	0.445421	**Stk24**	-0.2283
Odc1	0.441261	**Otulin**	-0.22964
Klhdc2	0.437685	**mt-Nd2**	-0.23144
Scand1	0.43708	**Npm1**	-0.23382
Macroh2a1	0.434541	**Nxn**	-0.23477
Pgp	0.434268	**Pim1**	-0.23675
Tmpo	0.427579	**Rpl27a**	-0.24253
Nr2f1	0.427314	**Rpl36**	-0.24544
Bag1	0.422689	**Mthfd2l**	-0.2465
Elavl1	0.42015	**Akirin2**	-0.24678
Arglu1	0.418185	**Gna11**	-0.2468
Tmed2	0.417778	**Gnb1**	-0.24797
Nfix	0.412603	**Suds3**	-0.25088
Kras	0.409235	**Rtn4**	-0.25155

Ptov1	0.408081	**Zbtb12**	-0.25675
Tle5	0.406621	**Mrps30**	-0.2576
0610012G03Rik	0.40093	**Sac3d1**	-0.25812
Vapa	0.394065	**Fgfr2**	-0.2582
Smarca5	0.392672	**Uri1**	-0.25931
Pcbp1	0.390937	**Sap30l**	-0.26054
Marcks	0.390023	**Ubn1**	-0.26086
1810026B05Rik	0.38874	**Rab24**	-0.26547
Mtch1	0.387461	**Mycn**	-0.26945
Cdk2ap1	0.387221	**Etl4**	-0.27014
Mpped2	0.387081	**Fam49b**	-0.27246
Dcun1d5	0.386046	**Raly**	-0.27473
Sfrp1	0.385521	**Asf1a**	-0.28071
Emx1	0.384911	**Yy1**	-0.28099
Btg1	0.384616	**Rala**	-0.28431
Luc7l2	0.383164	**Yrdc**	-0.28689
Flrt3	0.380116	**Tmem165**	-0.28925
Usp1	0.379854	**Mir6236**	-0.29096
Frat2	0.379844	**mt-Rnr2**	-0.29592
Trim27	0.3789	**Pnrc1**	-0.29624
Cdon	0.375954	**Tmem160**	-0.29952
Rrs1	0.373957	**Zmynd19**	-0.30015
Topbp1	0.373106	**Alcam**	-0.30098
Uba52	0.372629	**Sfpq**	-0.30523
Nfia	0.370791	**Rfxap**	-0.30548
D030056L22Rik	0.369739	**Gatad1**	-0.30943
Suz12	0.363915	**Hs2st1**	-0.31169
Zfp771	0.362055	**Kdm1a**	-0.31598
Rnf187	0.361718	**Etaa1**	-0.31602
Imp3	0.361447	**Isoc1**	-0.31645
Gnas	0.360556	**Dhx36**	-0.31854
mt-Atp8	0.358756	**Carnmt1**	-0.3194
Ier5	0.352633	**Gsr**	-0.32006
Rhobtb3	0.347885	**Kmt5a**	-0.32039
Lmo1	0.345999	**Plagl1**	-0.32198

Table 5. Genes directly adjacent to peaks identified in ChIP-seq analysis of mRobo1-ICD-flag and Crispr-Dll1 performed *in vitro* in P19 cells. The top 25 genes that Robo1-flag binds at intergenic, intronic, exonic and promoter regions are listed as indicated.

Intergenic	Intronic	Exonic	Promoter
Gene Name			
Lrrc4c	Chl1	Robo1	Mir466d
Mir101c	Mdga2	Robo1	Rps29
Gm5458	Filip1l	Robo1	4931408C20Rik
4933422A05Rik	Txndc11	Robo1	Pisd-ps2
Rab10os	Cldn34d	Robo1	Rn4.5s
Mir101c	Ppp1r9a	Limd1	Nek7
Mir101c	Kctd16	Vmn2r29	Dux
Gm5458	Brox	Rn45s	Bik
Mir101c	2700054A10Rik	Rn45s	Dip2a
Mir101c	Cobl	Erdr1	Ccm2
Mir101c	Cdk8	Slc30a4	Glud1
Fgf14	Vps45	Muc6	Phf20
Mir101c	Dtnbp1	Neurod1	Pou6f1
Mir101c	Smo	Ccl28	Gpbp1l1
Lrrc4c	E030030I06Rik	Pisd-ps2	Rn4.5s
Mir101c	Gphn	G530011O06Rik	Eaf2
Mir101c	Mir5623	Dux	Sirt1
Mrgprd	Ccl28	Speer4c	Tmcc1
Gm45871	Satl1	Dux	Agap1
Tmem196	Ank1	Cluh	Uros
Gm14496	Tmppe	Nxn	Gdf6
Mir101c	Erdr1	Naf1	Mycbp
Vmn2r87	Dock2	Muc3	Arhgef11
Mir101c	Tspan3	Odc1	Dll1
Csf2ra	Dlgap2	Asnsd1	Rn4.5s

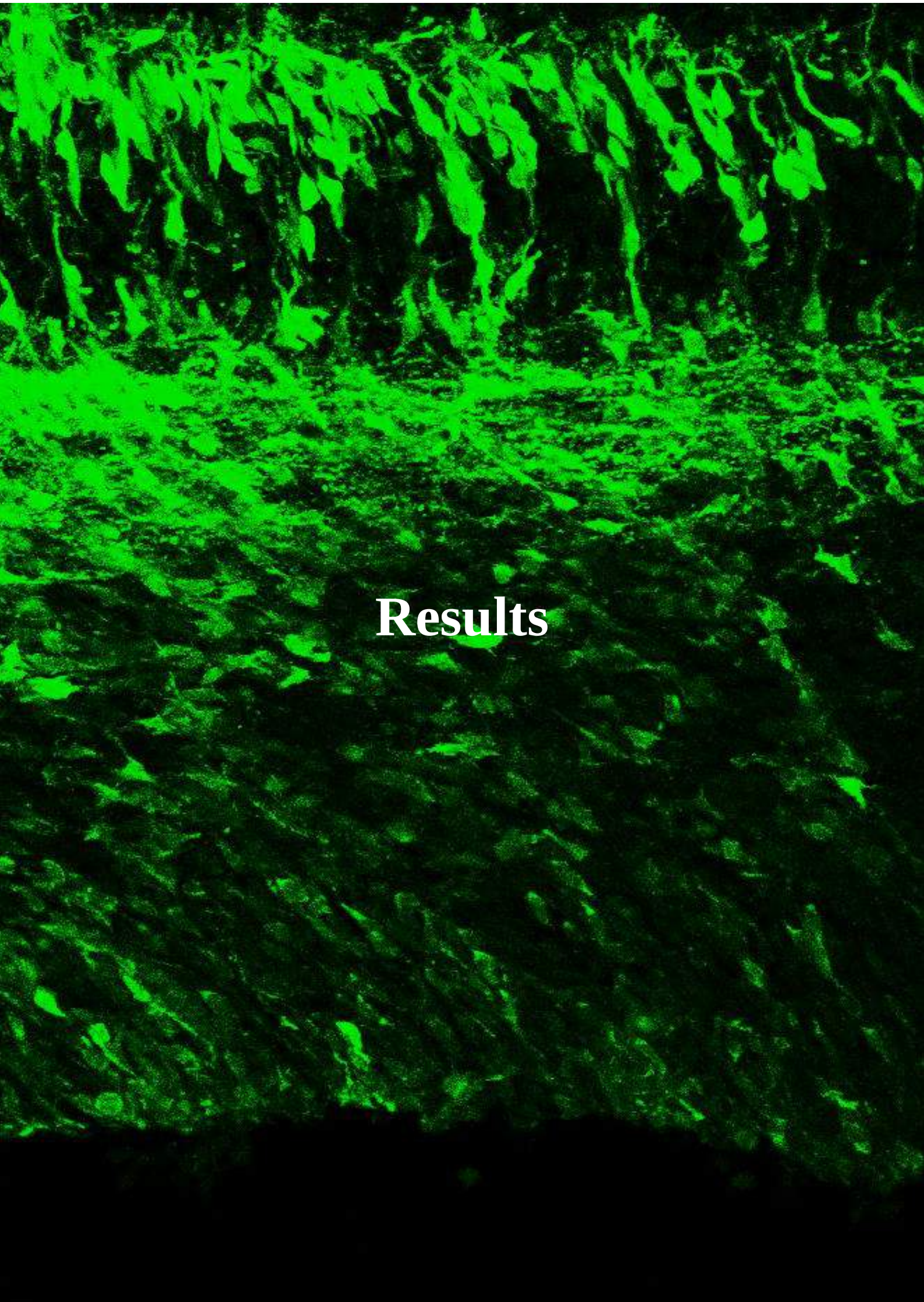

Results

Results

Part 1. Single cell transcriptomics reveals divergence between progenitors in the developing NCx and OB

1.1. Single cell sequencing analysis of the developing NCx and OB

The evolution of the mammalian neocortex involved a trade-off between different modes of neurogenesis, where suppression of direct neurogenesis promoted indirect neurogenesis (Cárdenas & Borrell, 2019). Our lab previously demonstrated that the differential growth of the OB and adjacent Neocortex (NCx) beginning at E12.5 was caused by increased neurogenesis within the OB primordium versus the NCx (Cárdenas et al., 2018). To determine the transcriptomic diversity and the heterogeneity between the NCx and OB on a single cell level, we implemented a single cell RNA sequencing (scRNA-seq) approach using 10X Genomics platform (**Fig. 1A**). We microdissected the olfactory bulb (OB) and the neocortex (NCx) of E12.5 mouse embryos (**Fig 1A**), followed by cell dissociation, processing with the 10X Genomics protocol and library sequencing, which yielded a total of 42,215 individual cells. We analysed three independent biological replicas for the NCx and two replicas for the OB. We performed quality control statistics with Seurat (v3.1.5) (**Fig. 1B**), and the high quality of the samples was confirmed. We identified 28 clusters that are present in the OB and NCx (**Fig. 1C**). Clusters (26) Cajal Retzius, (27) Erythrocytes, and (28) Microglia were excluded from further analysis due to their low abundance. Our analysis detected a continuum formed by the 28 clusters, which began with RGCs and progressed to IPCs before differentiating into neurons. (**Fig. 1D**).

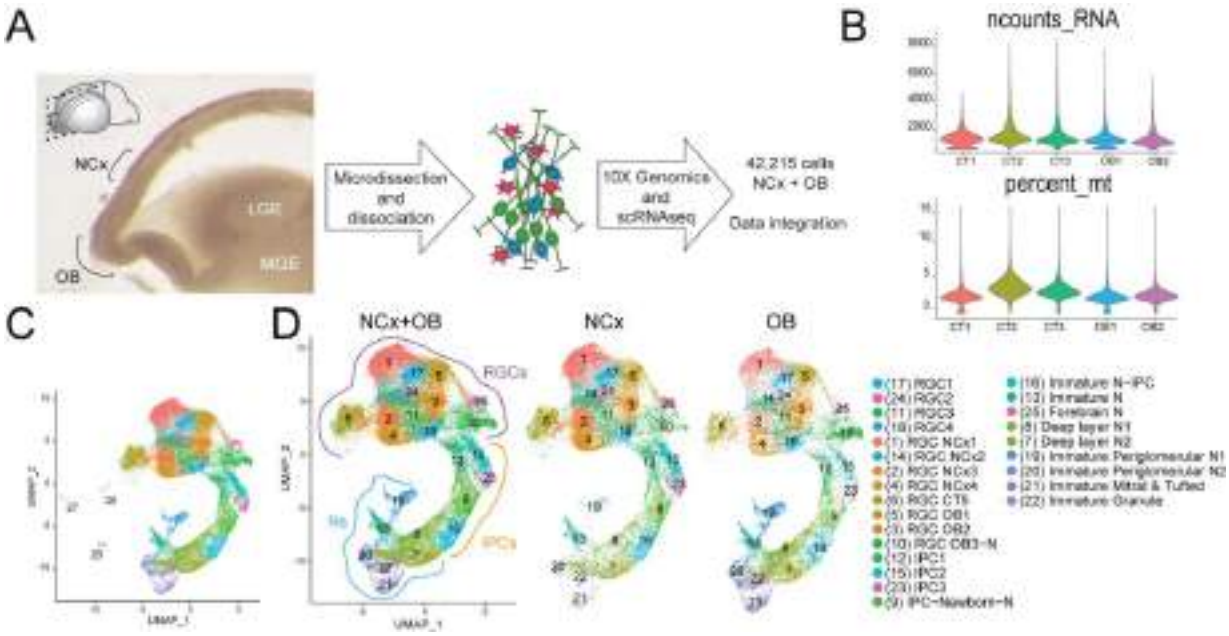

Figure 1. ScRNA-Seq of E12.5 mouse neocortex (NCx) and primodium of the olfactory bulb (OB). (A) Workflow for Single Cell RNA sequencing using 10X genomics platform. (B) Quality control statistics for the single cell RNA sequencing elucidated with Violin plot of detected number of UMI counts (nCount), and percentage of mitochondrial reads in each samples (NCx=3 replicates, OB=2 replicates). (C) UMAP visualization of the ScRNA-Seq data showing the 28 clusters identified for NCx and OB. Clusters (26) Cajal Retzius, (27) Erythrocytes, and (28) Microglia are in grey and are eliminated in the following UMAPs. (D) UMAP plot visualizing the different clusters for both NCx and OB. Radial glia cells (RGCs), intermediate progenitor cells (IPCs), and neurons (Ns) clusters are annotated on the UMAP.

1.2. ScRNA analysis reveals distinct cluster enrichment and cell trajectories in NCx and OB samples

We found differences in cluster enrichment between NCx and OB samples. Clusters (1) RGC CT 1, (14) RGC CT 2, (2) RGC CT 4, and (4) RGC CT 4, are Radial Glia Cell clusters enriched in NCx. Conversely, clusters (5) RGC OB 1, (3) RGC OB 2, and (10) RGC OB–Neuron are Radial Glia Cell clusters enriched in OB (**Fig. 2A, 2B**). We also found differences in IPC and neuron cluster enrichment between OB and NCx samples. In the case of IPCs, cluster (15) IPC2 and cluster (23) IPC3 are enriched in the NCx sample compared to the OB sample. This enrichment of IPC seemed to reflect the higher rate of indirect neurogenesis in the NCx compared to the OB (Di Bella et al., 2021; Moreau et al., 2021) (**Fig. 2A, 2B**). Furthermore, some neuronal clusters were more enriched in the OB samples than in the NCx samples, including cluster (7) Deep layer neuron 2, (8) Deep layer neuron 1, (13) immature neuron, (19) immature preiglomerular neuron 1, (20) immature preglomeluar neuron 2, (21) immature mitral and tufted cells, and (22) immature granule cells. This enrichment of

neuronal clusters observed in the OB samples compared to the NCx samples coincides with our previous findings of accelerated neurogenesis in the OB primodium compared to the NCx (Cárdenas et al., 2018).

To gain insight into cell lineages, we performed transcriptional trajectory reconstruction on the single cell data of the integrated NCx and OB samples using Monocle3b (**Fig. 1B**) (Qiu et al., 2017; Trapnell et al., 2014). Pseudotime ordering of cells showed the anticipated progression from the RGCs to neurons (**Fig. 2B**). Moreover, we discovered two distinct differentiation trajectories for RGCs from NCx and OB, one trajectory corresponding to indirect neurogenesis and another to direct neurogenesis. We found that NCx and OB RGCs indirect neurogenesis trajectory originate from cluster (11) RGC3, then passes through (12) IPC1, then cycling (15) IPC2 (S/G2/M) and (23) IPC3(S/G2/M), before becoming (9) IPCs-Newborn neurons. From there, IPCs diverge into two tracks, either through (8) Deep layers neurons 1 and then (22) immature Granule cells or as (16) immature neurons that then become (7) deep layer neurons 2. These (7) deep layer neurons 2, can differentiate into either (20) immature periglomerular neurons or generate (13) immature neurons, which then beome (21) immature mitral and tufts cells. (**Fig. 2C**). Interestingly, direct neurogenesis trajectory originates from OB RGCs. It starts from (5) RGCs OB1 then passes through (10) RGCs OB3-Neurons then differentiate into (19) immature periglomerular neurons 1 (**Fig. 2C**).

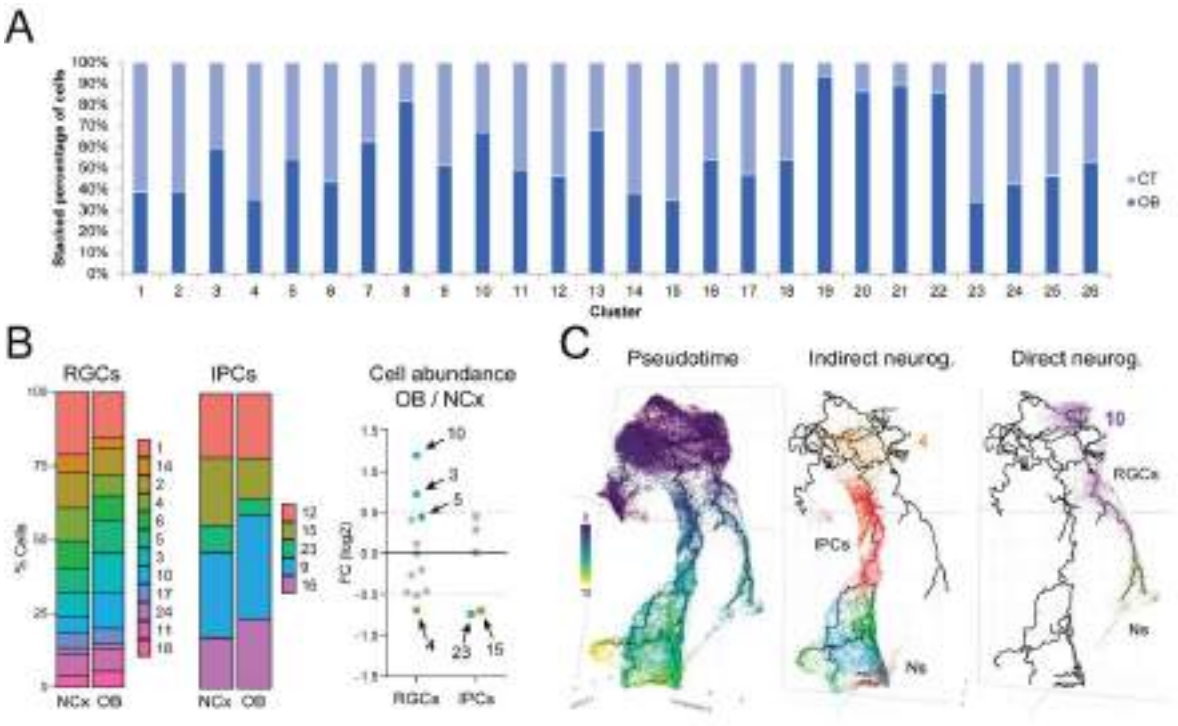

Figure 2. Different cluster enrichment and trajectories between NCx and OB. (A) stacked bar graph representing all the clusters and showing the proportion % for each cluster that originates from NCx or OB samples. (B) Average proportion of each RGC and IPC cluster in the NCx (n=3) and OB (n=2). A graph showing the ratio of cells in each cluster of the OB and NCx. (C) A UMAP plot of early-stage RGCs and late-stage neurons' pseudo-time trajectory. A UMAP plot demonstrating indirect neurogenesis trajectory for NCx and OB that originate from RGCs cluster (4). A UMAP plot demonstrating direct neurogenesis for OB RGCs derived from cluster (10).

1.3. Characterizing transcriptomic diversity between NCx and OB RGCs

To further characterize the transcriptomic diversity between NCx and OB RGCs, we checked the expression pattern of previously studied genes by our group in both the NCx and OB at E12.5 (Cárdenas et al., 2018). We observed that the expression of *Robo1* and *Robo2* is higher in the OB RGC clusters compared to the NCx RGC clusters, and *Dll1* expression is high in NCx RGCs clusters and OB RGCs clusters (**Fig. 3**). This observation was also validated with *in situ* hybridization (ISH) performed on E12.5 mouse embryos (**Fig. 3**). When focusing further on the expression of *Robo1, Robo2* and *Dll1* in RGCs cluster (4) and (10)-clusters where direct and indirect neurogenesis trajectory originate-, we found that *Robo1/2* have a slight higher expression in cluster (10) in the OB samples compared to NCx samples. On the other hand, we found that *Dll1* expression was slightly in cluster 10 in the OB samples compared to the NCx samples (**Fig. 3**).

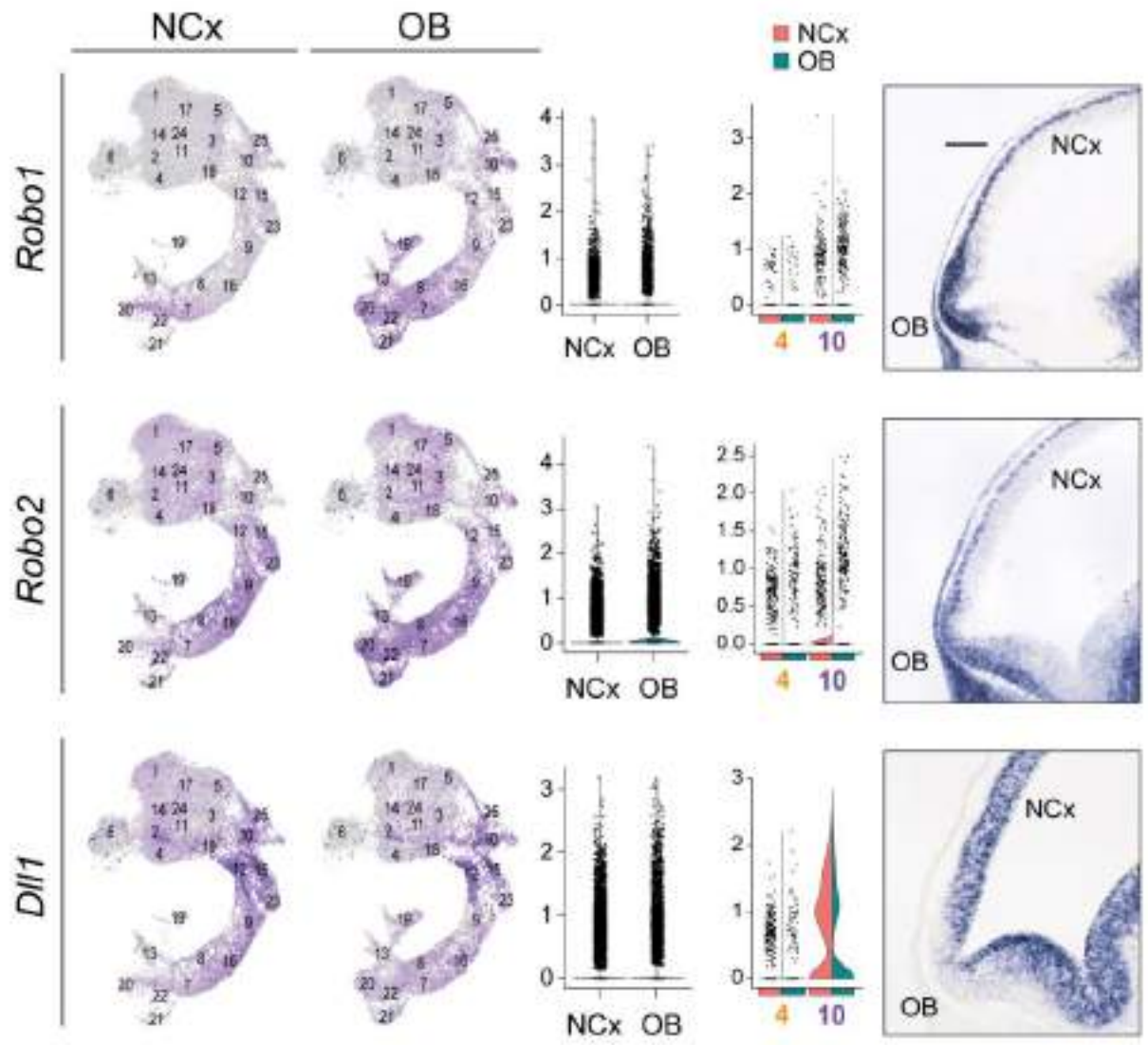

Figure 3. Validating *Robo1*, *Robo2* and *Dll1* expression patterns in NCx and OB scRNA data. UMAP plots showing the expression pattern for *Robo1, Robo2,* and *Dll1*in all clusters. Violin Plots showing the expression distribution of Robo1, Robo2, and Dll1 in RGCs clusters in NCx and OB samples. Sagittal brain sections of E12.5 mouse embryos showing the expression pattern of Robo1, Robo2, Dll1 in NCx and OB. Scale bar: 100µm.

Next, we looked at the expression patterns of other members of the Notch signalling pathway such as: *Hes1* and *Hes5* (which have previously been shown to play an important role in the maintenance of RGCs in the telencephalon) (Ohtsuka et al., 2001). We confirmed our previous findings that *Hes1* and *Hes5* expression levels were higher in NCx RGCs clusters than in OB RGCs (Cárdenas et al., 2018). *Hes1* and *Hes5* expression is reduced in cluster 4 and 10 in OB the sample. This observation further confirms the important role these genes

play in maintaining the progenitor pool. Pax6 —a highly conserved TF that is critical for cortical progenitor pool maintenance and its distribution in a rosto-lateral (higher) to a caudo-medial (lower) gradient is essential in establishing telencephalon rosto-lateral identities— had higher expression in NCx RGCs and OB RGCs clusters (**Fig. 4**). *Pax6* expression was high in both clusters (4) in both OB and NCx samples and in clusters (10) in both OB and NCx samples. We also detected higher expression of *Tbr1*—a transcription factor that is expressed in newly born neurons and upper layer neurons—in the OB clusters compared to the NCx clusters. These findings emphasize the higher rate of neurogenesis in the OB compared to the NCx at this stage of telencephalon development.

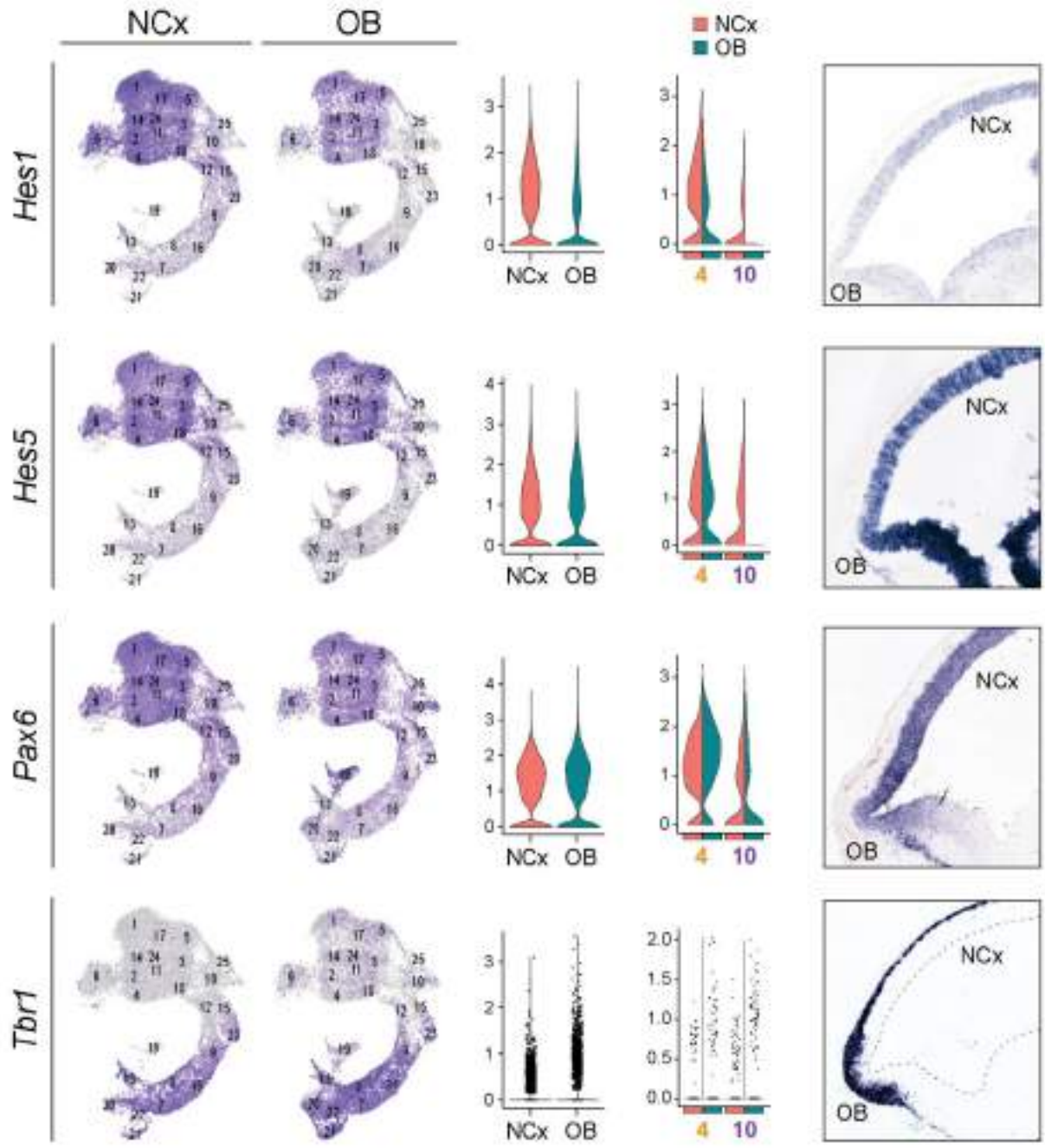

Figure 4. Expression patterns of different cortical development markers. UMAP plots of *Hes1, Hes5, Pax6,* and *Tbr1* expression patterns in different clusters. Violin Plots showing the expression distribution of *Hes1, Hes5, Pax6,* and *Tbr1*. Sagittal brain sections of E12.5 mouse embryos showing the expression patterns of *Hes1, Hes2, Pax6,* and *Tbr1* in NCx and OB.

To identify the genes that might play a role in the transcriptomic identity of RGCs clusters in mouse NCx and OB at E12.5, we searched for genes that were only found in one region or the other. Interestingly, we found that the expression of the *Etv4* gene (ETS variant transcription factor 4; this gene encodes a DNA-binding transcription factor involved in positive regulation

of transcription through RNA polymerase II) was exclusively higher in the OB RGCs clusters compared to the NCx RGCs clusters. Conversely, we discovered that *Hey2* gene expression (Hes Related Family BHLH Transcription Factor with YRPW Motif 2) was exclusively higher in NCx RGCs clusters compared to OB RGCs clusters. ISH assays of E12.5 mouse embryos confirmed the expression pattern observed for both genes (**Fig. 5**), confirming that *Etv4* and *Hey2* are specific markers for OB and NCx RGCs respectively, at E12.5 mouse.

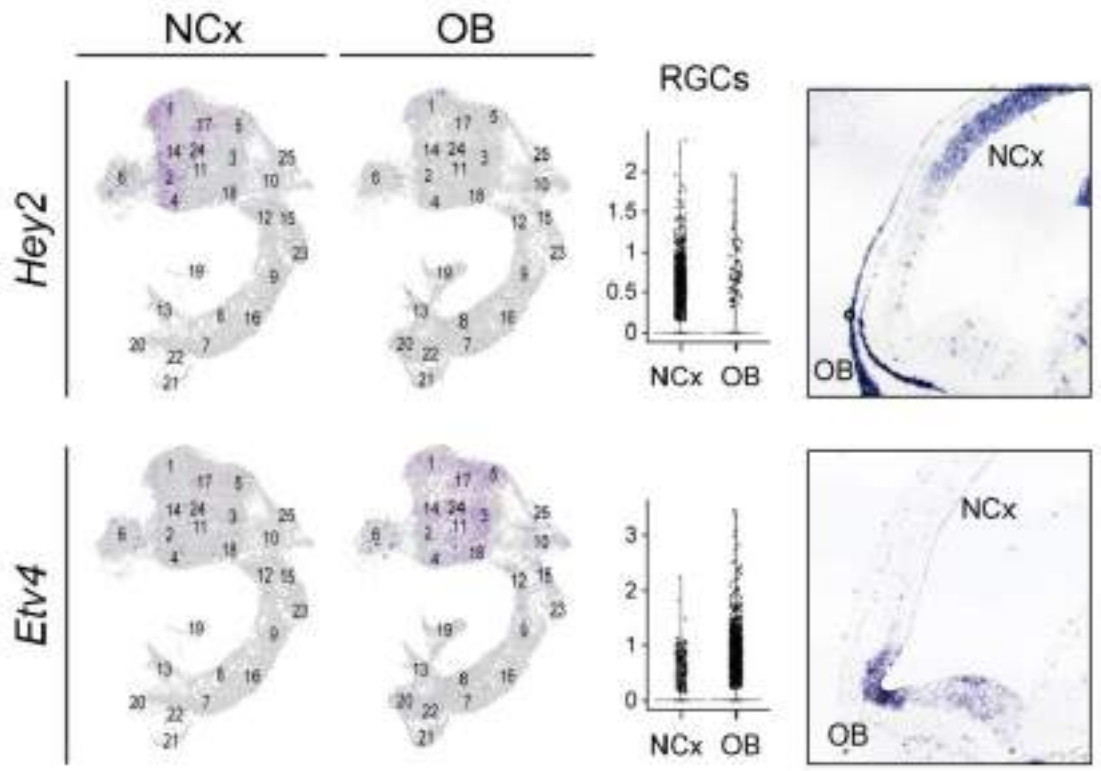

Figure 5. *Hey2* and *Etv4* exclusive markers for NCx and OB RGCs. UMAP plots showing the expression pattern for *Hey2* and *Etv4* in the different clusters. Violin Plots showing the expression *Hey2* and *Etv4*. Sagittal brain sections of E12.5 mouse embryos showing expression pattern of *Hey2* and *Etv4* in NCx and OB.

Previously, it has been reported that bRGCs in humans express canonical genes that are related to extracellular matrix formation, migration like *TNC, HOPX, PTPRZ1, LIFR* and *SLC1a3* (Pollen et al., 2015). Surprisingly, we observed that RGCs clusters in the OB samples at E12.5 had a higher expression of some of these bRGC markers like: *Hopx, Ptprz1*, and *Slc1a3*. To validate this observation, we performed ISH for *Hopx, Slc1a3*, and *Ptprz1* in WT E12.5 embryos (**Fig. 6**); we detected the high expression of these genes specifically in the primodium of the OB compared to the NCx. This finding is consistent with previous research

that found basal radial markers in humans are unlikely to show a specific expression pattern in mouse radial glia and are more likely to reflect regional and temporal heterogeneity of mouse RGCs (Pollen et al., 2015). We studied the expression levels of *Ptprz1* and *Slc1a3* in RGC clusters (4) and (10). We found that expression of these genes were higher in cluster 4 in OB samples, suggesting that these genes could play a role in progenitor proliferation rather than determining the mode of neurogenesis.

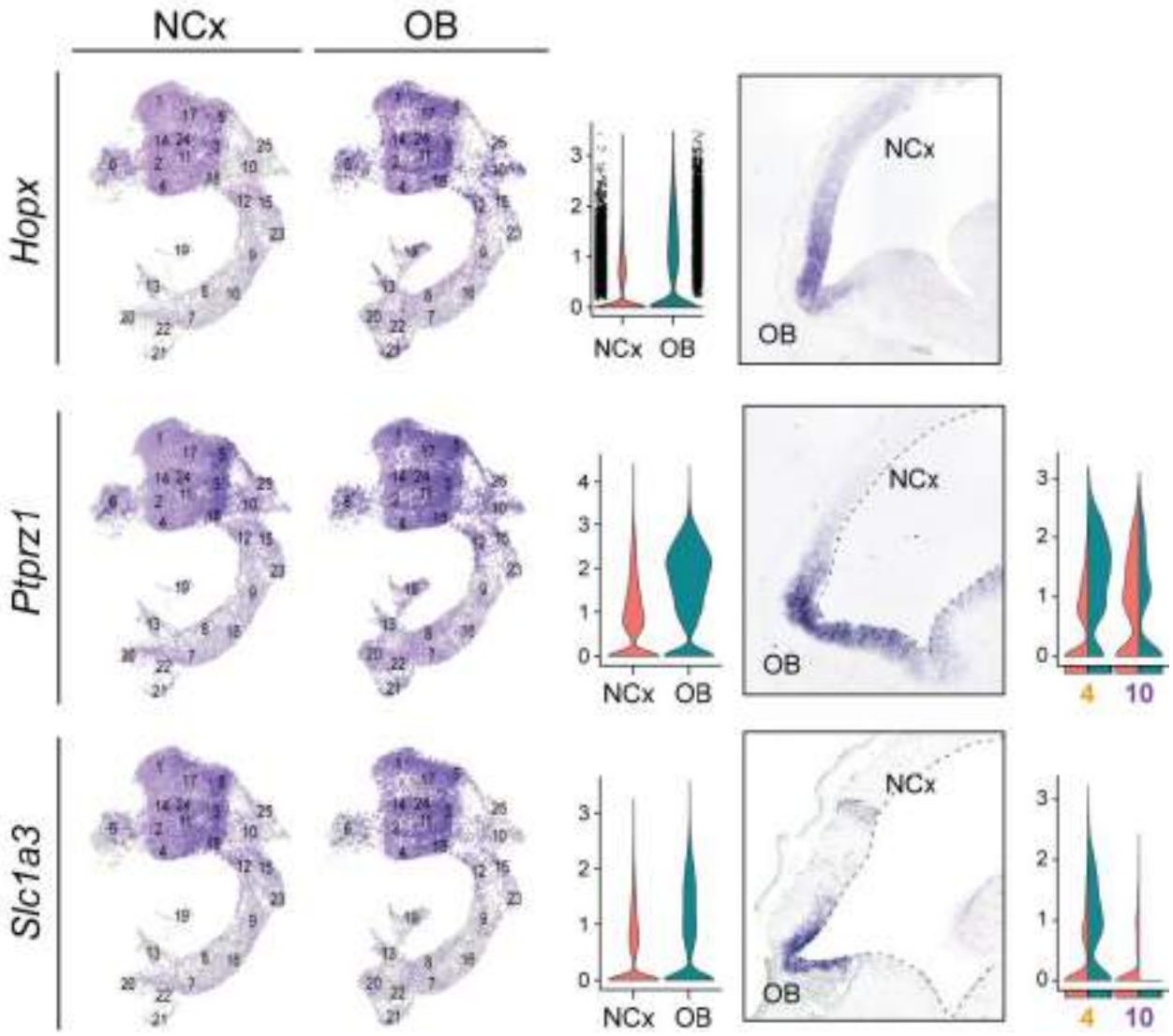

Figure 6. Expression of bRGCs markers higher in RGCs clusters of OB sample compared to NCx. patterns for a number of genes between NCx and OB. UMAP plots showing the expression pattern for *Hopx, Slc1a3,* and *Ptprz1* in the different cluster. Violin Plots showing the expressionof Hopx, Slc1a3, and Ptprz1. Sagittal brain sections of mouse E12.5 embryos showing the expression pattern of *Hopx, Slc1a3,* and *Ptprz1* in the NCx and OB.

Part 2. Characterizing Robo1/2 protein interactors

2.1. Proteomic analysis shows that Robo1/2 interact with different kinetochore assembly and spindle orientation proteins

Previously, we demonstrated that expression of myristoylated Robo1/2 intracellular cytoplasmic domain (mRobo1/2-ICD) (**Fig. 7A**) combined with low Dll1 expression promoted progenitors in the cortex to generate neurons directly. To understand the molecular signalling pathway that led to this phenotype, we opted to use liquid chromatography-mass spectrometry (LC-MS), in collaboration with Dr. Marc Gentzel, TU Dresden, and Dr. Alexandra Schambony, Friedrich-Alexander-Universität, Erlangen-Nürnberg, Germany. We immunoprecipitated the myristoylated form of Robo1/2 in the presence of Crispr Dll1 *in vitro* in P19 cells (**Fig. 7B**). The LC-MS analysis revealed the enrichment of more than 100 proteins in the cytoplasmic domain of Robo1/2 sample compared to the control.

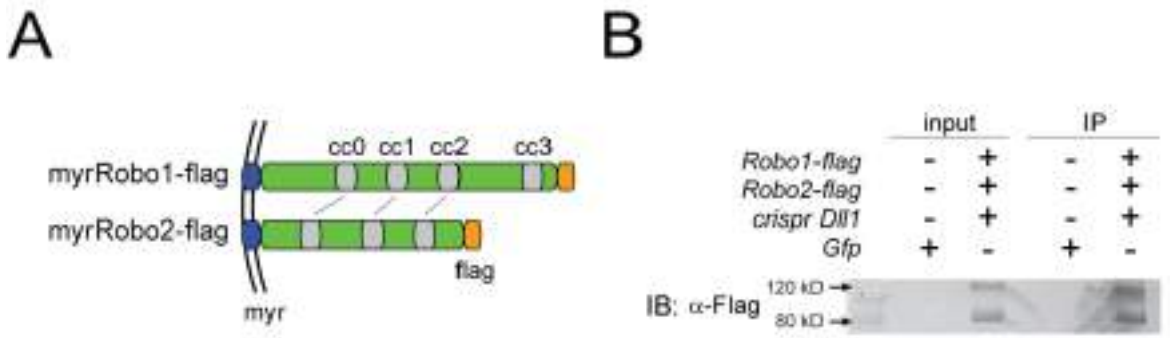

Figure 7. Immunoprecipitation of myristoylated form of Robo1/2 for mass spectrometry. (A) A schematic illustration showing myristoylated forms of Robo1/2 (mR1/2 flag) used in this study and the different cytoplasmic domains. (B) A western blot validating the immunoprecipitation of Robo1-Flag and Robo2-Flag accompanied with the knocking out of Dll1 using Crispr and a control sample in P19 cells. n=4.

As expected, mRobo1/2-ICD was pulled down with some of its known interactors, such as Nck1 and Nck2 (drosophila dock orthologues). These belong to a class of SH2-SH3 domain adaptor proteins and have been shown to be essential for achieving the physical connection between Robo and Son of sevenless (Sos). This protein complex binds to the cytoplasmic domains of Robo CC2-3, which is required for cytoskeleton dynamics and axon guidance across the midline (Fritz et al., 2015; Yang & Bashaw, 2006; Ypsilanti et al., 2010). Furthermore, Robo1/2-ICD interactors included Wipf1 and Wipf2 (WAS/WASL Interacting

Protein Family Member 1, WAS/WASL Interacting Protein Family Member 2). These proteins are known to contribute to the recruitment of WASL, which is essential in the actin polymerization molecular cascade (Rohatgi et al., 1999, 2000) (**Fig. 8A**). These interactors confirm the known role that mRobo1/2-ICD plays in cytoskeleton organization.

String analysis of our LC-MS results revealed an intriguing network of proteins that included nuclear proteins such as Nde1, Haus6, Dctn3, and Nup107 (**Fig. 8B**). These are associated with the kinetochore, mitotic spindle formation, and protein polyubiquitination, in addition to playing a role in cortical development (Cunha-Ferreira et al., 2018; Feng & Walsh, 2004; Splinter et al., 2012).

Interestingly, GO analysis (biological process) for these protein interactors revealed terms related to Robo signalling pathway, actin filament based proteins, regulation of RNA splicing, establishment of spindle localization, mitotic spindle orientation, and cell cycle progression. These findings suggest that Robo1/2-ICD interactions are not only restricted to cytoskeleton and axon guidance proteins but also include proteins that are associated with mitotic spindle organization and kinetochore assembly (**Fig. 8C**).

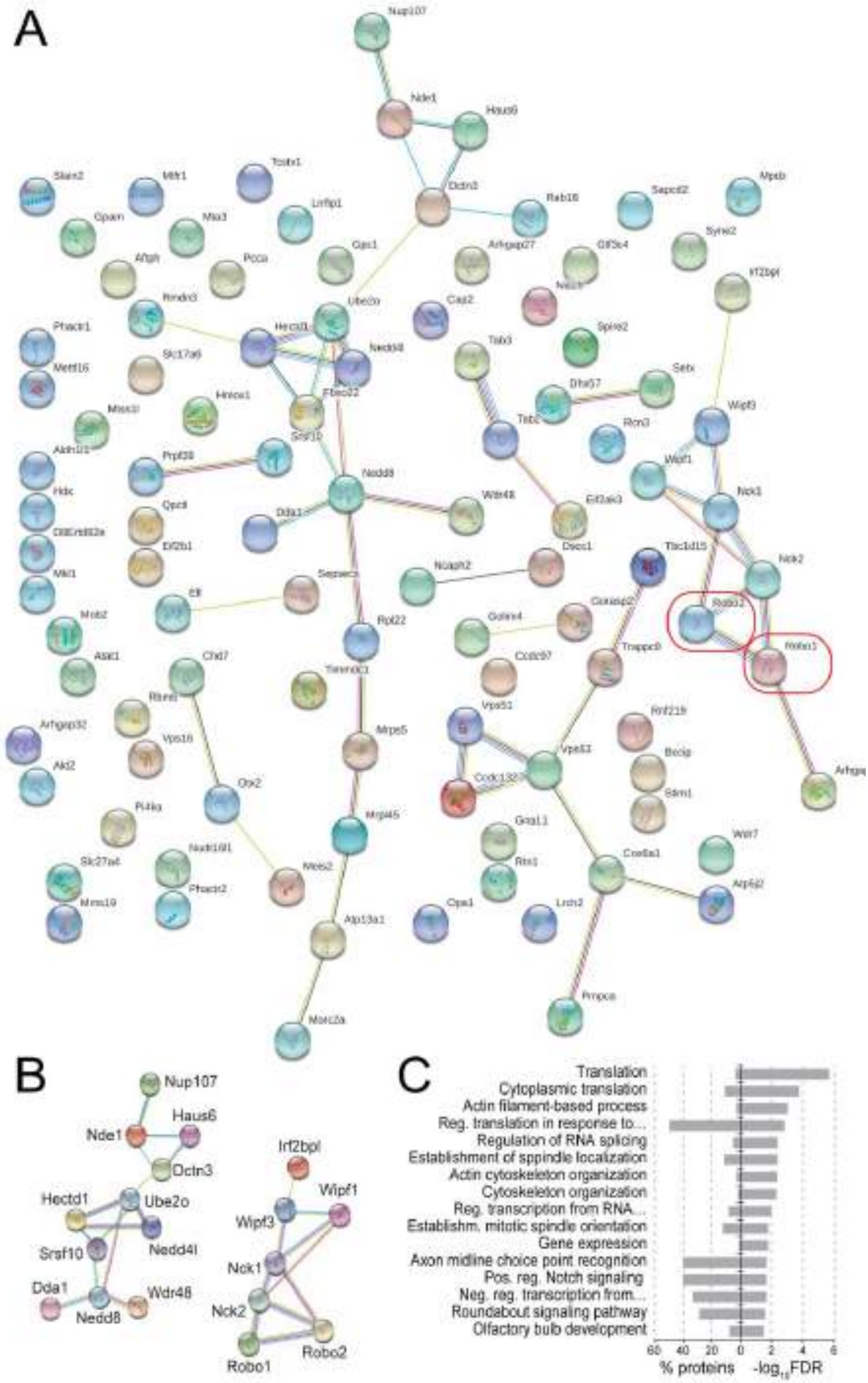
A
B
Nup107
Haus6
Nde1
Dctn3
Hectd1
Ube2o
Srsf10
Nedd4l
Dda1
Wdr48
Nedd8
Irf2bpl
Wipf1
Wipf3
Nck1
Nck2
Robo1
Robo2
C
Translation
Cytoplasmic translation
Actin filament-based process
Reg. translation in response to...
Regulation of RNA splicing
Establishment of sppindle localization
Actin cytoskeleton organization
Cytoskeleton organization
Reg. transcription from RNA...
Establishm. mitotic spindle orientation
Gene expression
Axon midline choice point recognition
Pos. reg. Notch signaling
Neg. reg. transcription from...
Roundabout signaling pathway
Olfactory bulb development
60 40 20 0 2 4 6
% proteins
-log10FDR

Figure 8. Robo1/2-ICD interactors are involved in cellular component biogenesis, translation, and spindle localization.(**A**) STRING functional protein association network performed on the 100 protein list.(B) Two networks depicting previously known Robo1/2 interactors as well as Robo1/2 nuclear and microtubule organisation related protein interactors. (C) The top enrichment GO terms' (biological process) significance is expressed as log10 FDR.

2.2 Robo1/2 cytoplasmic domains translocate to the nucleus

Previous research revealed that the Robo1-ICD translocates to the nucleus in cancer cells (Seki et al., 2010). Moreover, a recent study found that Robo1 localization to the nucleus may reflect a posttranslational regulation that is associated with a better prognosis and antitumor effect in bladder cancer patients (Krafft et al., 2020). To further delve into these previous findings, we used P19 cells for transfections and immunostaining of mRobo1/2-flag. Using superresolution microscopy, we discovered the presence of Robo1/2-ICD-flag protein in the cytoplasmic membrane as well as high abundance in the nucleus (**Fig. 9A**). To confirm this results, we transfected p19 cells with mRobo1/2-flag and immunoblotted them with anti-flag antibodies, anti-LaminB1 (to validate that we isolated the nuclear fraction), and anti-Gadph (to validate that we isolated the cytoplasmic and membrane fractions); indeed, mRobo1/2 ICD-flag showed a signal in both the cytoplasmic and membrane fractions, as well as a signal in the isolated nuclear fraction (**Fig. 9B**).

To determine whether the endogenous Robo1 cytoplasmic domain translocates to the nucleus, we used immunofluorescence on E12.5 cortical primary cultures with an antibody that recognises the cytoplasmic tail of Robo1. Cells that were co-stained with Sox2 and Roshowed the presence of Robo1-ICD in the nucleus and the cytoplasm (**Fig. 9C**).

We also validated this nuclear translocation of Robo1/2-ICD using antibodies that detect the endogenous signal for both Robo1 and Robo2-ICD. P19 cell lysates that were subjected to fractionation to isolate the nuclear fraction and cytoplasmic fraction were blotted by western blot. We used different antibodies for Robo1-ICD and Robo2-ICD. We found that both endogenous proteins were detectable in both the cytoplasmic and nuclear fractions of P19 cells (**Fig. 9D**).

In conclusion, these results demonstrate the presence of Robo1/2-ICD in the nucleus, implying a trafficking from the cell membrane to the nucleus that may have an impact on initiating the signalling cascade for Direct neurogenesis.

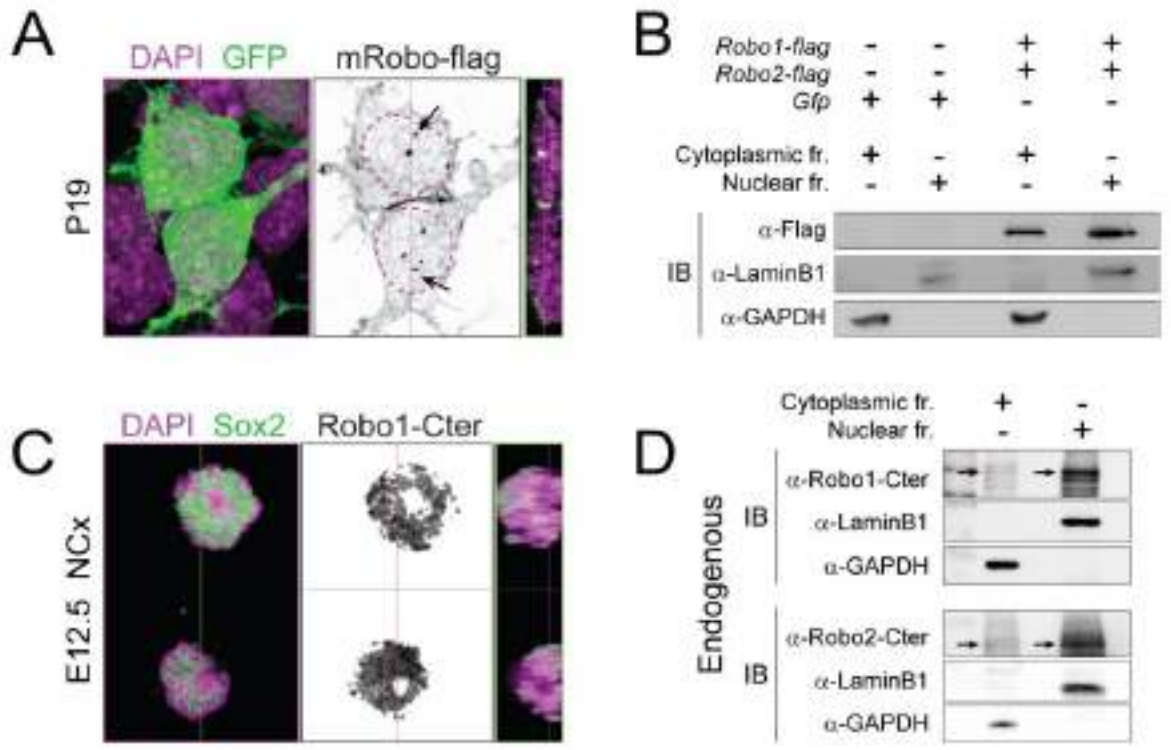

Figure 9. Robo ICD translocates to the nucleus. (A) Immunofluorescence of P19 transfected with mRobo flag, Showing DAPI (magenta), GFP (green), mRobo-flag (grey). The right panel displays a Z stack and orthogonal image of mRobo-flag (grey) and DAPI (magenta) with n = 3. Arrowheads point to the nuclear accumulation. (B) A representative western blot of cytoplasmic and nuclear fractions of P19 cell line transfected with mRobo1/2-flag. Robo-flag is detected in both nuclear and cytoplasmic fraction. GAPDH was used as a cytoplasmic marker, Lamin B1 as nuclear marker to exclude contamination during cell fraction isolation. n=3. (C) immunofluorescence of E12.5 primary culture, showing DAPI (magenta), Sox2 (green), Robo1-ICD antibody (grey). The panel on the right show Z stack and orthogonal image showing Robo1-ICD terminal antibody (grey) and DAPI (magenta) n=3. (D) A representative western blot of cytoplasmic and nuclear fractions of native P19 cell line, using specific antibodies for endogenous Robo1/2-ICD. The arrows indicate the position of endogenous Robo1/2-ICD in the cytoplasmic and the nuclear fraction. GAPDH was used as a cytoplasmic marker and Lamin B1 as nuclear marker to exclude contamination during cell fraction isolation.

2.3. Robo1/2-ICD have nuclear localization sequences

Following our above findings, we sought to determine whether Robo1/2-ICD contained nuclear localization sequences (NLSs), as mentioned in previous studies (Seki et al., 2010). Using the cNLS mapper (Kosugi et al., 2009), we found that Robo1-ICD has 2 NLS and Robo2-ICD has 3 NLS sequences (**Fig. 10**).

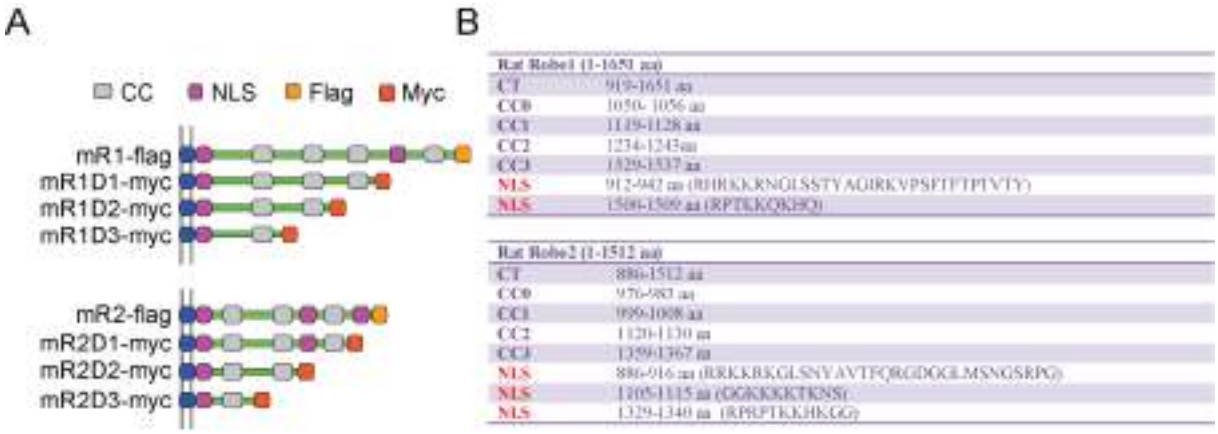

Figure 10. Robo1/2-ICD have nuclear localization sequences (NLSs). (A) A schematic illustration showing mRobo1/2-ICD with the different conserved cytoplasmic domains and predicted NLS sequences and tags present in each construct. (B) Tables showing the exact amino acid location of the different conserved cytoplasmic domains of rat Robo1/2 and the predicted NLSs.

2.4. Characterizing the potential of Robo1/2 truncated ICD in promoting direct neurogenesis

The cytoplasmic domains of Robo1/2-ICD are highly conserved (**Fig. 10A**). We investigated the necessity of these conserved cytoplasmic domains in the nuclear translocation of Robo1/2-ICD using truncated forms of Robo1-ICD (Robo1-D1, -D2, and -D3) and Robo2 (Robo2-D1, -D2, and -D3) (**Fig. 10A**). In p19 cells, each construct was transfected separately and the cytoplasmic and nuclear signals were quantified. The full length of both Robo1 and Robo2-ICD were found to be significantly more abundant in the nucleus than the other forms of truncated Robo1 and Robo2 (**Fig. 11**). As a result, we hypothesised that these cytoplasmic domains, along with the predicted NLSs, may interact with transporter molecules to facilitate the shuttle of Robo1/2-ICD to the cell nucleus.

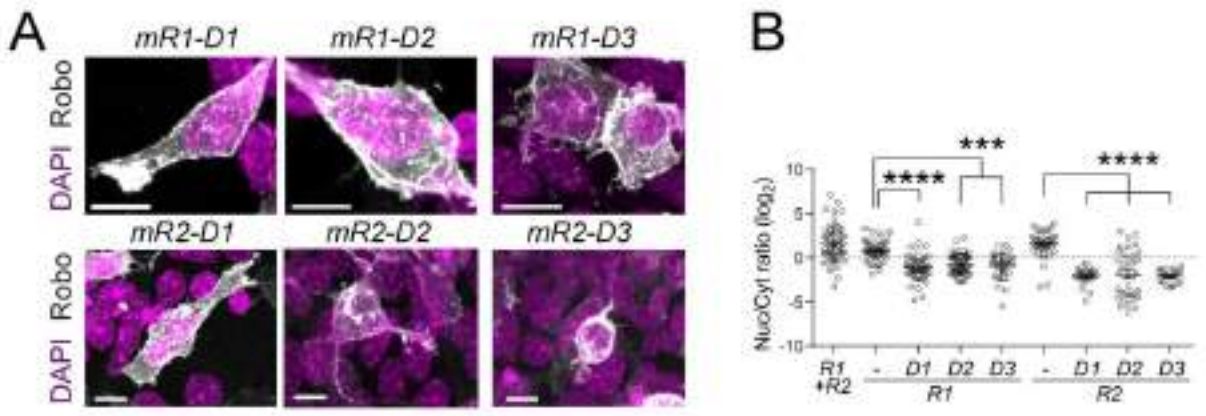

Figure 11. Characterizing the nuclear translocation of Robo1/2-ICD truncated forms in P19 cells. (A) Immunofluorescence Show DAPI (magenta), mRobo-myc (grey). (B) Quantification of Robo signal represented in log2 ratio between cytoplasmic and nuclear signal. n=3 coverslips per condition. Statistical analysis was performed using one-way ANOVA (multiple comparisons) followed by Turkey post hoc test. *P value< 0.05.mR1D1, mR1D2, mR1D3 photos were taken at 4X zoom, while mR2D1, mR2D2, mR2D3 photos were taken at zoom 1X.Sclae bar=10 µm.

After studying the ability of Robo1/2-ICD truncates to translocate to the nucleus, we wanted to see if different combinations of truncates have the ability to promote direct neurogenesis *in vivo* in mouse cortex. To test this hypothesis, we electroporated the full length myriostaleted form of Robo1/2-ICD with crispr-Dll1 in E12.5 mouse cortex and analysed the embryos at E14.5 (**Fig. 12A**). We were able to replicate the phenotype previously reported in (Cárdenas et al., 2018) of significantly promoting direct neurogenesis as compared to GFP or crispr-Dll1 alone (**Fig. 12B, 12C**). However, we discovered that mR1/2-D1+crispr-Dll1 and mR1/2-D2+crisprDll1 had a greater impact on promoting direct neurogenesis in the cortex than mR1/2-D3+crisprDll1 (**Fig. 12B, 12C**). These findings highlight the importance of the Robo1/2 CC (conserved cytoplasmic) domains in promoting Direct neurogenesis in the mouse cortex.

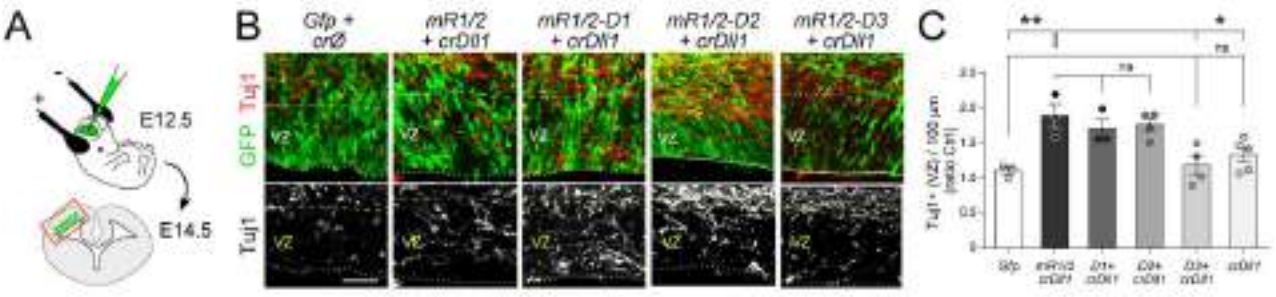

Figure 12. Characterizing the potential of Robo1/2 truncated ICD in promoting direct neurogenesis. (A) A representative scheme of NCX in-utero electroporation. (B) WT NCx electroporated with the indicated plasmid combinations (Immunofluorescence Show GFP (green), Tuj1 (red, grey). (C) Plot represents ratio of abundance of Tuj1+ cells in VZ between electroporated and non-electroporated hemispheres. Quantifications (n = 3-5 embryos per group; one-way ANOVA, followed by Tukey's multiple comparisons test, Values are mean + SEM; ns = not significant; * p<0.05; ** p<0.01. scale bar =50 µm.

2.5. Overexpression of Robo1/2-ICD promotes cell cycle exit and mitochondrial OXPHOS in cortical progenitors

To better understand the transcriptomic changes that occur upon overexpression of mRobo1/2-ICD and crispr-Dll1 in cortical progenitor cells -which results in Direct neurogenesis (Cárdenas et al., 2018), we performed bulk RNA sequencing of GFP^+ cells one day after *in utero* electroporation at E13.5 (**Fig. 13A**). Principal component analysis (PCA) and hierarchical clustering of transcriptomic profiles revealed a difference between control GFP^+ cells and mRobo1/2-ICD + crispr-Dll1 GFP^+ cells (**Fig. 13B,C**). Among the upregulated differentially expressed genes (DEGs) we found *Cdkn1a* (p21), *Ano3*, *Dglucy* and *Phlda3*; among the downregulated DEGs we found *Cntn2*, *Plxna4*, *Dok7*, *Cux2* (**Fig. 13D**). GO analysis showed that upregulated genes were enriched in the terms translation, cell cycle, cell division, mitotic cell cycle phase transition, rRNA processing, apoptotic process, negative regulation of epithelial cell proliferation, G1/S transition of mitotic cell cycle, nervous system development, and negative regulation of cell proliferation. On the other hand, GO terms enriched in downregulated genes included nervous system development, axon guidance, neuron projection development, synapse organization, axon fasciculation, Wnt signalling pathway, neurogenesis, and regulation of canonical Wnt signalling. These GO terms show mRobo1/2-ICD (accompanied with Dll1 knockdown) drives neurogenesis in mouse cortex by prompting cell cycle exit of cortical progenitors (**Fig. 13E**).

The normalised enrichment score (NES) of the gene set enrichment analysis (GSEA) revealed that upregulated genes upon overexpression of mRobo1/2-ICD plus Dll1-KD in the mouse cortex were enriched in the terms mitochondrial respiratory chain, endocardial morphogenesis, ribosomal subunit, interferon pathway, cell cycle arrest, viral genome replication, heart specification, ribonucleotide biogenesis, toxic substance detoxification, and chemokine. Furthermore, GSEA enriched terms of downregulated genes were related to cholesterol regulation, neurotransmitter receptor, synaptic membrane, synaptic vesicle, potassium channel, postsynapse assembly, and axon guidance (**Fig. 13F, 13G**). This analysis

further indicated the correlation between expression levels of mRobo1/2-ICD and of genes related to cell cycle exit. Moreover, we found an upregulation in genes related to mitochondrial processes and GSEA terms related to oxidative phosphorylation (OXPHOS) and respiratory chain genes. These results suggest that Robo1/2-ICD promotes direct neurogenesis of cortical progenitors by regulating neuronal oxidative phosphorylation (Zheng et al., 2016).

Interestingly, we found that genes related to neuronal differentiation were down regulated in both GSEA and GO analyses. To further understand this, we used the dataset from (Denoth-Lippuner et al., 2021) that describes the transcriptomic profile of neurons produced at E13.5 directly from aRGCs or indirectly from IPCs. Indeed we found that the percentage of up regulated genes from cells expressing Robo1/2 ICD and low Dll1 were correlated to the transcriptomic profile of neurons produced directly. Concomitantly, the percentage of downregulated genes in cells expressing Robo1/2-ICD and low Dll1 correlated with the transcriptomic profile of neurons produced indirectly via IPCs.This result shows that high expression of Robo1/2-ICD and low Dll1 expression induces direct neurogenesis by changing the transcriptomic profile of cortical progenitors (**Fig. 13H**).

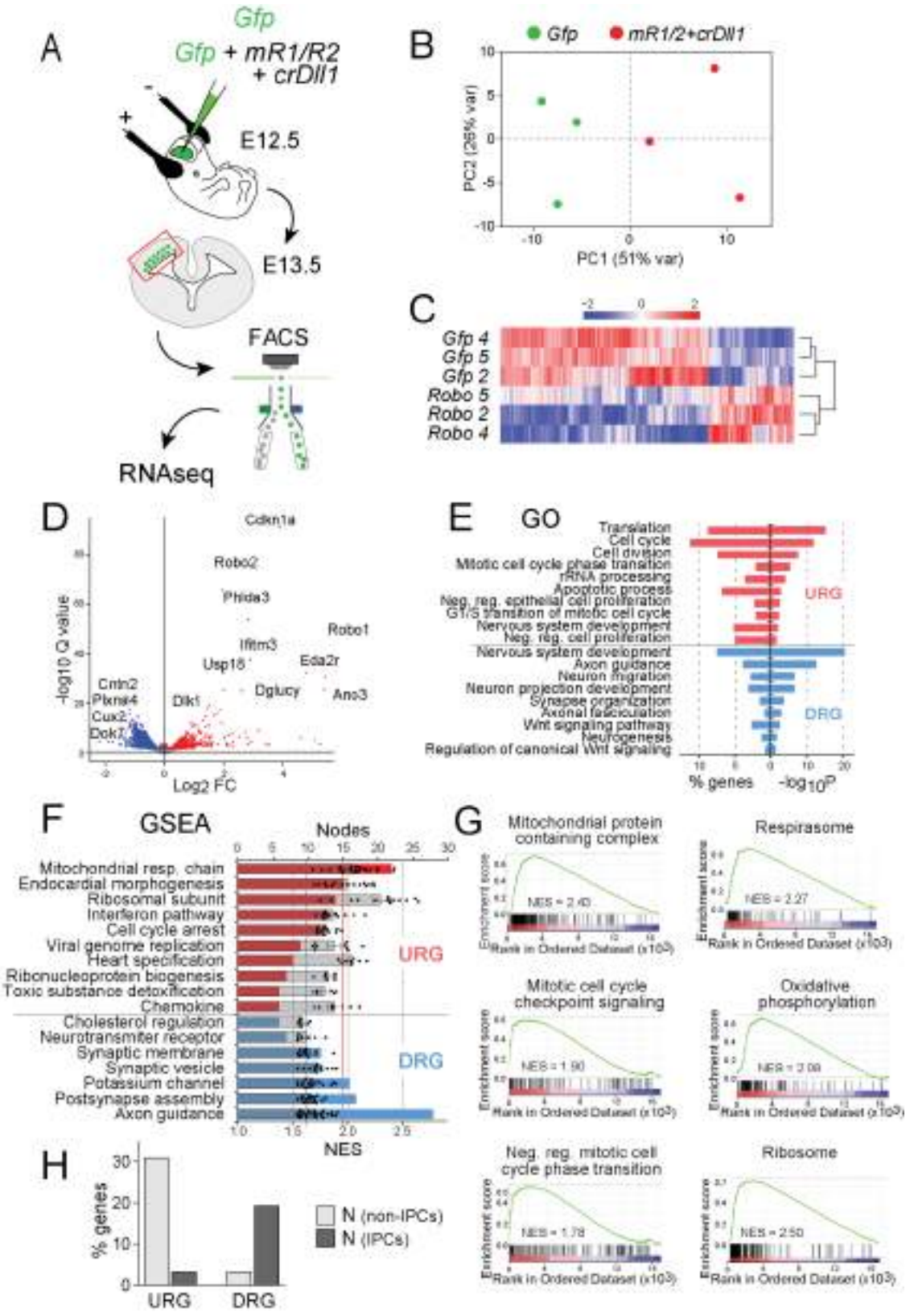

Figure 13. Robo1/2 ICD overexpression and Dll1 Knockout promote cell cycle exit and activiate OXPHOS. (A) Schema of experimental design: E12.5 mouse embryos were electroporated with GFP or GFP + mR1/2 and Crispr Dll1-encoding plasmids; at E13.5 their brains were microdissected and dissociated, cells expressing high levels of GFP were purified by FACS sorting, and their pooled RNA

expression profiles were analyzed by RNAseq. (B) Principal component analysis (PCA) showing GFP (green dots) and mR1&2+Crispr Dll1 (red dots). Samples clustered according to their gene expression. Each dot represents one sample. (C) A heat map shows the top 1537 highly variant genes between GFP and GFP plus mR1/2-ICD and Crispr Dll1 samples (in red: upregulation, in blue: downregulation). Statistical significance (FDR) is indicated. (D) A volcano plot representing the distribution of log2 fold change in gene expression. Differentially Expressed Genes (DEGs; Adj. P < 0.01). In red (upregulated genes, UGR) and blue (downregulated genes, DGR). On the plot, the top DEGs are depicted. (E) A Plot representing Gene ontology (GO) terms ranked by percentage of genes and $-\log_{10}$P value. (F) A forest plot showing Gene Set Enrichment Analysis (GSEA) terms that represent in red (upregulated genes, UGR) and blue (downregulated genes DGR) and their respective normalized enrichment scores (NES). (G) Enrichment plots from GSEA for mitochondrial protein containing complex (NES = 2.43; NOM p-val=0.00), respiraosome (NES= 2.27, NOM p-val=0.00), oxidative phosphorylation (NES=2.08, NOM p-val=0.00), mitotic cell cycle checkpoint signalling (NES=1.90, NOM p-val=0.00), negative regulation of mitotic cell cycle transition (NES=1.78, NOM p-val=0.00), ribosome (NES=2.50, NOM p-val=0.00). (H) A quantitative plot showing the percentage of up regulated and down regulated genes that correlate with genes that are expressed in progenitors that differentiating into neurons (N) directly or producing neurons through intermediate progenitors (IPCs) (Denoth-Lippuner et al., 2021).

Part 3. Robo ICD a possible transcription factor

3.1. Robo1 ICD possesses transcription factor characteristics

Next we used open online tool for predicting protein functional domains (Bernhofer et al., 2021) to enquire about the potential presence of DNA binding sites in Robo1/2-ICD. Intriguiungly, we found that Robo1/2-ICD in both mouse and rat have predicted DNA binding sites, with a similar size and distribution as in canonical transcription factors like Sox2, Pax6, Ngn1 (**Fig. 14A**). Next, we checked for the presence of DNA binding sites in Robo1-ICD across species (**Fig. 14B**). We detected a conservation of the predicted DNA binding sites in human, marmoset, mouse, pig, cow , dog, ferret, panda, cat , lizard, and snake (Bernhofer et al., 2021). These sites were somehow less conserved in species such as rat, chicken, zebrafinch, and zebrafish, with some point differences. Overall, these findings suggest that Robo1/2-ICD may bind DNA and subsequently change gene transcription across evolution.

To check whether these predicted DNA binding sites found in Robo1-ICD grant it the qualification of transcription factor (TF), we used DeepTFactor (Kim et al., 2021) ―a deep learning-based tool that predicts whether an interrogated protein is candidate to be TF― and tested Robo-ICD in mouse, human and ferret, alongside known human canonical TFs such as ZIC2, PAX6, TBR1, NMYC, MEIS2 (**Fig. 14C**). Surprisingly, mouse, human and ferret Robo1-ICD, along with human and ferret Robo3-ICD, scored highly in TF prediction, similar to canonical TFs. Comparing these TF prediction results of Robo1 and Robo3 to other transmembrane proteins with a cytoplasmic terminal, we found that these proteins scored

much lower than Robo family cytoplasmic domains and canonical TFs. Next we checked the TF prediction score for Robo family members across species (human, rhesus, marmoset, mouse, rat ferret, cat, pig, chick, and snake) using DeepTFactor (**Fig. 14D**). We found that Robo1-ICD scored highest in all species along with Robo3-ICD in human, marmoset, ferret, pig, and snake, compared to Robo2 and Robo4 ICDs. These results emphasize that Robo1/3 ICD possess the conserved protein characteristics to act as TFs.

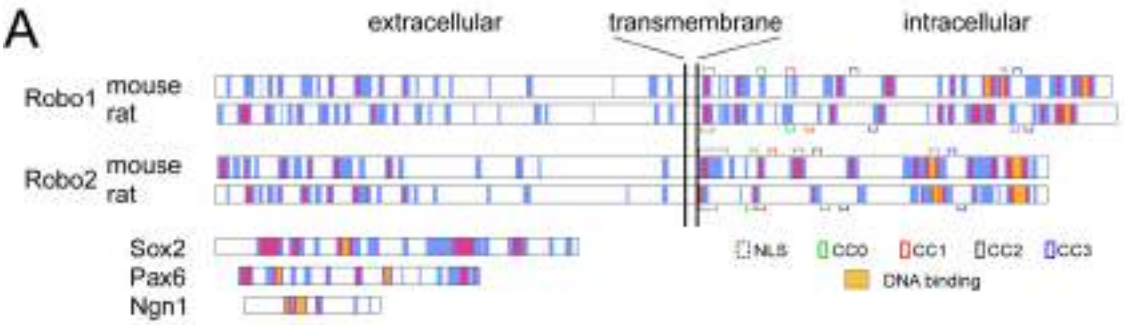

B

	CITOSOLIC ROBO1				
HUMAN	923-KKRNGL-928	1387-RSSVS-1391	1431-HFHASQCPRP-1440	1459-RPAKK-1463	1605 – SSMSSRGSGSR – 1615
RHESUS	KKRNGL	RSSVS	HFHASQCPRP	RPAKK	SSMSSRGSGSR
MARMOSET	KKRNGL	RSSVS	HFHASQCPRP	RPAKKQ	SSMSSRGSGSR
TARSIER	KKRSGL	RSSVS	HFHASPCPRP	RPAKK	SSMSSRGSGSR
MOUSE	KKRNGL	RSSVS	HFHASQCPRP	RPAKKQ	SSMSSRGSGSR
RAT	KKRNGL	RSSVS	HFHASQCPRP	RPTKKQ	SSMSSRGSGSR
PIG	KKRNGL	RSSVS	HFHASQCPRP	RPAKKQ	SSMSSRGSGGRQ
COW	KKRNGL	RSSVS	HFHASQCPRP	RPAKKQ	SSMSSRGSGSR
DOG	KKRNGL	RSSVS	HFHASQCPRP	RPAKKQ	SSMSSRGSGSR
FERRET	KKRNGL	RSSVS	HFHASQCPRP	RPAKKQ	SSMSSRGSGSR
PANDA	KKRNGL	RSSVS	HFHASQCPRP	RPAKKQ	SSMSSRGSGSR
CAT	KKRNGL	RSSVS	HFHASQCPRP	RPAKKQ	SSMSSRGSGSR
CHICK	KKRNGL	RSSVS	HFHASHCPRP	RPAKKQ	SSMSSRGSGGRQ
ZEBRA FINCH	KKRNGL	RSSVS	HFHASHCPRP	RPAKKQ	SSMSSRGSGGRQ
LIZARD	KKRNGL	RSSVS	YHAS	RPVKKQKHQQG	SSMSSRGSGSR
SNAKE	KKRNGL	RSSVS	YHAS	RPAKKQKHQQG	SSMSSRGSGSR
ZEBRA FISH	KKRNGL	RSSAVS	KYQNLPAGHRP	RPLKRQKQHPAAQTG	ISLSSRGSGGRRRGEGPPGARF

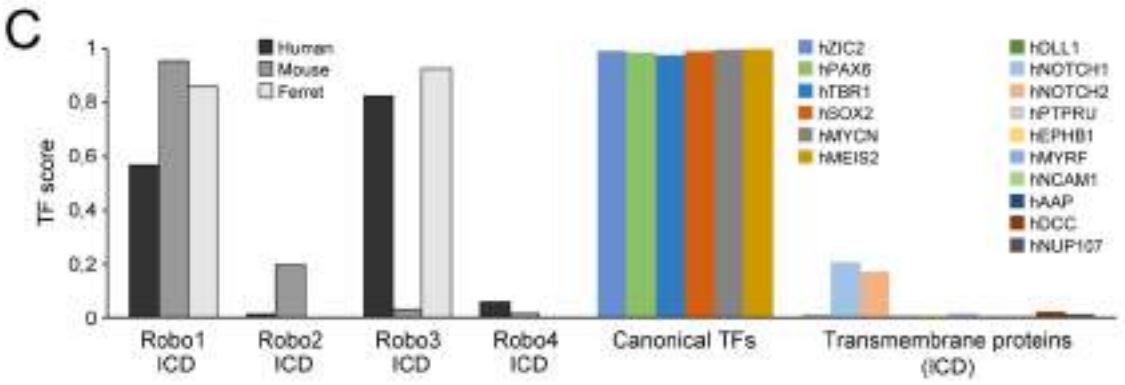

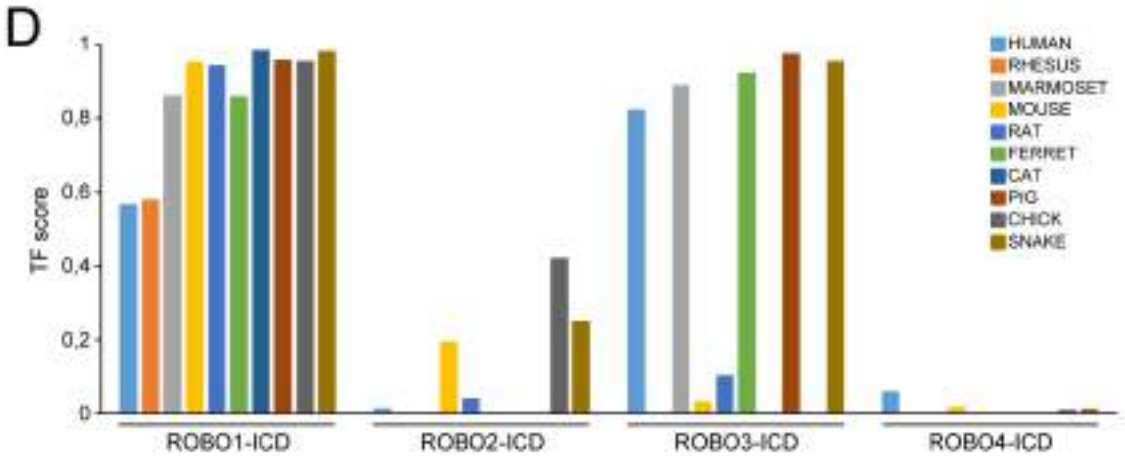

Figure 14. Robo1 ICD has TF characteristics. (A) Illustration of the extracellular, transmembrane, and intercellular regions of mouse and rat Robo 1/2 full-length proteins. Cytoplasmic domains (CC0 (green), CC1 (red), CC2 (black), and CC3 (blue)) are indicated in the protein sequences. Nuclear localization sequences (NLS) are indicated in dashed lines. DNA binding predicted (yellow) sequences are indicated in the intracellular region of the protein. Schematic representation of DNA binding regions in canonical transcription factors (Sox2, Pax6, Ngn1) (B) A table displaying predicted DNA binding sequences based on the Robo1 ICD amino acid sequence in various species, as determined by the predict protein tool (Bernhofer et al., 2021). Sequences in pink are different from other species due to point mutations. (C) A plot created with DeeptFactor tool depicting the Robo family ICD transcription factor score in mouse, human, and ferret, as well as canonical transcription factors and other trans membrane proteins (Kim et al., 2021). (D) A plot created with DeeptFactor tool showing the transcription factor scores of the Robo family ICD in different species (Kim et al., 2021).

3.2. Chip-seq reveals Robo1-ICD binding sites on genomic DNA

P19 cells were used to investigate the potential location of Robo1/2-ICD to chromatin. We began by performing *in situ* subcellular fractionation (CSK) on cells transfected to express mRobo1/2-ICD-Flag (**Fig. 15A**). We removed different compartments of the cell membrane and organelles using CSK buffers. We observed Robo1/2-ICD-flag in the tightly held nuclear fraction, together with the staining of the nuclear envelope by lamin B1. After using additional stringent CSK buffers, we also detected Robo1/2-ICD-flag signal in the chromatin fraction of these cells; this signal coincided with Histone1 signal, which stains the top of the structure that keeps the DNA in place wrapped around the nucleosome (**Fig. 15B**). This suggests that Robo1/2-ICD binds DNA or is in very close proximity to DNA and may play a role in transcriptional regulation.

Based on our previous bioinformatics data that predicted Robo1 ICD acting as a TF, we wanted to investigate the possible genomic binding sites of Robo1 ICD. We performed chromatin immunoprecipitation followed by chromatin deep sequencing (Chip-seq) in P19 cells transfected with mRobo1-ICD flag and crispr-Dll1 (**Fig. 15A**). This experimental setup allowed us to understand the chromatin modifying aspect of Robo1-ICD overexpresssion and knocking out of Dll1 exert on progenitors to induce direct neurogenesis. Data was normalized using the input of Chip-seq from native p19 cells. We identified a total of 871 peak, distributed along 5UTR, promoter, exonic, intronic, and intergenic DNA regions, with a high preference to bind intergenic and intronic DNA regions (**Fig. 15C**).

Next, we cross-analyzed the genes with Robo1-ICD ChIP peaks with the DEGs derived from the previous transcriptomic analyses. We found 63 DEGs that contained Robo1 ICD peaks, and 22 DEGs with Robo1-ICD peaks at their promoter regions (**Fig. 15G**). Indeed, the majority of DEGs showed Robo1-ICD binding in their exonic and promoter regions (**Fig.**

15F). We found that Robo1-ICD binds to DEGs including its own exonic region, the *Bcl7a* intronic region, the *Rnf38* promoter region, the *Pou6f1* promoter region, and the *Dll1* promoter region (**Fig. 15E**). Validation of this binding via Chip-qPCR showed enrichment of Robo1-ICD on the exonic region of *Robo1*, *Dll1* promoter, and *Bcl7a* intronic region (**Fig. 15D**). These findings suggest that Robo1-ICD binding different genomic regions could play a direct role in transcription control.

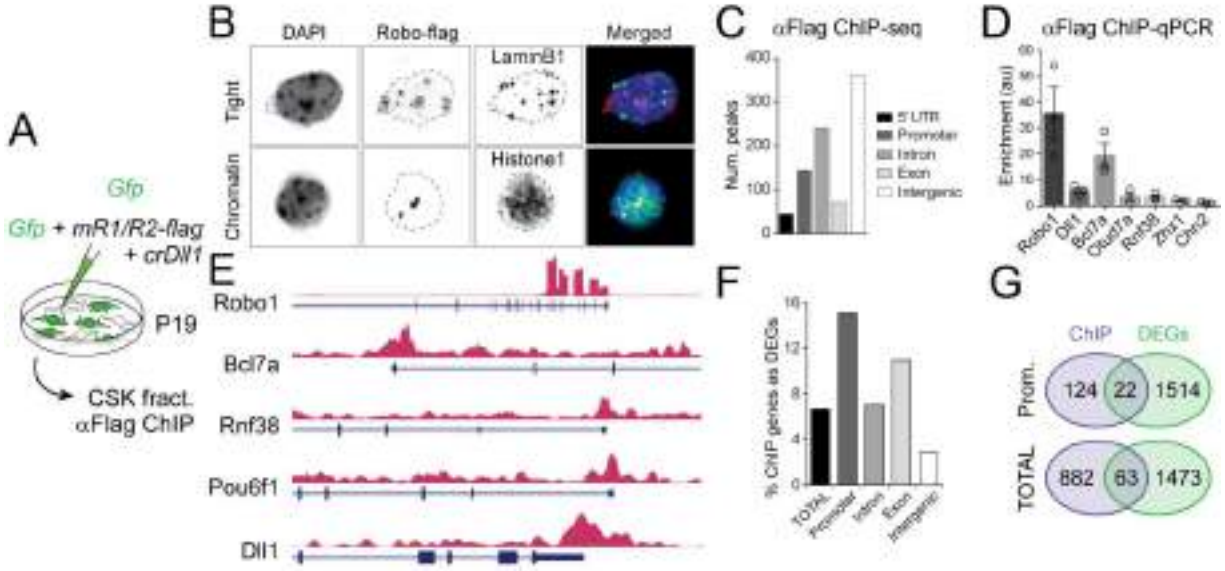

Figure 15. Robo1 ICD localizes to the chromatin and binds to a variety of genomic regions. (A) A schematic representation illustrating the experimental design using P19 cells transfected with GFP and GFP+ mRobo1/2-ICD flag+ Crispr Dll1; these cells were used to perform CSK fractionation and anti-Flag Chip. (B) P19 cells treated with CSK buffer to reveal the tightly held nuclear portion and chromatin. Cells where then subjected to immunofluorescence. (Dapi, grey), (Robo-flag,grey), (laminb1, grey), (histone1, grey), channels merged showing (dapi, blue), (Robo-flag,red), (lamin b1, green), (histone1, green). (C) A bar graph illustrating the distribution of Robo1 ICD flag binding peaks from Chip-seq and their functional categories. (D) A bar graph illustrating Chip fold enrichment of DNA fragments using Chip-qPCR analysis of *Robo1*, *Dll1*, *Bcl7a*, *Outd7a*, *Rnf38*, *Zhx1*, and *Chn2*. Each value represent mean SD (n=3). Chip-qPCR was performed to elucidate the regulatory role of Robo1 in regulating the transcription of predicted target genes. (E) Chip-seq tracks for Robo1-flag occupancy. Representative tracks for *Roob1*, *Bcl7a*, *Rnf38*, *Pou6f1*, and *Dll1*. The corresponding gene is displayed in (blue), the direction of transcription is marked with blue arrows within the gene. (F) A bar plot displaying the percentage of DEGs from mRobo1/2-ICD + Crispr Dll1 RNA sequencing obtained from electroporated cortical progenitors at E13.5 that appear in the Robo1-flag chip peaks, as well as their functional categories. (G) A Venn diagram illustrating the intersection of Chip peaks in the promoter region and total peaks with DEGs obtained from electroporated cortical progenitors at E13.5 using mRobo1/2-ICD + Crispr Dll1 RNA seq.

3.3. Robo 1 activates neuronal differentiation *in vitro* in P19 cells

According to transcription factor prediction analysis, Robo1-ICD has a higher likelihood of acting as a transcription factor. Immunofluorescence, nuclear fractionation, CSK fractionation assay, and Chip-seq experiments all show Robo1-ICD translocation to the nucleus and DNA binding. To elucidate the role of Robo1-ICD in regulating transcription, we performed bulk RNA-seq of P19 cells overexpressing mRobo1 ICD flag and control GFP expressing cells. FACS sorting GFP+ expressing cells was followed by bulk RNA extraction and sequencing (**Fig. 16A**). PCA analysis yielded two principal components that successfully discriminated between the samples based on their RNA profiles (**Fig. 16B**). This confirmed that the six samples (three biological replicates per condition) of GFP and mRobo1-ICD had very high levels of reproducibility. We identified 3798 DEGs with (Adj. P<0.01), in the samples overexpressing mRobo1 ICD. We found that 51% of the DEGs were down regulated genes, while 49% of the DEGs were up regulated genes (**Fig. 16C**). Interestingly, we discovered that some of the up-regulated DEGs were associated with the Notch pathway, such as *Lfng*, *Dll1*, and *Jag1*. Furthermore, *Dmbx1* and *Tlx2* were among the upregulated DEGs. *Dmbx1* is a homeobox transcription factor that controls cell cycle exit and differentiation in retinal progenitors (L. Wong et al., 2010). *Tlx2*, a transcription belonging to the homebox family, was found to be important in controlling the timing of neurogenesis in the developing cortex (Roy et al., 2004). GO analysis was performed to reflect the biological relevance of the DEGs. GO analysis on the up regulated DEGs highlighted biological processes such as Neurogenesis, cell morphogenesis involved in differentiation, and cellular protein localization (**Fig. 16D**). However, GO analysis of down regulated DEGs highlighted biological processes such as: RNA processing, translation, and Ribonucleoprotein complex biogenesis (**Fig. 16D**). This observation concerning the downregulation of translation and ribosomal biogenesis genes could be explained by the sequential downregulation of ribosomal biogenesis required for the transition from pluripotency to differentiated neurons (Hetman & Slomnicki, 2019).

Finally, our transcriptomic analysis demonstrates Robo1-ICD's ability to induce transcriptomic changes that affect fate determination.

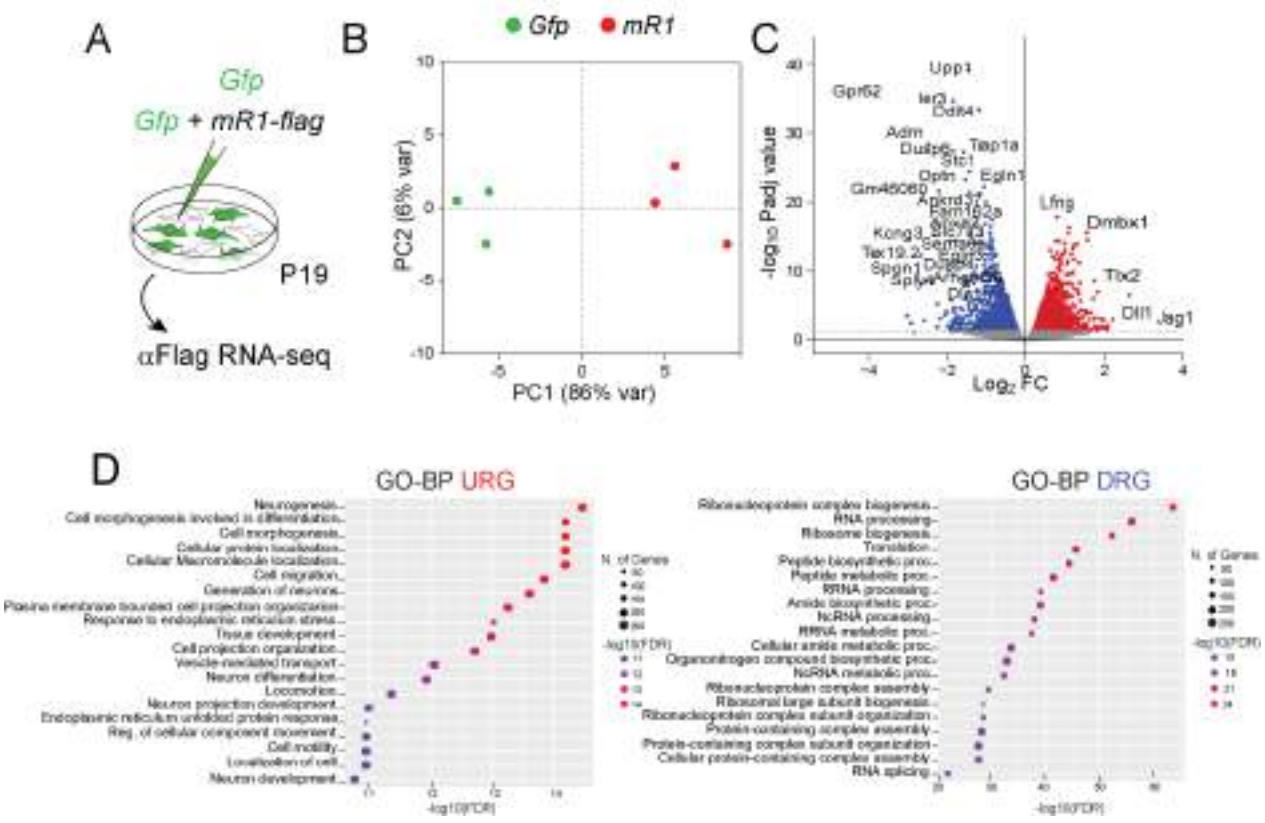

Figure16. Robo1 ICD promotes neurogenesis and cell morphogenesis *in vitro*. (A) A schematic representation illustrating the experimental design. P19 cells were transfected with GFP or mRobo1-ICD flag; cells expressing GFP were purified using FACS sorting, and their pooled RNA was then analyzed by bulk RNA sequencing. (B) Principal component analysis (PCA) showing GFP (green dots) and mR1 (red dots). Samples were clustered according to their gene expression. Each dot represents one sample. (C) Volcano plot representing the distribution of log2 fold change in gene expression. Differentially Expressed Genes (DEGs; Adj. P < 0.01), in red (upregulated genes, UGR) and blue (downregulated genes, DGR). the top DEGs are depicted on the plot. (D) Functional enrichment analysis of the DEGs, showing the most significant enriched GO terms for URG and DRG. Ontology: Biological Process.

3.4. Robo1 binds to and regulates the *Dll1* promoter region

We previously showed that high levels of Robo1/2-ICDs and low level of Dll1 promote direct neurogenesis across amniotes cortices (Cárdenas et al., 2018). Furthermore, we showed in this thesis that Robo1-ICD flag binds to Dll1 promoter region, this occurred in an experimental setup where we are using Crispr Dll1. In order to address the DNA binding potential of Robo 1-ICD without the interference of Crispr Dll1, we performed Chip qpcr assay using anti-Flag antibody to determine the enrichment of Robo1 on the chromatin of *Robo1*, *Dll1*, *Bcl7a*, *Outd7a*, *Rnf38*, and *Zhx1* (**Fig. 17A**). Robo1-ICD binding was highly enriched on Robo1 exonic region and Dll1 promoter region compared to the other genes. Moreover, Robo1

enrichment on Robo1 exonic region in the CHIP-qPCR against mRobo1 had a similar value to CHIP-qPCR mRobo1 and Crispr Dll1, but Robo1 enrichment on Dll1 promoter was at a higher value in the CHIP-qPCR against mRobo1-ICD alone. This result already validates the efficiency of Crispr Dll1 directly on Dll1 genome transcription and confirms that Robo1 ICD could be directly affecting *Dll1* transcription via binding *Dll1* promotor (**Fig. 17B**).

To investigate the effect of mRobo1-ICD on *Dll1* promoter activity, we performed luciferase assays comparing the effects of mRobo1/2 ICD, mRobo1-ICD myc, mRobo1-ICD flag and Jag1 on *Dll1* promoter activity. We found that mRobo1/2-ICD, mRobo1-ICD myc, and mRobo1-ICD flag gain of function were able to decrease Dll1 promoter significantly (**Fig. 17C, 17D**). This result, combined with the previous finding of Robo1 enrichment over Dll1 promoter region, confirms the ability of Robo1-ICD to modify *Dll1* activity.

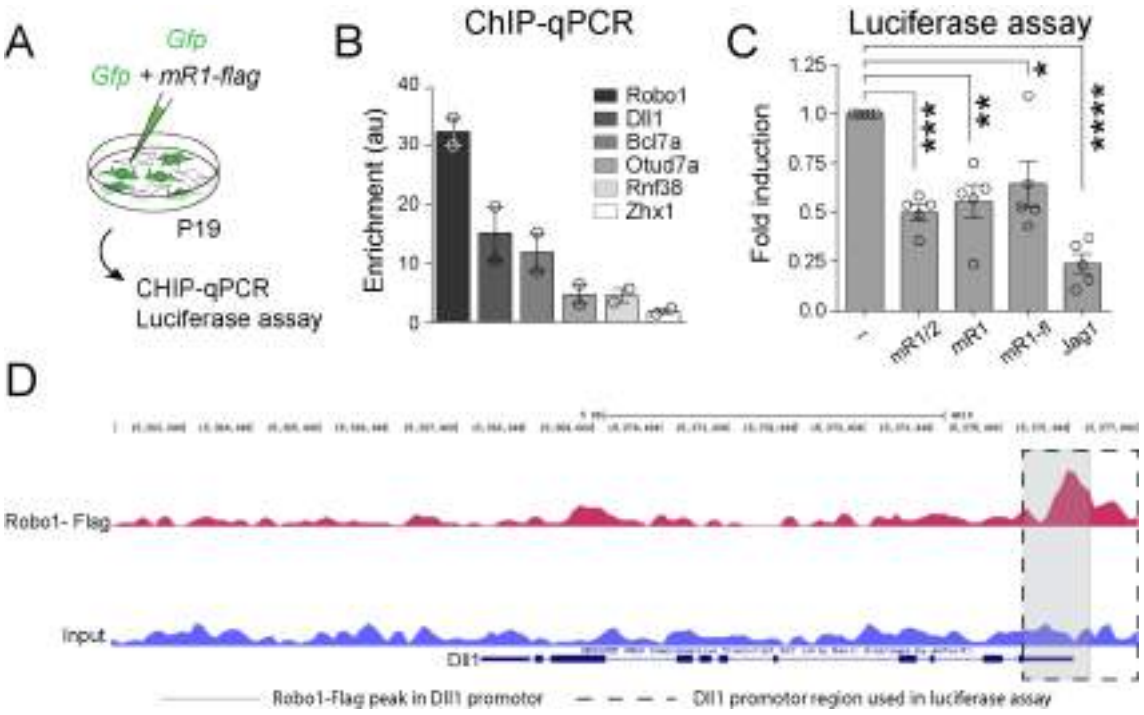

Figure17. Robo1 ICD binds to *Dll1* promoter. (A) A schematic representation illustrating the experimental design used, where P19 cells were transfected with mRobo1-ICD flag and subjected to Chip-qPCR and luciferase assays using Dll1 luciferase plasmid to measure *Dll1* promoter activity. (B) Chip-qPCR showing the regulatory role of Robo1 ICD in regulating transcription of predicted key target genes of *Robo1*, *Dll1*, *Bcl7a*, *Outd7a*, *Rnf38*, *Zhx1*, and *Chn2*. Chromatin of P19 cells transfected with Robo1 ICD Flag and immunoprecipitated using anti-flag antibody. Each value represent mean SD (n=3). (C) P19 cells were transfected with Dll1 Luc alone or with mRobo1/2, mR1, mR1-flag, Jag1, or an empty pcDNA (mock) vector and normalized to the activity of pcl Renilla. After 24 hours of incubation, luciferase activity was measured. Each value represents the mean SD (n=5), where five independent experiments were performed in triplicates. Groups were compared by one-way ANOVA followed by Turkey's post hoc test. *, significantly different from control (mock), $p < 0.05$. (D) Genome browser tracks show Robo1 flag Chip-seq in the presence of Crispr Dll1 and input over *Dll1* gene. Ref seq annotations are shown below the tracks. The *Dll1*

promoter region is denoted by a dashed line, and the RoboFlag binding region in the *Dll1* promoter is denoted by a grey line.

3.5. The Robo interacting protein Nup107 has a conserved role in promoting Direct neurogenesis

We previously demonstrated that Robo1/2-ICD interacted with proteins involved in kinetochore assembly, spindle microtubule dynamics, and transcription factors, including Nup107. We were intrigued by the presence of this protein in the dataset because it is a key component in the formation of nuclear pore complexes (NPCs), and all molecules entering or exiting the nucleus are actively transported or diffuse across the nuclear membrane via an NPC protein. First, we conducted a co-immunoprecipitation experiment in P19 cells to confirm the interaction of Robo ICD and Nup107 (**Fig. 18A**). Given that NPC proteins are known to have an evolutionary conserved role in cell cycle progression, mitosis, and transcriptional regulation (Ibarra & Hetzer, 2015). We wanted to investigate the expression pattern of *Nup107* in different amniotic species; therefore we performed ISH in mouse, chicken, and snake at different timepoints of development. At E8, *Nup107* expression was found only in the SVZ region of the snake pallium. *Nup107* expression in mouse telencephalon at E12.5 was lower in the OB compared to the adjacent NCx, and it was higher in the lateral dorsal pallium (lDP) compared to the medial dorsal pallium (mDP) throughout E6 chick pallium (**Fig. 18B**). Taken together, we find that the coincidences of low *Nup107* expression with areas have higher *Robo1/2* expression suggest a possible role of Nup107 in progenitor's fate determination.

Then we wanted to test the hypothesis that *Nup107* low expression in OB progenitors was part of the signalling cascade promoting direct neurogenesis. We used a Crispr guide against mouse *Nup107*, which was cloned into a plasmid encoding for all the CRISPR machinery, including the gRNA scaffold, Cas9 and GFP as a reporter of transduced cells. To validate that we were targeting the expression of *Nup107*, we transfected crispr-Nup107 into P19 and performed western blot analysis on FACs sorted transfected cells. We confirmed that that our crispr guides were able to abate Nup107 protein levels (**Fig. 18D**). After validating the Crispr guide, we moved forward with testing them *in vivo*. We electroporated the guide together with Cas9 into the NCx of E12.5 mice, using an empty crispr plasmid as a control, and the phenotype was analysed at E14.5 (**Fig. 18C**). We quantified $Tuj1^+$ cells in the VZ to assess changes in Direct neurogenesis. We found that Nup107 crispr increased the ratio of $Tuj1^+$

cells significantly compared to control Crispr elctroporated samples (these ratios were normalized to non-electroporated contralateral NCx section) (**Fig. 18E,F**). Thus, we conclude that a decrease of *Nup107* expression in mouse NCx progenitors is sufficient to promote Direct neurogenesis.

In a previous study we showed that overexpressing mRobo1/2 ICD and knocking out Dll1 expression in chick lDp at E4 was sufficient to promote Direct neurogenesis by two days after *in ovo* electroporation, increasing $Tbr1^+$ cells in VZ and decreasing basal $PH3^+$ cells (Cárdenas et al., 2018) . To elucidate whether decreasing *Nup107* expression in the chick lDp is sufficient to increase Direct neurogenesis, we used a crispr guide against chicken sequence of *Nup107* and performed *in ovo* electroporation at E4 and analysed the embryos 2 days post electroporation. We found a significant decrease in basal $PH3^+$ cells and a significant increase in $Tbr1^+$ cells in VZ of *Nup107* KD embryos in comparison to controls (**Fig. 18G**). These results demonstrate that Nup107 has an evolutionary conserved function in promoting Indirect neurogenesis in the NCx across amniotes.

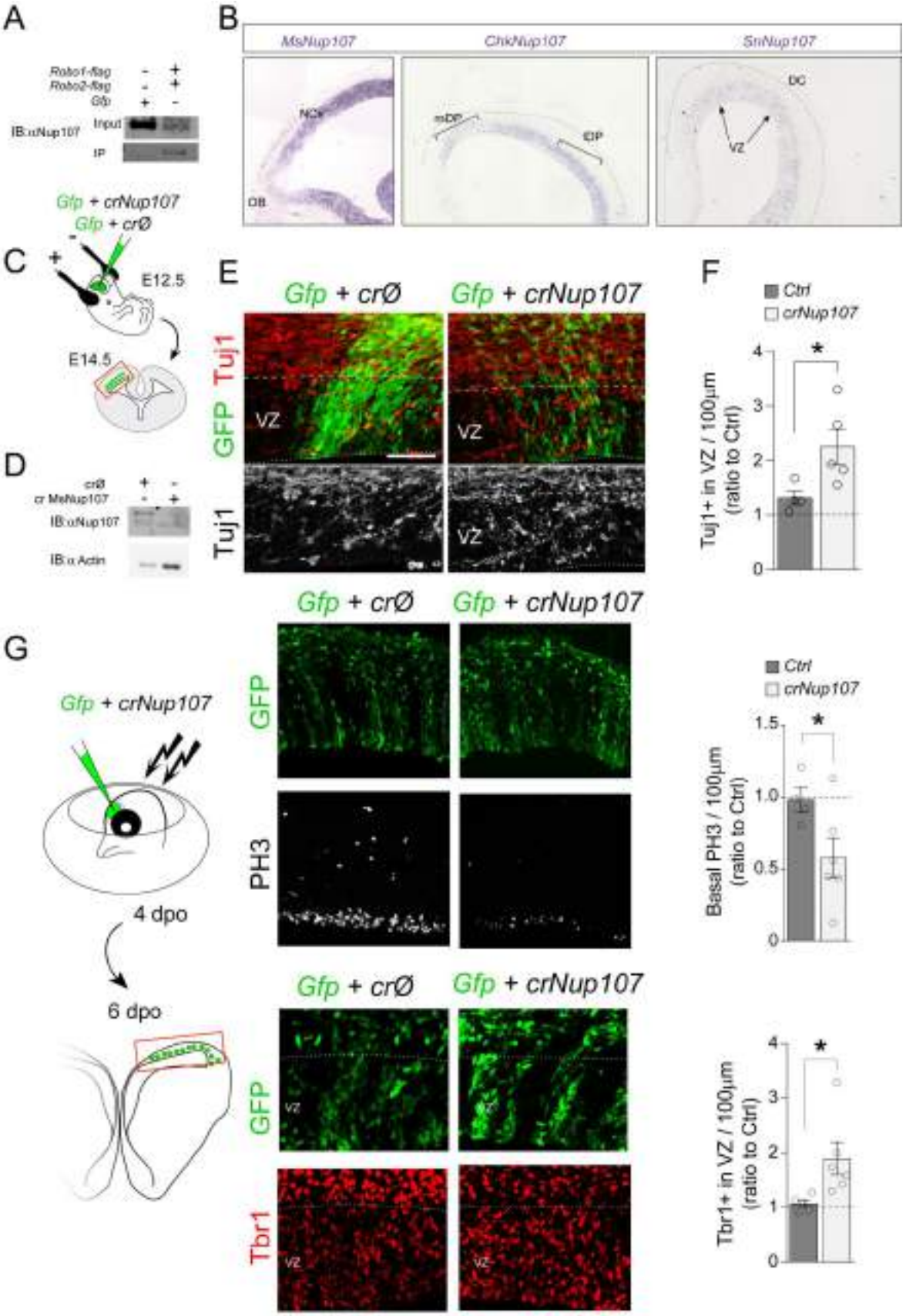
A
Robo1-flag
Robo2-flag
Gfp
IB:αNup107
Input
IP
B
MsNup107
ChkNup107
SnNup107
NCx
OB
nIZP
IZP
VZ
DC
C
Gfp + crNup107
Gfp + crØ
E12.5
E14.5
D
crØ
cr MsNup107
IB:αNup107
IB:α Actin
E
Gfp + crØ
Gfp + crNup107
GFP Tuj1
Tuj1
VZ
F
Ctrl
crNup107
Tuj1+ in VZ / 100µm
(ratio to Ctrl)
G
Gfp + crNup107
4 dpo
6 dpo
GFP
PH3
Basal PH3 / 100µm
(ratio to Ctrl)
Tbr1
Tbr1+ in VZ / 100µm
(ratio to Ctrl)

Figure 18. Nup107 induces direct neurogenesis in developing mouse NCx and Chick pallium. (A) Co-immunoprecipitation (Co-IP) assay showing interaction of Nup107 with Robo1/2 ICD. Robo1/2 ICD-flag and control GFP were expressed in independent samples transiently in P19 cells in vitro. (B) ISH stains for Nup107 in mouse at E12.5, chick at dpo E6 and snake at dpo E8. (C) Schema of experimental design: E12.5 mouse embryos were electroporated with Crispr plasmid without guide or Crispr plasmid with guide for mouse Nup107, at E14.5 embryos were sacrificed and processed for immunofluorescence. (D) A western blot validating mouse Nup107 crispr, the western blot samples used where of P19 cells lysate expressing Crispr plasmid without guide or Crispr plasmid with guide against mouse Nup107. (E) WT NCx at E14.5 electroporated as indicated in (C), immunofluorescence show GFP (green) and Tuj1(red, black). (F) Quantification showing the ratio of $Tuj1^+$ cells in the VZ between electroporated and non-electroporated hemispheres using t test. Values are shown in SEM, n=3-5 embryos per group, *P value<0.05. (G) Schema of experimental design: at day 4 dpo chick embryos were electroporated with Crispr plasmid without guide or Crispr plasmid with guide for mouse Nup107 and at day 6 dpo, embryos were sacrificed and processed for immunofluorescence. Immunofluorescence and quantification in the VZ of day 6 dpo chick embryos with the indicated plasmids, GFP (green), PH3(black), and Tbr1(red).Quantifications showing the ratios of basal mitoses ($PH3^+$) and neurons ($Tbr1^+$) in the VZ between electroporated and non-electroporated hemispheres using unpaired t-tests. Values are shown in SEM with n=3-5 per group. *P value<0.05.

Discussion

Discussion

Heterogeneity and lineage of progenitor cell populations in the developing NCx and OB

Recent single cell studies have focused on understanding the neuronal and progenitor cell diversity in the developing mouse neocortex, as well as correlating it to temporal and spatial gene expression (Moreau et al., 2021; Ruan et al., 2021). We recently showed that direct neurogenesis accounts for less than 5% of total apical mitosis in mice at E12.5. In contrast, at E12.5 mouse OB, we demonstrated that the direct mode of neurogenesis accounted for 20% of the neuronal yield (Cárdenas et al., 2018; Cárdenas & Borrell, 2019). To understand the root of the difference between the OB and NCx in the aspect of neurogenesis, we performed single cell RNA sequencing on samples microdissected from the OB region and adjacent NCx at E12.5. We decided to conduct this analysis at E12.5, because it is the time when the difference between the OB and NCx begins to appear, and it is only maintained for a short period of time before all developmental statuses standardise again. We were able to unravel the transcriptomic changes between the developing NCx and OB using this technique. We found differences in progenitor (RGCs, IPCs) and neuronal cluster enrichment between the two regions. This difference in clustering enrichment between the two regions could be explained by our previous findings, which showed that the peak of neurogenesis at the OB occurs between E11.5 and E13.5 (Cárdenas et al., 2018). Cell lineage analysis of the integrated clusters from both regions revealed, as expected, a transition from RGCs to IPCs, followed by a transition to deep layer neurons or OB specific neurons. We discovered two RGC trajectories: one transitioning from RGCs to IPCs and then differentiating into deep layer neurons, immature neurons, or OB specific. In contrast, we found a cell lineage trajectory that emerges from an RGC-OB-enriched cluster and directly differentiates to OB specific neurons. This data clearly demonstrates the two modes of neurogenesis that we previously demonstrated in the OB (Cárdenas et al., 2018).

Slit/Robo and Notch signalling have an impact on the mode of neurogenesis adapted by progenitors in the NCx and OB, where *Robo1/2* expression in the developing NCx maintains the balance between aRGCs and IPCs progenitor pools, this role involves *Hes1* transcriptional activation (Borrell et al., 2012). Moreover, high levels of *Robo1/2*-ICD expression and low levels of *Dll1* expression promote direct neurogenesis from aRGCs in the NCx and OB (Cárdenas et al., 2018). Our single cell RNA seq data confirms the higher expression of

Robo1/2 in the OB RGCs compared to the NCx RGCs. Interestingly, *Robo1/2* expression was higher in OB cluster 10 (where direct neurogenesis lineages originate) than in NCx cluster 10.

During cortical development neural progenitors exhibit a salt and pepper pattern that is credited to notch lateral inhibition (Kunisch et al., 1994; Miller et al., 2009). Curiously, our single cell dataset shows that *Dll1* expression is slightly higher in cluster 10 in the OB (where direct neurogenesis trajectory originates). This observation could be explained by the fact that differentiating cells upregulate proneural transcription factors, which in return upegulate *Dll1* expression. *Dll1* expression is critical for maintaining lateral inhibition by keeping neighbouring cells in an undifferentiaited state (Sprinzak et al., 2010).

Our analysis revealed that *Hes1* and *Hes5* expression levels were higher in the NCx RGCs clusters than in the OB RGCs clusters. As a result, these findings are consistent with the traditional role of hey genes in inhibiting RGCS differentiation in developing telencephalon (Pierfelice et al., 2011; Yoon & Gaiano, 2005). Coinciding with these results, *Tbr1* expression was higher in OB RGCs clusters compared to NCx clusters. Thus, this points to the accelerated rate of neurogenesis occurring at this point in the OB compared to the adjacent NCx at this point of development.

Intriguingly, genes identified as bRGC makers were found to be enriched in OB progenitor clusters (Pollen et al., 2014, 2015). ISH of *Hopx*, *Ptprz1* and *Slc1a3* in mouse E12.5 revealed that these genes were more expressed in OB progenitors than in NCx progenitors. These genes were found to be highly expressed in Cluster (4) of the OB, which is where indirect neurogenesis begins in our cell lineage trajectory. Besides that, a recent study found that $Hopx^{+}$ bRGCs in developing gyrencaplic cortex have higher self-renewal capcity and are more abundant in developing gyral regions (Matsumoto et al., 2020). These findings led us to believe that the enrichment of these genes in the OB could play a role in regulating progenitor proliferation and indirect neurogenesis.

Furthermore, we found that *Hey2* expression was significantly higher in NCx RGCs clusters compared to the OB RGCs clusters. *Hey2*, one of Notch effector genes, inhibits the neuronal bHLH genes *Mash1* and *Math3* and promotes the maintenance of the progenitor pool in the cortex (Piper et al., 2010; Sakamoto et al., 2003). On the other hand, we found that *Etv4* is expressed in OB progenitor clusters significantly more than NCx progenitors. *Etv4* is a member of the ETS transcription factor family, which plays an important role in the developing cortex (Arber et al., 2000) as well as hippocampal dendritic development and arborization (Fontanet et al., 2018). One possible explanation for the enrichment of *Hey2* and *Etv4* expression in the NCx and OB is that *Hey2* plays a role in the preservation of the

progenitor pool in the NCx, whereas *ETv4* higher expression in the OB could be important for neuronal differentiation and the formation of neuronal circuitry.

Identifying Novel interactors of Robo1/2 ICD

Robo1/2-ICDs lack autonomous catalytic activities; therefore, Robo intracellular signalling occurs by interacting with other molecules in order to initiate signalling (Chédotal, 2007). Robo signaling is moderated by secondary molecules such as: GAPs, SrGAPs, GEFs and other receptors such as: Netrin 1 receptor Dcc and N-cadherin that bind to Robo cytoplasmic terminal directly or to its conserved cytoplasmic domains (Heasman & Ridley, 2008; Lundström et al., 2004; Whitford et al., 2002; Yang & Bashaw, 2006). As expected, our MS analysis revealed that Robo1/2-ICDs interact with previously described proteins involved in actin binding and cytoskeleton dynamics (Arhgap32, Arhgap27, Arhgap39, Wipf1, Nisch, Nck1, Nck2) (Fan et al., 2003; Round & Sun, 2011; K. Wong et al., 2001). Interestingly, we discovered that Robo1/2-ICD interacts with various transcription factors (Hdx, Otx2, Meis2, Akt2), as well as proteins involved in microtubule spindle assembly and kinetochore formation (Haus6, Dctn3, Nde1, Ndel1, Dscc).

Our GO analysis of Robo-ICD interactors revealed terms like centrosome localization, microtubule nucleation, actin cytoskeleton organisation, translation regulation, and positive regulation of transcription from the RNA polymerase II promoter. Our findings also show that Robo1/2-ICDs can interact with proteins from various cellular compartments, including the nucleus, mitochondria, and endoplasmic reticulum. These findings point to the possibility of Robo-ICD trafficking between different cellular components.

It has been described that Robo-ICD undergoes Clathrin-dependent endocytosis, which is critical for Robo's axon guidance function ((Chance & Bashaw, 2015). Our findings show that Robo-ICD interacts with a variety of proteins associated with endosomes and endomembrane-bound vesicles (Arp13a1, Rab18, Vps51, Vps53, Vps16, Afph, Spire2), implying that endocytosis occurs in our Robo ICD model. Although Robo endocytosis has been described as a Slit-dependent mechanism, our experiments show that a constitutively active myristolated Robo does not require Slit activation (Borrell et al., 2012; Cárdenas et al., 2018).

Cell cycle regulation and interkinetic nuclear movement (INM) have a strong relationship; this relationship implicates interkinetic nuclear movement in other mitosis-related dynein-regulated processes such as nuclear envelope breakdown. In our MS analysis, we observed proteins related to INM, such as Ndel1, Syne2, and Dctn3. Ndel1 is involved in the

breakdown of the nuclear envelope, whereas Syne1 and Dctn3 mediate microtubule binding to the nucleus by interacting with other dynein and dynactin complexes. We postulate that Robo-ICD's interaction with these INM-related proteins is explained by Robo-ICD's role in not only controlling cell cycle progression in progenitors but also in radial neuronal migration and axon guidance in neurons (Reiner et al., 2012).

Characterzing Robo1/2-ICD translocation to the nucleus

To initiate the signalling cascade, Robo/Slits must be proteolytically processed. According to structural studies, the interaction of the Robo1 extracellular domain with the ECM-immobilized Slit causes molecular tension in the Robo receptor structure. This receptor tension reveals the metalloproteinase cleavage site. This site is highly conserved across species, and signalling requires the cleavage of the Robo receptor. This is supported by the fact that the uncleavable Robo receptor in Drosophila is incapable of restoring Robo dependent midline repulsion. It has previously been reported that in human cancer cells, Robo1 undergoes a two-step proteolysis with secretase that results in two carboxy terminal fragments of 129 kDa and 118 kDa. This cleaved Robo1 terminal has been demonstrated to translocate to the nucleus (Chance & Bashaw, 2015; Coleman et al., 2010; Seki et al., 2010). In contrast, it was recently discovered that Robo1-ICD cleavage by an unknown protease and translocation to the nucleus is unaffected by Slit, prior extracellular domain shedding, or membrane anchoring (Bianchi et al., 2021). Our results suggest that Robo1/2 ICDs translocate to the nucleus of P19 cells and is also found in the nucleus of E12.5 neuronal primary cultures. Furthermore, nuclear fractionation of P19 cells revealed that both ectopic and native Robo1/2-ICDs translocate to the nucleus.

Although we are expressing Robo1/2-ICDs sequences that lack the transmembrane sequence cleaved by secreatase in our experiments, it has a Myr sequence in the N-terminus that allows it to bind to the membrane (Borrell et al., 2012; Cárdenas et al., 2018). Seki et al. observed a very intense Robo signal in the nucleus despite not using a Myr sequence before the Robo1 ICD construct used in their experiments (Seki et al., 2010). Moreover, in the study describing how Robo1 undergoes endocytosis, they observed that the cells expressing Robo1 -ICD constructs without having any sequence tethering them to the membrane, were unable to form processes properly (Chance & Bashaw, 2015). In contrast, we found that the construct expressing myr-Robo1-ICD can induce exuberant branching in embryonic rat dorsal ganglion cells independent of Slit expression (Cárdenas et al., 2018). These results suggest that Robo

cytoplasmic terminal attachment to the membrane is enough to maintain axonal branching and doesn't hinder Robo ICD translocation to the nucleus.

Given that Robo-CD undergoes endocytosis (Chance & Bashaw, 2015; Coleman et al., 2010), and the presence of other transcription factors and proteins involved in microtubule assembly and translation in our MS dataset, we hypothesised that Robo-ICD belongs to a class of membrane transcription factors (MTFs) that undergo endocytosis before entering the nucleus and participating in transcription machinery.

How does Robo-ICD translocate to the nucleus?

Nucleocytoplasmic transport is an indispensable process in mammalian cells. Multiple proteins, such as transcription factor, histones, and cell cycle regulators, require the presence of nuclear localization sequence (NLS). NLS is recognized by nuclear transporters, which facilitate the transport of proteins from the cytoplasm to the nucleus through NPC (Oka & Yoneda, 2018). We found that Robo1/2-ICDs have classical NLSs. This finding may help to explain how Robo1/2-ICDs translocate to the nucleus. However, experiments mutating these NLSs in Robo1 ICD didn't abate its translocation to the nucleus (Seki et al., 2010). To this end, we reasoned that Robo-ICD transportation to the nucleus could additionally require clatherin mediated endocytosis like other TFs such as Epidermal Growth Factor Receptor (EGFR) and Human Epidermal Growth Factor Receptor 2 (HER-2). These TFs are transported to the nucleus through interaction of their NLS sequence with nuclear transporters followed by endocytosis. Experiments inhibiting endocytosis lead to an extreme reduction of their nuclear translocation of up to 80% (Bild et al., 2002; Lo et al., 2006).

Robo conserved cytoplasmic domains are necessary for direct neurogenesis phenotype

We mentioned previously that Robo conserved cytoplasmic domains don't have autonomous catalytic activity. Nevertheless, these domains have been shown to interact with several molecules to exert repulsion, control of cytoskeletal dynamics, cell polarity and adhesion (Rhee et al., 2002, 2007; K. Wong et al., 2001). In this thesis we truncated Robo1/2-ICDs by removing different cytoplasmic domain and quantifying the signal in the nucleus versus cytoplasm and membrane in P19 transfected cells. We found that Robo1/2-ICD combined or separately had a higher nuclear signal compared to other truncations. This could be explained

by a possible interaction between these cytoplasmic domains and some nuclear transporters that is reduced with the removal of these domains.

We showed that the gain of function of mRobo1/2-ICD combined with the knockout of Crispr Dll1 was enough to induce direct neurogenesis in the developing mouse cortex (Cárdenas et al., 2018). Following up on these results by investigating whether mR1/2-ICD different truncations are able to recapitulate this phenotype, we found that both mR1/2-D1 and D2 had potential to increase direct neurogenesis in the cortex, while mR1/2-D3 failed to promote direct neurogenesis in the cortex. These results led us to hypothesize the Robo1/2 conserved cytoplasmic domains could be interacting with important interactors that are crucial in fate determination.

Overexpression of mR1/2-ICD and knocking out Dll1 changes cell cycle dynamics and metabolism in cortical progenitors

Neurogenesis entails a balance between proliferation and neurogenesis, and in the context of cell cycle, this means cell cycle exit and cell cycle re-entry. Progenitors need to exit the cell cycle in G1 and enter G0 bypassing cell cycle restriction points. This can be achieved by overexpressing CdkI, which can block cell cycle progression at G1, hence promoting differentiation (Ohnuma & Harris, 2003). Our results show that gain of function of mRobo1/2- ICDs combined with knocking out of Dll1 in cortical progenitors promotes direct neurogenesis via cell cycle exit at G1 by upregulation of Cdkn1a (P21). Moreover, our transcriptomic analysis revealed GSEA terms related to cell cycle exit, such as negative regulation of mitotic cell cycle phase transition. These findings are consistent with our results comparing cell cycle exit between OB (where Robo1/2 is highly expressed in OB progenitors) and NCx in the developing mouse telencephalon, where we found that progenitors exit the cell cycle at a higher rate in the OB compared to NCx (Cárdenas et al., 2018).

Changes in the metabolic program are critical during neurogenesis. Progenitors mainly rely on glycolysis, while neurons mainly depend on mitochondrial oxidative phosphorylation. Single cell transcriptomics of adult neural progenitors shows that OXPHOS marks the commencement of neurogenesis. GSEA terms related to mitochondrial respiratory chain, respirome, and oxidative phosphorylation are included in our transcriptomic analysis. Interestingly, both Cox6b2 (Cytochrome C Oxidase Subunit 6B2) and Ndufa12 (NADH:Ubiquinone Oxidoreductase Subunit A12)-which take part in the OXPHOS process-

were among the upregulated DEGs in our dataset (Rath et al., 2021), suggesting that the Direct neurogenesis observed after mRobo1/2-ICDs gain function and Dll1 knockout is caused by transcriptional changes that affect cell cycle progression and cellular metabolism.

Recent studies showed that Robo1-ICD is required for multiple myeloma adhesion to bone marrow stromal and endothelial cells (Bianchi et al., 2021). Proteomics and RNA sequencing results from this study coincide with our results, confirming the role of Robo1-ICD in RNA processing and metabolic processes.

Furthermore, Robo1-ICD translocation to the nucleus is thought to indicate a better prognosis in patients with bladder cancer (Krafft et al., 2020). These findings, which speculate on the therapeutic impact of Robo nuclear translocation on cancer progression, support our hypothesis of Robo1-ICD transcriptional potential in cortical development.

Robo 1-ICD binds DNA and regulates transcriptional activity

Axon guidance receptors have been described recently for their ability to control gene expression. Dcc, neogin (Neo1), and Frazzled (Fra) have the ability to act as transcriptional activators, where the cytoplasmic domain of these receptors translocates to the nucleus upon cleavage with γ secretase or a metalloprotease, making this cleavage necessary to activate their transcription (Goldschneider et al., 2008; Neuhaus-Follini & Bashaw, 2015). Here, we found that Robo1/2-ICDs have DNA binding sequences that are conserved across most species. We showed that Robo1-ICD scores similarly to other canonical transcription factors, and this score is maintained across other species. Interestingly, CSK fractionation assay showed that Robo1-ICD is present in the tightly held fraction and chromatin fraction. these results suggest the transcriptional role of Robo1-ICD.

Experiments in this thesis showed that Robo1-ICD interacts with chromatin of specific genes, binding to promoter, intronic, intragenic, or exonic regions. These findings are similar to previous research on neogenin intercellular domain (NeICD) that showed its translocation to the nucleus, interactions with transcription-related proteins, and chromatin binding (Goldschneider et al., 2008). Nonetheless, the Chip-seq dataset we generated using the mRobo1-flag-ICD gain of function and Dll1 knockout coincided with a number enes that were differentially expressed in our *invivo* bulk RNA dataset. These findings suggest that Robo1-ICD DNA binding and transcriptional regulation is required for direct neurogenesis.

To gain more insight on Robo1-ICD acting as a transcription factor, we perfomed Motif analysis using the Homer database reveals an enrichment of Robo1 binding sequences for transcription factors when compared to the background in both known and de novo motifs (**Fig. 19**). Interestingly, we found that Hdx -one of the transcription factors that are significant in the de novo Robo 1 binding motifs- is one of the Robo1/2-ICDs highly enriched protein interactors. This could be explained by a possible interaction between Robo1 ICD and Hdx in the context of transcription factor, Co-factor that ultimately could affect gene transcription. This interaction should be thoroughly investigated in order to comprehend its dynamics and the implications for direct neurogenesis *in vivo*.

Top known motifs enriched at Robo1 binding sites

Rank	Motifs	Name	p-val	% of targets
1		Irf3	1e-6	6.41
2		Pax3	1e-4	4.27
3		Pax7	1e-4	2.14
4	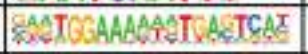	Nfat	1e-4	3.56
5		Bmi1	1e-3	5.54
6		Oct4-Sox2-Tcf-Nanog	1e-3	3.40
7		Irf3	1e-3	2.37
8		Hnf1	1e-3	2.37
9		Irf8	1e-3	6.17
10		bZIP:IRF	1e-3	7.59

Top de-novo motifs enriched at Robo1 binding sites

Rank	Motifs	Best Match	p-val	% of targets
1		Foxh1	1e-69	2.14
2		E2f8	1e-68	2.61
3		Stat2, Pou6f1	1e-68	2.61
4		Runx	1e-66	2.06
5		Dmrt6	1e-60	3.01
6		Irf4	1e-58	2.69
7		Hdx	1e-55	2.29
8		Zfp691	1e-53	1.96
9		Sox11	1e-45	2.22
10		Foxp1	1e-26	2.29

Figure 19. Known and de novo predictions on Robo1 binding sites. Homer was used to predict the DNA binding motifs of proteins that were strongly linked to Robo1 binding sites. The percentage of targets represents the enrichment of target sequences for transcription factors (TFs) in comparison to the background.

Robo1-ICD binds to the *Dll1* locus

We showed that the overexpression of mRobo1-ICD flag in P19 cells causes the upregulation of genes associated with neurogenesis and cytoskeleton rearrangement. We previously demonstrated that the Robo2-ICD stimulates transcriptional activity of the *Hes1* promoter in Neuro2a cells that lack Notch signalling. Furthermore, we found that both the Robo2-ICD and the Notch intracellular domain (NICD) increased *Hes1* transcriptional activity (Borrell et al., 2012). Moreover, we showed previously that Notch signalling in the NCx and OB in Robo mutants have a similar pattern of expression, unlike in WT embryos (Cárdenas et al., 2018). Transcriptomic analysis of this dataset revealed that some Notch pathway ligands, such as *Lnfg*, *Jag1*, and *Dll1*, were upregulated. To elucidate the interaction between Robo1-ICD and Dll1, we used a Luciferase assay, which revealed that Robo1-ICD reduces the transcriptional activity of the *Dll1* promoter. Furthermore, Chip-qPCR experiments revealed that the Robo1-ICD is abundant in the *DLL1* promoter region. As a result of these findings, we propose that Robo signalling can play a role in modulating Notch signalling.

The upregulation of Notch ligands in the Robo1-ICD RNA-seq dataset could be explained by Notch lateral inhibition (LeBon et al., 2014). Notch/Dll1-mediated Cis inhibition permits the generation of a huge variety of cell types (Cepko, 2014; Furukawa et al., 2000; Jadhav, Cho, et al., 2006; Jadhav, Mason, et al., 2006; Kageyama, Ohtsuka, Shimojo, et al., 2008; Mizeracka et al., 2013). Notch lateral inhibition is characterized by the rise of the ligand's expression and the decline of the receptor's expression. It is initiated when Dll1, located on differentiating cells, activates a Notch receptor in an adjacent progenitor. Trans-activation causes cleavage of the Notch receptor and release of NICD which then translocate to the nucleus and forms a complex with the DNA-binding protein RbpJ, ultimately activating the expression of Hes1 and Hes5. Hence, this keeps the trans-activated progenitor in an undifferentiated state (Schuurmans & Guillemot, 2002). This Notch signalling response could explain the upregulation of *Dll1* expression observed in Robo1-ICD RNA seq data, which happens when proneural genes in differentiating cells upregulate *Dll1* expression (Kunisch et al., 1994). However, it must be put in perspective that the results were obtained *in vitro*, and further research *in vivo* is required to confirm Robo's ICD role.

Nup107 impact on Direct neurogenesis across evolution

Most nucleoporins are evolutionary conserved from yeast to mammals, and consequently the NPC structure is also well conserved (Khan et al., 2020). Our MS data showed that Nup107 was among Robo1/2-ICD interactors. This association between Nup107 and Robo1/2-ICD suggests that Robo1/2-ICD may play a role in kinetochore formation during mitosis. Furthermore, Nup107 is a component of NPC, and its association with the kinetochore in vertebrates is well established (Antonin et al., 2005; Orjalo et al., 2006; Walther et al., 2003).
Further investigation into Nup107 expression in amniotes revealed that Nup107 expression is conserved in cortical progenitors such as Robo1/2 and Dll1; even so, Nup107 expression pattern is similar to Dll1 in both mouse telencephalon and chick pallium. We showed that loss of function experiments of Nup107 in mouse NCx and chick pallium resulted in an increase in Direct neurogenesis, suggesting the role Nup107 plays in modersting indirect neurogenesis.
This direct interaction between Nup107 and Robo1/2 ICDs could be explained by Robo-ICD acting as a transcription factor and forming a complex with Nup107 that controls transcription programs. This explanation is in accord with the interaction discovered between Sox2 and Nup153 (Toda et al., 2017), where Genome-wide analyses showed the binding of Nup153 and Sox2 co-regulate many genes, Thus it will be interesting to determine the spatial changes in nuclear architecture that this interaction between Robo1/2-ICD and Nup107 exert on progenitor maintenance and fate determination.

Conclusions

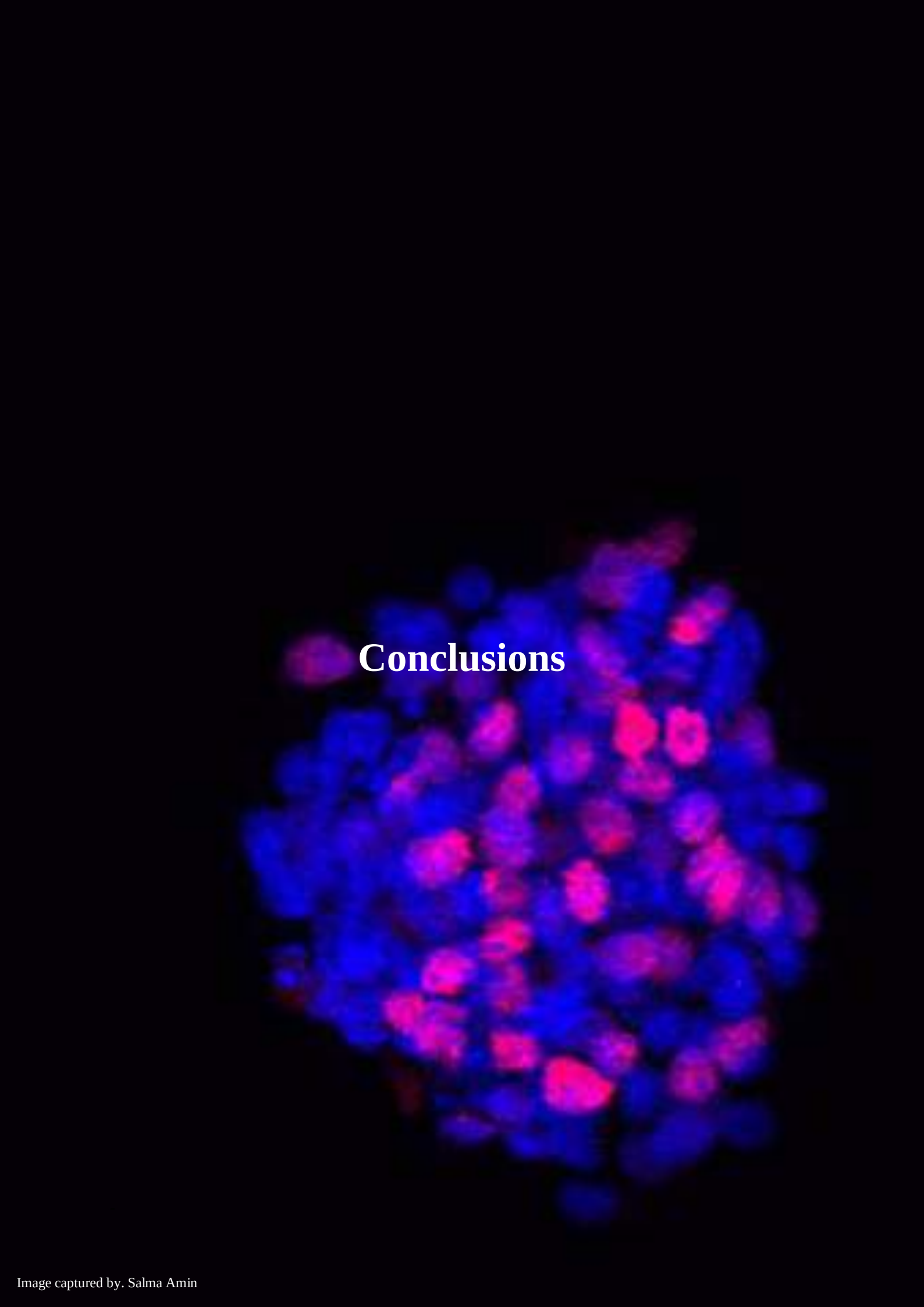

Image captured by. Salma Amin

Conclusions

1. Distinct progenitor cell populations are selectively enriched in the NCx and OB of mouse embryos, linked to the generation of neurons Directly or Indirectly.
2. Robo interacts intracellularly with a variety of protein types, including transporters, transcription factors and nuclear proteins.
3. Following Robo receptor activation, the intracellular domain (ICD) is shuttled to the nucleus of neural progenitor cells.
4. High levels of Robo1/2-ICD combined with low levels of *Dll1* promote Direct neurogenesis in the NCx by inducing transcriptional changes in cortical progenitor cells, namely via upregulation of OX-PHOS and cell cycle exit genes.
5. The protein sequence of Robo1-ICD is predicted to be a transcription factor, including the conserved cytoplasmic domain CC3 and C-terminus, which are important for nuclear shuttling and to drive Direct neurogenesis.
6. Robo1-ICD directly regulates gene expression by binding to specific gene regulatory elements, including promoters and enhancers, such as in the *Dll1* locus.
7. Robo-ICD interacts with the nuclear pore protein Nup107. Loss of Nup107 promotes Direct neurogenesis in an evolutionarily-conserved manner, similar to the gain of Robo signaling.

Conclusiones

1. Distintas poblaciones de células progenitoras se enriquecen selectivamente en NCx y OB de embriones de ratón, vinculadas a la generación de neuronas directa o indirectamente.
2. Robo interactúa intracelularmente con una variedad de tipos de proteínas, incluidos transportadores, factores de transcripción y proteínas nucleares.
3. Después de la activación del receptor Robo, el dominio intracelular (ICD) se transporta al núcleo de las células progenitoras neurales.
4. Los niveles altos de Robo1/2-ICD combinados con niveles bajos de Dll1 promueven la neurogénesis directa en el NCx al inducir cambios transcripcionales en las células progenitoras corticales, concretamente a través de la regulación al alza de OX-PHOS y genes de salida del ciclo celular.
5. Se prevé que la secuencia proteica de Robo1-ICD sea un factor de transcripción, incluido el dominio citoplasmático conservado CC3 y C-terminal, que son importantes para el transporte nuclear y para impulsar la neurogénesis directa.
6. Robo1-ICD regula directamente la expresión génica al unirse a elementos reguladores de genes específicos, incluidos promotores y potenciadores, como en el locus Dll1.
7. Robo-ICD interactúa con la proteína de poro nuclear Nup107. La pérdida de Nup107 promueve la neurogénesis directa de una manera conservada evolutivamente, similar a la ganancia de señalización de Robo.

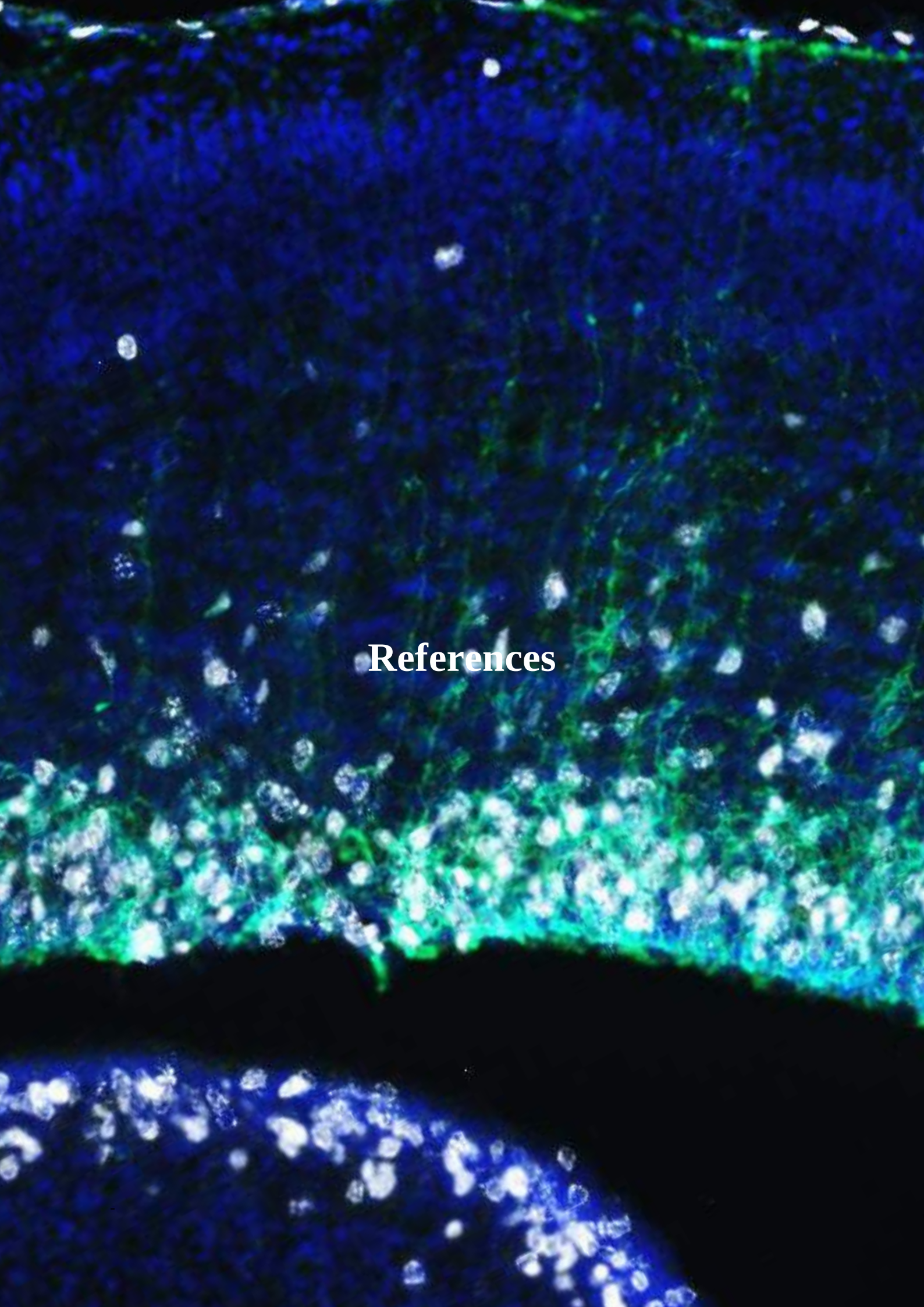

References

References

Ables, J. L., Breunig, J. J., Eisch, A. J., & Rakic, P. (2011). Not(ch) just development: Notch signalling in the adult brain. *Nature Reviews Neuroscience*, *12*(5), 269–283. https://doi.org/10.1038/nrn3024

Ahmed, S., Brickner, D. G., Light, W. H., Cajigas, I., McDonough, M., Froyshteter, A. B., Volpe, T., & Brickner, J. H. (2010). DNA zip codes control an ancient mechanism for gene targeting to the nuclear periphery. *Nature Cell Biology*, *12*(2), 111–118. https://doi.org/10.1038/ncb2011

Akhtar, A., & Gasser, S. M. (2007). The nuclear envelope and transcriptional control. *Nature Reviews Genetics*, *8*(7), 507–517. https://doi.org/10.1038/nrg2122

Alvarez-Buylla, A., & Garcıa-Verdugo, J. M. (2002). Neurogenesis in adult subventricular zone. *Journal of Neuroscience*, *22*(3), 629–634.

Amin, S., & Borrell, V. (2020). The Extracellular Matrix in the Evolution of Cortical Development and Folding. *Frontiers in Cell and Developmental Biology*, *8*(December). https://doi.org/10.3389/fcell.2020.604448

Anders, S., Pyl, P. T., & Huber, W. (2015). HTSeq-A Python framework to work with high-throughput sequencing data. *Bioinformatics*. https://doi.org/10.1093/bioinformatics/btu638

Andrés, V., & González, J. M. (2009). Role of A-type lamins in signaling, transcription, and chromatin organization. *Journal of Cell Biology*, *187*(7), 945–957. https://doi.org/10.1083/jcb.200904124

Andrews, W., Barber, M., Hernadez-Miranda, L. R., Xian, J., Rakic, S., Sundaresan, V., Rabbitts, T. H., Pannell, R., Rabbitts, P., Thompson, H., Erskine, L., Murakami, F., & Parnavelas, J. G. (2008). The role of Slit-Robo signaling in the generation, migration and morphological differentiation of cortical interneurons. *Developmental Biology*, *313*(2), 648–658. https://doi.org/10.1016/j.ydbio.2007.10.052

Andrews, W. D., Barber, M., & Parnavelas, J. G. (2007). Slit-Robo interactions during cortical development. *Journal of Anatomy*, *211*(2), 188–198. https://doi.org/10.1111/j.1469-7580.2007.00750.x

Antonin, W., Franz, C., Haselmann, U., Antony, C., & Mattaj, I. W. (2005). The integral membrane nucleoporin pom121 functionally links nuclear pore complex assembly and nuclear envelope formation. *Molecular Cell*, *17*(1), 83–92. https://doi.org/10.1016/j.molcel.2004.12.010

Arai, Y., & Pierani, A. (2014). Development and evolution of cortical fields. *Neuroscience Research*, *86*, 66–76. https://doi.org/10.1016/j.neures.2014.06.005

Arai, Y., & Taverna, E. (2017). Neural progenitor cell polarity and cortical development. *Frontiers in Cellular Neuroscience*, *11*(December), 1–11. https://doi.org/10.3389/fncel.2017.00384

Arber, S., Ladle, D. R., Lin, J. H., Frank, E., & Jessell, T. M. (2000). ETS gene Er81 controls the formation of functional connections between group Ia sensory afferents and motor

neurons. *Cell*, *101*(5), 485–498. https://doi.org/10.1016/S0092-8674(00)80859-4

Arnold, S. J., Huang, G. J., Cheung, A. F. P., Era, T., Nishikawa, S. I., Bikoff, E. K., Molnár, Z., Robertson, E. J., & Groszer, M. (2008). The T-box transcription factor Eomes/Tbr2 regulates neurogenesis in the cortical subventricular zone. *Genes and Development*, *22*(18), 2479–2484. https://doi.org/10.1101/gad.475408

Asakawa, H., Kojidani, T., Yang, H. J., Ohtsuki, C., Osakada, H., Matsuda, A., Iwamoto, M., Chikashige, Y., Nagao, K., Obuse, C., Hiraoka, Y., & Haraguchi, T. (2019). Asymmetrical localization of nup107-160 subcomplex components within the nuclear pore complex in fission yeast. *PLoS Genetics*, *15*(6), 1–30. https://doi.org/10.1371/journal.pgen.1008061

Attardo, A., Calegari, F., Haubensak, W., Wilsch-Bräuninger, M., & Huttner, W. B. (2008). Live imaging at the onset of cortical neurogenesis reveals differential appearance of the neuronal phenotype in apical versus basal progenitor progeny. *PLoS ONE*, *3*(6), 14–18. https://doi.org/10.1371/journal.pone.0002388

Ballard, M. S., & Hinck, L. (2012). A Roundabout Way to Cancer. In *Advances in Cancer Research* (1st ed., Vol. 114). Elsevier Inc. https://doi.org/10.1016/B978-0-12-386503-8.00005-3

Bar, I., Lambert de Rouvroit, C., & Goffinet, A. M. (2000). The evolution of cortical development. An hypothesis based on the role of the Reelin signaling pathway. *Trends in Neurosciences*, *23*(12), 633–638. https://doi.org/10.1016/S0166-2236(00)01675-1

Barkovich, A. J., Guerrini, R., Kuzniecky, R. I., Jackson, G. D., & Dobyns, W. B. (2012). A developmental and genetic classification for malformations of cortical development: Update 2012. *Brain*, *135*(5), 1348–1369. https://doi.org/10.1093/brain/aws019

Batista-Brito, R., Close, J., Machold, R., & Fishell, G. (2008). The distinct temporal origins of olfactory bulb interneuron subtypes. *Journal of Neuroscience*, *28*(15), 3966–3975. https://doi.org/10.1523/JNEUROSCI.5625-07.2008

Bauer, K., Dowejko, A., Bosserhoff, A. K., Reichert, T. E., & Bauer, R. (2011). Slit-2 facilitates interaction of P-cadherin with Robo-3 and inhibits cell migration in an oral squamous cell carcinoma cell line. *Carcinogenesis*, *32*(6), 935–943. https://doi.org/10.1093/carcin/bgr059

Bernhofer, M., Dallago, C., Karl, T., Satagopam, V., Heinzinger, M., Littmann, M., Olenyi, T., Qiu, J., Schütze, K., Yachdav, G., Ashkenazy, H., Ben-Tal, N., Bromberg, Y., Goldberg, T., Kajan, L., O'Donoghue, S., Sander, C., Schafferhans, A., Schlessinger, A., … Rost, B. (2021). PredictProtein - Predicting Protein Structure and Function for 29 Years. *Nucleic Acids Research*, *49*(W1), W535–W540. https://doi.org/10.1093/nar/gkab354

Bertrand, N., Castro, D. S., & Guillemot, F. (2002). Proneural genes and the specification of neural cell types. *Nature Reviews Neuroscience*, *3*(7), 517–530. https://doi.org/10.1038/nrn874

Betizeau, M., Cortay, V., Patti, D., Pfister, S., Gautier, E., Bellemin-Ménard, A., Afanassieff, M., Huissoud, C., Douglas, R. J., Kennedy, H., & Dehay, C. (2013). Precursor Diversity and Complexity of Lineage Relationships in the Outer Subventricular Zone of the

Primate. *Neuron*, *80*(2), 442–457. https://doi.org/10.1016/j.neuron.2013.09.032

Betizeau, M., & Dehay, C. (2016). From stem cells to comparative corticogenesis: A bridge too far? *Stem Cell Investigation*, *2016*(AUG), 1–8. https://doi.org/10.21037/sci.2016.08.02

Betts, J. G., Young, K. A., Wise, J. A., Johnson, E., Poe, B., Kruse, D. H., Korol, O., Johnson, J. E., Womble, M., & DeSaix, P. (2013). *Anatomy and physiology*.

Bianchi, G., Czarnecki, P. G., Ho, M., Roccaro, A. M., Sacco, A., Kawano, Y., Gullà, A., Samur, A. A., Chen, T., Wen, K., Tai, Y. T., Moscvin, M., Wu, X., Camci-Unal, G., Da Vià, M. C., Bolli, N., Sewastianik, T., Carrasco, R. D., Ghobrial, I. M., & Anderson, K. C. (2021). ROBO1 Promotes Homing, Dissemination, and Survival of Multiple Myeloma within the Bone Marrow Microenvironment. *Cancer Discovery*, *2*(4), 338–353. https://doi.org/10.1158/2643-3230.BCD-20-0164

Bild, A. H., Turkson, J., & Jove, R. (2002). Cytoplasmic transport of Stat3 by receptor-mediated endocytosis. *EMBO Journal*, *21*(13), 3255–3263. https://doi.org/10.1093/emboj/cdf351

Bilodeau, S., Roussel-Gervais, A., & Drouin, J. (2009). Distinct Developmental Roles of Cell Cycle Inhibitors p57 Kip2 and p27 Kip1 Distinguish Pituitary Progenitor Cell Cycle Exit from Cell Cycle Reentry of Differentiated Cells . *Molecular and Cellular Biology*, *29*(7), 1895–1908. https://doi.org/10.1128/mcb.01885-08

Borello, U., Cobos, I., Long, J. E., Murre, C., & Rubenstein, J. L. R. (2008). FGF15 promotes neurogenesis and opposes FGF8 function during neocortical development. *Neural Development*, *3*(1). https://doi.org/10.1186/1749-8104-3-17

Borrell, V., Cárdenas, A., Ciceri, G., Galcerán, J., Flames, N., Pla, R., Nóbrega-Pereira, S., García-Frigola, C., Peregrín, S., & Zhao, Z. (2012). Slit/Robo signaling modulates the proliferation of central nervous system progenitors. *Neuron*, *76*(2), 338–352.

Borrell, V., & Götz, M. (2014). Role of radial glial cells in cerebral cortex folding. *Current Opinion in Neurobiology*, *27*, 39–46. https://doi.org/10.1016/j.conb.2014.02.007

Borrell, V., & Reillo, I. (2012). Emerging roles of neural stem cells in cerebral cortex development and evolution. *Developmental Neurobiology*, *72*(7), 955–971. https://doi.org/10.1002/dneu.22013

Bradl, M., & Lassmann, H. (2010). Oligodendrocytes: Biology and pathology. *Acta Neuropathologica*, *119*(1), 37–53. https://doi.org/10.1007/s00401-009-0601-5

Braunreiter, K. M., & Cole, S. E. (2019). A tale of two clocks: phosphorylation of NICD by CDK s links cell cycle and segmentation clock . *EMBO Reports*, *20*(7), 3–5. https://doi.org/10.15252/embr.201948247

Brose, K., Bland, K. S., Kuan, H. W., Arnott, D., Henzel, W., Goodman, C. S., Tessier-Lavigne, M., & Kidd, T. (1999). Slit proteins bind robo receptors and have an evolutionarily conserved role in repulsive axon guidance. *Cell*, *96*(6), 795–806. https://doi.org/10.1016/S0092-8674(00)80590-5

Burke, B. (2019). Chain reaction: LINC complexes and nuclear positioning. *F1000Research*, *8*(0), 136. https://doi.org/10.12688/f1000research.16877.1

Burke, B., & Ellenberg, J. (2002). Remodelling the walls of the nucleus. *Nature Reviews Molecular Cell Biology*, *3*(7), 487–497. https://doi.org/10.1038/nrm860

Butler, A. B., & Hodos, W. (2005). *Comparative vertebrate neuroanatomy: evolution and adaptation*. John Wiley & Sons.

Butler, A., Hoffman, P., Smibert, P., Papalexi, E., & Satija, R. (2018). Integrating single-cell transcriptomic data across different conditions, technologies, and species. *Nature Biotechnology*, *36*(5), 411–420. https://doi.org/10.1038/nbt.4096

Bystron, I., Blakemore, C., & Rakic, P. (2008). Development of the human cerebral cortex: Boulder Committee revisited. *Nature Reviews Neuroscience*, *9*(2), 110–122. https://doi.org/10.1038/nrn2252

Cadwell, C. R., Bhaduri, A., Mostajo-Radji, M. A., Keefe, M. G., & Nowakowski, T. J. (2019). Development and Arealization of the Cerebral Cortex. *Neuron*, *103*(6), 980–1004. https://doi.org/10.1016/j.neuron.2019.07.009

Calegari, F., Haubensak, W., Haffher, C., & Huttner, W. B. (2005). Selective lengthening of the cell cycle in the neurogenic subpopulation of neural progenitor cells during mouse brain development. *Journal of Neuroscience*, *25*(28), 6533–6538. https://doi.org/10.1523/JNEUROSCI.0778-05.2005

Calegari, F., & Huttner, W. B. (2003). An inhibition of cyclin-dependent kinases that lengthens, but does not arrest, neuroepithelial cell cycle induces premature neurogenesis. *Journal of Cell Science*, *116*(24), 4947–4955. https://doi.org/10.1242/jcs.00825

Cárdenas, A., & Borrell, V. (2019). Molecular and cellular evolution of corticogenesis in amniotes. *Cellular and Molecular Life Sciences*, *0123456789*. https://doi.org/10.1007/s00018-019-03315-x

Cárdenas, A., Villalba, A., de Juan Romero, C., Picó, E., Kyrousi, C., Tzika, A. C., Tessier-Lavigne, M., Ma, L., Drukker, M., & Cappello, S. (2018). Evolution of cortical neurogenesis in amniotes controlled by robo signaling levels. *Cell*, *174*(3), 590–606.

Casolari, J. M., Brown, C. R., Komili, S., West, J., Hieronymus, H., & Silver, P. A. (2004). Genome-wide localization of the nuclear transport machinery couples transcriptional status and nuclear organization. *Cell*, *117*(4), 427–439. https://doi.org/10.1016/S0092-8674(04)00448-9

Castro, D. S., Skowronska-Krawczyk, D., Armant, O., Donaldson, I. J., Parras, C., Hunt, C., Critchley, J. A., Nguyen, L., Gossler, A., Göttgens, B., Matter, J. M., & Guillemot, F. (2006). Proneural bHLH and Brn Proteins Coregulate a Neurogenic Program through Cooperative Binding to a Conserved DNA Motif. *Developmental Cell*, *11*(6), 831–844. https://doi.org/10.1016/j.devcel.2006.10.006

Caviness, V. S., Goto, T., Tarui, T., Takahashi, T., Bhide, P. G., & Nowakowski, R. S. (2003). Cell output, cell cycle duration and neuronal specification: A model of integrated mechanisms of the neocortical proliferative process. *Cerebral Cortex*, *13*(6), 592–598. https://doi.org/10.1093/cercor/13.6.592

Cepko, C. (2014). Intrinsically different retinal progenitor cells produce specific types of progeny. *Nature Reviews Neuroscience*, *15*(9), 615–627.

Chance, R. K., & Bashaw, G. J. (2015). Slit-Dependent Endocytic Trafficking of the Robo Receptor Is Required for Son of Sevenless Recruitment and Midline Axon Repulsion. *PLoS Genetics*, *11*(9). https://doi.org/10.1371/journal.pgen.1005402

Chandel, N. S. (2014). *Mitochondria as signaling organelles*.

Charvet, C. J., Owerkowicz, T., & Striedter, G. F. (2009). Phylogeny of the telencephalic subventricular zone in sauropsids: Evidence for the sequential evolution of pallial and subpallial subventricular zones. *Brain, Behavior and Evolution*, *73*(4), 285–294. https://doi.org/10.1159/000230673

Chédotal, A. (2007). Slits and their receptors. *Axon Growth and Guidance*, 65–80.

Cheeseman, I. M., & Desai, A. (2008). Molecular architecture of the kinetochore-microtubule interface. *Nature Reviews Molecular Cell Biology*, *9*(1), 33–46. https://doi.org/10.1038/nrm2310

Chenn, A., & Walsh, C. A. (2002). Regulation of cerebral cortical size by control of cell cycle exit in neural precursors. *Science*, *297*(5580), 365–369.

Cheung, A. F. P., Pollen, A. A., Tavare, A., Deproto, J., & Molnár, Z. (2007). Comparative aspects of cortical neurogenesis in vertebrates. *Journal of Anatomy*, *211*(2), 164–176. https://doi.org/10.1111/j.1469-7580.2007.00769.x

Cohen, M., Feinstein, N., Wilson, K. L., & Gruenbaum, Y. (2003). Nuclear pore protein gp210 is essential for viability in HeLa cells and Caenorhabditis elegans. *Molecular Biology of the Cell*, *14*(10), 4230–4237.

Colasante, G., Sessa, A., Crispi, S., Calogero, R., Mansouri, A., Collombat, P., & Broccoli, V. (2009). Arx acts as a regional key selector gene in the ventral telencephalon mainly through its transcriptional repression activity. *Developmental Biology*, *334*(1), 59–71. https://doi.org/10.1016/j.ydbio.2009.07.014

Coleman, H. A., Labrador, J. P., Chance, R. K., & Bashaw, G. J. (2010). The Adam family metalloprotease Kuzbanian regulates the cleavage of the roundabout receptor to control axon repulsion at the midline. *Development*, *137*(14), 2417–2426. https://doi.org/10.1242/dev.047993

Courvalin, J. C., Segil, N., Blobel, G., & Worman, H. J. (1992). The lamin B receptor of the inner nuclear membrane undergoes mitosis- specific phosphorylation and is a substrate for p34(cdc2)-type protein kinase. *Journal of Biological Chemistry*, *267*(27), 19035–19038. https://doi.org/10.1016/s0021-9258(18)41734-6

Cubelos, B., Sebastián-Serrano, A., Kim, S., Moreno-Ortiz, C., Redondo, J. M., Walsh, C. A., & Nieto, M. (2008). Cux-2 controls the proliferation of neuronal intermediate precursors of the cortical subventricular zone. *Cerebral Cortex*, *18*(8), 1758–1770. https://doi.org/10.1093/cercor/bhm199

Cunha-Ferreira, I., Chazeau, A., Buijs, R. R., Stucchi, R., Will, L., Pan, X., Adolfs, Y., van der Meer, C., Wolthuis, J. C., Kahn, O. I., Schätzle, P., Altelaar, M., Pasterkamp, R. J., Kapitein, L. C., & Hoogenraad, C. C. (2018). The HAUS Complex Is a Key Regulator of Non-centrosomal Microtubule Organization during Neuronal Development. *Cell Reports*, *24*(4), 791–800. https://doi.org/10.1016/j.celrep.2018.06.093

D'Angelo, M. A., Gomez-Cavazos, J. S., Mei, A., Lackner, D. H., & Hetzer, M. W. (2012). A Change in Nuclear Pore Complex Composition Regulates Cell Differentiation. *Developmental Cell*, *22*(2), 446–458. https://doi.org/10.1016/j.devcel.2011.11.021

Danecek, P., Bonfield, J. K., Liddle, J., Marshall, J., Ohan, V., Pollard, M. O., Whitwham, A., Keane, T., McCarthy, S. A., Davies, R. M., & Li, H. (2021). Twelve years of SAMtools and BCFtools. *GigaScience*, *10*(2), 1–4. https://doi.org/10.1093/gigascience/giab008

De Juan Romero, C., & Borrell, V. (2015). Coevolution of radial glial cells and the cerebral cortex. *Glia*, *63*(8), 1303–1319. https://doi.org/10.1002/glia.22827

de Juan Romero, C., Bruder, C., Tomasello, U., Sanz-Anquela, J. M., & Borrell, V. (2015). Discrete domains of gene expression in germinal layers distinguish the development of gyrencephaly. *The EMBO Journal*, *34*(14), 1859–1874. https://doi.org/10.15252/embj.201591176

Dechat, T., Adam, S. A., Taimen, P., Shimi, T., & Goldman, R. D. (2010). Nuclear lamins. *Cold Spring Harbor Perspectives in Biology*, *2*(11), 1–22. https://doi.org/10.1101/cshperspect.a000547

DeFelipe, J., & Fariñas, I. (1992). The pyramidal neuron of the cerebral cortex: Morphological and chemical characteristics of the synaptic inputs. *Progress in Neurobiology*, *39*(6), 563–607. https://doi.org/10.1016/0301-0082(92)90015-7

Dehay, C., & Kennedy, H. (2007). Cell-cycle control and cortical development. *Nature Reviews Neuroscience*, *8*(6), 438–450. https://doi.org/10.1038/nrn2097

Dehay, C., Kennedy, H., & Kosik, K. S. (2015). The Outer Subventricular Zone and Primate-Specific Cortical Complexification. *Neuron*, *85*(4), 683–694. https://doi.org/10.1016/j.neuron.2014.12.060

Denoth-Lippuner, A., Jaeger, B. N., Liang, T., Royall, L. N., Chie, S. E., Buthey, K., Machado, D., Korobeynyk, V. I., Kruse, M., Munz, C. M., Gerbaulet, A., Simons, B. D., & Jessberger, S. (2021). Visualization of individual cell division history in complex tissues using iCOUNT. *Cell Stem Cell*, *28*(11), 2020-2034.e12. https://doi.org/10.1016/j.stem.2021.08.012

Desfilis, E., Abellán, A., Sentandreu, V., & Medina, L. (2018). Expression of regulatory genes in the embryonic brain of a lizard and implications for understanding pallial organization and evolution. *Journal of Comparative Neurology*, *526*(1), 166–202. https://doi.org/10.1002/cne.24329

Di Bella, D. J., Habibi, E., Stickels, R. R., Scalia, G., Brown, J., Yadollahpour, P., Yang, S. M., Abbate, C., Biancalani, T., Macosko, E. Z., Chen, F., Regev, A., & Arlotta, P. (2021). Molecular logic of cellular diversification in the mouse cerebral cortex. *Nature*, *595*(7868), 554–559. https://doi.org/10.1038/s41586-021-03670-5

Díaz-Guerra, E., Pignatelli, J., Nieto-Estévez, V., & Vicario-Abejón, C. (2013). Transcriptional regulation of olfactory bulb neurogenesis. *Anatomical Record*, *296*(9), 1364–1382. https://doi.org/10.1002/ar.22733

Dobin, A., Davis, C. A., Schlesinger, F., Drenkow, J., Zaleski, C., Jha, S., Batut, P., Chaisson, M., & Gingeras, T. R. (2013). STAR: ultrafast universal RNA-seq aligner. *Bioinformatics (Oxford, England)*, *29*(1), 15–21.

https://doi.org/10.1093/bioinformatics/bts635

Dugas-Ford, J., & Ragsdale, C. W. (2015). Levels of Homology and the Problem of Neocortex. *Annual Review of Neuroscience*, *38*, 351–368. https://doi.org/10.1146/annurev-neuro-071714-033911

Dultz, E., Zanin, E., Wurzenberger, C., Braun, M., Rabut, G., Sironi, L., & Ellenberg, J. (2008). Systematic kinetic analysis of mitotic dis- and reassembly of the nuclear pore in living cells. *Journal of Cell Biology*, *180*(5), 857–865. https://doi.org/10.1083/jcb.200707026

Eccles, J. C. (1981). The modular operation of the cerebral neocortex considered as the material basis of mental events. *Neuroscience*, *6*(10), 1839–1855. https://doi.org/10.1016/0306-4522(81)90027-0

Eguchi, A., Lee, G. O., Wan, F., Erwin, G. S., & Ansari, A. Z. (2014). Controlling gene networks and cell fate with precision-targeted DNA-binding proteins and small-molecule-based genome readers. *Biochemical Journal*, *462*(3), 397–413.

Engeland, K. (2018). Cell cycle arrest through indirect transcriptional repression by p53: I have a DREAM. *Cell Death and Differentiation*, *25*(1), 114–132. https://doi.org/10.1038/cdd.2017.172

Englund, C., Fink, A., Lau, C., Pham, D., Daza, R. A. M., Bulfone, A., Kowalczyk, T., & Hevner, R. F. (2005). Pax6, Tbr2, and Tbr1 are expressed sequentially by radial glia, intermediate progenitor cells, and postmitotic neurons in developing neocortex. *Journal of Neuroscience*, *25*(1), 247–251. https://doi.org/10.1523/JNEUROSCI.2899-04.2005

Enninga, J., Levay, A., & Fontoura, B. M. A. (2003). Sec13 Shuttles between the Nucleus and the Cytoplasm and Stably Interacts with Nup96 at the Nuclear Pore Complex. *Molecular and Cellular Biology*, *23*(20), 7271–7284. https://doi.org/10.1128/mcb.23.20.7271-7284.2003

Fahrenkrog, B. (2006). The nuclear pore complex, nuclear transport, and apoptosis. *Canadian Journal of Physiology and Pharmacology*, *84*(3–4), 279–286. https://doi.org/10.1139/Y05-100

Fan, X., Labrador, J. P., Hing, H., & Bashaw, G. J. (2003). Slit Stimulation Recruits Dock and Pak to the Roundabout Receptor and Increases Rac Activity to Regulate Axon Repulsion at the CNS Midline Studies of Slit-mediated axon repulsion in Drosophila and C. elegans, together with studies of Slit-mediated neurona. *Neuron*, *40*(Cc), 113–127.

Farah, M. H., Olson, J. M., Sucic, H. B., Hume, R. I., Tapscott, S. J., & Turner, D. L. (2000). *Generation of neurons by transient expression of neural bHLH proteins in mammalian cells*. *702*, 693–702.

Fatterpekar, G. M., Naidich, T. P., Delman, B. N., Aguinaldo, J. G., Gultekin, S. H., Sherwood, C. C., Hof, P. R., Drayer, B. P., & Fayad, Z. A. (2002). Cytoarchitecture of the human cerebral cortex: MR microscopy of excised specimens at 9.4 Tesla. *American Journal of Neuroradiology*, *23*(8), 1313–1321.

Feng, Y., & Walsh, C. A. (2004). Mitotic spindle regulation by Nde1 controls cerebral cortical size. *Neuron*, *44*(2), 279–293. https://doi.org/10.1016/j.neuron.2004.09.023

Fernández, V., Llinares-Benadero, C., & Borrell, V. (2016). Cerebral cortex expansion and folding: what have we learned? *The EMBO Journal*, *35*(10), 1021–1044. https://doi.org/10.15252/embj.201593701

Fietz, S. A., Kelava, I., Vogt, J., Wilsch-Bräuninger, M., Stenzel, D., Fish, J. L., Corbeil, D., Riehn, A., Distler, W., Nitsch, R., & Huttner, W. B. (2010). OSVZ progenitors of human and ferret neocortex are epithelial-like and expand by integrin signaling. *Nature Neuroscience*, *13*(6), 690–699. https://doi.org/10.1038/nn.2553

Fietz, S. A., Lachmann, R., Brandl, H., Kircher, M., Samusik, N., Schröder, R., Lakshmanaperumal, N., Henry, I., Vogt, J., Riehn, A., Distler, W., Nitsch, R., Enard, W., Pääbo, S., & Huttner, W. B. (2012). Transcriptomes of germinal zones of human and mouse fetal neocortex suggest a role of extracellular matrix in progenitor self-renewal. *Proceedings of the National Academy of Sciences of the United States of America*, *109*(29), 11836–11841. https://doi.org/10.1073/pnas.1209647109

Fish, J. L., Dehay, C., Kennedy, H., & Huttner, W. B. (2008). Making bigger brains - The evolution of neural-progenitor-cell division. *Journal of Cell Science*, *121*(17), 2783–2793. https://doi.org/10.1242/jcs.023465

Fish, J. L., Kosodo, Y., Enard, W., Pääbo, S., & Huttner, W. B. (2006). Aspm specifically maintains symmetric proliferative divisions of neuroepithelial cells. *Proceedings of the National Academy of Sciences of the United States of America*, *103*(27), 10438–10443. https://doi.org/10.1073/pnas.0604066103

Flames, N., Pla, R., Gelman, D. M., Rubenstein, J. L. R., Puelles, L., & Marín, O. (2007). Delineation of multiple subpallial progenitor domains by the combinatorial expression of transcriptional codes. *Journal of Neuroscience*, *27*(36), 9682–9695. https://doi.org/10.1523/JNEUROSCI.2750-07.2007

Florio, M., & Huttner, W. B. (2014). Neural progenitors, neurogenesis and the evolution of the neocortex. *Development (Cambridge)*, *141*(11), 2182–2194. https://doi.org/10.1242/dev.090571

Florio, M., Namba, T., Paabo, S., Hiller, M., & Huttner, W. B. (2016). A single splice site mutation in human-specific ARHGAP11B causes basal progenitor amplification. *Science Advances*, *2*(12). https://doi.org/10.1126/sciadv.1601941

Fode, C., Ma, Q., Casarosa, S., Ang, S. L., Anderson, D. J., & Guillemot, F. (2000). A role for neural determination genes in specifying the dorsoventral identity of telencephalic neurons. *Genes and Development*, *14*(1), 67–80. https://doi.org/10.1101/gad.14.1.67

Fontanet, P. A., Ríos, A. S., Alsina, F. C., Paratcha, G., & Ledda, F. (2018). Pea3 transcription factors, Etv4 and Etv5, are required for proper hippocampal dendrite development and plasticity. *Cerebral Cortex*, *28*(1), 236–249. https://doi.org/10.1093/cercor/bhw372

Frey, S., & Görlich, D. (2009). FG/FxFG as well as GLFG repeats form a selective permeability barrier with self-healing properties. *EMBO Journal*, *28*(17), 2554–2567. https://doi.org/10.1038/emboj.2009.199

Fritz, R. D., Menshykau, D., Martin, K., Reimann, A., Pontelli, V., & Pertz, O. (2015). SrGAP2-Dependent Integration of Membrane Geometry and Slit-Robo-Repulsive Cues

Regulates Fibroblast Contact Inhibition of Locomotion. *Developmental Cell*, *35*(1), 78–92. https://doi.org/10.1016/j.devcel.2015.09.002

Furukawa, T., Mukherjee, S., Bao, Z. Z., Morrow, E. M., & Cepko, C. L. (2000). rax, Hes1, and notch1 promote the formation of Muller glia by postnatal retinal progenitor cells. *Neuron*, *26*(2), 383–394. https://doi.org/10.1016/S0896-6273(00)81171-X

Gaiano, N., & Fishell, G. (2002). The role of notch in promoting glial and neural stem cell fates. *Annual Review of Neuroscience*, *25*(1), 471–490.

Gaidatzis, D., Lerch, A., Hahne, F., & Stadler, M. B. (2015). QuasR: quantification and annotation of short reads in R. *Bioinformatics (Oxford, England)*, *31*(7), 1130–1132. https://doi.org/10.1093/bioinformatics/btu781

Gao, P., Postiglione, M. P., Krieger, T. G., Hernandez, L., Wang, C., Han, Z., Streicher, C., Papusheva, E., Insolera, R., Chugh, K., Kodish, O., Huang, K., Simons, B. D., Luo, L., Hippenmeyer, S., & Shi, S. H. (2014). Deterministic progenitor behavior and unitary production of neurons in the neocortex. *Cell*, *159*(4), 775–788. https://doi.org/10.1016/j.cell.2014.10.027

Garey, L. J. (1999). *Brodmann's' localisation in the cerebral cortex'*. World Scientific.

Gelman, D. M., & Marín, O. (2010). Generation of interneuron diversity in the mouse cerebral cortex. *European Journal of Neuroscience*, *31*(12), 2136–2141. https://doi.org/10.1111/j.1460-9568.2010.07267.x

Gertz, C. C., & Kriegstein, A. R. (2015). Neuronal migration dynamics in the developing ferret cortex. *Journal of Neuroscience*, *35*(42), 14307–14315. https://doi.org/10.1523/JNEUROSCI.2198-15.2015

Geschwind, D. H., & Rakic, P. (2013). Cortical evolution: Judge the brain by its cover. *Neuron*, *80*(3), 633–647. https://doi.org/10.1016/j.neuron.2013.10.045

Goffinet, A. M. (2017). The evolution of cortical development: The synapsid-diapsid divergence. *Development (Cambridge)*, *144*(22), 4061–4077. https://doi.org/10.1242/dev.153908

Goldschneider, D., Rama, N., Guix, C., & Mehlen, P. (2008). The neogenin intracellular domain regulates gene transcription via nuclear translocation. *Molecular and Cellular Biology*, *28*(12), 4068–4079. https://doi.org/10.1128/MCB.02114-07

Gonda, Y., Andrews, W. D., Tabata, H., Namba, T., Parnavelas, J. G., Nakajima, K., Kohsaka, S., Hanashima, C., & Uchino, S. (2013). Robo1 regulates the migration and laminar distribution of upper-layer pyramidal neurons of the cerebral cortex. *Cerebral Cortex*, *23*(6), 1495–1508. https://doi.org/10.1093/cercor/bhs141

Götz, M., & Huttner, W. B. (2005). The cell biology of neurogenesis. *Nature Reviews Molecular Cell Biology*, *6*(10), 777–788. https://doi.org/10.1038/nrm1739

Groessl, M., Luksch, H., Rösen-Wolff, A., Shevchenko, A., & Gentzel, M. (2012). Profiling of the human monocytic cell secretome by quantitative label-free mass spectrometry identifies stimulus-specific cytokines and proinflammatory proteins. *Proteomics*, *12*(18), 2833–2842. https://doi.org/10.1002/pmic.201200108

Güttinger, S., Laurell, E., & Kutay, U. (2009). Orchestrating nuclear envelope disassembly and reassembly during mitosis. *Nature Reviews Molecular Cell Biology*, *10*(3), 178–191. https://doi.org/10.1038/nrm2641

Hansen, D. V., Lui, J. H., Parker, P. R. L., & Kriegstein, A. R. (2010). Neurogenic radial glia in the outer subventricular zone of human neocortex. *Nature*, *464*(7288), 554–561. https://doi.org/10.1038/nature08845

Hardwick, L. J. A., Ali, F. R., Azzarelli, R., & Philpott, A. (2015). Cell cycle regulation of proliferation versus differentiation in the central nervous system. *Cell and Tissue Research*, *359*(1), 187–200. https://doi.org/10.1007/s00441-014-1895-8

Hardwick, L. J. A., & Philpott, A. (2014). Nervous decision-making: To divide or differentiate. *Trends in Genetics*, *30*(6), 254–261. https://doi.org/10.1016/j.tig.2014.04.001

Haubensak, W., Attardo, A., Denk, W., & Huttner, W. B. (2004). Neurons arise in the basal neuroepithelium of the early mammalian telencephalon: A major site of neurogenesis. *Proceedings of the National Academy of Sciences of the United States of America*, *101*(9), 3196–3201. https://doi.org/10.1073/pnas.0308600100

Heasman, S. J., & Ridley, A. J. (2008). Mammalian Rho GTPases: New insights into their functions from in vivo studies. *Nature Reviews Molecular Cell Biology*, *9*(9), 690–701. https://doi.org/10.1038/nrm2476

Hébert, J. M. (2011). FGFs: Neurodevelopment's jack-of-all-trades - How do they do it? *Frontiers in Neuroscience*, *5*(DEC), 1–10. https://doi.org/10.3389/fnins.2011.00133

Heinz, S., Benner, C., Spann, N., Bertolino, E., Lin, Y. C., Laslo, P., Cheng, J. X., Murre, C., Singh, H., & Glass, C. K. (2010). Simple Combinations of Lineage-Determining Transcription Factors Prime cis-Regulatory Elements Required for Macrophage and B Cell Identities. *Molecular Cell*, *38*(4), 576–589. https://doi.org/10.1016/j.molcel.2010.05.004

Hetman, M., & Slomnicki, L. P. (2019). Ribosomal biogenesis as an emerging target of neurodevelopmental pathologies. *Journal of Neurochemistry*, *148*(3), 325–347.

Hetzer, M. W. (2010). The nuclear envelope. *Cold Spring Harbor Perspectives in Biology*, *2*(3). https://doi.org/10.1101/cshperspect.a000539

Hevner, R. F. (2006). From radial glia to pyramidal-projection neuron: Transcription factor cascades in cerebral cortex development. *Molecular Neurobiology*, *33*(1), 33–50. https://doi.org/10.1385/mn:33:1:033

Hill, R. S., & Walsh, C. A. (2005). Molecular insights into human brain evolution. *Nature*, *437*(7055), 64–67. https://doi.org/10.1038/nature04103

Hohenester, E. (2008). Structural insight into Slit-Robo signalling. *Biochemical Society Transactions*, *36*(2), 251–256. https://doi.org/10.1042/BST0360251

Hori, K., Sen, A., & Artavanis-Tsakonas, S. (2013). Notch signaling at a glance. *Journal of Cell Science*, *126*(10), 2135–2140. https://doi.org/10.1242/jcs.127308

Hou, C., & Corces, V. G. (2010). Nups take leave of the nuclear envelope to regulate

transcription. *Cell*, *140*(3), 306–308.

Huttner, W. B., & Kosodo, Y. (2005). Symmetric versus asymmetric cell division during neurogenesis in the developing vertebrate central nervous system. *Current Opinion in Cell Biology*, *17*(6), 648–657. https://doi.org/10.1016/j.ceb.2005.10.005

Ibarra, A., & Hetzer, M. W. (2015). Nuclear pore proteins and the control of genome functions. *Genes and Development*, *29*(4), 337–349. https://doi.org/10.1101/gad.256495.114

Imamura, F., Ayoub, A. E., Rakic, P., & Greer, C. A. (2011). Timing of neurogenesis is a determinant of olfactory circuitry. *Nature Neuroscience*, *14*(3), 331–337. https://doi.org/10.1038/nn.2754

Imayoshi, I., Isomura, A., Harima, Y., Kawaguchi, K., Kori, H., Miyachi, H., Fujiwara, T., Ishidate, F., & Kageyama, R. (2013). Oscillatory control of factors determining multipotency and fate in mouse neural progenitors. *Science*, *342*(6163), 1203–1208.

Insausti, R. (1993). Comparative anatomy of the entorhinal cortex and hippocampus in mammals. *Hippocampus*, *3*(1 S), 19–26. https://doi.org/10.1002/hipo.1993.4500030705

Insausti, R., & Amaral, D. G. (2003). Hippocampal Formation. In *The Human Nervous System: Second Edition* (Issue December). https://doi.org/10.1016/B978-012547626-3/50024-7

Iwata, R., Casimir, P., & Vanderhaeghen, P. (2020). Mitochondrial dynamics in postmitotic cells regulate neurogenesis. *Science*, *369*(6505), 858–862. https://doi.org/10.1126/science.aba9760

Iwata, T., & Hevner, R. F. (2009). Fibroblast growth factor signaling in development of the cerebral cortex. *Development Growth and Differentiation*, *51*(3), 299–323. https://doi.org/10.1111/j.1440-169X.2009.01104.x

Jadhav, A. P., Cho, S.-H., & Cepko, C. L. (2006). Notch activity permits retinal cells to progress through multiple progenitor states and acquire a stem cell property. *Proceedings of the National Academy of Sciences*, *103*(50), 18998–19003.

Jadhav, A. P., Mason, H. A., & Cepko, C. L. (2006). *Notch 1 inhibits photoreceptor production in the developing mammalian retina*.

Jäkel, S., & Dimou, L. (2017). Glial cells and their function in the adult brain: A journey through the history of their ablation. *Frontiers in Cellular Neuroscience*, *11*(February), 1–17. https://doi.org/10.3389/fncel.2017.00024

Jarvis, E. D., Güntürkün, O., Bruce, L., Csillag, A., Karten, H., Kuenzel, W., Ball, G. F., Dugas-ford, J., Durand, S. E., Hough, G. E., Husband, S., Lee, D. W., Mello, C. V, Powers, A., Siang, C., & Smulders, T. V. (2005). Avian Brain and Vertebrate Brain Evolution. *Nature Reviews Neuroscience*, *6*(2), 151–159.

Jiang, X., & Nardelli, J. (2016a). Cellular and molecular introduction to brain development. *Neurobiology of Disease*, *92*(Part A), 3–17. https://doi.org/10.1016/j.nbd.2015.07.007

Jiang, X., & Nardelli, J. (2016b). Cellular and molecular introduction to brain development. *Neurobiology of Disease*, *92*(Part A), 3–17. https://doi.org/10.1016/j.nbd.2015.07.007

Kageyama, R., Ohtsuka, T., & Kobayashi, T. (2008). Roles of Hes genes in neural development. *Development Growth and Differentiation*, *50*(SUPPL. 1). https://doi.org/10.1111/j.1440-169X.2008.00993.x

Kageyama, R., Ohtsuka, T., Shimojo, H., & Imayoshi, I. (2008). Dynamic Notch signaling in neural progenitor cells and a revised view of lateral inhibition. *Nature Neuroscience*, *11*(11), 1247–1251. https://doi.org/10.1038/nn.2208

Kalebic, N., Gilardi, C., Stepien, B., Wilsch-Bräuninger, M., Long, K. R., Namba, T., Florio, M., Langen, B., Lombardot, B., Shevchenko, A., Kilimann, M. W., Kawasaki, H., Wimberger, P., & Huttner, W. B. (2019). Neocortical Expansion Due to Increased Proliferation of Basal Progenitors Is Linked to Changes in Their Morphology. *Cell Stem Cell*, *24*(4), 535-550.e9. https://doi.org/10.1016/j.stem.2019.02.017

Kampmann, M., & Blobel, G. (2009). Three-dimensional structure and flexibility of a membrane-coating module of the nuclear pore complex. *Nature Structural and Molecular Biology*, *16*(7), 782–788. https://doi.org/10.1038/nsmb.1618

Kandel, E. R., Schwartz, J. H., Jessell, T. M., Siegelbaum, S., Hudspeth, A. J., & Mack, S. (2000). *Principles of neural science* (Vol. 4). McGraw-hill New York.

Kang, W., Wong, L. C., Shi, S. H., & Hébert, J. M. (2009). The transition from radial glial to intermediate progenitor cell is inhibited by FGF signaling during corticogenesis. *Journal of Neuroscience*, *29*(46), 14571–14580. https://doi.org/10.1523/JNEUROSCI.3844-09.2009

Katsani, K. R., Karess, R. E., Dostatni, N., & Doye, V. (2008). In vivo dynamics of Drosophila nuclear envelope components. *Molecular Biology of the Cell*, *19*(9), 3652–3666.

Katz, L. C., & Callaway, E. M. (1992). Development of local circuits in mammalian visual cortex. *Annual Review of Neuroscience*, *15*(1), 31–56.

Kawauchi, T., Sekine, K., Shikanai, M., Chihama, K., Tomita, K., Kubo, K. ichiro, Nakajima, K., Nabeshima, Y. ichi, & Hoshino, M. (2010). Rab GTPases-dependent endocytic pathways regulate neuronal migration and maturation through N-cadherin trafficking. *Neuron*, *67*(4), 588–602. https://doi.org/10.1016/j.neuron.2010.07.007

Kelava, I., Reillo, I., Murayama, A. Y., Kalinka, A. T., Stenzel, D., Tomancak, P., Matsuzaki, F., Lebrand, C., Sasaki, E., Schwamborn, J. C., Okano, H., Huttner, W. B., & Borrell, V. (2012). Abundant occurrence of basal radial glia in the subventricular zone of embryonic neocortex of a lissencephalic primate, the common marmoset callithrix jacchus. *Cerebral Cortex*, *22*(2), 469–481. https://doi.org/10.1093/cercor/bhr301

Khacho, M., Harris, R., & Slack, R. S. (2019). Mitochondria as central regulators of neural stem cell fate and cognitive function. *Nature Reviews Neuroscience*, *20*(1), 34–48. https://doi.org/10.1038/s41583-018-0091-3

Khacho, M., & Slack, R. S. (2018). Mitochondrial dynamics in the regulation of neurogenesis: From development to the adult brain. *Developmental Dynamics*, *247*(1), 47–53. https://doi.org/10.1002/dvdy.24538

Khan, A. U., Qu, R., Ouyang, J., & Dai, J. (2020). Role of Nucleoporins and Transport Receptors in Cell Differentiation. *Frontiers in Physiology*, *11*(April), 1–12.

https://doi.org/10.3389/fphys.2020.00239

Kidd, T., Brose, K., Mitchell, K. J., Fetter, R. D., Tessier-Lavigne, M., Goodman, C. S., & Tear, G. (1998). Roundabout controls axon crossing of the CNS midline and defines a novel subfamily of evolutionarily conserved guidance receptors. *Cell*, *92*(2), 205–215. https://doi.org/10.1016/S0092-8674(00)80915-0

Kim, D., Langmead, B., & Salzberg, S. L. (2015). HISAT: A fast spliced aligner with low memory requirements. *Nature Methods*. https://doi.org/10.1038/nmeth.3317

Kim, G. B., Gao, Y., Palsson, B. O., & Lee, S. Y. (2021). DeepTFactor: A deep learning-based tool for the prediction of transcription factors. *Proceedings of the National Academy of Sciences of the United States of America*, *118*(2). https://doi.org/10.1073/pnas.2021171118

Knoblich, J. A. (2001). Asymmetric cell division during animal development. *Nature Reviews Molecular Cell Biology*, *2*(1), 11–20. https://doi.org/10.1038/35048085

Kornack, D. R., & Rakic, P. (1995). Radial and horizontal deployment of clonally related cells in the primate neocortex: Relationship to distinct mitotic lineages. *Neuron*, *15*(2), 311–321. https://doi.org/10.1016/0896-6273(95)90036-5

Kostovic, I., & Rakic, P. (1990). Developmental history of the transient subplate zone in the visual and somatosensory cortex of the macaque monkey and human brain. *Journal of Comparative Neurology*, *297*(3), 441–470. https://doi.org/10.1002/cne.902970309

Kosugi, S., Hasebe, M., Tomita, M., & Yanagawa, H. (2009). Systematic identification of cell cycle-dependent yeast nucleocytoplasmic shuttling proteins by prediction of composite motifs. *Proceedings of the National Academy of Sciences of the United States of America*, *106*(25), 10171–10176. https://doi.org/10.1073/pnas.0900604106

Kowalczyk, T., Pontious, A., Englund, C., Daza, R. A. M., Bedogni, F., Hodge, R., Attardo, A., Bell, C., Huttner, W. B., & Hevner, R. F. (2009). Intermediate neuronal progenitors (basal progenitors) produce pyramidal-projection neurons for all layers of cerebral cortex. *Cerebral Cortex*, *19*(10), 2439–2450. https://doi.org/10.1093/cercor/bhn260

Krafft, U., Reis, H., Ingenwerth, M., Kovalszky, I., Becker, M., Niedworok, C., Darr, C., Nyirády, P., Hadaschik, B., & Szarvas, T. (2020). Nuclear Localization of Robo is Associated with Better Survival in Bladder Cancer. *Pathology and Oncology Research*, *26*(1), 253–261. https://doi.org/10.1007/s12253-018-0447-z

Kreis, N. N., Louwen, F., & Yuan, J. (2019). The multifaceted p21 (Cip1/Waf1/CDKN1A) in cell differentiation, migration and cancer therapy. *Cancers*, *11*(9), 14–16. https://doi.org/10.3390/cancers11091220

Kriegstein, A., Noctor, S., & Martínez-Cerdeño, V. (2006). Patterns of neural stem and progenitor cell division may underlie evolutionary cortical expansion. *Nature Reviews Neuroscience*, *7*(11), 883–890. https://doi.org/10.1038/nrn2008

Kriegstein, A. R., & Götz, M. (2003). Radial glia diversity: A matter of cell fate. *Glia*, *43*(1), 37–43. https://doi.org/10.1002/glia.10250

Kriegstein, A. R., & Noctor, S. C. (2004). Patterns of neuronal migration in the embryonic cortex. *Trends in Neurosciences*, *27*(7), 392–399.

https://doi.org/10.1016/j.tins.2004.05.001

Kriegstein, & Alvarez-Buylla. (2009). The glial nature of embryonic and adult neural stem cells. *Annual Review of Neuroscience*, *32*, 149–184. https://doi.org/10.1146/annurev.neuro.051508.135600

Krubitzer, L., & Kaas, J. (2005). The evolution of the neocortex in mammals: How is phenotypic diversity generated? *Current Opinion in Neurobiology*, *15*(4), 444–453. https://doi.org/10.1016/j.conb.2005.07.003

Kuersten, S., Ohno, M., & Mattaj, I. W. (2001). Nucleocytoplasmic transport: Ran, beta and beyond. *Trends in Cell Biology*, *11*(12), 497–503. https://doi.org/10.1016/S0962-8924(01)02144-4

Kunisch, M., Haenlin, M., & Campos-Ortega, J. A. (1994). Lateral inhibition mediated by the Drosophila neurogenic gene delta is enhanced by proneural proteins. *Proceedings of the National Academy of Sciences of the United States of America*, *91*(21), 10139–10143. https://doi.org/10.1073/pnas.91.21.10139

Kutay, U., & Hetzer, M. W. (2008). Reorganization of the nuclear envelope during open mitosis. *Current Opinion in Cell Biology*, *20*(6), 669–677. https://doi.org/10.1016/j.ceb.2008.09.010

Lancaster, M. A., & Knoblich, J. A. (2012). Spindle orientation in mammalian cerebral cortical development. *Current Opinion in Neurobiology*, *22*(5), 737–746. https://doi.org/10.1016/j.conb.2012.04.003

Lange, A., Mills, R. E., Lange, C. J., Stewart, M., Devine, S. E., & Corbett, A. H. (2007). Classical nuclear localization signals: Definition, function, and interaction with importin α. *Journal of Biological Chemistry*, *282*(8), 5101–5105. https://doi.org/10.1074/jbc.R600026200

Langmead, B., & Salzberg, S. L. (2012). Fast gapped-read alignment with Bowtie 2. *Nature Methods*, *9*(4), 357–359. https://doi.org/10.1038/nmeth.1923

LeBon, L., Lee, T. V., Sprinzak, D., Jafar-Nejad, H., & Elowitz, M. B. (2014). Fringe proteins modulate Notch-ligand cis and trans interactions to specify signaling states. *ELife*, *3*(October), e02950. https://doi.org/10.7554/eLife.02950

Lee, D. C., Welton, K. L., Smith, E. D., & Kennedy, B. K. (2009). A-type nuclear lamins act as transcriptional repressors when targeted to promoters. *Experimental Cell Research*, *315*(6), 996–1007. https://doi.org/10.1016/j.yexcr.2009.01.003

Lee, J. K., Cho, J. H., Hwang, W. S., Lee, Y. D., Reu, D. S., & Suh-Kim, H. (2000). Expression of neuroD/BETA2 in mitotic and postmitotic neuronal cells during the development of nervous system. *Developmental Dynamics*, *217*(4), 361–367. https://doi.org/10.1002/(SICI)1097-0177(200004)217:4<361::AID-DVDY3>3.0.CO;2-8

Lewitus, E., Kelava, I., & Huttner, W. B. (2013). Conical expansion of the outer subventricular zone and the role of neocortical folding in evolution and development. *Frontiers in Human Neuroscience*, *7*(JUL), 1–12. https://doi.org/10.3389/fnhum.2013.00424

Liu, Z., Patel, K., Schmidt, H., Andrews, W., Pini, A., & Sundaresan, V. (2004). Extracellular

Ig domains 1 and 2 of Robo are important for ligand (Slit) binding. *Molecular and Cellular Neuroscience*, *26*(2), 232–240. https://doi.org/10.1016/j.mcn.2004.01.002

Llinares-Benadero, C., & Borrell, V. (2019). Deconstructing cortical folding: genetic, cellular and mechanical determinants. *Nature Reviews Neuroscience*, *20*(3), 161–176. https://doi.org/10.1038/s41583-018-0112-2

Llorca, A., & Marín, O. (2021). Orchestrated freedom: new insights into cortical neurogenesis. *Current Opinion in Neurobiology*, *66*, 48–56. https://doi.org/10.1016/j.conb.2020.09.004

Lo, H. W., Ali-Seyed, M., Wu, Y., Bartholomeusz, G., Hsu, S. C., & Hung, M. C. (2006). Nuclear-cytoplasmic transport of EGFR involves receptor endocytosis, importin β1 and CRM1. *Journal of Cellular Biochemistry*, *98*(6), 1570–1583. https://doi.org/10.1002/jcb.20876

Long, H., Sabatier, C., Ma, L., Plump, A., Yuan, W., Ornitz, D. M., Tamada, A., Murakami, F., Goodman, C. S., & Tessier-Lavigne, M. (2004). Conserved roles for Slit and Robo proteins in midline commissural axon guidance. *Neuron*, *42*(2), 213–223. https://doi.org/10.1016/S0896-6273(04)00179-5

Long, K. R., & Huttner, W. B. (2019). How the extracellular matrix shapes neural development. *Open Biology*, *9*(1). https://doi.org/10.1098/rsob.180216

Long, K. R., Newland, B., Florio, M., Kalebic, N., Langen, B., Kolterer, A., Wimberger, P., & Huttner, W. B. (2018). Extracellular Matrix Components HAPLN1, Lumican, and Collagen I Cause Hyaluronic Acid-Dependent Folding of the Developing Human Neocortex. *Neuron*, *99*(4), 702-719.e7. https://doi.org/10.1016/j.neuron.2018.07.013

Love, M. I., Huber, W., & Anders, S. (2014). Moderated estimation of fold change and dispersion for RNA-seq data with DESeq2. *Genome Biology*. https://doi.org/10.1186/s13059-014-0550-8

Lu, J., Wu, T., Zhang, B., Liu, S., Song, W., Qiao, J., & Ruan, H. (2021). Types of nuclear localization signals and mechanisms of protein import into the nucleus. *Cell Communication and Signaling*, *19*(1), 1–10. https://doi.org/10.1186/s12964-021-00741-y

Lukaszewicz, A., Savatier, P., Cortay, V., Kennedy, H., & Dehay, C. (2002). Contrasting effects of basic fibroblast growth factor and neurotrophin 3 on cell cycle kinetics of mouse cortical stem cells. *Journal of Neuroscience*, *22*(15), 6610–6622. https://doi.org/10.1523/jneurosci.22-15-06610.2002

Lun, A. T. L., Riesenfeld, S., Andrews, T., Dao, T. P., Gomes, T., & Marioni, J. C. (2019). EmptyDrops: distinguishing cells from empty droplets in droplet-based single-cell RNA sequencing data. *Genome Biology*, *20*(1), 63. https://doi.org/10.1186/s13059-019-1662-y

Lundström, A., Gallio, M., Englund, C., Steneberg, P., Hemphälä, J., Aspenström, P., Keleman, K., Falileeva, L., Dickson, B. J., & Samakovlis, C. (2004). Vilse, a conserved Rac/Cdc42 GAP mediating Robo repulsion in tracheal cells and axons. *Genes and Development*, *18*(17), 2161–2171. https://doi.org/10.1101/gad.310204

Luzzati, F. (2015). A hypothesis for the evolution of the upper layers of the neocortex through co-option of the olfactory cortex developmental program. *Frontiers in Neuroscience*, *9*(APR), 1–12. https://doi.org/10.3389/fnins.2015.00162

MacDonald, B. T., Tamai, K., & He, X. (2009). Wnt/β-catenin signaling: components, mechanisms, and diseases. *Developmental Cell*, *17*(1), 9–26.

Machon, O., Van Den Bout, C. J., Backman, M., Kemler, R., & Krauss, S. (2003). Role of β-catenin in the developing cortical and hippocampal neuroepithelium. *Neuroscience*, *122*(1), 129–143.

Maeda, N. (2015). Proteoglycans and neuronal migration in the cerebral cortex during development and disease. *Frontiers in Neuroscience*, *9*(MAR), 1–15. https://doi.org/10.3389/fnins.2015.00098

Mai, J. K., & Paxinos, G. (2011). *The human nervous system*. Academic press.

Manger, P. R., Slutsky, D. A., & Molnár, Z. (2002). Visual subdivisions of the dorsal ventricular ridge of the Iguana (Iguana iguana) as determined by electrophysiologic mapping. *Journal of Comparative Neurology*, *453*(3), 226–246. https://doi.org/10.1002/cne.10373

Mansfeld, J., Güttinger, S., Hawryluk-Gara, L. A., Panté, N., Mall, M., Galy, V., Haselmann, U., Mühlhäusser, P., Wozniak, R. W., Mattaj, I. W., Kutay, U., & Antonin, W. (2006). The Conserved Transmembrane Nucleoporin NDC1 Is Required for Nuclear Pore Complex Assembly in Vertebrate Cells. *Molecular Cell*, *22*(1), 93–103. https://doi.org/10.1016/j.molcel.2006.02.015

Manuel, M. N., Mi, D., Masonand, J. O., & Price, D. J. (2015). Regulation of cerebral cortical neurogenesis by the Pax6 transcription factor. *Frontiers in Cellular Neuroscience*, *9*(March), 1–21. https://doi.org/10.3389/fncel.2015.00070

Marillat, V., Cases, O., Nguyenf-Ba-Charvet, K. T., Tessier-Lavigne, M., Sotelo, C., & Chédotal, A. (2002). Spatiotemporal expression patterns of slit and robo genes in the rat brain. *Journal of Comparative Neurology*, *442*(2), 130–155. https://doi.org/10.1002/cne.10068

Marín, O., & Rubenstein, J. L. R. (2001). A long, remarkable journey: tangential migration in the telencephalon. *Nature Reviews Neuroscience*, *2*(11), 780–790.

Marín, O., & Rubenstein, J. L. R. (2003). Cell migration in the forebrain. *Annual Review of Neuroscience*, *26*(1), 441–483.

Martínez-cerdeño, V., Cunningham, C. L., Camacho, J., Janet, A., Ariza, J., Lovern, M., & Noctor, S. C. (2017). *Subventricular Zone in the Developing Cortex*. *524*(3), 433–447. https://doi.org/10.1002/cne.23879.Evolutionary

Martínez-Cerdeño, Verónica, Cunningham, C. L., Camacho, J., Antczak, J. L., Prakash, A. N., Cziep, M. E., Walker, A. I., & Noctor, S. C. (2012). Comparative analysis of the subventricular zone in rat, ferret and macaque: Evidence for an outer subventricular zone in rodents. *PLoS ONE*, *7*(1). https://doi.org/10.1371/journal.pone.0030178

Martínez-Cerdeño, Veronica, Noctor, S. C., & Kriegstein, A. R. (2006). The role of intermediate progenitor cells in the evolutionary expansion of the cerebral cortex. *Cerebral Cortex*, *16*(SUPPL. 1). https://doi.org/10.1093/cercor/bhk017

Matsumoto, N., Tanaka, S., Horiike, T., Shinmyo, Y., & Kawasaki, H. (2020). A discrete subtype of neural progenitor crucial for cortical folding in the gyrencephalic mammalian

brain. *ELife*, *9*, 1–26. https://doi.org/10.7554/eLife.54873

Medina, L. (2007). Do birds and reptiles possess homologues of mammalian visual, somatosensory, and motor cortices? *Evolution of Nervous Systems*, *2*, 163–194. https://doi.org/10.1016/B0-12-370878-8/00132-4

Mekhail, K., & Moazed, D. (2010). The nuclear envelope in genome organization, expression and stability. *Nature Reviews Molecular Cell Biology*, *11*(5), 317–328. https://doi.org/10.1038/nrm2894

Merico, D., Isserlin, R., Stueker, O., Emili, A., & Bader, G. D. (2010). Enrichment map: A network-based method for gene-set enrichment visualization and interpretation. *PLoS ONE*. https://doi.org/10.1371/journal.pone.0013984

Miller, A. C., Lyons, E. L., & Herman, T. G. (2009). cis-Inhibition of Notch by Endogenous Delta Biases the Outcome of Lateral Inhibition. *Current Biology*, *19*(16), 1378–1383. https://doi.org/10.1016/j.cub.2009.06.042

Mishra, R. K., Chakraborty, P., Arnaoutov, A., Fontoura, B. M. A., & Dasso, M. (2010). The Nup107-160 complex and γ-TuRC regulate microtubule polymerization at kinetochores. *Nature Cell Biology*, *12*(2), 164–169. https://doi.org/10.1038/ncb2016

Miyata, T., Kawaguchi, A., Saito, K., Kawano, M., Muto, T., & Ogawa, M. (2004). Asymmetric production of surface-dividing and non-surface-dividing cortical progenitor cells. *Development*, *131*(13), 3133–3145. https://doi.org/10.1242/dev.01173

Miyata, T., Kawaguchi, D., Kawaguchi, A., & Gotoh, Y. (2010). Mechanisms that regulate the number of neurons during mouse neocortical development. *Current Opinion in Neurobiology*, *20*(1), 22–28. https://doi.org/10.1016/j.conb.2010.01.001

Mizeracka, K., DeMaso, C. R., & Cepko, C. L. (2013). Notch1 is required in newly postmitotic cells to inhibit the rod photoreceptor fate. *Development*, *140*(15), 3188–3197.

Mizutani, K. I., Yoon, K., Dang, L., Tokunaga, A., & Gaiano, N. (2007). Differential Notch signalling distinguishes neural stem cells from intermediate progenitors. *Nature*, *449*(7160), 351–355. https://doi.org/10.1038/nature06090

Mohr, D., Frey, S., Fischer, T., Güttler, T., & Görlich, D. (2009). Characterisation of the passive permeability barrier of nuclear pore complexes. *EMBO Journal*, *28*(17), 2541–2553. https://doi.org/10.1038/emboj.2009.200

Molnár, Z. (2011). Evolution of cerebral cortical development. *Brain, Behavior and Evolution*, *78*(1), 94–107. https://doi.org/10.1159/000327325

Molnár, Z., & Pollen, A. (2014). How unique is the human neocortex? *Development (Cambridge)*, *141*(1), 11–16. https://doi.org/10.1242/dev.101279

Molyneaux, B. J., Arlotta, P., Menezes, J. R. L., & Macklis, J. D. (2007). Neuronal subtype specification in the cerebral cortex. *Nature Reviews Neuroscience*, *8*(6), 427–437. https://doi.org/10.1038/nrn2151

Moreau, M. X., Saillour, Y., Cwetsch, A. W., Pierani, A., & Causeret, F. (2021). Single-cell transcriptomics of the early developing mouse cerebral cortex disentangle the spatial and temporal components of neuronal fate acquisition. *Development (Cambridge)*, *148*(14).

https://doi.org/10.1242/DEV.197962

Morlot, C., Thielens, N. M., Ravelli, R. B. G., Hemrika, W., Romijn, R. A., Gros, P., Cusack, S., & McCarthy, A. A. (2007). Structural insights into the Slit-Robo complex. *Proceedings of the National Academy of Sciences of the United States of America*, *104*(38), 14923–14928. https://doi.org/10.1073/pnas.0705310104

Mountcastle, V. B. (1997). The columnar organization of the neocortex. *Brain*, *120*(4), 701–722. https://doi.org/10.1093/brain/120.4.701

Munji, R. N., Choe, Y., Li, G., Siegenthaler, J. A., & Pleasure, S. J. (2011). *Wnt Signaling Regulates Neuronal Differentiation of Cortical Intermediate Progenitors*. *31*(5), 1676–1687. https://doi.org/10.1523/JNEUROSCI.5404-10.2011

Muzio, L., DiBenedetto, B., Stoykova, A., Boncinelli, E., Gruss, P., & Mallamaci, A. (2002). Conversion of cerebral cortex into basal ganglia in Emx2−/− Pax6Sey/Sey double-mutant mice. *Nature Neuroscience*, *5*(8), 737–745. https://doi.org/10.1038/nn892

Namba, T., & Huttner, W. B. (2017). Neural progenitor cells and their role in the development and evolutionary expansion of the neocortex. *Wiley Interdisciplinary Reviews: Developmental Biology*, *6*(1). https://doi.org/10.1002/wdev.256

Neuhaus-Follini, A., & Bashaw, G. J. (2015). The Intracellular Domain of the Frazzled/DCC Receptor Is a Transcription Factor Required for Commissural Axon Guidance. *Neuron*, *87*(4), 751–763. https://doi.org/10.1016/j.neuron.2015.08.006

Newton, K., Dugger, D. L., Sengupta-Ghosh, A., Ferrando, R. E., Chu, F., Tao, J., Lam, W., Haller, S., Chan, S., Sa, S., Dunlap, D., Eastham-Anderson, J., Ngu, H., Hung, J., French, D. M., Webster, J. D., Bolon, B., Liu, J., Reja, R., … Dixit, V. M. (2018). Ubiquitin ligase COP1 coordinates transcriptional programs that control cell type specification in the developing mouse brain. *Proceedings of the National Academy of Sciences of the United States of America*, *115*(44), 11244–11249. https://doi.org/10.1073/pnas.1805033115

Nieto, M., Schuurmans, C., Britz, O., & Guillemot, F. (2001). Neural bHLH genes control the neuronal versus glial fate decision in cortical progenitors. *Neuron*, *29*(2), 401–413. https://doi.org/10.1016/S0896-6273(01)00214-8

Noctor, S. C., Flint, A. C., Weissman, T. A., Wong, W. S., Clinton, B. K., & Kriegstein, A. R. (2002). Dividing precursor cells of the embryonic cortical ventricular zone have morphological and molecular characteristics of radial glia. *Journal of Neuroscience*, *22*(8), 3161–3173. https://doi.org/10.1523/jneurosci.22-08-03161.2002

Noctor, S. C., Martinez-Cerdeño, V., Ivic, L., & Kriegstein, A. R. (2004). Cortical neurons arise in symmetric and asymmetric division zones and migrate through specific phases. *Nature Neuroscience*, *7*(2), 136–144. https://doi.org/10.1038/nn1172

Noctor, S. C., Martínez-Cerdeño, V., & Kriegstein, A. R. (2008). Distinct behaviors of neural stem and progenitor cells underlie cortical neurogenesis. *Journal of Comparative Neurology*, *508*(1), 28–44. https://doi.org/10.1002/cne.21669

Nomura, T., & Hanashima, C. (2014). Neocortical development and evolution. *Neuroscience Research*, *86*, 1–2. https://doi.org/10.1016/j.neures.2014.10.010

Nomura, T., Kawaguchi, M., Ono, K., & Murakami, Y. (2013). Reptiles: A new model for brain evo-devo research. *Journal of Experimental Zoology Part B: Molecular and Developmental Evolution*, *320*(2), 57–73. https://doi.org/10.1002/jez.b.22484

Nonaka-Kinoshita, M., Reillo, I., Artegiani, B., Ángeles Martínez-Martínez, M., Nelson, M., Borrell, V., & Calegari, F. (2013). Regulation of cerebral cortex size and folding by expansion of basal progenitors. *EMBO Journal*, *32*(13), 1817–1828. https://doi.org/10.1038/emboj.2013.96

O'Leary, D. D. M., Chou, S. J., & Sahara, S. (2007). Area patterning of the mammalian cortex. *Neuron*, *56*(2), 252–269. https://doi.org/10.1016/j.neuron.2007.10.010

Oesper, L., Merico, D., Isserlin, R., & Bader, G. D. (2011). WordCloud: A Cytoscape plugin to create a visual semantic summary of networks. *Source Code for Biology and Medicine*. https://doi.org/10.1186/1751-0473-6-7

Ohata, S., Aoki, R., Kinoshita, S., Yamaguchi, M., Tsuruoka-Kinoshita, S., Tanaka, H., Wada, H., Watabe, S., Tsuboi, T., Masai, I., & Okamoto, H. (2011). Dual roles of notch in regulation of apically restricted mitosis and apicobasal polarity of neuroepithelial cells. *Neuron*, *69*(2), 215–230. https://doi.org/10.1016/j.neuron.2010.12.026

Ohnuma, S. I., & Harris, W. A. (2003). Neurogenesis and the cell cycle. *Neuron*, *40*(2), 199–208. https://doi.org/10.1016/S0896-6273(03)00632-9

Ohtsuka, T., Sakamoto, M., Guillemot, F., & Kageyama, R. (2001). Roles of the Basic Helix-Loop-Helix Genes Hes1 and Hes5 in Expansion of Neural Stem Cells of the Developing Brain. *Journal of Biological Chemistry*, *276*(32), 30467–30474. https://doi.org/10.1074/jbc.M102420200

Oka, M., & Yoneda, Y. (2018). Importin α: Functions as a nuclear transport factor and beyond. *Proceedings of the Japan Academy Series B: Physical and Biological Sciences*, *94*(7), 259–274. https://doi.org/10.2183/pjab.94.018

Orjalo, A. V, Arnaoutov, A., Shen, Z., Boyarchuk, Y., Zeitlin, S. G., Fontoura, B., Briggs, S., Dasso, M., & Forbes, D. J. (2006). The Nup107-160 nucleoporin complex is required for correct bipolar spindle assembly. *Molecular Biology of the Cell*, *17*(9), 3806–3818.

Panaliappan, T. K., Wittmann, W., Jidigam, V. K., Mercurio, S., Bertolini, J. A., Sghari, S., Bose, R., Patthey, C., Nicolis, S. K., & Gunhaga, L. (2018). Sox2 is required for olfactory pit formation and olfactory neurogenesis through BMP restriction and Hes5 upregulation. *Development (Cambridge)*, *145*(2). https://doi.org/10.1242/dev.153791

Paridaen, J. T. M. L., & Huttner, W. B. (2014). *Neurogenesis during development of the vertebrate central nervous system*. *15*(4), 351–364.

Park, Y., Rangel, C., Reynolds, M. M., Caldwell, M. C., Johns, M., Nayak, M., Welsh, C. J. R., McDermott, S., & Datta, S. (2003). Drosophila Perlecan modulates FGF and Hedgehog signals to activate neural stem cell division. *Developmental Biology*, *253*(2), 247–257. https://doi.org/10.1016/S0012-1606(02)00019-2

Pataskar, A., Jung, J., Smialowski, P., Noack, F., Calegari, F., Straub, T., & Tiwari, V. K. (2016). NeuroD1 reprograms chromatin and transcription factor landscapes to induce the neuronal program. *The EMBO Journal*, *35*(1), 24–45. https://doi.org/10.15252/embj.201591206

Pepenella, S., & Hayes, J. (2007). Global histone acetylation induces functional genomic reorganization at mammalian nuclear pore complexes: Commentary. *Chemtracts*, *20*(10), 406–409. https://doi.org/10.1101/gad.1632708.4

Perkins, D. N., Pappin, D. J., Creasy, D. M., & Cottrell, J. S. (1999). Probability-based protein identification by searching sequence databases using mass spectrometry data. *Electrophoresis*, *20*(18), 3551–3567. https://doi.org/10.1002/(SICI)1522-2683(19991201)20:18<3551::AID-ELPS3551>3.0.CO;2-2

Petanjek, Z., Judaš, M., Šimić, G., Rašin, M. R., Uylings, H. B. M., Rakic, P., & Kostović, I. (2011). Extraordinary neoteny of synaptic spines in the human prefrontal cortex. *Proceedings of the National Academy of Sciences of the United States of America*, *108*(32), 13281–13286. https://doi.org/10.1073/pnas.1105108108

Pierfelice, T., Alberi, L., & Gaiano, N. (2011). Notch in the Vertebrate Nervous System: An Old Dog with New Tricks. *Neuron*, *69*(5), 840–855. https://doi.org/10.1016/j.neuron.2011.02.031

Pilz, G. A., Shitamukai, A., Reillo, I., Pacary, E., Schwausch, J., Stahl, R., Ninkovic, J., Snippert, H. J., Clevers, H., Godinho, L., Guillemot, F., Borrell, V., Matsuzaki, F., & Götz, M. (2013). Amplification of progenitors in the mammalian telencephalon includes a new radial glial cell type. *Nature Communications*, *4*, 1–11. https://doi.org/10.1038/ncomms3125

Piper, M., Barry, G., Hawkins, J., Mason, S., Lindwall, C., Little, E., Sarkar, A., Smith, A. G., Moldrich, R. X., Boyle, G. M., Tole, S., Gronostajski, R. M., Bailey, T. L., & Richards, L. J. (2010). NFIA controls telencephalic progenitor cell differentiation through repression of the Notch effector Hes1. *Journal of Neuroscience*, *30*(27), 9127–9139. https://doi.org/10.1523/JNEUROSCI.6167-09.2010

Platani, M., Santarella-Mellwig, R., Posch, M., Walczak, R., Swedlow, J. R., & Mattaj, I. W. (2009). The Nup107-160 nucleoporin complex promotes mitotic events via control of the localization state of the chromosome passenger complex. *Molecular Biology of the Cell*, *20*(24), 5260–5275.

Pollen, A. A., Nowakowski, T. J., Chen, J., Retallack, H., Sandoval-Espinosa, C., Nicholas, C. R., Shuga, J., Liu, S. J., Oldham, M. C., & Diaz, A. (2015). Molecular identity of human outer radial glia during cortical development. *Cell*, *163*(1), 55–67.

Pollen, A. A., Nowakowski, T. J., Shuga, J., Wang, X., Leyrat, A. A., Lui, J. H., Li, N., Szpankowski, L., Fowler, B., Chen, P., Ramalingam, N., Sun, G., Thu, M., Norris, M., Lebofsky, R., Toppani, D., Kemp, D. W., Wong, M., Clerkson, B., … West, J. A. A. (2014). Low-coverage single-cell mRNA sequencing reveals cellular heterogeneity and activated signaling pathways in developing cerebral cortex. *Nature Biotechnology*, *32*(10), 1053–1058. https://doi.org/10.1038/nbt.2967

Portier, N., Audhya, A., Maddox, P. S., Green, R. A., Dammermann, A., Desai, A., & Oegema, K. (2007). A Microtubule-Independent Role for Centrosomes and Aurora A in Nuclear Envelope Breakdown. *Developmental Cell*, *12*(4), 515–529. https://doi.org/10.1016/j.devcel.2007.01.019

Puelles, L., Sandoval, J. E., Ayad, A., del Corral, R., Alonso, A., Ferran, J. L., & Martínez-de-la-Torre, M. (2016). The Pallium in Reptiles and Birds in the Light of the Updated

Tetrapartite Pallium Model. In *Evolution of Nervous Systems: Second Edition* (Vols. 1–4, Issue January). https://doi.org/10.1016/B978-0-12-804042-3.00014-2

Puelles, Luis. (2017). Comments on the updated tetrapartite pallium model in the mouse and chick, featuring a homologous claustro-insular complex. *Brain, Behavior and Evolution*, *90*(2), 171–189.

Puelles, Luis, Harrison, M., Paxinos, G., & Watson, C. (2013). A developmental ontology for the mammalian brain based on the prosomeric model. *Trends in Neurosciences*, *36*(10), 570–578. https://doi.org/10.1016/j.tins.2013.06.004

Purves, D., Augustine, G. J., Fitzpatrick, D., Hall, W., LaMantia, A.-S., & White, L. (2019). *Neurosciences*. De Boeck Supérieur.

Qiu, X., Mao, Q., Tang, Y., Wang, L., Chawla, R., Pliner, H. A., & Trapnell, C. (2017). Reversed graph embedding resolves complex single-cell trajectories. *Nature Methods*, *14*(10), 979–982. https://doi.org/10.1038/nmeth.4402

Raballo, R., Rhee, J., Lyn-Cook, R., Leckman, J. F., Schwartz, M. L., & Vaccarino, F. M. (2000). Basic fibroblast growth factor (Fgf2) is necessary for cell proliferation and neurogenesis in the developing cerebral cortex. *Journal of Neuroscience*, *20*(13), 5012–5023. https://doi.org/10.1523/jneurosci.20-13-05012.2000

Rabut, G., Lénárt, P., & Ellenberg, J. (2004). Dynamics of nuclear pore complex organization through the cell cycle. *Current Opinion in Cell Biology*, *16*(3), 314–321. https://doi.org/10.1016/j.ceb.2004.04.001

Rakic, P. (2007). The radial edifice of cortical architecture: From neuronal silhouettes to genetic engineering. *Brain Research Reviews*, *55*(2 SPEC. ISS.), 204–219. https://doi.org/10.1016/j.brainresrev.2007.02.010

Raney, B. J., Dreszer, T. R., Barber, G. P., Clawson, H., Fujita, P. A., Wang, T., Nguyen, N., Paten, B., Zweig, A. S., Karolchik, D., & Kent, W. J. (2014). Track data hubs enable visualization of user-defined genome-wide annotations on the UCSC Genome Browser. *Bioinformatics (Oxford, England)*, *30*(7), 1003–1005. https://doi.org/10.1093/bioinformatics/btt637

Rasala, B. A., Orjalo, A. V., Shen, Z., Briggs, S., & Forbes, D. J. (2006). ELYS is a dual nucleoporin/kinetochore protein required for nuclear pore assembly and proper cell division. *Proceedings of the National Academy of Sciences of the United States of America*, *103*(47), 17801–17806. https://doi.org/10.1073/pnas.0608484103

Rash, B. G., & Grove, E. A. (2006). Area and layer patterning in the developing cerebral cortex. *Current Opinion in Neurobiology*, *16*(1), 25–34. https://doi.org/10.1016/j.conb.2006.01.004

Rath, S., Sharma, R., Gupta, R., Ast, T., Chan, C., Durham, T. J., Goodman, R. P., Grabarek, Z., Haas, M. E., Hung, W. H. W., Joshi, P. R., Jourdain, A. A., Kim, S. H., Kotrys, A. V., Lam, S. S., McCoy, J. G., Meisel, J. D., Miranda, M., Panda, A., … Mootha, V. K. (2021). MitoCarta3.0: An updated mitochondrial proteome now with sub-organelle localization and pathway annotations. *Nucleic Acids Research*, *49*(D1), D1541–D1547. https://doi.org/10.1093/nar/gkaa1011

Reillo, I., De Juan Romero, C., García-Cabezas, M. Á., & Borrell, V. (2011). A Role for

intermediate radial glia in the tangential expansion of the mammalian cerebral cortex. *Cerebral Cortex*, *21*(7), 1674–1694. https://doi.org/10.1093/cercor/bhq238

Reiner, A., Yamamoto, K., & Karten, H. J. (2005). Organization and evolution of the avian forebrain. *Anatomical Record - Part A Discoveries in Molecular, Cellular, and Evolutionary Biology*, *287*(1), 1080–1102. https://doi.org/10.1002/ar.a.20253

Reiner, O., Sapir, T., & Gerlitz, G. (2012). *Interkinetic Nuclear Movement in the Ventricular Zone of the Cortex*. 516–526. https://doi.org/10.1007/s12031-011-9633-0

Rhee, J., Buchan, T., Zukerberg, L., Lilien, J., & Balsamo, J. (2007). Cables links Robo-bound Abl kinase to N-cadherin-bound β-catenin to mediate Slit-induced modulation of adhesion and transcription. *Nature Cell Biology*, *9*(8), 883–892. https://doi.org/10.1038/ncb1614

Rhee, J., Mahfooz, N. S., Arregui, C., Lilien, J., Balsamo, J., & VanBerkum, M. F. A. (2002). Activation of the repulsive receptor roundabout inhibits N-cadherin-mediated cell adhesion. *Nature Cell Biology*, *4*(10), 798–805. https://doi.org/10.1038/ncb858

Ródenas, E., González-Aguilera, C., Ayuso, C., & Askjaer, P. (2012). Dissection of the NUP107 nuclear pore subcomplex reveals a novel interaction with spindle assembly checkpoint protein MAD1 in Caenorhabditis elegans. *Molecular Biology of the Cell*, *23*(5), 930–944. https://doi.org/10.1091/mbc.E11-11-0927

Rohatgi, R., Ho, H. Y. H., & Kirschner, M. W. (2000). Mechanism of N-WASP activation by CDC42 and phosphatidylinositol 4,5-bisphosphate. *Journal of Cell Biology*, *150*(6), 1299–1309. https://doi.org/10.1083/jcb.150.6.1299

Rohatgi, R., Ma, L., Miki, H., Lopez, M., Kirchhausen, T., Takenawa, T., & Kirschner, M. W. (1999). The interaction between N-WASP and the Arp2/3 complex links Cdc42-dependent signals to actin assembly. *Cell*, *97*(2), 221–231. https://doi.org/10.1016/S0092-8674(00)80732-1

Ross, M. E., & Walsh, C. A. (2001). Human brain malformations and their lessons for neuronal migration. *Annual Review of Neuroscience*, *24*(July 2014), 1041–1070. https://doi.org/10.1146/annurev.neuro.24.1.1041

Round, J. E., & Sun, H. (2011). The adaptor protein Nck2 mediates Slit1-induced changes in cortical neuron morphology. *Molecular and Cellular Neuroscience*, *47*(4), 265–273. https://doi.org/10.1016/j.mcn.2011.04.009

Roy, K., Kuznicki, K., Wu, Q., Sun, Z., Bock, D., Schutz, G., Vranich, N., & Monaghan, A. P. (2004). The tlx gene regulates the timing of neurogenesis in the cortex. *Journal of Neuroscience*, *24*(38), 8333–8345. https://doi.org/10.1523/JNEUROSCI.1148-04.2004

Ruan, X., Kang, B., Qi, C., Lin, W., Wang, J., & Zhang, X. (2021). Progenitor cell diversity in the developing mouse neocortex. *Proceedings of the National Academy of Sciences*, *118*(10), e2018866118.

Rubenstein, J. L. R., Shimamura, K., Martinez, S., & Puelles, L. (1998). Regionalization of the prosencephalic neural plate. *Annual Review of Neuroscience*, *21*(February 2016), 445–477. https://doi.org/10.1146/annurev.neuro.21.1.445

Sahara, S., & O'Leary, D. D. M. (2009). Fgf10 regulates transition period of cortical stem cell

differentiation to radial glia controlling generation of neurons and basal progenitors. *Neuron*, *63*(1), 48–62.

Sakamoto, M., Hirata, H., Ohtsuka, T., Bessho, Y., & Kageyama, R. (2003). The Basic Helix-Loop-Helix Genes Hesr1/Hey1 and Hesr2/Hey2 Regulate Maintenance of Neural Precursor Cells in the Brain. *Journal of Biological Chemistry*, *278*(45), 44808–44815. https://doi.org/10.1074/jbc.M300448200

Salatino, D. R. (2014). *PSYCHE - Structure and Function* (Issue December). https://doi.org/10.13140/2.1.4912.5448

Satomura, A., & Brickner, J. H. (2017). Nuclear Pore Complexes: A Scaffold Regulating Developmental Transcription? *Trends in Cell Biology*, *27*(9), 621–622. https://doi.org/10.1016/j.tcb.2017.07.002

Sawasdichai, A., Chen, H. T., Hamid, N. A., Jayaraman, P. S., & Gaston, K. (2010). In situ subcellular fractionation of Adherent and non-adherent mammalian cells. *Journal of Visualized Experiments*, *6*(41), 1–5. https://doi.org/10.3791/1958

Scardigli, R., Bäumer, N., Gruss, P., Guillemot, F., & Le Roux, I. (2003). Direct and concentration-dependent regulation of the proneural gene Neurogenin2 by Pax6. *Development*, *130*(14), 3269–3281. https://doi.org/10.1242/dev.00539

Schrimer, E. C., & Gerace, L. (2002). Organellar proteomics: The prizes and pitfalls of opening the nuclear envelope. *Genome Biology*, *3*(4). https://doi.org/10.1186/gb-2002-3-4-reviews1008

Schuurmans, C., & Guillemot, F. (2002). Molecular mechanisms underlying cell fate specification in the developing telencephalon. *Current Opinion in Neurobiology*, *12*(1), 26–34. https://doi.org/10.1016/S0959-4388(02)00286-6

Seiradake, E., von Philipsborn, A. C., Henry, M., Fritz, M., Lortat-Jacob, H., Jamin, M., Hemrika, W., Bastmeyer, M., Cusack, S., & McCarthy, A. A. (2009). Structure and functional relevance of the Slit2 homodimerization domain. *EMBO Reports*, *10*(7), 736–741. https://doi.org/10.1038/embor.2009.95

Seki, M., Watanabe, A., Enomoto, S., Kawamura, T., Ito, H., Kodama, T., Hamakubo, T., & Aburatani, H. (2010). Human ROBO1 is cleaved by metalloproteinases and γ-secretase and migrates to the nucleus in cancer cells. *FEBS Letters*, *584*(13), 2909–2915. https://doi.org/10.1016/j.febslet.2010.05.009

Sessa, A., Mao, C. A., Colasante, G., Nini, A., Klein, W. H., & Broccoli, V. (2010). Tbr2-positive intermediate (basal) neuronal progenitors safeguard cerebral cortex expansion by controlling amplification of pallial glutamatergic neurons and attraction of subpallial GABAergic interneurons. *Genes and Development*, *24*(16), 1816–1826. https://doi.org/10.1101/gad.575410

Shannon, P., Markiel, A., Ozier, O., Baliga, N. S., Wang, J. T., Ramage, D., Amin, N., Schwikowski, B., & Ideker, T. (2003). Cytoscape: A software Environment for integrated models of biomolecular interaction networks. *Genome Research*. https://doi.org/10.1101/gr.1239303

Shevchenko, A., Wilm, M., Vorm, O., & Mann, M. (1996). Mass spectrometric sequencing of proteins silver-stained polyacrylamide gels. *Analytical Chemistry*, *68*(5), 850–858.

https://doi.org/10.1021/ac950914h

Shikata, Y., Okada, T., Hashimoto, M., Ellis, T., Matsumaru, D., Shiroishi, T., Ogawa, M., Wainwright, B., & Motoyama, J. (2011). Ptch1-mediated dosage-dependent action of Shh signaling regulates neural progenitor development at late gestational stages. *Developmental Biology*, *349*(2), 147–159. https://doi.org/10.1016/j.ydbio.2010.10.014

Shimojo, H., Ohtsuka, T., & Kageyama, R. (2011). Dynamic expression of Notch signaling genes in neural stem/ progenitor cells. *Frontiers in Neuroscience*, *5*(JUN), 1–7. https://doi.org/10.3389/fnins.2011.00078

Shitamukai, A., Konno, D., & Matsuzaki, F. (2011). *Oblique Radial Glial Divisions in the Developing Mouse Neocortex Induce Self-Renewing Progenitors outside the Germinal Zone That Resemble Primate Outer Subventricular Zone Progenitors*. *31*(10), 3683–3695. https://doi.org/10.1523/JNEUROSCI.4773-10.2011

Sidman, R. L., & Rakic, P. (1973). Neuronal migration, with special reference to developing human brain: a review. *Brain Research*, *62*(1), 1–35. https://doi.org/https://doi.org/10.1016/0006-8993(73)90617-3

Silva, J. C., Gorenstein, M. V, Li, G.-Z., Vissers, J. P. C., & Geromanos, S. J. (2006). Absolute quantification of proteins by LCMSE: a virtue of parallel MS acquisition. *Molecular & Cellular Proteomics : MCP*, *5*(1), 144–156. https://doi.org/10.1074/mcp.M500230-MCP200

Silver, D. L. (2016). Genomic divergence and brain evolution: How regulatory DNA influences development of the cerebral cortex. *BioEssays*, *38*(2), 162–171. https://doi.org/10.1002/bies.201500108

Silver, D. L., Rakic, P., Grove, E. A., Haydar, T. F., Hensch, T. K., Huttner, W. B., Molnár, Z., Rubenstein, J. L., Sestan, N., Stryker, M. P., Sur, M., Tosches, M. A., & Walsh, C. A. (2020). Evolution and Ontogenetic Development of Cortical Structures. In *The Neocortex* (Vol. 27). https://doi.org/10.7551/mitpress/12593.003.0008

Sindhu, C., Samavarchi-Tehrani, P., & Meissner, A. (2012). Transcription factor-mediated epigenetic reprogramming. *Journal of Biological Chemistry*, *287*(37), 30922–30931. https://doi.org/10.1074/jbc.R111.319046

Sirko, S., Akita, K., Von Holst, A., & Faissner, A. (2010). Structural and functional analysis of chondroitin sulfate proteoglycans in the neural stem cell niche. In *Methods in Enzymology* (1st ed., Vol. 479, Issue C). Elsevier Inc. https://doi.org/10.1016/S0076-6879(10)79003-0

Smart, I. H. M. (2002). Unique Morphological Features of the Proliferative Zones and Postmitotic Compartments of the Neural Epithelium Giving Rise to Striate and Extrastriate Cortex in the Monkey. *Cerebral Cortex*, *12*(1), 37–53. https://doi.org/10.1093/cercor/12.1.37

Soriano, E., & Del Río, J. A. (2005). The cells of cajal-retzius: Still a mystery one century after. *Neuron*, *46*(3), 389–394. https://doi.org/10.1016/j.neuron.2005.04.019

Sousa, A. M. M., Meyer, K. A., Santpere, G., Gulden, F. O., & Sestan, N. (2017). Evolution of the Human Nervous System Function, Structure, and Development. *Cell*, *170*(2), 226–247. https://doi.org/10.1016/j.cell.2017.06.036

Splinter, D., Razafsky, D. S., Schlager, M. A., Serra-Marques, A., Grigoriev, I., Demmers, J., Keijzer, N., Jiang, K., Poser, I., Hyman, A. A., Hoogenraad, C. C., King, S. J., & Akhmanova, A. (2012). BICD2, dynactin, and LIS1 cooperate in regulating dynein recruitment to cellular structures. *Molecular Biology of the Cell*, *23*(21), 4226–4241. https://doi.org/10.1091/mbc.E12-03-0210

Sprinzak, D., Lakhanpal, A., Lebon, L., Santat, L. A., Fontes, M. E., Anderson, G. A., Garcia-Ojalvo, J., & Elowitz, M. B. (2010). Cis-interactions between Notch and Delta generate mutually exclusive signalling states. *Nature*, *465*(7294), 86–90. https://doi.org/10.1038/nature08959

Stahl, R., Walcher, T., De Juan Romero, C., Pilz, G. A., Cappello, S., Irmler, M., Sanz-Aquela, J. M., Beckers, J., Blum, R., Borrell, V., & Götz, M. (2013). Trnp1 regulates expansion and folding of the mammalian cerebral cortex by control of radial glial fate. *Cell*, *153*(3), 535–549. https://doi.org/10.1016/j.cell.2013.03.027

Stepniewska, I., Preuss, T. M., & Kaas, J. H. (2007). Thalamic connections of the dorsal and ventral premotor areas in New World owl monkeys. *Neuroscience*, *147*(3), 727–745. https://doi.org/10.1016/j.neuroscience.2007.03.054

Strambio-De-Castillia, C., Niepel, M., & Rout, M. P. (2010). The nuclear pore complex: Bridging nuclear transport and gene regulation. *Nature Reviews Molecular Cell Biology*, *11*(7), 490–501. https://doi.org/10.1038/nrm2928

Subramanian, A., Tamayo, P., Mootha, V. K., Mukherjee, S., Ebert, B. L., Gillette, M. A., Paulovich, A., Pomeroy, S. L., Golub, T. R., Lander, E. S., & Mesirov, J. P. (2005). Gene set enrichment analysis: A knowledge-based approach for interpreting genome-wide expression profiles. *Proceedings of the National Academy of Sciences of the United States of America*. https://doi.org/10.1073/pnas.0506580102

Sultan, K. T., & Shi, S. (2018). Generation of diverse cortical inhibitory interneurons. *Wiley Interdisciplinary Reviews: Developmental Biology*, *7*(2), e306.

Suzuki, I. K., & Hirata, T. (2013). Neocortical neurogenesis is not really "neo": A new evolutionary model derived from a comparative study of chick pallial development. *Development Growth and Differentiation*, *55*(1), 173–187. https://doi.org/10.1111/dgd.12020

Tanaka, H., Yamashita, T., Asada, M., Mizutani, S., Yoshikawa, H., & Tohyama, M. (2002). Cytoplasmic p21Cip1/WAF1 regulates neurite remodeling by inhibiting Rho-kinase activity. *Journal of Cell Biology*, *158*(2), 321–329. https://doi.org/10.1083/jcb.200202071

Tarui, T., Takahashi, T., Nowakowski, R. S., Hayes, N. L., Bhide, P. G., & Caviness, V. S. (2005). Overexpression of p27Kip1, probability of cell cycle exit, and laminar destination of neocortical neurons. *Cerebral Cortex*, *15*(9), 1343–1355. https://doi.org/10.1093/cercor/bhi017

Taverna, E., Götz, M., & Huttner, W. B. (2014). The Cell Biology of Neurogenesis: Toward an Understanding of the Development and Evolution of the Neocortex. In *Annual Review of Cell and Developmental Biology* (Vol. 30, Issue 1). https://doi.org/10.1146/annurev-cellbio-101011-155801

Toda, T., Hsu, J. Y., Linker, S. B., Hu, L., Schafer, S. T., Mertens, J., Jacinto, F. V, Hetzer, M. W., & Gage, F. H. (2017). Nup153 interacts with Sox2 to enable bimodal gene regulation and maintenance of neural progenitor cells. *Cell Stem Cell*, *21*(5), 618–634.

Tong, M., Jun, T., Nie, Y., Hao, J., & Fan, D. (2019). The role of the SLIT/Robo signaling pathway. *Journal of Cancer*, *10*(12), 2694–2705. https://doi.org/10.7150/jca.31877

Torii, M., Hashimoto-Torii, K., Levitt, P., & Rakic, P. (2009). Integration of neuronal clones in the radial cortical columns by EphA and ephrin-A signalling. *Nature*, *461*(7263), 524–528. https://doi.org/10.1038/nature08362

Tosches, M. A., Yamawaki, T. M., Naumann, R. K., Jacobi, A. A., Tushev, G., & Laurent, G. (2018). Evolution of pallium, hippocampus, and cortical cell types revealed by single-cell transcriptomics in reptiles. *Science*, *360*(6391), 881–888. https://doi.org/10.1126/science.aar4237

Trapnell, C., Cacchiarelli, D., Grimsby, J., Pokharel, P., Li, S., Morse, M., Lennon, N. J., Livak, K. J., Mikkelsen, T. S., & Rinn, J. L. (2014). The dynamics and regulators of cell fate decisions are revealed by pseudotemporal ordering of single cells. *Nature Biotechnology*, *32*(4), 381–386. https://doi.org/10.1038/nbt.2859

Tsai, L. H., & Gleeson, J. G. (2005). Nucleokinesis in neuronal migration. *Neuron*, *46*(3), 383–388. https://doi.org/10.1016/j.neuron.2005.04.013

Tury, A., Mairet-Coello, G., & Dicicco-Bloom, E. (2011). The cyclin-dependent kinase inhibitor p57Kip2 regulates cell cycle exit, differentiation, and migration of embryonic cerebral cortical precursors. *Cerebral Cortex*, *21*(8), 1840–1856. https://doi.org/10.1093/cercor/bhq254

Tzika, A. C., Helaers, R., Schramm, G., & Milinkovitch, M. C. (2011). Reptilian-transcriptome v1.0, a glimpse in the brain transcriptome of five divergent Sauropsida lineages and the phylogenetic position of turtles. *EvoDevo*, *2*(1). https://doi.org/10.1186/2041-9139-2-19

Vaage, S. (1969). The segmentation of the primitive neural tube in chick embryos (Gallus domesticus). A morphological, histochemical and autoradiographical investigation. *Ergebnisse Der Anatomie Und Entwicklungsgeschichte*, *41*(3), 3–87.

Vaid, S., & Huttner, W. B. (2020). Transcriptional regulators and human-specific/primate-specific genes in neocortical neurogenesis. *International Journal of Molecular Sciences*, *21*(13), 1–19. https://doi.org/10.3390/ijms21134614

Vasilj, A., Gentzel, M., Ueberham, E., Gebhardt, R., & Shevchenko, A. (2012). Tissue proteomics by one-dimensional gel electrophoresis combined with label-free protein quantification. *Journal of Proteome Research*, *11*(7), 3680–3689. https://doi.org/10.1021/pr300147z

Vitalis, T., & Rossier, J. (2011). New insights into cortical interneurons development and classification: Contribution of developmental studies. *Developmental Neurobiology*, *71*(1), 34–44. https://doi.org/10.1002/dneu.20810

Walther, T. C., Alves, A., Pickersgill, H., Loïodice, I., Hetzer, M., Galy, V., Hülsmann, B. B., Köcher, T., Wilm, M., Allen, T., Mattaj, I. W., & Doye, V. (2003). The conserved Nup107-160 complex is critical for nuclear pore complex assembly. *Cell*, *113*(2), 195–

206. https://doi.org/10.1016/S0092-8674(03)00235-6

Wandke, C., & Kutay, U. (2013). Enclosing chromatin: Reassembly of the nucleus after open mitosis. *Cell*, *152*(6), 1222–1225. https://doi.org/10.1016/j.cell.2013.02.046

Wang, B., Xiao, Y., Ding, B. B., Zhang, N., Yuan, X. Bin, Gui, L., Qian, K. X., Duan, S., Chen, Z., Rao, Y., & Geng, J. G. (2003). Induction of tumor angiogenesis by Slit-Robo signaling and inhibition of cancer growth by blocking Robo activity. *Cancer Cell*, *4*(1), 19–29. https://doi.org/10.1016/S1535-6108(03)00164-8

Waterston, R. H., Lindblad-Toh, K., Birney, E., Rogers, J., Abril, J. F., Agarwal, P., Agarwala, R., Ainscough, R., Alexandersson, M., An, P., Antonarakis, S. E., Attwood, J., Baertsch, R., Bailey, J., Barlow, K., Beck, S., Berry, E., Birren, B., Bloom, T., … Lander, E. S. (2002). Initial sequencing and comparative analysis of the mouse genome. *Nature*, *420*(6915), 520–562. https://doi.org/10.1038/nature01262

Whitford, K. L., Marillat, V., Stein, E., Goodman, C. S., Tessier-Lavigne, M., Chédotal, A., & Ghosh, A. (2002). Regulation of cortical dendrite development by Slit-Robo interactions. *Neuron*, *33*(1), 47–61. https://doi.org/10.1016/S0896-6273(01)00566-9

Wilkinson, G., Dennis, D., & Schuurmans, C. (2013). Proneural genes in neocortical development. *Neuroscience*, *253*, 256–273. https://doi.org/10.1016/j.neuroscience.2013.08.029

Wills, Z., Emerson, M., Rusch, J., Bikoff, J., Baum, B., Perrimon, N., & Van Vactor, D. (2002). A Drosophila homolog of cyclase-associated proteins collaborates with the Abl tyrosine kinase to control midline axon pathfinding. *Neuron*, *36*(4), 611–622. https://doi.org/10.1016/S0896-6273(02)01022-X

Wong, K., Ren, X. R., Huang, Y. Z., Xie, Y., Liu, G., Saito, H., Tang, H., Wen, L., Brady-Kalnay, S. M., Mei, L., Wu, J. Y., Xiong, W. C., & Rao, Y. (2001). Signal transduction in neuronal migration: roles of GTPase activating proteins and the small GTPase Cdc42 in the Slit-Robo pathway. *Cell*, *107*(2), 209–221. https://doi.org/10.1016/s0092-8674(01)00530-x

Wong, L., Weadick, C. J., Kuo, C., Chang, B. S., & Tropepe, V. (2010). Duplicate dmbx1 genes regulate progenitor cell cycle and differentiation during zebrafish midbrain and retinal development. *BMC Developmental Biology*, *10*, 1–24. https://doi.org/10.1186/1471-213X-10-100

Woodhead, G. J., Mutch, C. A., Olson, E. C., & Chenn, A. (2006). *Cell-Autonomous* - *Catenin Signaling Regulates Cortical Precursor Proliferation*. *26*(48), 12620–12630. https://doi.org/10.1523/JNEUROSCI.3180-06.2006

Yang, L., & Bashaw, G. J. (2006). Son of Sevenless Directly Links the Robo Receptor to Rac Activation to Control Axon Repulsion at the Midline. *Neuron*, *52*(4), 595–607. https://doi.org/10.1016/j.neuron.2006.09.039

Yao, Z., van Velthoven, C. T. J., Nguyen, T. N., Goldy, J., Sedeno-Cortes, A. E., Baftizadeh, F., Bertagnolli, D., Casper, T., Chiang, M., Crichton, K., Ding, S. L., Fong, O., Garren, E., Glandon, A., Gouwens, N. W., Gray, J., Graybuck, L. T., Hawrylycz, M. J., Hirschstein, D., … Zeng, H. (2021). A taxonomy of transcriptomic cell types across the isocortex and hippocampal formation. *Cell*, *184*(12), 3222-3241.e26.

https://doi.org/10.1016/j.cell.2021.04.021

Yoon, K., & Gaiano, N. (2005). *Notch signaling in the mammalian central nervous system : insights from mouse mutants*. *8*(6), 709–715. https://doi.org/10.1038/nn1475

Ypsilanti, A. R., Zagar, Y., & Chédotal, A. (2010). Moving away from the midline: New developments for Slit and Robo. *Development*, *137*(12), 1939–1952. https://doi.org/10.1242/dev.044511

Zheng, W., Geng, A. Q., Li, P. F., Wang, Y., & Yuan, X. B. (2012). Robo4 regulates the radial migration of newborn neurons in developing neocortex. *Cerebral Cortex*, *22*(11), 2587–2601. https://doi.org/10.1093/cercor/bhr330

Zheng, X., Boyer, L., Jin, M., Mertens, J., Kim, Y., Ma, L., Ma, L., Hamm, M., Gage, F. H., & Hunter, T. (2016). Metabolic reprogramming during neuronal differentiation from aerobic glycolysis to neuronal oxidative phosphorylation. *ELife*, *5*(JUN2016), 1–25. https://doi.org/10.7554/eLife.13374

Zuccolo, M., Alves, A., Galy, V., Bolhy, S., Formstecher, E., Racine, V., Sibarita, J. B., Fukagawa, T., Shiekhattar, R., Yen, T., & Doye, V. (2007). The human Nup107-160 nuclear pore subcomplex contributes to proper kinetochore functions. *EMBO Journal*, *26*(7), 1853–1864. https://doi.org/10.1038/sj.emboj.7601642

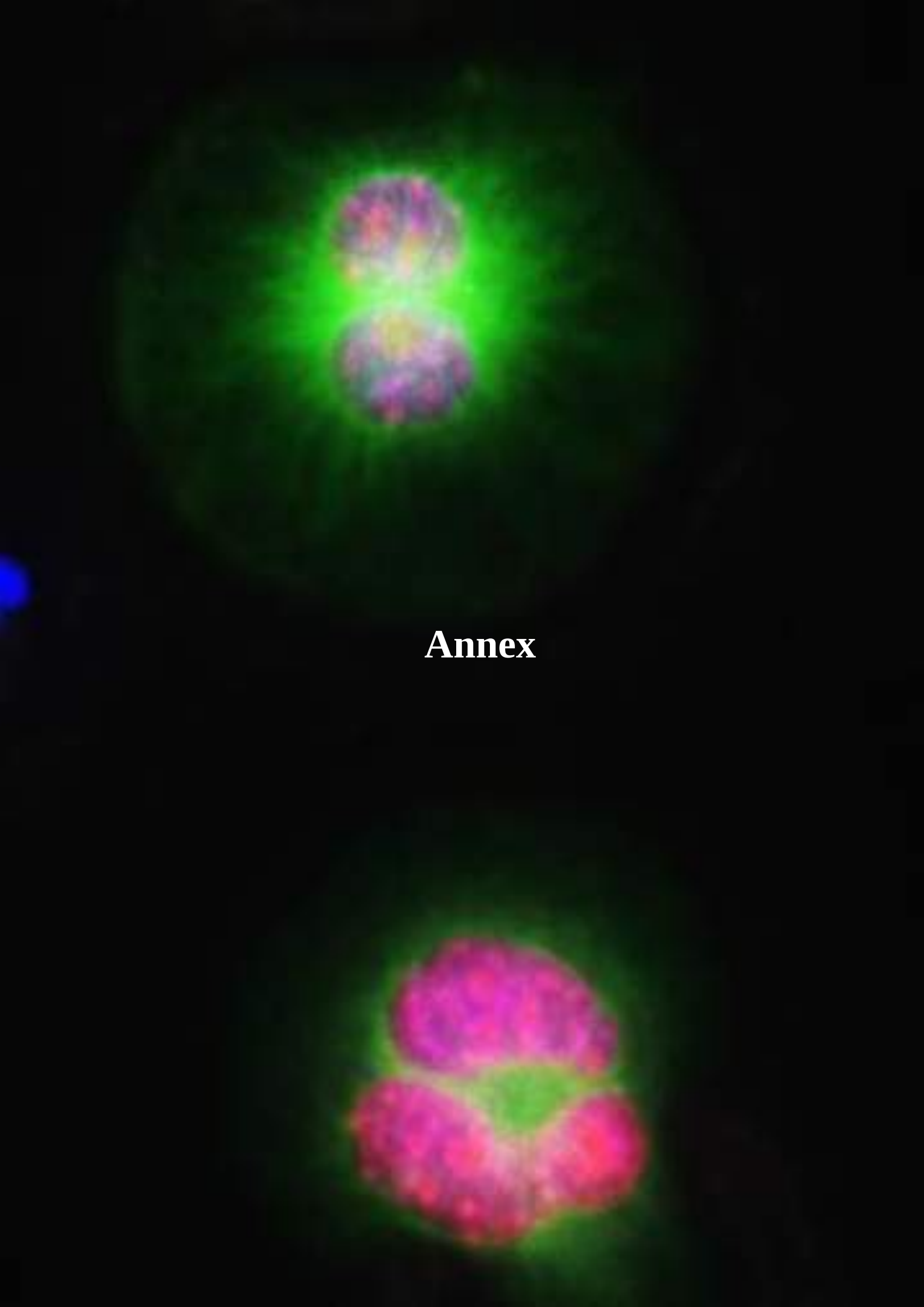

Annex

frontiers in Cell and Developmental Biology

REVIEW
published: 03 December 2020doi: 10.3389/fcell.2020.604448

The Extracellular Matrix in the Evolution of Cortical Developmentand Folding

*Salma Amin and Víctor Borrell**

Instituto de Neurociencias, Consejo Superior de Investigaciones Científicas and Universidad Miguel Hernández, Sant Joand'Alacant, Spain

The evolution of the mammalian cerebral cortex leading to humans involved a remarkable sophistication of developmental mechanisms. Specific adaptations of progenitor cell proliferation and neuronal migration mechanisms have been proposedto play major roles in this evolution of neocortical development. One of the central elements influencing neocortex development is the extracellular matrix (ECM). The ECM provides both a structural framework during tissue formation and to present signaling molecules to cells, which directly influences cell behavior and movement. Here we review recent advances in the understanding of the role of ECM molecules on progenitor cell proliferation and neuronal migration, and how these contribute to cerebral cortex expansion and folding. We discuss how transcriptomic studies in human, ferret and mouse identify components of ECM as being candidate key players in cortex expansion during development and evolution. Then we focus on recent functional studies showing that ECM components regulate cortical progenitor cell proliferation, neuron migration and the mechanical properties of the developing cortex. Finally, we discuss how these features differ between lissencephalic and gyrencephalic species, and how the molecular evolution of ECM components and their expression profiles may have been fundamental in the emergence and evolution of cortex folding across mammalian phylogeny.

Keywords: radial glia, gene expression, microenvironment, folding, evolutionary conservation, extracellular matrix

OPEN ACCESS

Edited by:
Mitsugu Fujita,Kindai University, Japan

Reviewed by:
Wieland B. Huttner,Max Planck Institute of Molecular CellBiology and Genetics, Max Planck Society (MPG), Germany
Hiroshi Kawasaki,Kanazawa University, Japan
Linda J. Richards,The University of Queensland, Australia

**Correspondence:*
Víctor Borrellvborrell@umh.es

Specialty section: This article was submitted toCell Adhesion and Migration,a section of the journal Frontiers in Cell and Developmental Biology

Received: 09 September 2020
Accepted: 12 November 2020
Published: 03 December 2020

Citation: Amin S and Borrell V (2020) The Extracellular Matrix in the Evolution of Cortical Development and Folding. Front. Cell Dev. Biol. 8:604448. doi: 10.3389/fcell.2020.604448

INTRODUCTION

The largest part of our brain is the cerebral cortex, or neocortex, which is considered the seat for our higher cognitive abilities and complex reasoning. The extraordinary size and complexity of the human cerebral cortex are the result of a sophisticated and exquisitely orchestrated developmental program, which emerged during mammalian evolution. This stemmed from an increase in the number of neuronal and glial cells, followed by a dramatic expansion in cortical size and folding. The selective pressure on these traits was the basis for the evolution of the mammalian cortex towards human (Florio and Huttner, 2014; De Juan Romero and Borrell, 2015). Recent efforts in understanding this remarkable process of mammalian cortex evolution have begun to shed light on key cellular and molecular mechanisms involved.

The neocortex is a large sheet of neural tissue characteristically organized in six main layers of neurons. This sheet may be smooth, typical of mammals with small brains like mice, or three-dimensionally arranged in folds and fissures, typical of mammals with a large brain like primates and carnivores, including human (De Juan Romero et al., 2015; Fernandez et al., 2016). The cerebral cortex originally develops from the early telencephalic primordium, a pseudostratified epithelium with apical-basal polarity composed by neuroepithelial cells (NECs; Götz and Huttner, 2005; Taverna et al., 2014). Cortical neurogenesis begins with the transformation of NECs into apical Radial Glia Cells (aRGCs), the lineage of which gives rise to all excitatory neurons of the neocortex. aRGCs are highly polarized and elongated cells, with an apical process contacting the ventricular surface, a basal process contacting the pial surface, and the cell body in the vicinity of the telencephalic ventricle, which altogether constitute the ventricular zone (VZ; Boulder_Committee, 1970). Similar to NECs, the cell body of aRGCs migrates apico-basally during the distinct phases of the cell cycle, in a movement known as interkinetic nuclear migration (INM). After mitosis at the apical surface, the cell nucleus moves basally during G1, undergoes DNA replication (S phase) at the basal side of the VZ, and moves apically during G2 to undergo mitosis again at the apical surface (Takahashi et al., 1993). aRGCs typically express the paired-box transcription factor Pax6, and may produce neurons either directly upon mitosis, or indirectly via producing Basal Progenitors (BPs; Noctor et al., 2001, 2004; Haubensak et al., 2004; Miyata et al., 2004). BPs generated by aRGCs migrate to the basal border of the VZ, where they coalesce forming the subventricular zone (SVZ) and divide to eventually produce neurons. There are two main types of BPs: intermediate progenitor cells (IPCs), which lack obvious polarity and characteristically express the T-box transcription factor Tbr2; basal radial glia cells (bRGCs), similar to aRGCs with a basal process contacting the pial surface, but without an apical process contacting the ventricle (Haubensak et al., 2004; Miyata et al., 2004; Noctor et al., 2004; Fietz et al., 2010; Hansen et al., 2010; Reillo et al., 2011; Shitamukai et al., 2011). In species with a smooth cortex (lissencephalic) like mouse, the SVZ is relatively thin and contains few BPs, with IPCs being the predominant type. These BPs largely undergo self-consuming neurogenic divisions, producing two neurons each. In contrast, in species with a folded cortex (gyrencephalic), the SVZ contains much larger numbers of BPs and is much thicker, displaying two cytoarchitectonically distinct sublayers: inner (ISVZ) and outer subventricular zone (OSVZ; Smart et al., 2002; Reillo et al., 2011). The high abundance of BPs in gyrencephalic species is largely due to their high potential for self-amplification (Fietzet al., 2010; Hansen et al., 2010; Betizeau et al., 2013). Both ISVZ and OSVZ are rich in bRGCs and IPCs, which after several rounds of self-amplification start producing massive numbers of neurons (Reillo et al., 2011; Betizeau et al., 2013; Martínez-Martínez et al., 2016). Neurogenesis from BPs occurs either by asymmetric self-renewing divisions (producing one neuron and one progenitor), or by terminal symmetric self-consuming divisions (producing two neurons). Thus, the abundance of BPs is ultimately proportional to the final number of cortical neurons and to cortical folding, these parameters being low in lissencephalic and high in gyrencephalic species (Borrell and Reillo, 2012; Betizeau et al., 2013; Pilz et al., 2013; Dehay et al., 2015; Llinares-Benadero and Borrell, 2019).

The extracellular matrix (ECM) is a key part of the cellular microenvironment during cortical development, contributing to define the local niche of the different cell populations. The ECM is formed by a complex combination of structural proteins and proteoglycans that act as a cell-supporting scaffold. However, in addition to this classical concept, recent studies show that the ECM plays fundamental roles in the polarity, survival, proliferation, migration and differentiation of cells (Hynes, 2009). Recent major breakthroughs in transcriptomic and functional analysis of cortical development in both lissencephalic and gyrencephalic species have identified ECM components as key factors regulating the proliferation of specific types of cortical progenitors, with a direct impact on the expansion and folding of the cerebral cortex (Fietz et al., 2012; Florio and Huttner, 2014; Florio et al., 2017; Long et al., 2018; Long and Huttner, 2019).

Here, we review how the expression of ECM components is regulated and patterned during cortical development, across cortical layers and progenitor cell populations, in lissencephalic and gyrencephalic species. Then we elaborate on the impact of the ECM on cortical progenitor cell proliferation and neuronal migration across mammalian phylogeny, and discuss its influence on the mechanical properties of cortical tissue, altogether affecting cortex folding. Finally, we hypothesize that the modification of ECM components and their expression patterns may have been critical to the remarkable expansion and folding of the mammalian neocortex during evolution.

EXPRESSION OF ECM COMPONENTS DURING CORTICAL DEVELOPMENT

Transcriptomic analyses of the developing human, mouse and ferret neocortex have been key to our understanding of the relevance of ECM in cortical development (Fietz et al., 2010, 2012; Camp et al., 2015; De Juan Romero et al., 2015; Florio et al., 2015; Pollen et al., 2015; Martínez- Martínez et al., 2016; Telley et al., 2019). High-throughput bulk RNA sequencing (RNAseq) analyses of isolated cortical germinal layers in mouse and human at mid-neurogenesis highlight that specific sets of ECM components are differentially expressed (Fietz et al., 2012). In human embryos, cortical germinal zones including VZ, ISVZ and OSVZ exhibit higher mRNA expression levels of ECM components and cytoskeletal proteins than the neuronal layer Cortical Plate (CP; **Table 1**). The mouse VZ also has a distinct signature of ECM gene expression, such that these genes are downregulated when progenitor cells are undergoing neurogenesis (Arai et al., 2011). Transcriptomic microarray data from the ferret neocortical VZ also revealed differential expression of ECM components, in this case along cortical developmental stages (**Table 1**; Martínez-Martínez et al., 2016).

Extracellular matrix components are extraordinarily diverse, and many of those expressed in the developing cerebral cortex

TABLE 1 | Differentially expressed extracellular matrix (ECM) components, Integrins, growth factors, and transferases, across lissencephalic, and gyrencephalic species.

ECM Genes		Human NCBI Gene ID	A Human (Fietz et al., 2012)			Mouse (Fietz et al., 2012)		B Ferret (Martínez-Martínez et al., 2016)			C Human cell populations (Florio et al., 2015)	
			hVZ	hISVZ = hOSVZ	hCP	mVZ	mCP	E34VZ-E30VZ	P1VZ-E34VZ	P1VZ-E30VZ	aRG > bRG > N	bRG ≥ aRG > N
Proteoglycans	ACAN	176	–	–	–	–	–	nr	nr	nr		ACAN
	BCAN	63827	–	–	–	–	–	BCAN	BCAN	BCAN	–	–
	BGN	633		BGN				nr	nr	nr	–	–
	DCN	1634					DCN	–	–	DCN	–	–
	HAPLN1	1404	–	–	–	–	–	nr	nr	nr	HAPLN1	
	HAPLN4	404037	HAPLN4					nr	nr	nr	–	–
	NCAN	1463	NCAN					–	NCAN	NCAN	–	–
	LUM	4060	–	–	–	–	–	nr	nr	nr	LUM	
	RELN	5649	–	–	–	–	–	–	–	RELN	–	–
	SCUBE3	222663					SCUBE3	–	–	SCUBE3	–	–
	SPARC	6678	–	–	–	–	–	–	SPARC	–	–	–
	SPARCL1	8404	–	–	–	–	–	–	SPARCL1	–	–	–
	SPOCK1	6695	–	–	–	–	–	–	SPOCK1	SPOCK1	–	–
	SPOCK2	9806	–	–	–	–	–	–	SPOCK2	SPOCK2	–	–
	SUSD1	64420	–	–	–	–	–	–	–	SUSD1	–	–
	VCAN	1462					VCAN	–	VCAN	VCAN	–	–
ECM proteins	ATRN	8455	–	–	–	–	–	–	ATRN	ATRN	–	–
	BMPER	168667				BMPER		nr	nr	nr		BMPER
	CD248	57124		CD248				nr	nr	nr	–	–
	CNTN4	152330			CNTN4			nr	nr	nr	–	–
	COCH	1690			COCH			nr	nr	nr	–	–
	ECM1	1893				ECM1		nr	nr	nr	–	–
	FBLN2	2199				FBLN2		–	FBLN2	FBLN2	–	–
	FBLN5	10516	FBLN5					nr	nr	nr	–	–
	LGALS3	3958	–	–	–	–	–	–	–	LGALS3	–	–
	LGALS8	3964			LGALS8			nr	nr	nr	–	–
	LGALSL	29094	–	–	–	–	–	–	LGALSL	LGALSL	–	–
	LTBP1	4052	–	–	–	–	–	–	LTBP1	–	–	–

(Continued)

TABLE 1 | Continued

ECM Genes		Human NCBI Gene ID	A Human (Fietz et al., 2012)			Mouse (Fietz et al., 2012)		B Ferret (Martínez-Martínez et al., 2016)			C Human cell populations (Florio et al., 2015)	
			hVZ	hISVZ = hOSVZ	hCP	mVZ	mCP	E34VZ-E30VZ	P1VZ-E34VZ	P1VZ-E30VZ	aRG > bRG > N	bRG ≥ aRG > N
	LTBP4	8425	–	–	–	–	–	–	LTBP4	LTBP4	–	–
	MATN2	4147	MATN2					–	MATN2	MATN2	–	–
	MFAP1	4236	–	–	–	–	–	–	MFAP1	MFAP1	–	–
	NTN1	9423		NTN1				nr	nr	nr	–	–
	NTN3	4917					NTN3	nr	nr	nr	–	–
	NTN4	59277				NTN4		nr	nr	nr	–	–
	NTNG1	22854	–	–	–	–	–	–	–	NTNG1	–	–
	PRELP	5549	–	–	–	–	–	nr	nr	nr	PRELP	
	RELN	5649	–	–	–	–	–	–	–	RELN	–	–
	TMEFF2	23671			TMEFF2			nr	nr	nr	–	–
	VIT VWF	5212	–	–		–	–	–	–	VIT	–	–
	COL1A1	7450			VWF			nr	nr	nr	–	–
Collagens	COL2A1	1277	–	–	–	–	–	–	–	COL1A1	–	–
	COL1A2	1280	COL2A1					–	–	COL2A1	–	–
	COL3A1	1278	–	–	–	–	–	nr	nr	nr	COL1A2	
	COL4A1	1281	–	–	–	–	–	–	–	COL3A1	–	–
	COL4A2	1282		COL4A1				–	COL4A1	COL4A1		COL4A1
	COL4A6	1284		COL4A2				nr	nr	nr	–	–
	COL5A2	1288	–	–	–	–	–	–	–	COL4A6	–	–
	COL5A3	1290	–	–	–	–	–	–	–	COL5A2	–	–
	COL8A1	50509	COL5A3					nr	nr	nr	–	–
	COL9A3	1295	–	–	–	–	–	nr	nr	nr		COL8A1
	COL11A1	1299		COL9A3				nr	nr	nr	–	–
	COL11A2	1301	–	–	–	–	–	–	–	COL11A1	–	–
	COL12A1	1302	COL11A2					nrnr	nr	nr	–	–
	COL15A1	1303				COL12A1		–	nr	nr	–	–
	COL16A1	1306				COL15A1		–	–	COL15A1	–	–
	COL17A1	1307	–	–	–	–	–	–	COL16A1	COL16A1	–	–
	COL18A1	1308	–	–	–	–	–	–	COL17A1	COL17A1	–	–
		80781				COL18A1			COL18A1	COL18A1	–	–

(Continued)

TABLE 1 | Continued

ECM Genes		Human NCBI Gene ID	A Human (Fietz et al., 2012)			Mouse (Fietz et al., 2012)		B Ferret (Martínez-Martínez et al., 2016)			C Human cell populations (Florio et al., 2015)	
			hVZ	hISVZ = hOSVZ	hCP	mVZ	mCP	E34VZ-E30VZ	P1VZ-E34VZ	P1VZ-E30VZ	aRG > bRG > N	bRG ≥ aRG > N
	COL21A1	81578	_	_	_	_	_	COL21A1	COL21A1	COL21A1	_	_
	COL22A1	169044	COL22A1					nr	nr	nr	_	_
	COL24A1	255631	_	_	_	_	_	_	COL24A1	COL24A1	_	_
	COL28A1	340267	_	_	_	_	_	nr	nr	nr	COL28A1	
	COLQ	8292	COLQ					nr	nr	nr	_	_
Laminins	LAMA1	284217	_	_	_	_	_	_	_	LAMA1	_	_
	LAMA3	3909	LAMA3					nr	nr	nr	_	_
	LAMA5	3911				LAMA5		nr	nr	nr	_	_
	LAMB1	3912	_	_	_	_	_	_	LAMB1	LAMB1	_	_
	LAMB2	3913	_	_	_	_	_	_	_	LAMB2	_	_
	LAMB4	22798	_	_	_	_	_	nr	nr	nr		LAMB4
	LAMC2	3918	_	_	_	_	_	nr	nr	nr		LAMC2
Integrins	ITGA1	3672		ITGA1				nr	nr	nr	_	_
	ITGA3	3675			ITGA3			nr	nr	nr	_	_
	ITGA5	3678				ITGA5		nr	nr	nr	_	_
	ITGA10	8515				ITGA10		nr	nr	nr	_	_
	ITGB5	3693	_	_	_	_	_	ITGB5	_	_	_	_
Growth Factors	BMP3	651					BMP3	nr	nr	nr	_	_
	CRELD1	78987	_	_	_	_	_	_	CRELD1	_	_	_
	EREG	2069	_	_	_	_	_	nr	nr	nr		EREG
	FGF5	2250	_	_	_	_	_	nr	nr	nr		FGF5
	FGF9	2254	_	_	_	_	_	FGF9	_	_	_	_
	FGF12	2257			FGF12			nr	nr	nr	_	_
	FGF18	8817					FGF18GDF1	nr	nr	nr	_	_
	GDF1	2657					GDF5	nr	nr	nr	_	_
	GDF5	8200						nr	nr	nr	_	_

(Continued)

TABLE 1 | Continued

ECM Genes		Human NCBI Gene ID	A Human (Fietz et al., 2012)			Mouse (Fietz et al., 2012)		B Ferret (Martínez-Martínez et al., 2016)			C Human cell populations (Florio et al., 2015)	
			hVZ	hISVZ = hOSVZ	hCP	mVZ	mCP	E34VZ-E30VZ	P1VZ-E34VZ	P1VZ-E30VZ	aRG > bRG > N	bRG ≥ aRG > N
	IGF2	3481	IGF2					nr	nr	nr	_	_
	INHA	3623					INHA	nr	nr	nr	_	_
	INHBA	3624			INHBA			nr	nr	nr	_	_
	MEGF6	1953		MEGF6				nr	nr	nr	_	_
	MEGF8	1954	_	_	_	_	_	_	_	MEGF8	_	_
	MEGF10	84466	_	_	_	_	_	_	MEGF10	_	_	_
	MSTN	2660	MSTN					nr	nr	nr	_	_
	PDGFA	5154			PDGFA			nr	nr	nr	_	_
	PDGFB	5155			PDGFB			nr	nr	nr	_	_
	PDGFC	56034				PDGFC		nr	nr	nr	_	_
	PDGFRA	5156			PDGFRA			nr	nr	nr	_	_
	TGFA	7039				TGFA		nr	nr	nr	_	_
	TGFB3	7043				TGFB3		nr	nr	nr	_	_
	TMEFF2	23671			TMEFF2			_	_	TMEFF2	_	_
	VEGFC	7424				VEGFC		nr	nr	nr	_	_
Transferase	CHPF	79586	CHPF					nr	nr	nr	_	_
	CHSY3	337876			CHSY3			nr	nr	nr	_	_
	HS2ST1	9653				HS2ST1		nr	nr	nr	_	_
	HS6ST1	9394					HS6ST1	nr	nr	nr	_	_
	NDST1	3340				NDST1		nr	nr	nr	_	_
	NDST2	8509				NDST2		nr	nr	nr	_	_
	ST3GAL2	6483			ST3GAL2			nr	nr	nr	_	_
	SULF1	23213	SULF1					nr	nr	nr	_	_
	SULT1B1	27284	_	_	_	_	_	nr	nr	nr		SULT1B1
	SULT1C2	6819	_	_	_	_	_	nr	nr	nr		SULT1C2
	SULT1C4	27233	_	_	_	_	_	nr	nr	nr	SULT1C4	

(A) Genes differentially expressed between cortical layers in human and mouse (Fietz et al., 2012). The gene name is indicated where it is expressed at significantly higher levels compared to the other layers; (-) means no significant difference. (B) Genes differentially expressed between embryonic (E) and postnatal (P) cortical Ventricular Zone (VZ) in ferret (Martínez-Martínez et al., 2016). The gene name is indicated whereit is differentially expressed; (−), no significant difference; (nr), not reported. (C) Genes differentially expressed between specific cell populations of the developing human cortex (Florio et al., 2015). The gene name is indicated in the comparison where it is differentially expressed; (−), no significant difference.

are polyvalent in regulating stem cell proliferation and niche maintenance (Fietz et al., 2010; Marthiens et al., 2010; Stenzel et al., 2014; Güven et al., 2020). Each mammalian species expresses in cortical germinal zones a unique combination of ECM components at unique relative levels, which suggests that their precise abundance and overall combined composition may be important in fine-tuning cortical progenitor proliferation, self-renewal and expansion, which are also unique among species. In the human OSVZ, very rich in highly proliferative BPs, specific ECM components are expressed at high levels (**Table 1**). A landmark study by Florio et al. (2015) compared thetranscriptomic profile of isolated aRGCs, bRGCs and neurons in the developing human and mouse cerebral cortex. This analysis revealed that ECM components and cell surface receptors were more highly expressed in human aRGCs and bRGCs than in mouse, pointing to the notion that these components may influence the proliferation of aRGCs and bRGCs in human versus mouse (Florio et al., 2015, 2016, 2017). Hence, a notion emerges that each species, either lissencephalic or gyrencephalic, elaborates its own ECM niche in germinal zones to implement the particular proliferative and neurogenic program for their unique set of progenitor cell composition, thus contributing to species differences in cortical development. Accordingly, changes in the expression of ECM components strongly regulate cortical progenitor proliferation and may have been central in the evolutionary expansion of the human neocortex (Fietz et al., 2012). Importantly, germinal zones appear to be a reservoir of ECM components. For example, HAPLN1 and collagen I mRNAs are expressed at high levels in human germinal zones (**Table 1**), but at the protein level these are concentrated in the CP and cortical wall. This shows that germinal zones are the site of transcription of these genes, but the proteins they encode are only active at the CP and cortical wall (Long et al., 2018).

One of the most salient features of mammalian cortex evolution is its folding. Transcriptomic studies in ferret have shed light on the genetic basis of cortex folding, which also appears to be strongly influenced by the ECM. By comparingthe transcriptomic profile of the cortical germinal zones prospectively forming the Splenial Gyrus and the Lateral Sulcus in the ferret visual cortex, we discovered a large number of genes differentially expressed between these two regions, including genes that encode for cell adhesion molecules and ECM components (De Juan Romero et al., 2015). This analysis also showed that the largest amount of differentially expressed genes, and the greatest differences in expression levels between prospective gyrus and sulcus, occur at the OSVZ, further supporting the central importance of this germinal layer in the differential expansion and folding of the cerebral cortex. This pioneer notion has been substantiated experimentally by, forexample, the disruption of Integrin receptor function in the OSVZ of ferret organotypic cortical slices (Fietz et al., 2010). The loss of function of Integrin $\alpha v\beta 3$ caused a significant reduction in the abundance of bRGCs, but not IPCs. This indicates that ECM components specifically enhance the amplification of bRGCs and, consequently, promote the expansion of the OSVZ andcortex folding (Fietz et al., 2010; De Juan Romero et al., 2015; Dehay et al., 2015).

Single cell RNA sequencing (scRNAseq) revolutionized the field of transcriptomic analysis by providing a snapshot of cell diversity. scRNAseq has been extensively used to characterize the developing cerebral cortex in a variety of mammals, from mouse to human, and newly emerged *in vitro* experimental models such as cerebral organoids (Camp et al., 2015; Pollen et al., 2015; Arlotta and Pasca, 2019; Kanton et al., 2019; Telley et al., 2019; Bhaduri et al., 2020). Aiming to identify the transcriptomic changes that caused the evolutionary expansionof the neocortex, studies have compared aRGCs and bRGCs in human and mouse. Findings highlight ECM genes as a correlate with the high proliferative activity of RGCs in human and ferret as compared to mouse (Lui et al., 2014; Johnson et al., 2015; Pollen et al., 2015). For example, human bRGCs have higher expression levels of ECM genes than mouse, including Laminin, Tenascins, and Integrins, along with HOPX, PTPRZ1, and other genes that modulate the interaction between ECM components, self-renewal of progenitor cells and migration of neurons (Pollen et al., 2015). ScRNAseq analyses have also revealed that RGCs possess unique typological and temporal transcriptomic profiles, distinguishing lineages between the dorsoventral and the rostrocaudal telencephalon. Accordingly, the well-known topographic differences and gradients of development in the telencephalon have been proposed to result from the existence of spatially patterned transcriptomic programs (Nowakowski et al., 2017). Similarly, during development of the mouse somatosensory cortex aRGCs gradually switch from proliferation to neurogenesis, and this appears to be evolutionarily conserved, as it is largely recapitulated inembryonic human aRGCs (Telley et al., 2019). This temporal and spatial change in the transcriptomic profile of progenitor cells during cortical development is linked to ECM components and microenvironmental cues, suggesting that they may have a relevant impact on neurogenesis and cortical patterning.

Recently, cerebral organoids have emerged as a valid *in vitro* model to study cortical development in diverse species (Lancasteret al., 2013; Lancaster and Knoblich, 2014; Camp et al., 2015; Qian et al., 2019; Velasco et al., 2019; Bhaduri et al., 2020). Accordingly, scRNAseq studies comparing progenitor cell populations in human fetal tissue and cerebral organoids have shown that aRGC populations express similar ECM components in both systems (Camp et al., 2015). Interestingly, scRNAseq in human and chimpanzee organoids uncovered subtle differences in the expression levels of genes encoding ECM components and cell adhesion molecules. Given the relevance of differences between human and chimpanzee to understand human evolution, even these small variations in the transcriptomic profiles and signaling pathways of cortical progenitor cells may be key in understanding the evolution and expansion of the human brain (Pollen et al., 2015, 2019; Mora-Bermudez et al., 2016).

ECM AND PROLIFERATION OF NEURAL PROGENITOR CELLS

The ECM plays many roles during neural development, from the formation of a meshwork for structural support, to the activation

of signaling pathways that stimulate progenitor proliferation, either directly or indirectly (Barros et al., 2011). Prior to the onset of neurogenesis, NECs in the cortical primordium augment their number by self-amplification via symmetric divisions (Miyataet al., 2010; Fernandez et al., 2016). Already at that early stage, the ECM provides the microenvironment necessary to modulate the behavior of NECs (Perris and Perissinotto, 2000; Zimmermann and Dours-Zimmermann, 2008). The developing cortex exhibits high concentration of extracellular matrix molecules, including chondroitin sulfate (CS) and heparan sulfate (HS) proteoglycans, hyaluronic acid (HA), Laminins, and glycoproteins like Tenascins (Maeda, 2015). Proteoglycans have an influential role on the proliferation of NECs. These are complex macromolecules composed of a central core with sulphated glycosaminoglycan (GAG) and O- or N-oligosaccharides covalently linked. There are four types of GAGs: CS, dermatan sulfate (DS), Heparin and HS; Schwartz and Domowicz, 2018). Heparan sulfate proteoglycans (HSPGs) include Syndecans, Glypicans, Agrin, and Perlecan (Sarrazin et al., 2011). Glypican is abundant in the cortical VZ during neurogenesis. Mouse embryos mutant for Glypican 1have an imbalance between proliferation and differentiation of NECs during one day of embryonic development (E8.5-9.5), which is sufficient to cause a significant reduction in brain size (**Figure 1**). At the signaling level, this reduction is due to the suppression of fibroblast growth factor signaling (FGF; Jen et al., 2009). The evolutionary conservation of the role of Glypican on NECs, and its relationship with FGF signaling, is evident in *Drosophila*, where it has been linked to organ development (Crickmore and Mann, 2007), and in *Xenopus* embryos, where Glypican 4 regulates dorsal forebrain development via FGF signaling activation (Galli et al., 2003).

Perlecan is an ECM component of the basement membrane important for both structural support and NEC proliferation (**Figure 1**). Mouse embryos mutant for Perlecan exhibit either exencephaly or microcephaly, the latter caused by a reduction in progenitor cell proliferation and impaired cell cycle progression. This phenotype results from a reduced dispersion of growth factors in the extracellular space mediated by Perlecan, such as FGF or SHH (Girós et al., 2007). Perlecan is also highly conserved, where the mutation of its *Drosophila* homolog *trol* leads to G1 cell cycle arrest, mediated by FGF and hedgehog (Hh) signaling (Park et al., 2003).

Syndecan-1 (Sdc1) is a transmembrane HSPG highly enriched in the cortical VZ. Knockdown of *Sdc1* in the developing mouse cortex led to a reduction in NEC proliferation and premature differentiation, accompanied by a reduction in ß-catenin. This suggests a possible implication of Sdc1 in regulating Wnt signaling (Wang et al., 2012; **Figure 1**). Another subclass of proteoglycan that plays a prominent role in NEC proliferation is chondroitin sulfate proteoglycans (CSPGs), which include the Lectican family (Brevican, Neurocan, Versican, and Aggrecan), Phosphacan, CD44 and the transmembrane component NG2 (Maeda, 2015). Previous studies have shown that depletion of CSPGs in mouse neurospheres *in vitro*, bymeans of the CSPG degrading enzyme Chondroitinase ABC, leads to a decrease in proliferation of NECs (Sirko et al., 2007). Intriguingly, a similar treatment with Chondroitinase ABC of rat neurospheres increased NEC proliferation and differentiation, indicating some functional divergence in this respect across species (Gu et al., 2009).

Laminins are a major class of ECM components with a role in cortical progenitor proliferation. Laminins are trimeric proteins composed of alpha, beta, and gamma subunits. They are expressed at high levels in stem cell niches like the VZ and SVZ, and are a major component of the VZ's apical surface (Lathia et al., 2007; Hall et al., 2008; Nirwane and Yao, 2019). Laminins exert their function by binding to Integrin and non- Integrin receptors, which transduce the Laminin signal in and out of the cell (Nirwane and Yao, 2019). *In vitro* studies illustrate that Laminin has an effect on expansion, maintenance and differentiation of mouse and human cortical progenitor cells (Drago et al., 1991; Kearns et al., 2003; Flanagan et al., 2007). Interestingly, enhanced expression of *Integrin-β1* in NECs of chick embryos led to two very distinct phenomena (Long et al., 2016). On the one hand, the generation of a population of cells that resemble subapical progenitors (SAPs) described in mouse (Pilz et al., 2013), dividing in the VZ away from the apical surface and producing IPCs. On the other hand, a non-cell autonomous effect where non-Integrin expressing cells undergo greater levels of neurogenesis driven by Wnt signaling and an increase in *Decorin* expression (Long et al., 2016). Because *Decorin* is only expressed in the OSVZ of the Human cortex (Fietz et al., 2012), this result further supports the notion thatthe ECM was key in the evolution of the mammalian cortex by enhancing the proliferation of progenitor cells and promoting cortical expansion and folding. So the next question regarding Laminins is: ¿how is their expression controlled during cortical development? A recent study reports that knock out of *Sox9* in thedeveloping ferret cortex leads to a reduction in the proliferation of IPCs and bRGCs in the OSVZ. Conversely, conditional overexpression of *Sox9* in the embryonic mouse cortex leads to anincrease in the proliferation of BPs, increased cell cycle re-entry and premature gliogenesis (**Figure 1**). In the long term, *Sox9* overexpression in mouse leads to an increase in the production of upper layer neurons, a hallmark of evolutionary cortical expansion. Importantly, *Sox9* overexpression in mouse cortex was accompanied by increased expression of ECM components, where Laminin 211 was the key in promoting BP proliferation (Güven et al., 2020).

Extracellular matrix components also influence the INM of NECs and aRGCs. Zebrafish *tab* mutants (analogue of *Laminin γ1*) exhibit abnormal INM in the neural tube, with nuclei entering mitosis prior to reaching the apical domain (Tsuda et al., 2010). Similarly, blockade of the β1-Integrin receptor in the VZ leads to detachment of aRGCs and affects INM and the cleavage plane of VZ progenitor cells (**Figure 1**; Lathiaet al., 2007; Loulier et al., 2009). These studies confirm the key and evolutionarily conserved influence of Laminins and their receptors on progenitor proliferation and cortical development.

The basement membrane, produced by the meningeal membranes, is crucial for the survival of RGCs. Loss of *Integrin-β1* in aRGCs of the developing mouse cortex leads to the detachment of their end feet, followed by apoptosis. This detachment is recapitulated by surgical removal of the meninges,

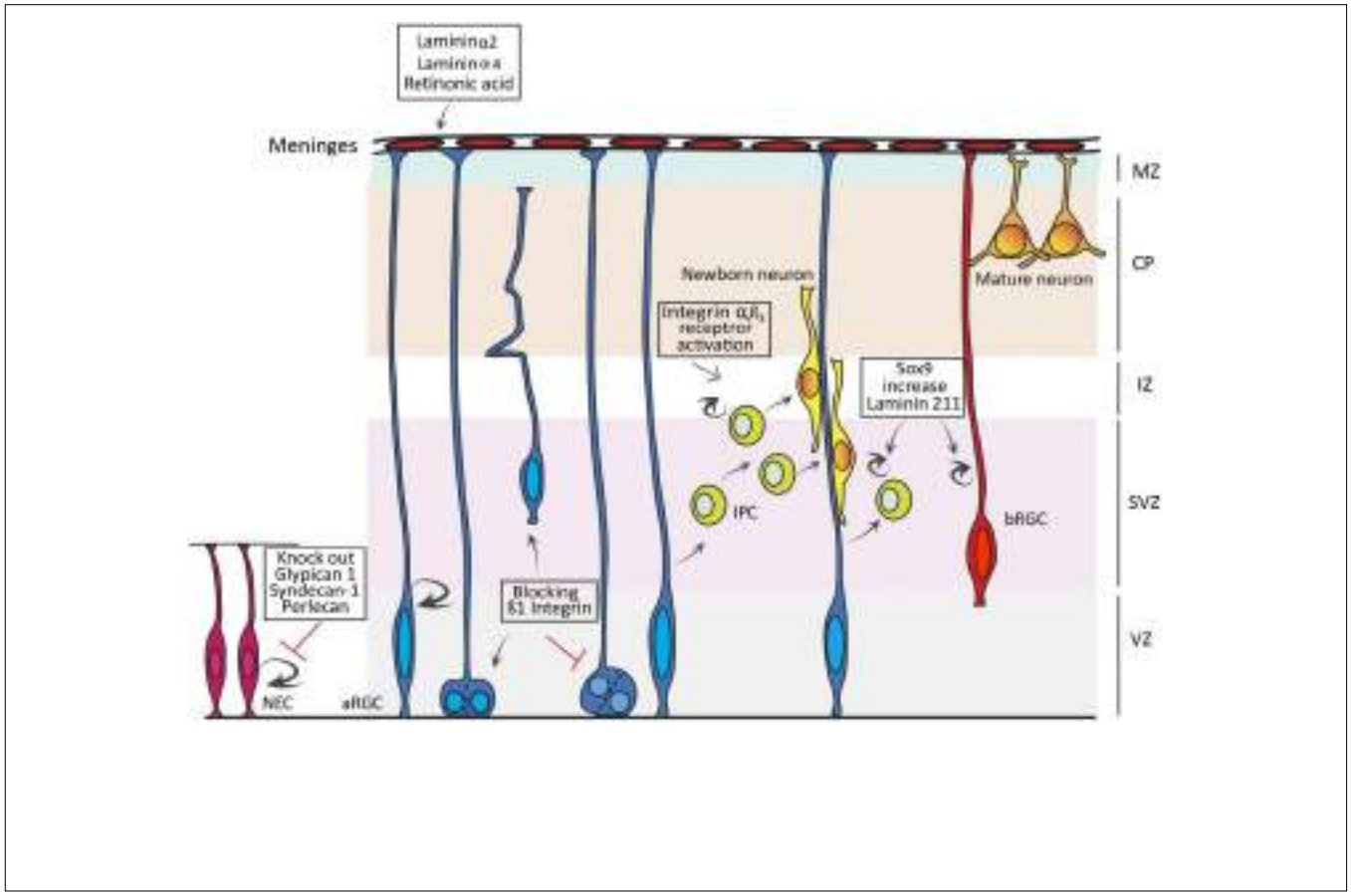

and in mice lacking *Laminin α2* and *4* in their basement membrane (**Figure 1**; Radakovits et al., 2009). Furthermore, mutant mice with disrupted meningeal development exhibit an expansion of NECs in detriment of IPC production and neurogenesis (Siegenthaler et al., 2009). This phenotype was rescued with retinoic acid (RA) treatment, showing the importance of the factors secreted from the meninges for propagating a normal neurogenesis (Siegenthaler et al., 2009).

The concept that the self-renewal capacity of cortical progenitors is the driving force for cortical expansion during evolution, where gyrencephalic species have a larger capital of NECs underlying the generation of more aRGCs, IPs and bRGCs, and subsequently more neurons, has been supported experimentally (Florio and Huttner, 2014; Fernandez et al., 2016). Integrin $\alpha v\beta 3$ is expressed at particularly high levels in human OSVZ, where highly proliferative bRGCs are abundant. Inhibition of Integrin $\alpha v\beta 3$ signaling in species endowed with abundant bRGCs, including human and ferret, decreases proliferation of bRGCs in OSVZ (Fietz et al., 2010; Reillo et al., 2011). Concomitantly, activation of the Integrin $\alpha v\beta 3$ receptor in mouse cortex leads to increased proliferation and cell cycle re-entry of IPs (Stenzel et al., 2014). Altogether, this strongly supports the notion that Integrin modulation of BPs plays an important role in cortical expansion, and that changes in ECM composition during mammalian evolution contributed critically to define the size and complexity of the cerebral cortex, including progenitor cell proliferation, neurogenesis and gliogenesis (Rash et al., 2019).

ECM IN CELL MIGRATION

Extracellular matrix molecules are also involved in regulating neuronal migration during cortical development (Franco and Müller, 2011; Franco et al., 2011). Excitatory cortical neurons travel radially from their place of birth in the germinal layers to their final destination in the CP, in a process known as radial migration (Rakic, 1972; Sidman and Rakic, 1973). In this process, neurons interact intimately with the basal process of aRGCs, known as radial glial fiber, which serves as guide and physical substrate for neuronal migration (Rakic, 1972; Sidman and Rakic, 1973). Thus, radial neuron migration depends on the integrity of RGCs, the actual movement of neurons, and the interaction between the two. Defects in neuron radial migration usually involve delayed or excessive migration, and lead to neuronal miss positioning and disorganization of cortical layers, direct causes of malformation of cortical development (Fernandez et al., 2016). Classically, studies of neuron radial migration have focused on intrinsic or cell-autonomous functions of candidate genes. However, radial neuron migration is also influenced by multiple non-cell autonomous signals, ranging from diffusible molecules to ECM proteins, and cell-cell interactions. This section mainly

focuses on the role of ECM components as primary non-cell autonomous factors that affect radial neuron migration.

Preservation of RGCs and the Basement Membrane

Radial neuron migration in the cerebral cortex depends on the integrity of RGCs, including the attachment of their basal process to the basement membrane, where ECM components are highly expressed. Laminins are critical for the structural integrity of the basement membrane, and patients with mutations in *Laminin beta-1* (*LAMB1*) develop cobblestone-lissencephaly. This is a neuronal migration disorder characterized by the breaching of the basement membrane, causing the detachment of the basal end-feet of aRGCs followed by the over migration of neurons, the loss of cortex folding and the acquisition of a bulgy appearance of the cortical surface (Timpl and Rohde, 1979; Radmanesh et al., 2013). Similarly, mutant mice deficient in *Laminin γ1III4* and *Perlecan* have severe defects on basement membrane integrity and neuron migration (Haubst et al., 2006), developing neuronal ectopias typical of cortical cobblestone (**Figure 2**).

Dystroglycan is another ECM component with an important role in neuron migration. This is a glycoprotein key in the dystrophin glycoprotein complex, which binds to α-Dystroglycan, a primary target for O-glycosylation. The Dystrophin glycoprotein complex is important for maintaining the integrity of the basement membrane by ensuring the attachment of the RGC end feet to the pial surface. Patients with genetic mutations resulting in hypoglycosylation of α- Dystroglycan display over-migration abnormalities and other malformations of cortical development (van Reeuwijk et al., 2005). This phenotype is mimicked in *Dag1* mutant mice, where RGCs fibers are truncated and the basement membrane is frequently breached, invaded by multiple cell types forming heterotopias (**Figure 2**; Myshrall et al., 2012).

The integrity of RGCs is also impaired upon the loss of the proteoglycan Syndecan-3 (Hienola et al., 2006) and of Endothelin Converting Enzyme 2 (ECE2; Buchsbaum et al., 2020). Both absence and overexpression of ECE2 in developing mouse embryos and human cerebral organoids lead to apical- basal detachment of RGCs and impaired radial neuron migration, resulting in the ectopic accumulation of neurons within the VZ. These features are typical of periventricular nodular heterotopia (PNH), a cortical malformation formed by clusters of cortical neurons that fail to undergo radial migration properly and accumulate next to the ventricular surface. Proteomic studies analyzing ECE2 mutant human cerebral organoids reveal a significant down regulation of ECM components such as *Laminin*, *Lumican* and six different collagens. These findings highlight the role of ECE2 in regulating the expression of ECM components that are important for normal neuron migration and cortical development (**Figure 2**; Buchsbaum et al.,2020).

Regulation of Neuron Movement

The role of ECM in cortical lamination also extends to a direct influence on migrating neurons. Reelin (Reln) is among the most studied, and yet most poorly understood, ECM molecules. Throughout cortical development, Reln is secreted by Cajal-Retzius (CR) cells in the marginal zone (D'Arcangelo et al., 1995; Alcantara et al., 1998). Reln binds to the VLDLR and/or ApoER2 lipoprotein receptors of target cells, driving the tyrosine phosphorylation of the adaptor protein Dab1 (Rice and Curran, 2001). Reln has been proposed to be a stop signal that instructs the end of radial migration to each new wave of cortical neurons, thus directly organizing the formation of cortical layers in an inside-out manner (older neurons occupy deep layers, newer neurons occupy superficial layers). Mutation of *RELN* leads to Norman-Roberts lissencephaly in humans (Hong et al., 2000) and to the *reeler* phenotype in mice (D'Arcangelo et al., 1995). Both human and mouse mutations disrupt cortical neuron migration, which in *reeler* mice is accentuated by the massive invasion of ectopic neurons into the marginal zone. This led to the suggestion that Reln acts as a "stop" signal to terminate neuronal migration at the cortical marginal zone (**Figure 2**; Curran and D'Arcangelo, 1998; Dulabon et al., 2000; Rice and Curran, 2001). CR cells and Reln have also been shown to be required for maintenance of the integrity of radial glia fibers in mouse (Super et al., 2000; Hartfuss et al., 2003), but this remains under debate as it seems not to be the case in ferret (Schaefer and Juliano, 2008). The sequence of Reln protein is conserved across more than 104 species (Manoharan et al., 2015), and the levels/patterns of expression of *Reln* and *Dab1* during cortical development in turtle, lizard, chicken and mouse are well corresponded with their respective laminar organization. In contrast to the subpial expression of *Reln* in mammals, in lizards it is expressed in a subcortical layer and cortical neurons are positioned in an inverted, outside-in manner. This suggests functional conservation of this extracellular protein in neuronal migration across amniotes. Its relevance in the well-defined laminar organization of the CP in mammals and lizards, as opposed to non-laminar in birds, is considered an example of homoplasy by convergent evolution (Bar et al., 2000).

Malformations of cortical development are also caused by delayed neuronal migration (Ross and Walsh, 2001). Targeted disruption of *Laminin γ1* expression in the cerebral cortex disrupts Integrin and Akt/Gsk-3β signaling, which impairs neuronal migration without affecting cell proliferation and neuronal cell death. The absence of Laminin γ1 – AKT signaling hinders the arrival of migrating neurons to the marginal zone and leads to defective cortical lamination (**Figure 2**; Chenet al., 2009). Neuroglycan C is a member of the family of CSPGs and a downstream interactor of PHF6, an X-linked protein mutated in the intellectual disability disorder Börjeson– Forssman–Lehmann. Loss of Neuroglycan C in mouse embryos leads to radial migration failure during cortical development (**Figure 2**; Zhang et al., 2013). The functional side chains of CSPGs possess a sulphated structure generated by a family of sulphotransferases, several of which are expressed during cortical development. Several sulphotransferases have been shown to play central roles in neuronal migration, by *in utero* electroporation of loss-of-function short hairpin RNAs. Following this manipulation, neuronal migration is

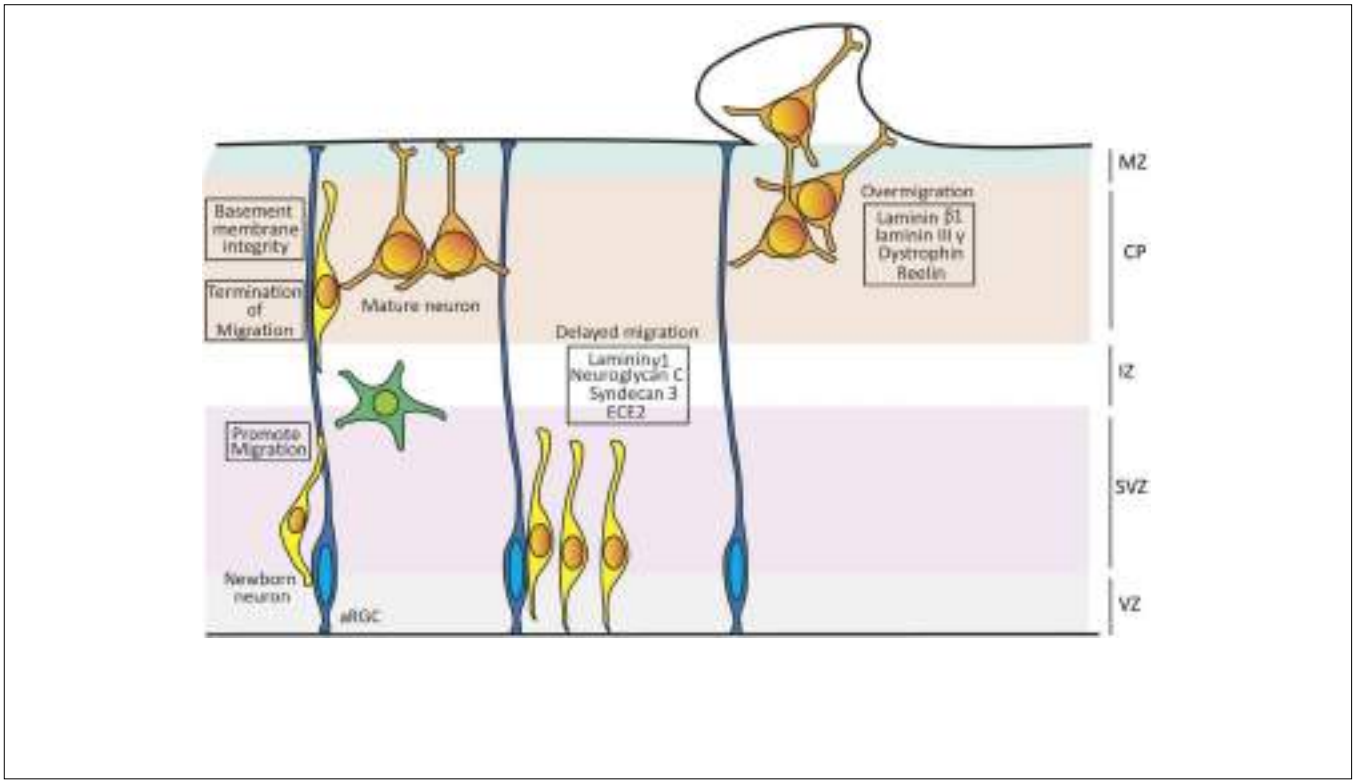

blocked at the multipolar-to-bipolar transition but not at the level of RGCs, suggesting that the specific sulphated side chains play an important role during radial migration (Akita et al., 2008; Ishii and Maeda, 2008). Altogether, it is clear that the ECM is involved in controlling many aspects of cortical neuronal migration, and that this is largely conserved across phylogeny, further supporting the importance of the ECM on the expansion and folding of the cerebral cortex during evolution.

ECM IN CEREBRAL CORTEX FOLDING

As mentioned above, transcriptomic studies have demonstrated that expression of ECM components is very different between cortical layers and species, supporting a process of cortical expansion and folding via progenitor cell proliferation and neuron migration. The ECM also defines the stiffness and biomechanical properties of the developing cortex, thus additionally influencing its folding. Accordingly, changes in ECM composition during mammalian evolution may have dictated the occurrence, degree and pattern of cortex folding across phylogeny (Llinares-Benadero and Borrell, 2019).

ECM in Cortical Expansion

The mechanisms responsible for folding of the mammalian cerebral cortex have been under debate for many years. A nearly attractive hypothesis was that animals with large brains have folded cortices because they undergo a disproportionate expansion of the outer cortical surface (gray matter, composed of neuron) in comparison to the inner part (white matter, composed of axons and glial cells), and this leads to folding of the cortex. Notable exceptions to this trend are represented by the American beaver and the Florida manatee, which have a smooth cortex but brain size similar to other species with a highly folded cortex, such as the chimpanzee (Welker, 1990). A refined version of this hypothesis proposes that cortex folding results from the differential expansion of the upper neuronal layers in comparison to deep cortical layers (Armstrong et al., 1991). The relative expansion of upper layers has been proposed to result from increases in BP abundance and the formation of the OSVZ (Smart et al., 2002; Kriegstein et al., 2006; Reillo et al., 2011; Borrell and Reillo, 2012). In combination with differential neurogenesis, the tangential dispersion of radially migrating neurons in gyrencephalic species is thought to significantly contribute to the expansion of cortical surface and the formation of folds (Borrell, 2018; Llinares-Benadero and Borrell, 2019).

As discussed above, the ECM is a very important factor in the regulation of cortical progenitor cell proliferation, and recent studies support that it is also important in cortex folding. Patients with mutations in *RELN* (see above) display abnormal neuronal migration and axonal connectivity, and in the long term resulting in lissencephaly (loss of cortical folds; Hong et al., 2000). The importance of proper neuron migration for cortical gyrification has been recently highlighted with the analysis of mice mutant for Flrt proteins. Flrts are a family of cell adhesion transmembrane proteins rich in Fibronectin and Leucine repeats, which are involved in the radial migration of cortical neurons. The analysis of mice double mutant for

Flrt1/3 revealed the formation of *bona fide* cortical folds and fissures in the otherwise smooth mouse cortex (del Toro et al., 2017). This phenotype emerges from an imbalance in adhesion-repulsion forces in migrating neurons. Importantly, these experimental results are validated by observations in the normally folded cortex of ferrets, where *Flrt1* and *Flrt3* are expressed at much lower levels in migrating neurons of cortical fissures than folds (De Juan Romero et al., 2015; del Toro et al., 2017).

Influence of the ECM on the Mechanical Properties of Cortex During Folding

Folding of the cerebral cortex is ultimately a physical process of deformation of developing neural tissue (Kroenke and Bayly, 2018). Cortical folding has been described as a mechanism where the differential expansion rate between upper and lower cortical layers leads to elastic instability (Richman et al., 1975; Bayly et al., 2014). Experimental testing with hydrogel models has been fundamental to our understanding of this process beyond mathematical models. Hydrogel models are composed of an inner core hydrogel covered with an outer layer of second hydrogel with similar or different physical properties (elasticity, resistance, etc.). When subject to expansion, these compound gel models sustain significant and measurable elastic instability and compression. The use of these models has demonstrated that when the outer layer swells (grows) faster than the inner core, this results in material strain and compression, which is released by buckling and the formation of seeming folds and fissures (Tallinen et al., 2014). For greater realism, three-dimensional hydrogel models have been designed with the shape of a mid- gestational human embryo brain, and then the differential expansion of the bi-layered hydrogel results in the formation of folds and fissures mimicking the adult human brain (Tallinen et al., 2016).

The above studies and related transcriptomic analyses (Sheppard et al., 1991; Fietz et al., 2012) suggest that the ECM regulates cortical folding not only by affecting progenitor cell proliferation and neuron migration, but also by contributing to define the mechanical properties of the developing cortex. A seminal study by Long and colleagues used living slices of embryonic human cortex cultured *in vitro* to demonstrate the critical role of the ECM on cortex folding (Long et al., 2018). Slices of human fetal neocortex in culture were treated with a cocktail of ECM components (HAPLN1, Lumican, and Collagen I), which induced the ultra-rapid folding of the cortical surface, not occurring in untreated slices. Related to an increase in tissue stiffness, this folding was accompanied by an increase in expression of HA and its receptor (CD168) in the CP, followed by ERK signaling activation. Intriguingly, this ECM cocktail did not induce folding by promoting progenitor proliferation or neuronal migration, but by decreasing cell density at the CP. This was recapitulated in untreated slices from older fetuses, supporting that this combination of ECM components increases stiffness and induces folding by the same physiological mechanism as nascent folds that develop at later stages in the non-manipulated human embryo (Long et al., 2018).

The advent of cerebral organoids has become an additional alternative to study and understand cortical folding, by physical manipulation *in vitro*. An innovative organoid on-a-chip approach allows growing cerebral organoids that wrinkle and fold (Karzbrun et al., 2018). This enables to culture human cerebral organoids in millimeter-thick chambers and image them in whole mount, including the formation of folds. Under these conditions, organoids developed from hiPSCs from lissencephalic patients, mutant for *LIS1*, wrinkle significantly less than control organoids from healthy donors. Transcriptomic analyses of these mutant organoids has revealed a significant downregulation of ECM and cytoskeletal genes, suggesting that the underlying cause of this deficit in cortical folding is a pathological softening of the cytoskeleton. Unfortunately, cortical folding of on-chip organoids is due to contraction of the VZ and expansion of the progenitor cell nucleus (Karzbrun et al., 2018), which completely differs from the expanded basal germinal zones and increased neurogenesis observed in animal models (Reillo et al., 2011; Heide et al., 2018; Karlinski and Reiner, 2018; Karzbrun et al., 2018). Nonetheless, these results support the relevance of the ECM in maintaining the tissue contractility and stiffness that induce cortex folding (Karlinski and Reiner, 2018; Karzbrun et al., 2018).

The balance between softness and stiffness in the CNS microenvironment is also a key factor in fate determination. Mounting evidence demonstrates that the mechanical properties of tissue microenvironment exerted by ECM components, including stiffness or viscoelasticity, play a significant role in cell fate determination, dictating the output of cellular lineages from differentiation to proliferation or apoptosis (Holle et al., 2018). For example, microenvironments as soft as brain tissue promote mesenchymal stem cells to adopt a neuronal lineage, whereas stiffer microenvironments promote the same cells to enter myogenic differentiation (Engler et al., 2006). Analyses of the stiffness of the developing mouse cortex using atomic force microscopy (AFM) have shown that VZ and SVZ gradually increase in stiffness during development, while the neuron- rich CP increases in stiffness only until E16.5, decreasing by E18.5. Stiffness of the CP is due not only to neurons, which are stiffer than other cells in the cortex, but also to changes in the composition of the ECM (Iwashita et al., 2014). Indeed, differences in ECM composition along the human cortical surface, causing variations in tissue stiffness, have been proposed as a mechanism contributing to cortex folding (Long et al., 2018; Wianny et al., 2018).

EVOLUTION OF ECM COMPONENTS AND THE EVOLUTION OF CORTICAL FOLDING

Recent progress in neuroimaging techniques and neuroanatomy are providing major insights into fundamental differences in cortical organization across phylogeny. Using multiple

approaches to compare cortical folding, parcellation and neural connectivity in mouse, marmoset, macaque and human, David Van Essen and colleagues have revealed dramatic differences in the total number and arrangement of cortical areas (Van Essen et al., 2019). In this study, they also report that cortical folding patterns vary dramatically across species, and that individual variability in cortical folding increases with cortical surface area. In line with this evidence, recent hypotheses propose that the sophistication of cortical folding and expansion in development and evolution may be attributed to both cell autonomous mechanisms (i.e., increased progenitor cell proliferation) and non-cell autonomous mechanisms (i.e., ECM composition) known to impinge on the former (Fietz et al.,2010; Güven et al., 2020). The notion that the evolution of ECM components may have significantly contributed to the evolution of cortical folding is directly supported by the effects of ECM treatment on folding of cortical slices in culture (Long et al., 2018). Ectopic administration of ECM molecules (HAPLN1, Lumican and Collagen I) caused the folding of livingcortical slices from human embryos, but not from ferrets or mice, although it did cause changes in tissue stiffness. Thisdifferent response suggests that the ECM and signaling pathways that induce gyrification in humans are different from those with a similar role in ferret, as shown in **Table 1**. These findings highlight human specific ECM components as a game changer in mechanical and signaling processes during cortical folding (Wianny et al., 2018). Interestingly, Cromar et al. (2014) showed that ECM proteins underwent domain gain that occurs exclusively at the divergence of primates from other mammals. In agreement with this, primate-specific miRNAs regulating the expression of ECM genes are differentially expressed in CP and germinal zones in primates (Arcila et al., 2014). Takentogether, this indicates the existence of evolutionary changes in the regulation of expression of ECM components, and supports the notion that the ECM contributes to regulate cortex size and folding (Fietz et al., 2012; Florio et al., 2017; Long et al., 2018).

A close inspection of the spatial and temporal patterns of expression of ECM components and cell adhesion molecules in the developing cerebral cortex highlights potential mechanisms evolved to induce cortical folding. As mentioned, *Flrt1/3* are expressed homogeneously and at high levels in the developing mouse cortex but not in ferret, where domains of medium and low expression alternate, correlating with the folding pattern. Interestingly, the loss of *Flrt1/3* in the mouse smooth cortex alters the adhesion-repulsion balance between migrating neurons thus promoting their tangential dispersion, leading to the formation of fissures and folds. This mimicks the native situation found in human and ferret, therefore emphasizing the importance of repression of *Flrt1/3* in the evolution of cortex folding (del Toro et al., 2017; Llinares-Benadero and Borrell, 2019).

The relevance of neuronal migration in the formation of cortical folds is further supported by comparative analyses in mouse and ferret (Gertz and Kriegstein, 2015; Martínez-Martínez et al., 2019). Whereas in mouse cortex radial neuron migration takes place in rather rectilinear trajectories, cortical neurons in ferret display much more tortuous and complex behaviors (Gertz and Kriegstein, 2015). Examination of the detailed cellular morphology and behavior demonstrates that, contrary to dogma, radially migrating cortical excitatory neurons extend a leading process that is frequently branched under normal physiological conditions, both in mouse and ferret (Martínez-Martínez et al., 2019). The frequency and degree of branching of this leading process are significantly greater in the gyrencephalic ferret than the lissencephalic mouse. We have proposed that this difference has a profound influence on the tangential dispersion of neurons migrating radially and, consequently, on cortical folding. Differences in branching between species may stem from differences in the expression profileof ECM and cell adhesion molecules (Fietz et al., 2012; Reillo et al., 2017).

In addition to the known and potential direct effects of ECM on cortex expansion and folding, a recent study in the developing ferret identified multiple cellular elements that may act as non-cell autonomous or "extrinsic" elements affecting cortical progenitor behavior and fate in different ways (Reillo et al., 2017). For example, axonal fiber tracts and tangentially migrating neurons with a marked laminar organization are proposedto be prominent sources of instructive signals onto cortical progenitor cells and radially migrating neurons. These extrinsic elements change quite dynamically during development, so their relevance on cortex development/folding are proposed to be also dynamic. This highlights the role that different combinations of ECM components and cell adhesion molecules may play in creating a complex laminar code of extrinsic influences, that modulate cortical development and folding in a selective manner (Nowakowski et al., 2017; Reillo et al., 2017).

CONCLUSION AND FUTUREPERSPECTIVES

The ECM is best known for providing structural support tocells and tissues. However, the burst of transcriptomic studies over the past few years has identified ECM components as prime candidates in controlling cerebral cortex development, expansion and folding, and the evolution of these features. A number of studies have shown the central importance of the ECM in regulating cortical progenitor proliferation and basal progenitor amplification, the basis for increased neurogenesis, expansion and folding. Other ECM molecules regulate neuron migration or define the stiffness of tissue, with profound implications in cell fate determination and cortex folding. Some of these functions are highly conserved across phylogeny, while others exert their function in a species- specific manner. Accordingly, functionally relevant interspecies differences in ECM composition suggest its co-evolution with thecortical phenotype.

New tools and technologies continuously provide unprecedented opportunities to increase our understandingof the ECM and its roles in brain development. Single cell

RNA sequencing now offers the unique opportunity to carefully examine differences in ECM expression profiles across progenitor cell populations and their lineages, and the impact of the ECM on transcriptional programs critical during cortical development. This may then allow identifying ECM signaling pathways implicated in the evolution and folding of the neocortex. A focus on the ECM is a promising strategy in the quest to reacha unified understanding of molecular mechanisms of cortical evolution and folding.

AUTHOR CONTRIBUTIONS

SA created the figures. SA and VB wrote the manuscript. Both authors contributed to the article and approved the submitted version.

FUNDING

SA was supported by a "La Caixa" international scholarship "Severo Ochoa". Work in our lab was supported by grants from European Research Council (309633) and the Spanish State Research Agency (PGC2018-102172-B-I00, as well as through the "Severo Ochoa" Program for Centers of Excellence in R&D, ref. SEV-2017-0723).

ACKNOWLEDGMENTS

We thank members of the Borrell lab for discussions and critical reading of the manuscript. We acknowledge support of the publication fee by the CSIC Open Access Publication Support Initiative through its Unit of Information Resources for Research (URICI).

REFERENCES

Akita, K., von Holst, A., Furukawa, Y., Mikami, T., Sugahara, K., and Faissner, A. (2008). Expression of multiple chondroitin/dermatan sulfotransferases in the neurogenic regions of the embryonic and adult central nervous system implies that complex chondroitin sulfates have a role in neural stem cell maintenance. *Stem Cells* 26, 798–809. doi: 10.1634/stemcells.2007-0448

Alcantara, S., Ruiz, M., D'Arcangelo, G., Ezan, F., de Lecea, L., Curran, T.,et al. (1998). Regional and cellular patterns of reelin mRNA expression in the forebrain of the developing and adult mouse. *J. Neurosci.* 18, 7779–7799.

Arai, Y., Pulvers, J. N., Haffner, C., Schilling, B., Nusslein, I., Calegari, F., et al. (2011). Neural stem and progenitor cells shorten S-phase on commitment to neuron production. *Nat. Commun.* 2:154.

Arcila, M. L., Betizeau, M., Cambronne, X. A., Guzman, E., Doerflinger, N., Bouhallier, F., et al. (2014). Novel primate miRNAs coevolved with ancient target genes in germinal zone-specific expression patterns. *Neuron* 81, 1255– 1262. doi: 10.1016/j.neuron.2014.01.017

Arlotta, P., and Pasca, S. P. (2019). Cell diversity in the human cerebral cortex: from the embryo to brain organoids. *Curr. Opin. Neurobiol.* 56, 194–198. doi: 10.1016/j.conb.2019.03.001

Armstrong, E., Curtis, M., Buxhoeveden, D. P., Fregoe, C., Zilles, K., Casanova, M. F., et al. (1991). Cortical gyrification in the rhesus monkey: a test of the mechanical folding hypothesis. *Cereb. Cortex* 1, 426–432.

Bar, I., Lambert de Rouvroit, C., and Goffinet, A. M. (2000). The evolution of cortical development. An hypothesis based on the role of the Reelin signaling pathway. *Trends Neurosci.* 23, 633–638. doi: 10.1016/S0166-2236(00)01675-1

Barros, C. S., Franco, S. J., and Müller, U. (2011). Extracellular Matrix: functionsin the nervous system. *Cold Spring Harb. Perspect. Biol.* 3, 1–24. doi: 10.1101/cshperspect.a005108

Bayly, P. V., Taber, L. A., and Kroenke, C. D. (2014). Mechanical forces in cerebral cortical folding: a review of measurements and models. *J. Mech. Behav. Biomed. Mater.* 29, 568–581. doi: 10.1016/j.jmbbm.2013.02.018

Betizeau, M., Cortay, V., Patti, D., Pfister, S., Gautier, E., Bellemin-Menard, A., et al. (2013). Precursor diversity and complexity of lineage relationships in the outer subventricular zone of the primate. *Neuron* 80, 442–457.

Bhaduri, A., Andrews, M. G., Mancia Leon, W., Jung, D., Shin, D., Allen,D., et al. (2020). Cell stress in cortical organoids impairs molecular subtype specification. *Nature* 578, 142–148. doi: 10.1038/s41586-020-1962-0

Borrell, V. (2018). How cells fold the cerebral cortex. *J. Neurosci.* 38, 776–783. doi: 10.1523/JNEUROSCI.1106-17.2017

Borrell, V., and Reillo, I. (2012). Emerging roles of neural stem cells in cerebral cortex development and evolution. *Dev. Neurobiol.* 72, 955–971. doi: 10.1002/dneu.22013

Boulder_Committee (1970). Embryonic vertebrate central nervous system: revised terminology. *Anat. Rec.* 166, 257–261.

Buchsbaum, I. Y., Kielkowski, P., Giorgio, G., O'Neill, A. C., Di Giaimo, R., Kyrousi, C., et al. (2020). ECE 2 regulates neurogenesis and neuronal migration during human cortical development. *EMBO Rep.* 21, 1–24. doi: 10.15252/embr.201948204

Camp, J. G., Badsha, F., Florio, M., Kanton, S., Gerber, T., Wilsch-Brauninger, M.,et al. (2015). Human cerebral organoids recapitulate gene expression programs of fetal neocortex development. *Proc. Natl. Acad. Sci. U.S.A.* 112, 15672–15677. doi: 10.1073/pnas.1520760112

Chen, Z.-L., Haegeli, V., Yu, H., and Strickland, S. (2009). Cortical deficiency of laminin γ1 impairs the AKT/GSK-3β signaling pathway and leads to defects in neurite outgrowth and neuronal migration. *Dev. Biol.* 327, 158–168. doi: 10.1038/jid.2014.371

Crickmore, M. A., and Mann, R. S. (2007). Hox control of morphogen mobility and organ development through regulation of glypican expression. *Development* 134, 327–334. doi: 10.1242/dev.02737

Cromar, G., Wong, K. C., Loughran, N., On, T., Song, H., Xiong, X., et al. (2014). New tricks for "old" domains: how novel architectures and promiscuous hubs contributed to the organization and evolution of the ECM. *Genome Biol. Evol.* 6, 2897–2917. doi: 10.1093/gbe/evu228

Curran, T., and D'Arcangelo, G. (1998). Role of Reelin in the control of brain development. *Brain Res. Rev.* 26, 285–294. doi: 10.1016/S0165-0173(97)00 035-0

D'Arcangelo, G., Miao, G. G., Chen, S. C., Soares, H. D., Morgan, J. I., and Curran, T. (1995). A protein related to extracellular matrix proteins deleted in the mouse mutant reeler. *Nature* 374, 719–723.

De Juan Romero, C., and Borrell, V. (2015). Coevolution of radial glial cells and the cerebral cortex. *Glia* 63, 1303–1319. doi: 10.1002/glia. 22827

De Juan Romero, C., Bruder, C., Tomasello, U., Sanz-Anquela, J. M., and Borrell, V. (2015). Discrete domains of gene expression in germinal layers distinguish the development of gyrencephaly. *EMBO J.* 34, 1859–1874. doi: 10.15252/embj.201591176

Dehay, C., Kennedy, H., and Kosik, K. S. (2015). The outer subventricular zone and primate-specific cortical complexification. *Neuron* 85, 683–694. doi: 10.1016/j.neuron.2014.12.060

del Toro, D., Ruff, T., Cederfjäll, E., Villalba, A., Seyit-Bremer, G., Borrell, V., et al. (2017). Regulation of cerebral cortex folding by controlling neuronal migration via flrt adhesion molecules. *Cell* 169, 621.e16–635.e16. doi: 10.1016/j.cell.2017. 04.012

Drago, J., Nurcombe, V., and Bartlett, P. F. (1991). Laminin through its long arm E8 fragment promotes the proliferation and differentiation of murine neuroepithelial cells in vitro. *Exp. Cell Res.* 192, 256–265. doi: 10.1016/0014-4827(91)90184-v

Dulabon, L., Olson, E. C., Taglienti, M. G., Eisenhuth, S., McGrath, B., Walsh, C. A., et al. (2000). Reelin binds alpha3beta1 integrin and inhibits neuronal migration.*Neuron* 27, 33–44.

Engler, A. J., Sen, S., Sweeney, H. L., and Discher, D. E. (2006). Matrix elasticity directs stem cell lineage specification. *Cell* 126, 677–689. doi: 10.1016/j.cell.2006.06.044

Fernandez, V., Llinares-Benadero, C., Borrell, V., Fernández, V., Llinares-Benadero, C., and Borrell, V. (2016). Cerebral cortex expansion and folding: what have we learned? *EMBO J.* 35, 1021–1044. doi: 10.15252/embj.20159 3701

Fietz, S. A., Kelava, I., Vogt, J., Wilsch-Brauninger, M., Stenzel, D., Fish, J. L., et al. (2010). OSVZ progenitors of human and ferret neocortex are epithelial-like and expand by integrin signaling. *Nat. Neurosci.* 13, 690–699.

Fietz, S. A., Lachmann, R., Brandl, H., Kircher, M., Samusik, N., Schroder, R., et al. (2012). Transcriptomes of germinal zones of human and mouse fetal neocortex suggest a role of extracellular matrix in progenitor self-renewal. *Proc. Natl. Acad. Sci. U.S.A.* 109, 11836–11841. doi: 10.1073/pnas.1209647109

Flanagan, L. A., Rebaza, L. M., Derzic, S., Schwartz, P. H., and Monuki, E. S. (2007). Regulation of human neural precursor cells by laminin and integrins. *J. Neurosci. Res.* 3253, 3244–3253. doi: 10.1002/jnr

Florio, M., Albert, M., Taverna, E., Namba, T., Brandl, H., Lewitus, E., et al. (2015). Human-specific gene ARHGAP11B promotes basal progenitor amplification and neocortex expansion. *Science* 347, 1465–1470. doi: 10.1126/science. aaa1975

Florio, M., Borrell, V., and Huttner, W. B. (2017). Human-specific genomic signatures of neocortical expansion. *Curr. Opin. Neurobiol.* 42, 33–44. doi: 10.1016/j.conb.2016.11.004

Florio, M., and Huttner, W. B. (2014). Neural progenitors, neurogenesis and the evolution of the neocortex. *Development* 141, 2182–2194. doi: 10.1242/dev.090571

Florio, M., Namba, T., Paabo, S., Hiller, M., and Huttner, W. B. (2016). A single splice site mutation in human-specific ARHGAP11B causes basal progenitor amplification. *Sci. Adv.* 2:e1601941. doi: 10.1126/sciadv.1601941

Franco, S. J., Martinez-Garay, I., Gil-Sanz, C., Harkins-Perry, S. R., and Müller, U. (2011). Reelin regulates cadherin function via Dab1/Rap1 to control neuronal migration and lamination in the neocortex. *Neuron* 69, 482–497. doi: 10.1016/j.neuron.2011.01.003

Franco, S. J., and Müller, U. (2011). Extracellular matrix functions during neuronal migration and lamination in the mammalian central nervous system. *Dev.Neurobiol.* 71, 889–900. doi: 10.1002/dneu.20946

Galli, A., Roure, A., Zeller, R., and Dono, R. (2003). Glypican 4 modulates FGF signalling and regulates dorsoventral forebrain patterning in Xenopus embryos. *Development* 130, 4919–4929. doi: 10.1242/dev.00706

Gertz, C. C., and Kriegstein, A. R. (2015). Neuronal migration dynamics inthe developing ferret cortex. *J. Neurosci.* 35, 14307–14315. doi: 10.1523/JNEUROSCI.2198-15.2015

Girós, A., Morante, J., Gil-Sanz, C., Fairén, A., and Costell, M. (2007). Perlecan controls neurogenesis in the developing telencephalon. *BMC Dev. Biol* 7:29. doi: 10.1186/1471-213X-7-29

Götz, M., and Huttner, W. B. (2005). The cell biology of neurogenesis. *Nat. Rev. Mol. Cell Biol.* 6, 777–788.

Gu, W. L., Fu, S. L., Wang, Y. X., Li, Y., Lü, H. Z., Xu, X. M., et al. (2009). Chondroitin sulfate proteoglycans regulate the growth, differentiation and migration of multipotent neural precursor cells through the integrin signaling pathway. *BMC Neurosci.* 10:128. doi: 10.1186/1471-2202-10-128

Güven, A., Kalebic, N., Long, K. R., Florio, M., Vaid, S., Brandl, H., et al. (2020). Extracellular matrix-inducing Sox9 promotes both basal progenitor proliferation and gliogenesis in developing neocortex. *Elife* 9:e49808. doi: 10.7554/eLife.49808

Hall, P. E., Lathia, J. D., Caldwell, M. A., and Ffrench-Constant, C. (2008). Laminin enhances the growth of human neural stem cells in defined culture media. *BMC Neurosci.* 9:71. doi: 10.1186/1471-2202-9-71

Hansen, D. V., Lui, J. H., Parker, P. R., and Kriegstein, A. R. (2010). Neurogenic radial glia in the outer subventricular zone of human neocortex. *Nature* 464, 554–561.

Hartfuss, E., Forster, E., Bock, H. H., Hack, M. A., Leprince, P., Luque, J. M., et al. (2003). Reelin signaling directly affects radial glia morphology and biochemical maturation. *Development* 130, 4597–4609.

Haubensak, W., Attardo, A., Denk, W., and Huttner, W. B. (2004). Neurons arise in the basal neuroepithelium of the early mammalian telencephalon: a major site of neurogenesis. *Proc. Natl. Acad. Sci. U.S.A.* 101, 3196–3201.

Haubst, N., Georges-Labouesse, E., De Arcangelis, A., Mayer, U., and Götz, M. (2006). Basement membrane attachment is dispensable for radial glial cell fate and for proliferation, but affects positioning of neuronal subtypes. *Development* 133, 3245–3254. doi: 10.1242/dev.02486

Heide, M., Huttner, W. B., and Mora-Bermúdez, F. (2018). Brain organoids as models to study human neocortex development and evolution. *Curr. Opin. CellBiol.* 55, 8–16. doi: 10.1016/j.ceb.2018.06.006

Hienola, A., Tumova, S., Kulesskiy, E., and Rauvala, H. (2006). N-syndecan deficiency impairs neural migration in brain. *J. Cell Biol.* 174, 569–580. doi: 10.1083/jcb.200602043

Holle, A. W., Young, J. L., Van Vliet, K. J., Kamm, R. D., Discher, D., Janmey, P., et al. (2018). Cell-extracellular matrix mechanobiology: forceful tools and emerging needs for basic and translational research. *Nano Lett.* 18, 1–8. doi: 10.1021/acs.nanolett.7b04982

Hong, S. E., Shugart, Y. Y., Huang, D. T., Shahwan, S. A., Grant, P. E., Hourihane, J. O., et al. (2000). Autosomal recessive lissencephaly with cerebellar hypoplasia is associated with human RELN mutations. *Nat. Genet.* 26, 93–96.

Hynes, R. O. (2009). The extracellular matrix: Not just pretty fibrils. *Science* 326, 1216–1219. doi: 10.1126/science.1176009

Ishii, M., and Maeda, N. (2008). Oversulfated chondroitin sulfate plays critical roles in the neuronal migration in the cerebral cortex. *J. Biol. Chem.* 283, 32610–32620. doi: 10.1074/jbc.M806331200

Iwashita, M., Kataoka, N., Toida, K., and Kosodo, Y. (2014). Systematic profiling of spatiotemporal tissue and cellular stiffness in the developing brain. *Development*141, 3793–3798. doi: 10.1242/dev.109637

Jen, Y. H. L., Musacchio, M., and Lander, A. D. (2009). Glypican-1 controls brain size through regulation of fibroblast growth factor signaling in early neurogenesis. *Neural Dev.* 4, 1–19. doi: 10.1186/1749-8104-4-33

Johnson, M. B., Wang, P. P., Atabay, K. D., Murphy, E. A., Doan, R. N., Hecht, J. L.,et al. (2015). Single-cell analysis reveals transcriptional heterogeneity of neural progenitors in human cortex. *Nat. Neurosci.* 18, 637–646. doi: 10.1038/nn.3980

Kanton, S., Boyle, M. J., He, Z., Santel, M., Weigert, A., Sanchís-Calleja, F., et al. (2019). Organoid single-cell genomic atlas uncovers human-specific features of brain development. *Nature* 574, 418-422. doi: 10.1038/s41586-019-1654-9 Karlinski, M., and Reiner, O. (2018). Unfolding the folds: how the biomechanics of the extracellular matrix contributes to cortical gyrification. *Opera Med. Physiol.* 4, 63–70. doi: 10.20388/omp2018.001.0058

Karzbrun, E., Kshirsagar, A., Cohen, S. R., Hanna, J. H., and Reiner, O. (2018). Human brain organoids on a chip reveal the physics of folding. *Nat. Phys.* 14, 515–522. doi: 10.1038/s41567-018-0046-7

Kearns, S. M., Laywell, E. D., Kukekov, V. K., and Steindler, D. A. (2003). Extracellular matrix effects on neurosphere cell motility. *Exp. Neurol.* 182, 240–244. doi: 10.1016/S0014-4886(03)00124-9

Kriegstein, A., Noctor, S., and Martinez-Cerdeno, V. (2006). Patterns of neural stem and progenitor cell division may underlie evolutionary cortical expansion. *Nat.Rev. Neurosci.* 7, 883–890.

Kroenke, C. D., and Bayly, P. V. (2018). How forces fold the cerebral cortex. *J. Neurosci.* 38, 767–775. doi: 10.1523/JNEUROSCI.1105-17.2017

Lancaster, M. A., and Knoblich, J. A. (2014). Organogenesis in a dish: modeling development and disease using organoid technologies. *Science* 345:1247125. doi: 10.1126/science.1247125

Lancaster, M. A., Renner, M., Martin, C. A., Wenzel, D., Bicknell, L. S., Hurles, M. E., et al. (2013). Cerebral organoids model human brain development and microcephaly. *Nature* 501, 373–379. doi: 10.1038/nature12517

Lathia, J. D., Patton, B., Eckley, D. M., Magnus, T., Mughal, M. R., Sasaki, T., et al. (2007). Patterns of laminins and integrins in the embryonic ventricular zone of the CNS. *J. Comp. Neurol.* 505, 630–643. doi: 10.1002/cne.21520

Llinares-Benadero, C., and Borrell, V. (2019). Deconstructing cortical folding: genetic, cellular and mechanical determinants. *Nat. Rev. Neurosci.* 20, 161–176. doi: 10.1038/s41583-018-0112-2

Long, K. R., and Huttner, W. B. (2019). How the extracellular matrix shapes neural development. *Open Biol.* 9:180216. doi: 10.1098/rsob.180216

Long, K. R., Moss, L., Laursen, L., Boulter, L., and Ffrench-Constant, C. (2016). Integrin signalling regulates the expansion of neuroepithelial progenitors and neurogenesis via Wnt7a and Decorin. *Nat. Commun.* 7:10354. doi: 10.1038/ncomms10354

Long, K. R., Newland, B., Florio, M., Kalebic, N., Langen, B., Kolterer, A., et al. (2018). Extracellular matrix components HAPLN1, lumican, and collagen I

cause hyaluronic acid-dependent folding of the developing human neocortex. *Neuron* 99:e7. doi: 10.1016/j.neuron.2018.07.013

Loulier, K., Lathia, J. D., Marthiens, V., Relucio, J., Mughal, M. R., Tang, S. C., et al. (2009). beta1 integrin maintains integrity of the embryonic neocortical stem cell niche. *PLoS Biol.* 7:e1000176. doi: 10.1371/journal.pbio.1000176

Lui, J. H., Nowakowski, T. J., Pollen, A. A., Javaherian, A., Kriegstein, A. R., and Oldham, M. C. (2014). Radial glia require PDGFD-PDGFRbeta signalling in human but not mouse neocortex. *Nature* 515, 264–268. doi: 10.1038/ nature13973

Maeda, N. (2015). Proteoglycans and neuronal migration in the cerebral cortex during development and disease. *Front. Neurosci.* 9:98. doi: 10.3389/fnins.2015. 00098

Manoharan, M., Muhammad, S. A., and Sowdhamini, R. (2015). Sequence analysis and evolutionary studies of reelin proteins. *Bioinform. Biol. Insights* 9, 187–193. doi: 10.4137/BBI.S26530

Marthiens, V., Kazanis, I., Moss, L., Long, K. R., and Ffrench-Constant, C. (2010). Adhesion molecules in the stem cell niche–more than just staying in shape? *J. Cell Sci.* 123, 1613–1622. doi: 10.1242/jcs.054312

Martínez-Martínez, M. Á, De Juan Romero, C., Fernández, V., Cárdenas, A., Götz, M., and Borrell, V. (2016). A restricted period for formation of outer subventricular zone defined by Cdh1 and Trnp1 levels. *Nat. Commun.* 7:11812. doi: 10.1038/ncomms11812

Martínez-Martínez, M. Á, Ciceri, G., Espinós, A., Fernández, V., Marín, O., and Borrell, V. (2019). Extensive branching of radially-migrating neurons in the mammalian cerebral cortex. *J. Comp. Neurol.* 527, 1558–1576. doi: 10.1002/cne. 24597

Miyata, T., Kawaguchi, A., Saito, K., Kawano, M., Muto, T., and Ogawa, M. (2004). Asymmetric production of surface-dividing and non-surface-dividing cortical progenitor cells. *Development* 131, 3133–3145.

Miyata, T., Kawaguchi, D., Kawaguchi, A., and Gotoh, Y. (2010). Mechanisms that regulate the number of neurons during mouse neocortical development. *Curr. Opin. Neurobiol.* 20, 22–28. doi: 10.1016/j.conb.2010.01.001

Mora-Bermudez, F., Badsha, F., Kanton, S., Camp, J. G., Vernot, B., Kohler, K., et al. (2016). Differences and similarities between human and chimpanzee neural progenitors during cerebral cortex development. *eLife* 5:e18683. doi: 10.7554/ eLife.18683

Myshrall, T. D., Moore, S. A., Ostendorf, A. P., Satz, J. S., Kowalczyk, T., Nguyen, H., et al. (2012). Dystroglycan on radial glia end feet is required for pial basement membrane integrity and columnar organization of the developing cerebral cortex. *J. Neuropathol. Exp. Neurol.* 71, 1047–1063. doi: 10.1097/NEN. 0b013e318274a128

Nirwane, A., and Yao, Y. (2019). Laminins and their receptors in the CNS. *Biol. Rev.* 94, 283–306. doi: 10.1111/brv.12454

Noctor, S. C., Flint, A. C., Weissman, T. A., Dammerman, R. S., and Kriegstein, A. R. (2001). Neurons derived from radial glial cells establish radial units in neocortex. *Nature* 409, 714–720.

Noctor, S. C., Martinez-Cerdeno, V., Ivic, L., and Kriegstein, A. R. (2004). Cortical neurons arise in symmetric and asymmetric division zones and migrate through specific phases. *Nat. Neurosci.* 7, 136–144.

Nowakowski, T. J., Bhaduri, A., Pollen, A. A., Alvarado, B., Mostajo-Radji, M. A., Di Lullo, E., et al. (2017). Spatiotemporal gene expression trajectories reveal developmental hierarchies of the human cortex. *Science* 358, 1318–1323. doi: 10.1126/science.aap8809

Park, Y., Rangel, C., Reynolds, M. M., Caldwell, M. C., Johns, M., Nayak, M., et al. (2003). Drosophila Perlecan modulates FGF and Hedgehog signals to activate neural stem cell division. *Dev. Biol.* 253, 247–257. doi: 10.1016/S0012-1606(02) 00019-2

Perris, R., and Perissinotto, D. (2000). Role of the extracellular matrix during neural crest cell migration. *Mech. Dev.* 95, 3–21. doi: 10.1016/S0925-4773(00)00365-8 Pilz, G. A., Shitamukai, A., Reillo, I., Pacary, E., Schwausch, J., Stahl, R., et al. (2013). Amplification of progenitors in the mammalian telencephalon includes a new radial glial cell type. *Nat. Commun.* 4:2125. doi: 10.1038/ncomms3125

Pollen, A. A., Bhaduri, A., Andrews, M. G., Nowakowski, T. J., Meyerson, O. S., Mostajo-Radji, M. A., et al. (2019). Establishing cerebral organoids as models of human-specific brain evolution. *Cell* 176:e17. doi: 10.1016/j.cell.2019.01.017

Pollen, A. A., Nowakowski, T. J., Chen, J., Retallack, H., Sandoval-Espinosa, C., Nicholas, C. R., et al. (2015). Molecular identity of human outer radial glia during cortical development. *Cell* 163, 55–67. doi: 10.1016/j.cell.2015.09.004

Qian, X., Song, H., and Ming, G. L. (2019). Brain organoids: advances, applications and challenges. *Development* 146:dev166074. doi: 10.1242/dev.166074

Radakovits, R., Barros, C. S., Belvindrah, R., Patton, B., and Müller, U. (2009). Regulation of radial glial survival by signals from the meninges. *J. Neurosci.* 29, 7694–7705. doi: 10.1523/JNEUROSCI.5537-08.2009

Radmanesh, F., Caglayan, A. O., Silhavy, J. L., Yilmaz, C., Cantagrel, V., Omar, T., et al. (2013). Mutations in LAMB1 cause cobblestone brain malformation without muscular or ocular abnormalities. *Am. J. Hum. Genet.* 92, 468–474. doi: 10.1016/j.ajhg.2013.02.005

Rakic, P. (1972). Mode of cell migration to the superficial layers of fetal monkey neocortex. *J. Comp. Neurol.* 145, 61–83.

Rash, B. G., Duque, A., Morozov, Y. M., Arellano, J. I., Micali, N., and Rakic, P. (2019). Gliogenesis in the outer subventricular zone promotes enlargement and gyrification of the primate cerebrum. *Proc. Natl. Acad. Sci. U.S.A.* 116, 7089–7094. doi: 10.1073/pnas.1822169116

Reillo, I., De Juan Romero, C., Cárdenas, A., Clascá, F., Martínez-Martinez, M. A., and Borrell, V. (2017). A complex code of extrinsic influences on cortical progenitor cells of higher mammals. *Cereb. Cortex* 27, 4586–4606. doi: 10.1093/ cercor/bhx171

Reillo, I., De Juan Romero, C., García-Cabezas, M. Á, and Borrell, V. (2011). A Role for intermediate radial glia in the tangential expansion of the mammalian cerebral cortex. *Cereb. Cortex* 21, 1674–1694. doi: 10.1093/cercor/bhq238

Rice, D. S., and Curran, T. (2001). Role of the reelin signaling pathway in central nervous system development. *Annu. Rev. Neurosci.* 24, 1005–1039.

Richman, D. P., Stewart, R. M., Hutchinson, J. W., and Caviness, V. S. Jr. (1975). Mechanical model of brain convolutional development. *Science* 189, 18–21.

Ross, M. E., and Walsh, C. A. (2001). Human brain malformations and their lessons for neuronal migration. *Annu. Rev. Neurosci.* 24, 1041–1070. doi: 10. 1146/annurev.neuro.24.1.1041

Sarrazin, S., Lamanna, W. C., and Esko, J. D. (2011). Heparan sulfate proteoglycans. *Cold Spring Harb. Perspect. Biol.* 3, 1–33. doi: 10.1101/cshperspect.a004952 Schaefer, A. W., and Juliano, S. L. (2008). Migration of transplanted neural progenitor cells in a ferret model of cortical dysplasia. *Exp. Neurol.* 210, 67–82.doi: 10.1016/j.expneurol.2007.10.005

Schwartz, N. B., and Domowicz, M. S. (2018). Proteoglycans in brain development and pathogenesis. *FEBS Lett.* 592, 3791–3805. doi: 10.1002/1873-3468.13026

Sheppard, A. M., Hamilton, S. K., and Pearlman, A. L. (1991). Changes in the distribution of extracellular matrix components accompany early morphogenetic events of mammalian cortical development. *J. Neurosci.* 11, 3928–3942. doi: 10.1523/jneurosci.11-12-0392 8.1991

Shitamukai, A., Konno, D., and Matsuzaki, F. (2011). Oblique radial glial divisions in the developing mouse neocortex induce self-renewing progenitors outside the germinal zone that resemble primate outer subventricular zone progenitors. *J. Neurosci.* 31, 3683–3695.

Sidman, R. L., and Rakic, P. (1973). Neuronal migration, with special reference to developing human brain: a review. *Brain Res.* 62, 1–35.

Siegenthaler, J. A., Ashique, A. M., Zarbalis, K., Patterson, K. P., Hecht, J. H., Kane, M. A., et al. (2009). Retinoic acid from the meninges regulates cortical neuron generation. *Cell* 139, 597–609.

Sirko, S., Von Holst, A., Wizenmann, A., Götz, M., and Faissner, A. (2007). Chondroitin sulfate glycosaminoglycans control proliferation, radial glia cell differentiation and neurogenesis in neural stem/progenitor cells. *Development* 134, 2727–2738. doi: 10.1242/dev.02871

Smart, I. H., Dehay, C., Giroud, P., Berland, M., and Kennedy, H. (2002). Unique morphological features of the proliferative zones and postmitotic compartments of the neural epithelium giving rise to striate and extrastriate cortex in the monkey. *Cereb. Cortex* 12, 37–53.

Stenzel, D., Wilsch-Brauninger, M., Wong, F. K., Heuer, H., and Huttner, W. B. (2014). Integrin alphavbeta3 and thyroid hormones promote expansion of progenitors in embryonic neocortex. *Development* 141, 795–806.

Super, H., Del Rio, J. A., Martinez, A., Perez-Sust, P., and Soriano, E. (2000). Disruption of neuronal migration and radial glia in the developing cerebral cortex following ablation of Cajal-Retzius cells. *Cereb. Cortex* 10, 602–613.

Takahashi, T., Nowakowski, R. S., and Caviness, V. S. Jr. (1993). Cell cycle parameters and patterns of nuclear movement in the neocortical proliferative zone of the fetal mouse. *J. Neurosci.* 13, 820–833.

Tallinen, T., Chung, J. Y., Biggins, J. S., and Mahadevan, L. (2014). Gyrification from constrained cortical expansion. *Proc. Natl. Acad. Sci. U.S.A.* 111, 12667–12672. doi: 10.1073/pnas.1406015111

Tallinen, T., Chung, J. Y., Rousseau, F., Girard, N., Lefèvre, J., and Mahadevan, L.(2016). On the growth and form of cortical convolutions. *Nat. Phys.* 12:588.

Taverna, E., Götz, M., and Huttner, W. B. (2014). The cell biology of neurogenesis:toward an understanding of the development and evolution of the neocortex. *Annu. Rev. Cell Dev. Biol.* 30, 465–502. doi: 10.1146/annurev-cellbio-101011-155801

Telley, L., Agirman, G., Prados, J., Amberg, N., Fièvre, S., Oberst, P., et al. (2019).Temporal patterning of apical progenitors and their daughter neurons in the developing neocortex. *Science* 364:eaav2522. doi: 10.1126/science.aav2522

Timpl, R., and Rohde, H. (1979). Laminin-A glycoprotein from basement membranes. *J. Biol. Chem.* 254, 9933–9937.

Tsuda, S., Kitagawa, T., Takashima, S., Asakawa, S., Shimizu, N., Mitani, H., et al.(2010). FAK-mediated extracellular signals are essential for interkinetic nuclearmigration and planar divisions in the neuroepithelium. *J. Cell Sci.* 123, 484–496. doi: 10.1242/jcs.057851

Van Essen, D. C., Donahue, C. J., Coalson, T. S., Kennedy, H., Hayashi, T., and Glasser, M. F. (2019). Cerebral cortical folding, parcellation, and connectivity in humans, nonhuman primates, and mice. *Proc. Natl. Acad. Sci. U.S.A.* 116, 26173–26180. doi: 10.1073/pnas.1902299116

van Reeuwijk, J., Janssen, M., van den Elzen, C., Beltran-Valero de Bernabe,D., Sabatelli, P., Merlini, L., et al. (2005). POMT2 mutations cause alpha- dystroglycan hypoglycosylation and Walker-Warburg syndrome. *J. Med. Genet.* 42, 907–912.

Velasco, S., Kedaigle, A. J., Simmons, S. K., Nash, A., Rocha, M., Quadrato, G., et al. (2019). Individual brain organoids reproducibly form cell diversity of the human cerebral cortex. *Nature* 570, 523–527. doi: 10.1038/s41586-019-1289-x

Wang, Q., Yang, L., Alexander, C., and Temple, S. (2012). The niche factor syndecan-1 regulates the maintenance and proliferation of neural progenitor cells during mammalian cortical development. *PLoS One* 7:e0042883. doi: 10.1371/journal.pone.0042883
Welker, W. (1990). "Why does cerebral cortex fissure and fold? A review of determinants of gyri and sulci," in *Cerebral Cortex*, eds A. Peters and E. G. Jones (London: Plenum Press), 3–136.
Wianny, F., Kennedy, H., and Dehay, C. (2018). Bridging the gap between mechanics and genetics in cortical folding: ecm as a major driving force. *Neuron*99, 625–627. doi: 10.1016/j.neuron.2018.08.012
Zhang, C., Mejia, L. A., Huang, J., Valnegri, P., Bennett, E. J., Anckar, J., et al. (2013).The X-linked intellectual disability protein PHF6 associates with the PAF1 complex and regulates neuronal migration in the mammalian brain. *Neuron*78, 986–993. doi: 10.1016/j.neuron.2013.04.021
Zimmermann, D. R., and Dours-Zimmermann, M. T. (2008). Extracellular matrix of the central nervous system: from neglect to challenge. *Histochem. Cell Biol.* 130, 635–653. doi: 10.1007/s00418-008-0485-9

Conflict of Interest: The authors declare that the research was conducted in the absence of any commercial or financial relationships that could be construed as a potential conflict of interest.

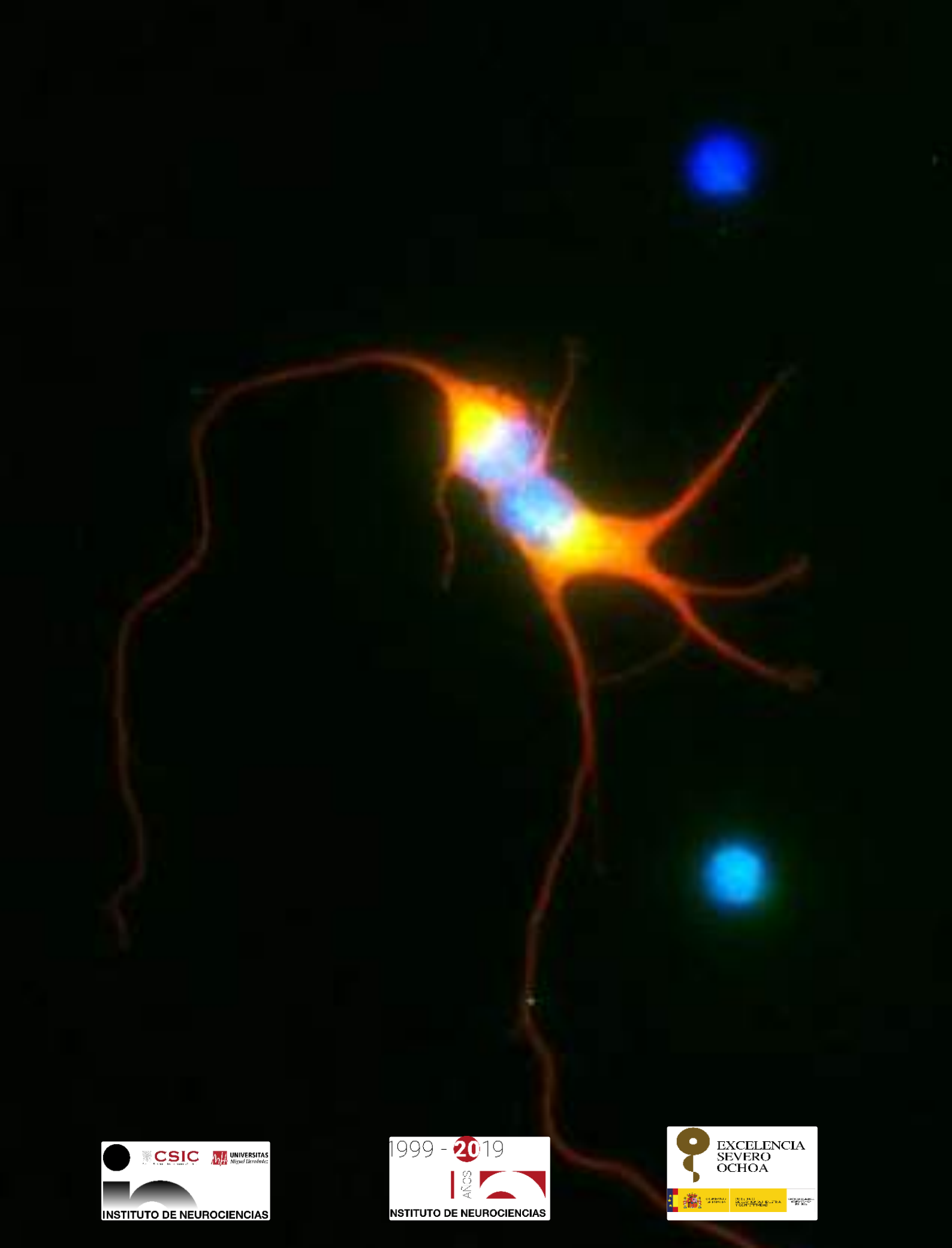

INSTITUTO DE NEUROCIENCIAS

1999 - 2019 20 AÑOS

INSTITUTO DE NEUROCIENCIAS

EXCELENCIA SEVERO OCHOA